ABUNDANCES AND KINEMATICS

OF

K GIANTS IN THE GALACTIC NUCLEAR BULGE

Thesis by

Robert Michael Rich

In Partial Fulfillment of the Requirements

for the Degree of

Doctor of Philosophy

California Institute of Technology

Pasadena, California

1986

(Submitted April 17, 1986)

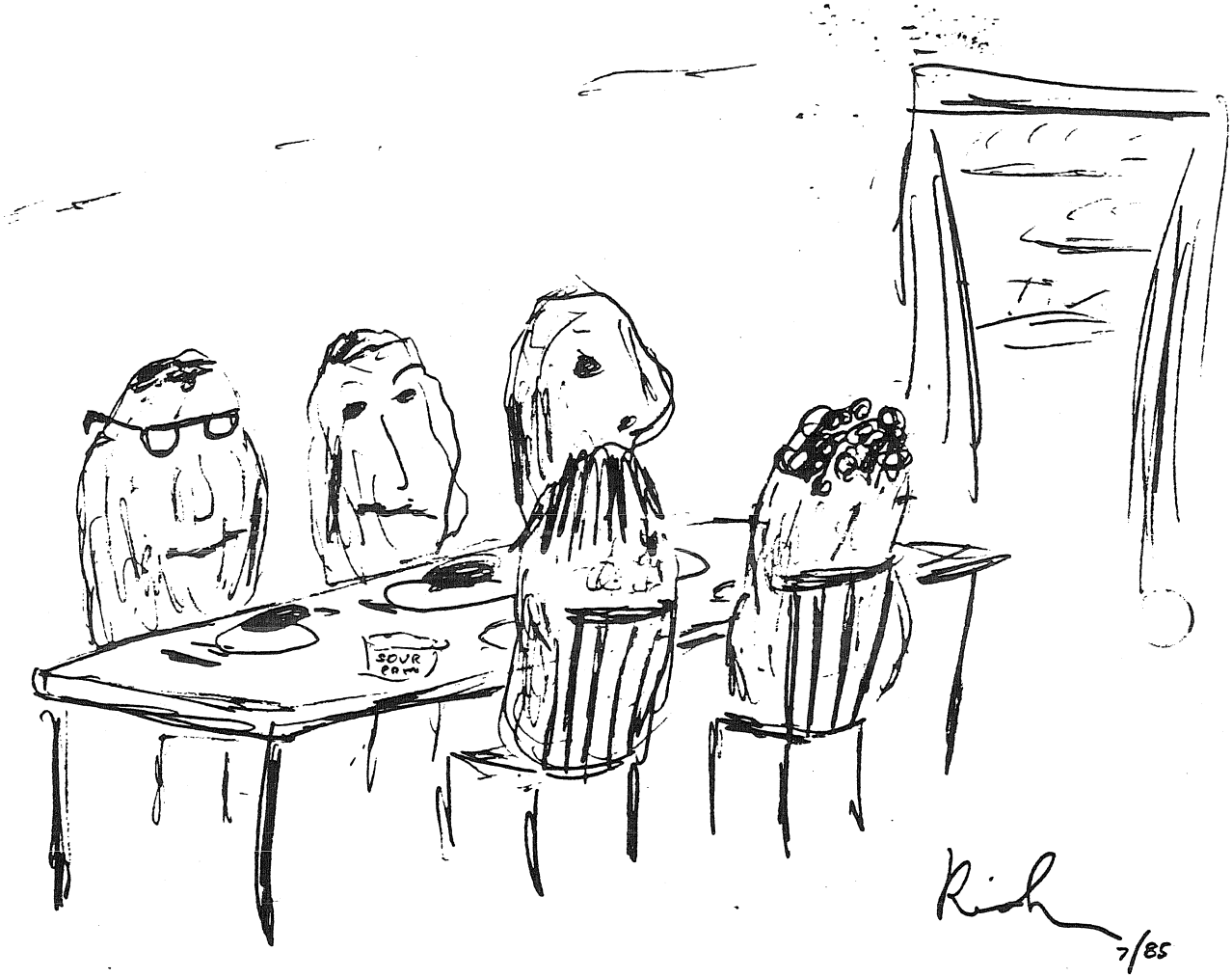

"YOU KNOW BEV, I HATE TO COMPLAIN TOO. BUT SIX STRAIGHT NIGHTS OF BAKED POTATOES?.."

To the memory of my father

Jay Baum Rich

Acknowledgements

The kindness, friendship, and support of a great many people was a great source of sustenance and joy during these years at Caltech. I have benefitted immeasurably from the faculty, support staff, students, personal friends, and family. These years have spanned the greatest emotional peaks and valleys in my life. To those of you who became and remained my friends, I have great and deep appreciation.

Jeremy Mould has guided this work with personal interest, support, and patience above and beyond the call of duty. He gave me the opportunity to pursue this research, for the most part, unhindered by any other responsibilities. He was supportive and patient in every respect.

I also want to express thanks to A. E. Whitford, who gave the initial inspiration for this research and provided financial support during the first years.

I am grateful to George Preston who, as director of the Mt. Wilson and Las Campanas Observatories sustained this research with generous allocations of telescope time and who directed an outstanding observatory at Las Campanas. At Las Campanas, I am especially grateful to Oscar Duhalde, Angel Guerra, Fernando Peralta, Ljubo Papic, Bill Robinson, and Hernan Solis.

I am also grateful to Gerry Neugebauer for allocations of observing time at Palomar Observatory.

And I am grateful to those faculty who doggedly upheld the freedom of students to choose their own research, and to those students who exercised that freedom.

I treasured my many conversations with Wal Sargent about the fate of the Dodgers, crumpet, and life in general.

I also benefitted from conversations with Maarten Schmidt, Jesse Greenstein, Bev Oke, the late Peter Young, and Gerry Neugebauer (who taught me cowboy billiards) and, at Lick Observatory, Sandy Faber and Steve Vogt.

I am indebted to Keith Shortridge for writing FIGARO, the set of programs used to reduce these data, as well as for many chats over a beer. I am also grateful to Peter Parnicky for efficient maintenance of the Vaxes. I am also grateful to Jay Frogel for providing data in advance of publication, and to Don Terndrup for the use of his photometry program.

There are three sets of people to whom I owe special thanks. My fellow students and postdocs, friends, and family.

The man most responsible for this work, in the end, wouldn't have read much past the first few pages, had he lived to read them. Yet my father treasured knowledge, and valued highly even that which he did not comprehend. While he was not highly educated, he knew of Beethoven, Shakespeare, and understood some basic science. He supported my drive to become an astronomer although there was seemingly no practical application. Most of all, he valued education for its own sake, and he gave more of himself than any reader can imagine so that this dream could come true.

I also owe a great debt to my brother Peter, and his wife Elizabeth, for their

kind hospitality and support over the years, as well as to Hildegard, and the Wilson family, who provided great friendship and support.

I am also grateful to my friends, those mentioned and unmentioned: John Biretta, Alex Filippenko, Dan Hofstadter, Keith Horne, Steve Lichten, Matthew Malkan, Jim McCarthy, Eugene Mezereny, Martha Moore, Jim Nemec, Jeff Pier, Don Penrod, Alain Porter, Abi Saha, Don Schneider, Ed Shaya, and Dave Tytler.

To future generations of students, these words. Think independently, and come up with your own research ideas. The faculty are great here; they'll support you. The going may get rough, but don't kid yourself: this is the world's greatest place to do astronomy. Remember, you have each other. Look after each other. The best times I ever had here were because people cared. The taste for Armenian food and late night dinners at the Shaker will not leave me soon. This is a group of people I have gained from greatly, and whom I will miss.

ABSTRACT

Spectroscopy and photometry has been obtained for 100 K giants in Baade's Window at $l = 1°, b = -4°$. For a galactocentric distance 7.5 kpc the line of sight passes 522 pc below the nucleus. The abundance distribution of the nuclear bulge K giants has been derived relative to 45 stars of known abundance. The abundances run from -1 to nearly $+1$ dex, with a peak at 0.3 dex, or twice the solar abundance. Of the 88 stars with derived abundances, 22% exceeded the abundance of the most metal rich local K giants; 50% exceeded the solar abundance, and 10% were metal poor (< -0.6 dex).

Radial velocities have been measured for 53 nuclear bulge K giants which also have derived abundances. Their velocity dispersion is 104 km/sec. The mean velocity is -19 ± 14 km/sec; within 1σ of the solar Π velocity of -10 km/sec. When this sample is divided into 3 subsets based on the abundances, the subset of 21 stars > 0.3 dex has $\sigma = 92 \pm 14$ km/sec and the metal poor subset of 16 stars < -0.3 dex has $\sigma = 126 \pm 22$ km/sec. An intermediate set of 16 stars has $\sigma = 97 \pm 17$ km/sec. The most metal rich stars may have a bulk velocity of -38 ± 14 km/sec, 1σ less than the -19 km/sec of the metal poor stars.

The abundance distribution function is found to be fit very well by the simple model of chemical evolution with complete gas consumption.

The smaller velocity dispersion for the metal rich stars can be interpreted as supporting a steep power law for their spatial distribution $\rho \sim r^{-7}$. The metal

rich stars may belong to a special central component of the Galaxy, which cuts off completely at 1kpc.

No evidence was found that either the metal rich or metal poor stars follow the galactic rotation curve; hence neither population appears to be rotation supported.

Optical and infrared photometry is presented for nuclear bulge K giants The colors of these stars are shown to be to hot for their derived metal abundances.

Analysis of color-magnitude diagrams in bulge fields at $-4°$ (Baade's Window) and $-8°$shows that there cannot be a 1 Gyr old population of main sequence stars in the galactic bulge. A turnoff population is detected at $-8°$, and comparison with isochrones indicates that the population is older than 5 Gyr. For the first time, there is a clear indication of a horizontal branch, or "globular cluster feature" in the luminosity function of the galactic bulge.

TABLE OF CONTENTS

Dedication iii

Acknowledgements iv

Abstract vii

Introduction 1

Introductory Note 7

Chapter 1: Metal Content of K Giants in the Nuclear Bulge of the Galaxy 8

Chapter 2: Abundances of 88 Nuclear Bulge K Giants 19

Chapter 3: Abundances and Kinematics of K Giants in the Galactic Nuclear Bulge 124

Appendix 1: Photometry of K Giants in the Nuclear Bulge of the Galaxy 179

Appendix 2: New Results on the Galactic Bulge Population: Relevence to the Population II Variables 187

Introduction

If you look straight overhead at midnight in June, and you are at Las Campanas Observatory, you will see the brightest portion of the Milky Way – the galactic bulge. It requires only a little imagination to pretend you are outside the Galaxy, looking towards the center. It is a sight we do not really see from the northern hemisphere, where the Sagittarius star clouds lay close to the horizon. The region containing Baade's Window is visually the brightest portion of the Milky Way.

The subject of this research is use of the K giant population in Baade's Window, at $l = 1°, b = -4°$ to understand the history of formation of the galactic bulge. The abundances and kinematics of the K giants, due to the long relaxation time, preserve information from the time when they were formed.

The galactic bulge is the ultimate star cluster. It is, most likely, both the first and final stages of the Galaxy's collapse. We study the galactic bulge because we hope to compare its population with other old, metal rich galaxy populations such as are seen in other spiral and elliptical galaxies. The galactic bulge has a special role in this because it is by far the nearest resolved population of this type – 100 times as close as M31, the next nearest example. When Baade first surveyed the bulge, he was interested only in proving that it was in fact a galactic bulge, and in finding the distance to the center from the RR Lyrae stars. (Baade, 1951,1963). Baade used the 18-inch Schmidt at Palomar mountain to discover windows of low obscuration toward the galactic center. One window in particular was interesting,

for it had a familiar object – a globular cluster, NGC 6522, well placed in the center. This cluster could be used to obtain a precise reddening value. This window is the most famous of several which Baade identified, and is known as Baade's Window. While its name gives the impression that it is the only window through which one may see the bulge, this is actually incorrect. At latitudes below $-4°$, the bulge is nearly entirely accessible, although the reddening is variable.

The discovery of numerous RR Lyrae stars in this field was accomplished using 137 plates taken from 1945 to 1949 at the 100 inch Hooker reflector at Mt. Wilson. The landmark analysis of these data (Baade, 1951) arrived at a distance to the center $R_o = 8.16$ kpc, very close to the best accepted values of today of 7.95 ± 0.69 or 6.94 ± 0.58 kpc, depending on assumptions about the intrinsic luminosity of RR Lyrae variables (Blanco and Blanco, 1985). Proof that there was in fact a nuclear bulge came from the narrow width of the peak in the distribution of the RR Lyrae stars (FWHM of 0.7 mag) and the completeness of the survey to two magnitudes past the peak.

Because of the large numbers of RR Lyrae stars, or cluster variables, a comparison was made between the galactic bulge and metal poor globular clusters. This was somewhat unfortunate, because it should have been apparent that there was in fact a wide abundance range in the bulge. Among the many clues were the large numbers of late M giants found by Nassau and Blanco (1958) in the direction of Baade's Window. Later, Blanco, McCarthy, and Blanco (1984) repeated Baade's experiment for the M giants, finding a similarly narrow peak, and surveying well

past it, again demonstrating conclusively the existence of a nuclear bulge. Globular clusters do not have late giants and RR Lyrae stars together.

Photometry of over 1000 stars in Baade's Window was accomplished by Arp (1965). The first color-magnitude diagram to clearly show a giant branch was that of Whitford and Blanco (1979), done in R and I. The late M giants have TiO bands which blanket the B, V bandpasses, preventing $(B-V)$ from getting redder for cooler stars. This caused confusion in the interpretation of Arp's first color magnitude diagram, in B and V.

The Whitford and Blanco color-magnitude diagram allowed selection of a sample of K giants for spectroscopy in Baade's Window. The goal was to obtain the distribution function of stellar abundances, and to discover if the metal rich and metal poor stars have different kinemtics. This initial survey could not really be a complete, carefully selected sample. Care had to be taken to select stars with measurable abundances, which were clearly not foreground stars. While the sample is unbiased, a complete sample must await completion of CCD surveys currently in progress.

The initial study of 21 bulge giants, with the a new method for measuring stellar abundances in the heavily reddened field, is described in Chapter 1. Here, the first indications of the extremely high abundances of the Baade's Window K giants come to light.

Expansion of the survey to a total of 88 bulge K giants is described in Chapter 2. This chapter also contains a great deal of information about local K giants,

for the Baade's Window stars are compared with 45 stars with well determined abundances, which are either members of globular clusters or are local K giants.

A study of the velocity dispersion of the Baade's Window K giants, and an interpretation of the abundance distribution function in terms of chemical evolution of the Galaxy is discussed in Chapter 3. In this chapter, it is proposed that the metal rich stars may belong to a special central bulge component of the Galaxy (Oort, 1977), which is required from both infrared data and the rotation curve. The abundance distribution, which ranges from -1 to $+1$ dex, is explained to arise as a result of the simple one-zone model of chemical evolution.

This chapter also contains a look towards the future – the possibility of obtaining high dispersion spectra to confirm or refute the high abundances assigned to bulge stars, surveys of other kinematic probes in the bulge, and a narrow band CCD survey designed to obtain the abundance distribution function at different galactic latitudes.

In appendix 1, photometry is presented which supports the abundance determinations in chapters 1 and 2, as well as illustrates the peculiar nature of the Baade's Window K giants.

In appendix 2, evidence for a possible age range in the bulge is considered. Photometry in two bulge windows is presented, with the result that very young (1 Gyr old) stars probably are not present in the bulge, but 5-10 Gyr old stars cannot be ruled out based on deep photometry. There may be an age range, but it is confused by the spatial depth of the bulge.

The finding that the K giants have a wide abundance range implies that extragalactic metal rich populations also have wide abundance ranges, a factor that should be taken into account when they are modeled. The apparent contradiction of a population which contains both RR Lyraes and late M giants is resolved by the wide abundance range. The metal rich stars have a smaller velocity dispersion, as expected if they were formed in the final phase of a dissipative collapse of the Galaxy.

References

Arp, H. 1965, *Ap. J.*, **141**, 45.

Baade W. 1951, *Pub.Obs.Univ.Mich.*, **10**, 7.

Baade, W. 1963, in *Evolution of Stars and Galaxies*, ed. C. P. Gaposchkin (Cambridge: Harvard University Press), p. 287.

Blanco, V. and Blanco, B. 1985, *Mem.S.A.It.*, **56**, 15.

Blanco, V. M., M. F. McCarthy, S. J., and Blanco, B. M. 1984, *A. J.*, **89**, 636.

Nassau J. J., and Blanco, V. M. 1958, *Ap. J.*, **128**, 46.

Oort, J. 1977, *Ann. Rev. Astr. Ap.*, **15**, 295.

Whitford, A. E., and Blanco, B. M. 1979, *Bull. AAS*, **11**, 675.

Introductory Note

The chapters comprising this thesis have been written essentially as individual papers to be submitted to refereed journals. Chapter 1 is reprinted from *The Astrophysical Journal.* Chapter 2 will be submitted to *The Astrophysical Journal Supplement* and Chapter 3 to the *Astrophysical Journal.*

A. E. Whitford contributed significantly to Chapter 1. He also participated in much of the observing for Chapter 2, and will be a coauthor on the paper to ultimately result from that work. Jay Frogel actually wrote nearly all of Appendix 1, which is included mainly because it forms the basis for supporting observations for Chapters 1 and 2.

CHAPTER 1

METAL CONTENT OF K GIANTS IN THE NUCLEAR BULGE OF THE GALAXY

A. E. Whitford and R. M. Rich

Reprinted from the *Astrophysical Journal* (1983, **274** 723–732).

THE ASTROPHYSICAL JOURNAL, 274:723–732, 1983 November 15

METAL CONTENT OF K GIANTS IN THE NUCLEAR BULGE OF THE GALAXY[1,2]

A. E. WHITFORD
Lick Observatory, Board of Studies in Astronomy and Astrophysics, University of California, Santa Cruz, California
AND
R. M. RICH
California Institute of Technology
Received 1983 March 21; accepted 1983 April 13

ABSTRACT

The metallicity of 21 K giants in Baade's window has been determined by comparison of the strengths of strong iron lines and the Mg *b* feature with those in 22 calibration stars having high-resolution abundance analyses. $(J-K)$ colors were used to separate the effects of temperature and metallicity on line strengths. The majority of the stars are super–metal-rich with a mean $\langle[Fe/H]\rangle = 0.29$ or 0.44 and an upper extreme $[Fe/H] = 0.7$ or 1.0, depending on the method of extrapolation for stars more metal-rich than any solar neighborhood calibration stars. These values for individual stars support the super–metal-rich explanation of very strong lines in the spectra of unresolved external galaxies. The minority fraction of metal-poor stars, for which $\langle[Fe/H]\rangle \approx -1.0$, includes the progenitors of Baade's RR Lyrae variables. The small-number statistics of the present sample leave the relative proportion of the metal-poor stars and their possible status as a separate group uncertain.

Subject headings: galaxies: Milky Way — galaxies: stellar content — stars: abundances — stars: late-type

I. INTRODUCTION

The stars in the nuclear bulge of the Galaxy seen relatively unobscured in Baade's window (BW) around NGC 6522 (Baade 1963) are members of the nearest, best resolved example of the type of old galaxy population that is characteristic of ellipticals and the bulges of spirals. Stars down to the base of the giant branch, the source of most of the light, can be subjected to individual analysis. The stellar content can therefore be investigated in much greater detail than is possible by methods that seek to match the spectrum of the integrated light of unresolved systems by a population synthesis. The close similarity of the spectral characteristics of the integrated light from patches of BW to those of the nuclear regions of other galaxies (Whitford 1978) gives reason to believe that a sample of giants in BW should be representative of old galaxy populations in general, and that a star-by-star determination of their properties could yield information on the evolutionary history of such systems.

In this paper we report the first results from a study of metallicity of bulge giants in BW. A super–metal-rich (SMR)[3] composition for the stellar population in the nuclear region of unresolved galaxies was first proposed by McClure (1969) and by Spinrad and Taylor (1971) in order to account for spectral features stronger than those observed in typical solar neighborhood giants. A more general study of the spectral characteristics of spheroidal systems by Faber (1972, 1973) established the close dependence of feature strength on the luminosity of a galaxy; the metallicity of the more luminous galaxies was found to be about twice solar. Certain galaxy population models have used the strong-lined group of local giants as prototypes in a synthesis fitted to the spectrum of the integrated light (e.g., O'Connell 1976; Gunn, Stryker, and Tinsley 1981, hereafter GST). In adapting Tinsley's evolutionary models for old populations (Tinsley 1972, 1978; Tinsley and Gunn 1976) to incorporate the most recent observational data, GST used theoretical isochrones for a metal content up to $Z = 0.04$.

The objectives of the observations reported here were (1) to ascertain whether the BW giants are in fact sufficiently SMR to explain the strong-line characteristics of the spectrum of unresolved galaxies, and (2) to

[1] Lick Observatory Bulletin No. B964.
[2] This research is based on observations at the Las Campanas Observatory of the Carnegie Institution of Washington.

[3] In this paper SMR signifies a metal content such that [Fe/H] > 0.

find the range of metallicities present and their distribution function. Line strengths in the spectrum of the integrated light can of course do no more than show the average metallicity; finding the spread of values contained in such an average requires individual observations of a sufficient number of stars, as was undertaken in the present work.

The K giants were a natural choice for the observed sample of bulge stars. Several strong features in their spectra have previously been used to compare the metallicity of galaxies and to trace internal abundance gradients (e.g., Spinrad and Taylor 1971; Faber 1972, 1977). These features are readily measurable on the relatively low-dispersion spectra that must be used to obtain an adequate sample of 16th mag stars. A sample limited to K giants avoids the heavy molecular blanketing of certain metallicity-sensitive features by the TiO bands seen in the M giants. Furthermore, such a sample is unbiased, since every star evolving past the turnoff in an old population becomes a K giant, no matter whether it goes on to become an M giant or suffers termination of its giant evolution through mass loss (Renzini 1977).

The metallicity of the bulge stars was determined by comparing their line strengths with those of standard stars having high-resolution abundance analyses. Line strengths for both groups were measured on spectra at the same dispersion, observed in identical fashion on the same telescope.

The observations are described in § II. The measurement of the line strengths and the analysis leading to the determination of the metallicities of the bulge stars are set forth in § III. The conclusions and their implications are discussed in § IV.

II. OBSERVATIONS

All the spectra for the evaluation of line strengths were obtained with the intensified Reticon detector

TABLE 1

LINE STRENGTHS FOR STANDARD STARS

No. (1)	Name/ Messier (2)	V_0 (3)	K_0 (4)	$(J-K)_0$ (5)	W_λ (Å) Fe 43 (6)	Fe 52 (7)	Fe 53 (8)	Mg b (9)	Na D (10)	log ΣW_λ (11)	[Fe/H] (12)	Sources (13)
489.....	ν Psc	4.44	1.24	0.83	8.78	4.72	2.73	11.60	2.25	1.44	−0.32	a
1953.....	γ Men	5.18	2.65	0.64	9.73	5.18	2.43	12.97	2.40	1.48	0.30	1,2;a
3905.....	μ Leo	3.88	1.22	0.66	10.41	5.44	3.47	11.77	3.35	1.49	0.48	b
4608.....	o Vir	4.12	1.89	0.52	6.03	3.01	2.13	5.13	0.47	1.21	−0.50	3;a
4695.....	16 Vir	4.96	2.19	0.68	7.64	4.07	2.04	9.59	0.58	1.37	−0.11	a
4932.....	ϵ Vir	2.84	0.80	0.52	6.27	3.89	2.47	5.18	0.77	1.25	0.00	a
5340.....	α Boo	−0.05	−3.00	0.76	6.83	4.48	2.73	10.01	0.81	1.38	−0.50	a
5370.....	20 Boo	4.86	2.14	0.66	8.72	5.41	2.96	11.57	2.31	1.46	0.30	4;c
5777.....	37 Lib	4.62	2.25	0.58	6.63	4.20	2.33	9.15	1.22	1.35	−0.14	a
5854.....	α Ser	2.64	0.06	0.65	8.04	5.18	3.03	10.25	2.57	1.42	0.23	a
6299.....	κ Oph	3.20	0.64	0.66	9.49	4.96	2.98	10.01	1.79	1.44	0.00	a
165195.....	...	6.50:	4.00	0.65	0.00	1.77	0.75	3.17	0.38	0.76	−1.90	5;d
7429.....	μ Aql	4.45	1.76	0.69	10.54	4.47	2.58	12.12	1.93	1.47	0.30	a
7869.....	α Ind	3.10	0.86	0.54	7.46	3.64	2.56	6.38	1.00	1.30	0.25	1,4;a
2426.....	47 Tuc	11.98	8.48	0.90	6.30	3.61	2.08	11.75	1.86	1.38	−1.09	6;e
4415.....	47 Tuc	12.22	9.85	0.59	7.22	3.27	1.40	7.63	1.23	1.29	−0.33	6;f
I68.....	M5	12.33	9.07	0.85	4.96	2.86	1.45	7.05	0.52	1.21	−1.13	7;e
IV28.....	M5	14.41	11.86	0.64	3.96	2.14	1.38	3.71	0.63	1.05	−1.13	7;e
IV47.....	M5	12.33	9.00	0.88	2.94	2.94	2.00	6.10	1.11	1.15	−1.13	7;e
IV81.....	M5	12.11	8.62	0.89	5.32	3.74	2.51	8.49	0.49	1.30	−1.13	7;e
II2.....	M15	12.41	9.40	0.73	3.81	1.02	0.92	2.14	0.97	0.90	−1.76	7;e
II64.....	M15	13.15	10.55	0.64	2.57	1.05	1.25	2.10	1.17	0.84	−1.76	7;e

NOTES.—Col. (1) HR/HD/star number in cluster. Col. (2) Star name, or cluster in which star is located. Cols. (3)–(4) V, K mag from Johnson 1966, unless other source is noted in col. (13); zero reddening assumed. Col. (5) Unless other source is noted in col. (13), $(J-K)_0$ is from Johnson 1966, transformed to the Caltech system by the relation $(J-K)=0.94(J_J-K)-0.01$, derived from data given by Frogel *et al.* 1978. Cols. (6)–(10) Measured line strengths (see § III*a*). Col. (11) Logarithm of the sum of the line strengths, Na D omitted. Col. (12) Adopted metallicity; sources in col. (13). Col. (13) Sources for magnitudes, colors: 1. V from Yale Bright Stars. 2. K, $(J-K)$ from J. A. Frogel, private communication. 3. K, $(J-K)$ from Frogel *et al.* 1978. 4. K, $(J-K)$ from Las Campanas observations, Whitford and Rich, unpublished. 5. V_0, K_0, $(J-K)_0$ derived from observed K mag and reddening data given by Pilachowski 1978. 6. Star designation, V_0, K_0, $(J-K)_0$ from Frogel, Persson, and Cohen 1981. 7. Star designation, V_0, K_0, $(J-K)_0$ from Frogel, Persson, and Cohen 1983. Sources for [Fe/H]: (a) Cayrel de Strobel *et al.* 1980; see text. (b) Branch, Bonnell, and Tomkin 1978. (c) Gustafsson, Kjaergaard, and Andersen 1974. (d) Leep and Wallerstein 1981. (e) Pilachowski, Sneden, and Wallerstein 1983. (f) R. Gratton, private communication (not a cluster member).

(Shectman 1978) on the Cassegrain spectrograph of the 2.5 m du Pont telescope of the Las Campanas Observatory. The observations were made in 1980 June–July. The dispersion at the first cathode was 114 Å mm^{-1}. For the bulge giants the exposures were typically 30–40 minutes. The second of the two entrance apertures (each $2'' \times 4''$) was positioned with some care to give a sky subtraction count rate representative of the background of unresolved bulge stars. Typical background rates were 30% of the net star rate, consistent with the bright background ($V = 20.0$ arcsec^{-2}; Arp 1965; Whitford 1978), due mainly to turnoff stars. Janes's (1977) image-tube spectra of three BW giants may have suffered some blending with background light because of the lack of a sky correction.

The observed bulge stars were selected to represent a reasonably even sampling along the giant sequence on the $(R - I)$, I color-magnitude diagram (Whitford and Blanco 1979); the very red late M giants were excluded. The stars on this diagram are all within the annulus covered by the Arp (1965) B,V photometry but are limited to those in the outer half between 2.5 and 4.0 from the center of NGC 6522. Most of the standard stars were taken from the Cayrel catalog of [Fe/H] determinations (Cayrel de Strobel *et al.* 1980). Among the bright K giants known to be appreciably more metal-rich than the Sun, nearly all those accessible from the site were observed. A number of metal-poor stars were selected from globular clusters having abundance analyses of individual stars.

Table 1 lists the standards and Table 2 the bulge giants. Column entries are explained in notes to these tables and in later paragraphs. Figure 1 shows the spectra of four standards and four bulge stars that cover the full range from very metal-rich to quite metal-poor. The spectra have been subjected to flat field division, and Gaussian smoothing over 3 pixels has reduced the original resolution from 4 Å to about 7 Å. Relative continuum intensities are distorted for bright standards because the heavy absorbers introduced to avoid exceeding a safe count rate were not completely neutral; the violet part has been depressed.

Table 1 also shows the $(J - K)$ color index used in the calibration (§ III*b*) to separate the effects of metallicity and temperature on line strength. This index was chosen as one not subject to appreciable blanketing in K giants; differential photoelectric observations with carefully chosen sky comparison areas have an ad-

TABLE 2

LINE STRENGTHS AND DERIVED METALLICITIES FOR BULGE GIANTS

				W_λ (Å)							
No. (1)	V (2)	K (3)	$(J-K)_0$ (4)	Fe 43 (5)	Fe 52 (6)	Fe 53 (7)	Mg *b* (8)	Na D (9)	Log ΣW_λ (10)	$[Fe/H]_1$ (11)	$[Fe/H]_2$ (12)
1025	16.46	12.67	0.67	11.54	6.93	4.05	16.01	5.46	1.59	0.54	0.79
1039	16.47	12.81	0.66	14.21	6.94	3.99	16.98	5.33	1.62	0.69	1.00
1053	16.49	13.57	0.45	4.39	2.39	1.47	4.91	2.50	1.12	−0.29	−0.50
1064	16.16	11.51	0.82	14.25	6.91	4.19	16.68	4.41	1.62	0.23	0.44
1076	15.53	11.08	0.77	11.92	6.71	4.15	16.89	4.53	1.60	0.30	0.50
1145	15.28	11.69	0.50	4.27	1.59	0.45	3.12	2.56	0.97	−0.89	−1.25*
1202	15.82	11.63	0.67	7.92	6.07	3.49	15.20	5.48	1.51	0.32	0.48
1322	14.21	10.08	0.72	11.36	4.80	2.61	12.87	2.39	1.50	0.13	0.24
2116	16.67	12.90	0.73	13.54	7.80	3.21	17.22	3.74	1.62	0.48	0.74
2122	14.27	9.48	0.90	6.70	4.84	2.39	13.50	2.72	1.44	−0.58	−0.72**
2146	15.65	11.64	0.59	7.45	4.13	1.57	8.36	4.10	1.33	−0.22	−0.05
2240	15.56	12.27	0.53	7.30	4.03	2.19	10.41	2.10	1.38	0.30	0.36
2244	16.14	11.56	0.78	11.79	4.25	2.76	11.29	2.87	1.48	−0.11	−0.06
3106	16.53	12.86	0.55	3.05	1.24	0.07	4.79	1.89	0.96	−1.07	−1.34*
3164	15.11	10.72	0.74	8.10	5.44	3.11	13.74	2.39	1.48	0.02	0.10
3209	16.33	11.98	0.73	13.20	6.84	4.24	15.56	5.91	1.60	0.42	0.65
4003	15.06	11.20	0.61	3.30	2.77	0.79	3.67	2.62	1.02	−1.05	−1.29*
4025	16.01	12.50	0.55	6.76	4.78	2.18	13.00	3.64	1.43	0.39	0.51
4203	13.81	8.93	0.92	5.71	4.03	2.21	9.65	2.01	1.33	−0.97	−1.03*
4325	16.42	12.76	0.64	8.52	6.27	3.71	13.07	4.76	1.50	0.36	0.51
4329	15.11	10.92	0.77	7.18	3.78	1.94	8.63	2.10	1.33	−0.54	−0.76**

NOTES.—Col. (1) Star number from Arp 1965; first digit denotes quadrant. Col. (2) Observed V mag from Arp. Cols. (3)–(4) Observed K mag and $(J - K)_0$ color from Frogel, Whitford, and Rich 1983. Reddening correction $E(J - K) = 0.23$, $A_V = 1.54$, $A_K = 0.14$ (see § III*c*). Cols. (5)–(9) Measured line strengths (see § III*a*). Col. (10) Logarithm of the sum of the line strengths, Na D omitted. Col. (11) Metallicity derived from solution 1, Table 4. Col. (12) Metallicity derived from solution 2a or 2b (*asterisk*), or for stars in the transition range, the mean of solutions 2a and 2b (*double asterisk*).

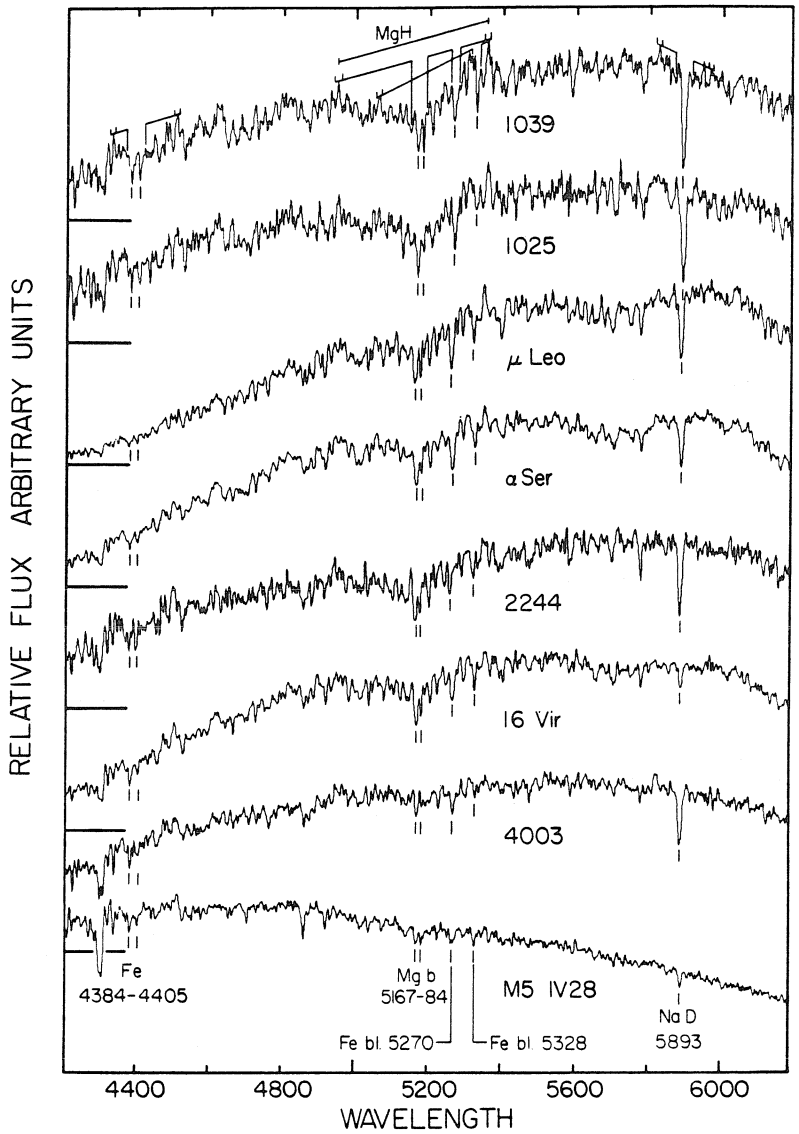

FIG. 1.—Spectra of four Baade's window K giants (four-digit numbers) and four standard stars. The vertical ticks mark the five features whose strength was measured; continuum placement and integration limits for these features are shown for the uppermost spectrum. The two bulge giants with the highest metallicity are at the top.

vantage in the crowded bulge field over other color indices dependent on iris photometry of photographic images.

The $(J - K)$ colors of bulge stars in Table 3 are from observations by Frogel, Whitford, and Rich (1983) with the CTIO InSb photometer on the 1.5 m and 4 m telescopes. Colors of standards are mostly from the literature; sources are given in notes to Table 1. All of these colors are on the Caltech system (Frogel *et al.* 1978).

III. DATA ANALYSIS

a) Measurement of Line Strengths

For the line strength analysis the five metallicity-sensitive features indicated in Figure 1 were selected as

TABLE 3

WAVELENGTHS USED IN LINE-STRENGTH MEASUREMENTS

Spectral Feature	Lower Sideband (Å)	Integration Limits F_1, F_2 (Å)	Upper Sideband (Å)
Fe 4384, 4405 ...	4325–4335	4365–4415	4503–4510
Mg *b*	4940–4955	5150–5190	5355–5361
Fe 5270 blend...	4940–4955	5255–5280	5355–5361
Fe 5328 blend...	5055–5060	5315–5340	5355–5361
Na D	5820–5840	5870–5910	5960–5975

being strong enough for reasonably accurate measurement on the observed spectra:

Fe 43: Fe 4384, 4405;

Mg *b*: Mg 5167, 5173, 5184 + MgH;

Fe 52: Fe 5270 blend;

Fe 53: Fe 5328 blend;

and

Na D: Na 5890, 5896.

These features do not include lines or molecular bands involving elements whose initial abundance could be subject to alteration by CNO processing during a star's giant evolution.

Line strengths were measured by integration of the depressions of the observed spectral intensity $I(\lambda)$ below a continuum intensity $I_c(\lambda)$ specified by a straight-line interpolation between the average intensity within selected sideband intervals:

$$W_\lambda(\text{Å}) = \int_{F_1}^{F_2} [1 - I(\lambda)/I_c(\lambda)]\, d\lambda. \qquad (1)$$

Table 3 gives the wavelengths of the upper and lower sideband intervals, and the limits F_1 and F_2 of the feature integration. Inspection of the *Arcturus Atlas* (Griffin 1968) guided the choice of relatively clean stretches of continuum for the sidebands. The sidebands and the integration limits for each of the five features are shown graphically in Figure 1. A computer program developed by Horace Smith and kindly made available by him was used to calculate the line strengths tabulated in columns (6)–(10) of Table 1 and columns (5)–(9) of Table 2.

Although the metallicity dependence shown by the relative strengths of the Na D feature in the spectra in Figure 1 is obvious, the interpretation is complicated by the contribution from interstellar Na, estimated to be of the order of 1.5 Å. Since this contamination could not be calibrated out via spectra of hot stars distributed over the field, Na D line strengths were not used in the later analysis. The sum of the line strengths of the other four features, called ΣW_λ, was adopted as the best overall index of metallicity; the logarithm is tabulated in column (11) of Table 1.

b) Calibration of Line Strengths against Metallicity

The [Fe/H] values adopted for the standards are given in column (12) of Table 1. The entries for the globular clusters are from the recent abundance determinations of Pilachowski, Sneden, and Wallerstein (1983), kindly made available in advance of publication. Those taken from the Cayrel catalog (Cayrel de Strobel *et al.* 1980) give preference when possible to determinations since 1970.

The value [Fe/H] = 0.48 for the prototype SMR star μ Leo is taken from Branch, Bonnell, and Tomkin (1978), who based their determination on the strength of weak iron lines in uncrowded parts of the spectrum near 7800 Å and 8700 Å, where the continuum level was not in doubt. Deming (1980) concluded that high weight must be given to this determination because the weak lines of excitation potential over 4 eV are formed deep in the atmosphere at a level insensitive to boundary cooling. Peterson (1976) had argued that boundary cooling would enhance the classic SMR features seen at low resolution (Spinrad and Taylor 1969), leading to an overestimate of metallicity. Two other determinations based on photometry of a group of weak lines in a narrow scanner band gave a result for μ Leo in close accord with that of Branch *et al.*: Gustafsson, Kjaergaard, and Andersen (1974) and Williams (1971) found [Fe/H] = 0.45 and 0.46, respectively. Pritchet and Campbell (1980) arrived at a different result for μ Leo from a photometric comparison of selected narrow bands in the deep red. These bands, however, gave less emphasis to weak lines than was the case in the other photometric determinations.

Bonnell and Branch (1979) showed that the near-solar abundance found in certain traditional curve-of-growth analyses of μ Leo (including Peterson 1976) could have resulted from an error in continuum placement and the consequent systematic underestimate of equivalent widths. Deming and Butler (1979) concluded that genuine supermetallicity is the only acceptable explanation for binaries where both the giant primary and the main-sequence secondary show strong-line characteristics; the temperature of the secondaries is too high for the formation of the molecules that are a necessary condition for boundary cooling.

We interpret the foregoing arguments as support for our adoption of a value for the metallicity of μ Leo which makes it truly SMR. The other five SMR stars in

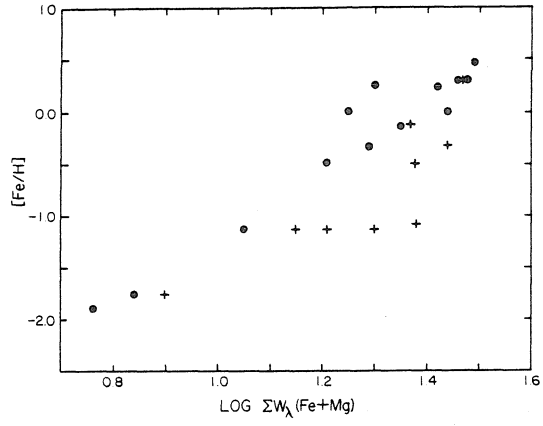

FIG. 2.—The relation between the summed line strengths of the standard stars and their adopted metallicity [Fe/H]. The + symbols denote stars for which the color $(J-K)_0 > 0.66$; the solid circles, all others.

Table 1, for which $0.23 \leq [Fe/H] \leq 0.30$, have not been the subject of comparable doubt and reexamination; hence the adopted values in column (12) do not involve selective judgment. Gustafsson *et al.* found [Fe/H] = 0.18 for α Ser by their narrow-band photometric method in fairly close agreement with the curve-of-growth result adopted here; their determination for 20 Boo is the only one available.

Figure 2 shows a plot of [Fe/H] versus $\log \Sigma W_\lambda$ for the 22 calibration stars. The scatter about the expected general trend is primarily the result of the dependence of line strength on temperature, as is shown by the separation of stars with $(J-K)_0 > 0.66$ from those with $(J-K)_0 \leq 0.66$. To take account of this effect a color term was included in the calibration equation:

$$[Fe/H] = A_0 + A_1(J-K)_0 + A_2 \log \Sigma W_\lambda. \quad (2)$$

A bivariate regression (Bevington 1969) using data from all 22 stars gave the coefficients listed under solution 1 in Table 4. To show the resultant fit on a simple linear plot, the two observed quantities are combined into a reduced width W_r:

$$\log W_r = \log \Sigma W_\lambda + A_1/A_2[(J-K)_0 - 0.66]. \quad (3)$$

In effect this procedure corrects the value of ΣW_λ for each star to one that would be observed for the same metallicity if the color were $(J-K)_0 = 0.66$.

Figure 3*a* shows the least squares regression line on a reduced-width plot of the data points. On such a plot the intercept is $A_0' = A_0 + 0.66A_1$. Inspection of the trend among the more metal-rich stars ([Fe/H] > −0.50) suggests a steeper slope than that given by solution 1. Solutions 2*a* and 2*b* were carried out separately for the metal-rich and metal-poor stars, and gave the somewhat better fit shown by the two regression lines of Figure 3*b*; the rms deviations in Table 4 are smaller than for solution 1.

For our atomic lines of Fe and Mg, Deutsch's (1966) simplified theory shows that at constant temperature the equivalent width $\log W \propto 0.5$ [Fe/H], with zero gravity dependence. On our low-resolution spectra of metal-poor stars, where the lines in question stand out from a continuum little disturbed by weak atomic and molecular lines, the line strength defined by equation (1) can be a close approximation to true equivalent width. Solution 2b, though determined from relatively few stars, does in fact give a slope $1/A_2 = 0.50 \pm 0.14$. With increasing metallicity, low-resolution measures become degraded as the clean stretches of the continuum are contaminated by many weak lines, and the wings of strong features blend into a depressed pseudocontinuum. The measured line strength then grows more slowly than the Deutsch prediction for true equivalent widths. The slopes from Table 4 are in the range $0.33 > 1/A_2 > 0.23$. Cohen (1982) found comparable dependency factors from spectra of similar resolution. It would appear that for metal-rich stars *any* practical definition of line strength will give an unavoidably diluted measure of a strong abundance-sensitive feature. To test whether the end result is dependent on the particular definitions adopted here, an alternate set of line strengths was measured against a lower pseudocontinuum defined by wave-

TABLE 4

COEFFICIENTS FROM BIVARIATE REGRESSIONS

Solution	A_0	A_1	A_2	σ_{rms}	R_{mult}[a]	Notes
1.....	−2.51	−2.89	3.14	0.16	0.975	All standards
	±0.32	±0.33	±0.18			
2a.....	−3.89	−3.46	4.41	0.14	0.900	[Fe/H] ≥ −0.50
	±0.68	±0.67	±0.65			
2b.....	−2.61	−1.17	1.99	0.12	0.929	[Fe/H] < −0.50
	±0.40	±1.02	±0.54			

[a] Multiple-correlation coefficient; Bevington 1969, p. 131.

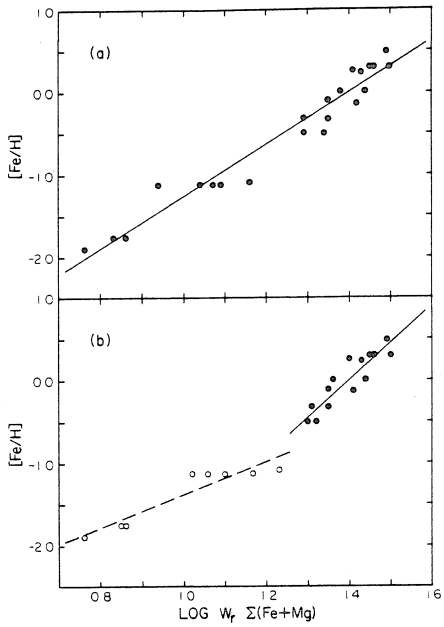

FIG. 3.—(*a*) [Fe/H] for standard stars as a function of the reduced line strength, i.e., the measured strength corrected for the temperature effect. The solid line is from solution 1, Table 4. (*b*) The same, with separate solutions 2a and 2b for metal-rich stars (*solid circles*) and metal-poor stars (*open circles*).

lengths closer to the line centers. The metallicity of the bulge giants read from the resulting calibration plot was not significantly changed.

c) *Metallicity of the Bulge Giants*

The intrinsic colors of the bulge giants needed to derive the metallicity of these stars from the calibration relations were obtained by applying a reddening correction $E(J-K)=0.23$ to the observed colors; the resulting values for $(J-K)_0$ are listed in column (4) of Table 2. Reddening determinations by Arp (1965) and Zinn (1980) give a mean $E(B-V)(A0)=0.48$. According to the reddening curve of Cohen *et al.* (1981), this corresponds to $A_V=1.54$, $E(V-K)=1.40$, and $E(J-K)=0.28$. The resulting dereddening vector with a slope $E(V-K)/E(J-K)=5.00$ transforms the observed colors of a larger sample of bulge giants (Frogel, Whitford, and Rich 1983) to a locus on the intrinsic $(V-K)$, $(J-K)$ plane that does not match the mean relation for local giants. A reexamination based on Lee's (1970) Johnson-system colors of 17 variously reddened M3–M4 supergiants yields $E(V-K)/E(J_J-K)=5.73\pm0.46$, close to the value 5.77 adopted by Glass and Feast (1982). On the Caltech system (see notes to Table 1) this becomes $E(V-K)/E(J-K)=6.15$ and $E(J-K)=0.23$, as adopted here; this value gives a satisfactory match to local giants on the $(V-K)$, $(J-K)$ plane.

Figure 4 shows the observed line strength ΣW_λ(Fe+Mg) versus the color $(J-K)_0$ for both bulge and calibration stars. It is immediately apparent that stars of the same color show a wide range of line strengths and hence metallicity. Half of the bulge stars are at or above the line strengths found in the calibration stars and for six of these the difference is conspicuous. Lines of constant metallicity from solution 2a for metal-rich stars show the influence of color on the metallicity inferred from a given line strength. The most metal-rich bulge stars are outside the range covered by the calibration and the derived metallicity must involve extrapolation. The two-segment solution 2a–2b (Table 4; Fig. 3*b*) is adopted as the best representation because of the smaller residuals for the SMR stars in the calibration group. The values of [Fe/H] so derived are tabulated in column (12) of Table 2. Those given by solution 1 are shown in column (11) for comparison.

To test whether the lumping of all the measured line strengths into a single parameter ΣW_λ has smoothed over a distinction between different elements, the strength of the Mg *b* feature is plotted against that of the summed Fe lines in Figure 5. The six most metal-rich bulge stars again stand apart. There is no significant separation of bulge and calibration stars. Since the MgH contribution to the total strength of the Mg *b* feature is gravity-sensitive, however, the possible bias introduced by comparing bulge stars with younger, more massive calibration stars needs to be considered: analysis shows the expected effect is actually rather small. In the conventional logarithmic notation used by Deutsch (1966), the strength of the molecular contribution should show a dependence $[W]=\frac{1}{2}[Z]+\frac{1}{2}[g]$ (Böhm-Vitense 1975). The dependence on the metallicity Z is already taken

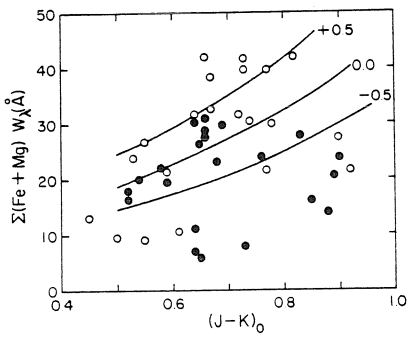

FIG. 4.—Observed summed line strengths of standards (*solid circles*) and bulge giants (*open circles*) as a function of color $(J-K)_0$. The lines of constant [Fe/H] are from solution 2a, Table 4, and apply only to metal-rich stars.

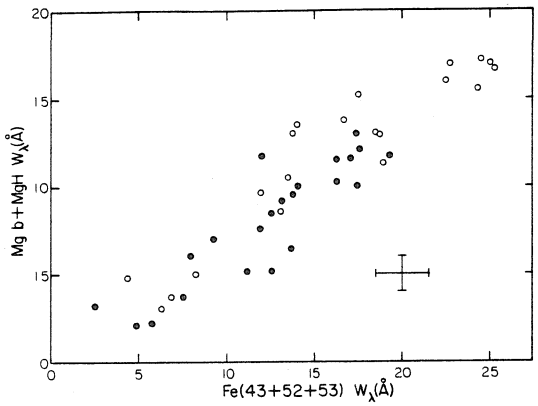

FIG. 5.—Observed strength of the Mg feature plotted against the summed strength of the three Fe features. Open circles denote bulge giants; closed circles, the standards.

care of in the range of calibration stars. For the constant T_e adopted in our reduced-width calibration, the gravity dependence derived from the basic (M, L, R, T_e) relations reduces to $[g] = [M] - [L]$. Interpolation on the Sweigart-Gross (1978) grid of evolution tracks yields $[L] \approx 1.6[M]$ at constant T_e, in close agreement with Renzini's (1977) parameterization (eq. [2.10]) of tracks for [Fe/H] < 0. Hence $[g] = -0.6[M]$ for the molecular contribution. The contribution of the gravity-independent atomic lines to the total feature strength dilutes the effect by at least a factor of 2. Mould's (1978) detailed modeling covered examples for [Fe/H] $\lesssim 0$, with the result $[W] \lesssim 0.2[g]$. If this applies over the whole range of metallicity encountered in the bulge, then for an average mass ratio (calibration stars/bulge stars) = 1.5 the change in feature strength $\Delta \log W \approx -0.02$ (calibration stars weaker). The difference is small enough to be lost in the scatter. The metallicity dependence of both the molecular and atomic contributions to the Mg feature is clearly the dominant effect.

The metallicity determinations for the bulge stars could rest entirely on the strength of the Fe lines, which have zero gravity dependence. The tight correlation shown in Figure 5, however, supports the widespread use of the Mg feature as a metallicity indicator.

d) *Metallicity Distribution Function*

Figure 6 shows the metallicity distribution function for the bulge giants plotted from the data in columns (11) and (12) of Table 2. Though the sample is not a large one, the results suggest a bimodal distribution with either choice of the calibration relation. The mean for the metal-rich majority group is $\langle$[Fe/H]$\rangle = 0.44$ for the preferred solution 2a, and $\langle$[Fe/H]$\rangle = 0.29$ for solution 1. The upper extremes are 1.0 and 0.7, respectively; this difference is a measure of the uncertainty resulting from the need to extrapolate. Within the range covered by the calibration, where line strengths can be treated as an empirical interpolation parameter, the uncertainty in the metallicity of a bulge star in the metal-rich group should be of the same order as the rms deviation of an average calibration star from the adopted relation: ~ 0.15 dex. The poorer signal-to-noise ratio for stars with [Fe/H] < −0.50 would result in a larger expected error. The measurement error in the line strengths for standards observed more than once was $\sigma(\log \Sigma W_\lambda) = 0.03$, corresponding to σ[Fe/H] = 0.10. This implies an uncertainty of similar magnitude in the values of [Fe/H] adopted for the standards. Bulge stars were observed only once.

It is apparent from equation (2) that the reddening correction for the bulge stars has a direct effect on the derived metallicities: Δ[Fe/H] $= -A_1 \Delta E(J-K)$. If the larger correction $E(J-K) = 0.28$ obtained from the reddening curve of Cohen *et al.* (1981) had been used instead of our adopted value $E(J-K) = 0.23$ (§ III*c*), then with the dependency factors in Table 4 the derived metallicity of metal-rich bulge giants would have been systematically increased by ~ 0.15 dex, and that of metal-poor giants via solution 2b by a lesser amount. The rather high values of [Fe/H] found for the most metal-rich bulge stars may thus be considered to be a conservative result.

IV. CONCLUSIONS AND DISCUSSION

1. Most of the K giants in the dominant metal-rich population in BW are found to be SMR. A significant fraction of them have metallicities in excess of that for

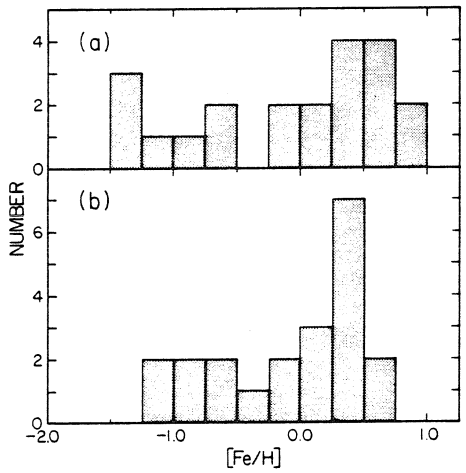

FIG. 6.—(*a*) Metallicity distribution of 21 bulge giants as determined from solutions 2a and 2b, Table 4 (Fig. 3*b*). (*b*) The same, but determined from solution 1, Table 4 (Fig. 3*a*).

any of the SMR prototypes in the solar neighborhood. This result for individual bulge stars gives strong qualitative support to the generally adopted SMR explanation of the line strengths in the integrated-light spectra of unresolved galaxies. The Mg *b* and Na D features follow the long-recognized enhancement of the corresponding features in galaxies. In order to make a similar comparison of the strength of Fe features, measures in galaxy spectra on the same system used in the present work are needed. Quantitative assessment of predicted and observed line strengths in galaxies will depend on a synthesis that takes into account the contributions of all components of the population (e.g., metal-poor giants, turnoff stars).

The line of sight through BW at $l = 1\overset{\circ}{.}0$, $b = -3\overset{\circ}{.}9$ passes 600 pc from the center of the Galaxy, far outside the active region close to the nucleus and in the surrounding parts of the galactic plane. At the distance of the Virgo Cluster, the corresponding off-nucleus angular distance would be about 10″. If the line-strength gradient reported by Faber (1977) for NGC 4472 and other galaxies is applicable along the minor axis of the nuclear bulge of the Galaxy, a halving of the distance to the nucleus would be expected to lead to an increase in average metallicity of the order of 0.1 dex. The actual inward gradient could be checked by a sampling of the metallicity distribution among giants in the Sgr I field at $b = -2\overset{\circ}{.}7$. (Baade 1963). Van den Bergh and Herbst (1974) noted a trend toward a less metal-rich population in going outward from BW to a field at $b = -8°$.

2. It would have been surprising if this first sample had not found some metal-poor giants to serve as progenitors of the RR Lyrae variables discovered by Baade (1963). The average metallicity of those observed is $\langle[Fe/H]\rangle \approx -1.0$, slightly lower than the average $\langle[Fe/H]\rangle = -0.65$ found for some of the BW RR Lyraes by Butler, Carbon, and Kraft (1976). The surprisingly large metal-poor fraction found in the present work (seven out of 21) is at least in part the result of biased sampling. An observational program that started with the brightest bulge giants selected in favor of stars on the thinly populated upper part of the evolution track near the red giant tip. Metal-poor stars like Nos. 2122 and 4203 in Table 2 are examples; they were automatically observed, but their metal-rich counterparts would be M giants and therefore excluded. When the comparison is made only for stars whose M_{bol} is at least 2 mag below the red giant tip, the metal-poor fraction ([Fe/H] < -0.25) shrinks to three out of 14, or about 20%, obviously a ratio of low statistical weight because of the small numbers.

The ratio of RR Lyraes to their K-giant progenitors in globular clusters is highly variable as a consequence of the second-parameter problem (e.g., Kraft 1980), but Butler, Carbon, and Kraft (1976) suggested 4% as a reasonable average; for M3 at the upper extreme the ratio is well over 10% (Sandage 1954). The surface density of RR Lyraes in Baade's (1963) zones I and II is $\rho_{RR} = 0.094$ arcmin^{-2}; with a 4% ratio the metal-poor K-giant density would be $\rho_{MPK} = 2.35$ arcmin^{-2}. The surface density of all K giants in BW, estimated to be 75% of the stars in Arp's (1965) photometry, is $\rho_K = 35$ arcmin^{-2}. The expected metal-poor fraction would then be about 7% of the total. No real disparity can be said to exist, however, because of the considerable uncertainty in both the expectation and the observed ratio. A quantitative discussion must await better statistics from a much larger sample of bulge K giants. Work in progress is directed to that end.

The presence of the RR Lyraes in the bulge shows that the population does indeed have a horizontal branch, a component not included in most galaxy population models. Such a component has been suggested by Wu *et al.* (1980) as a possible source of the strong ultraviolet radiation in the range 1500–2500 Å from the bulges of M31 and M81, but GST rejected such an explanation because the weak-lined K-giant progenitors would dilute the barely adequate strong-line spectral features predicted by their model. The number of bulge giants observed to have lines stronger than those in any of the local prototypes used in GST's model seems sufficient to balance out any such dilution, thus removing this objection to a horizontal branch component. Van den Bergh (1971) noted a few blue stars near $V = 17.0$ on his color-magnitude diagram as possible members of the horizontal branch. Deeper photometry by newer techniques that overcome the vulnerability of iris photometry to crowding and uneven background may show whether there are in fact enough very hot stars at the blue end of the horizontal branch in the bulge to explain the excess far ultraviolet radiation in external galaxies.

3. The considerable spread of metallicities observed among the bulge giants (~ 2 dex) can be understood in terms of Larson's (1974) dissipative collapse model for spheroidal systems. The metal-poor stars that formed at large radii early in the collapse may have retained the elongated elliptical orbits resulting from nearly radial infall. The high star formation rates associated with the high density near the end of the collapse were favorable to rapid enrichment, and the enrichment proceeded to a more advanced stage before exhaustion or expulsion of the gas than was the case in the delayed and much slower collapse of the disk (Larson 1976). Kinematic studies of the bulge stars may be able to show a difference in the motions of metal-poor and metal-rich components that has persisted since their formation in the early and late phases of the collapse.

The single average metallicity generally adopted in calculating models for old galaxy populations smooths over quite significant differences in the evolution paths followed by stars of high and low metallicity. The latter

will have a horizontal branch and no M giants. With increasing metallicity, tracks will have slightly redder turnoffs and cooler giant branches. As pointed out by Frogel and Whitford (1982) the higher mass at turnoff for old SMR stars can provide fuel that sustains M giants on their ascent of the upper asymptotic giant branch. The library of prototypes for a synthesis that takes into account these various paths will necessarily include examples from the SMR bulge giants.

4. Strongly SMR stars like those at the upper end of the BW metallicity distribution furnish a significant fraction of the light from elliptical galaxies and the bulges of spirals. Since there are no prototypes for these stars in the solar neighborhood, and since the derived metallicity rests thus far on extrapolation using line strengths in low-resolution spectra, a much more detailed study based on a high-resolution spectrum of a typical example in the BW population would be very desirable.

We are indebted to the Director of the Mount Wilson and Las Campanas Observatories for a generous assignment of telescope time. We acknowledge valuable conversations with David Burstein, Howard Bond, and Robert Kraft. We thank Sandra Faber for a careful reading of an earlier draft of this paper. This research was supported in part by grant AST 80-04467 from the National Science Foundation.

REFERENCES

Arp, H. 1965, *Ap. J.*, **141**, 45.
Baade, W. 1963, in *Evolution of Stars and Galaxies*, ed. C. P. Gaposchkin (Cambridge: Harvard University Press), p. 277 ff.
Bevington, P. R. 1969, *Data Reduction and Error Analysis for the Physical Sciences* (New York: McGraw-Hill), p. 127.
Böhm-Vitense, E. 1975, in *Problems of Stellar Atmospheres and Envelopes*, ed. B. Baschek, W. H. Kegel, and G. Traving (Berlin-New York: Springer-Verlag), p. 375.
Bonnell, J., and Branch, D. 1979, *Ap. J.*, **229**, 175.
Branch, D., Bonnell, J., and Tomkin, J. 1978, *Ap. J.*, **225**, 902.
Butler, D., Carbon, D., and Kraft, R. P. 1976, *Ap. J.*, **210**, 120.
Cayrel de Strobel, G., Bentolila, C., Hauck, B., and Curchod, A. 1980, *Astr. Ap. Suppl.*, **41**, 405.
Cohen, J. G., Frogel, J. A., Persson, S. E., and Elias, J. H. 1981, *Ap. J.*, **249**, 481.
Cohen, J. G. 1982, *Ap. J.*, **258**, 143.
Deming, D. 1980, *Ap. J.*, **236**, 230.
Deming, D., and Butler, D. 1979, *A.J.*, **84**, 839.
Deutsch, A. J., in *IAU Symposium 26, Abundance Determinations in Stellar Spectra* ed. H. Hubenet (London: Academic Press), p. 112.
Faber, S. M. 1972, *Astr. Ap.*, **20**, 361.
———. 1973, *Ap. J.*, **179**, 731.
———. 1977, in *The Evolution of Galaxies and Stellar Populations*, ed. B. M. Tinsley and R. B. Larson (New Haven: Yale University Observatory), p. 157.
Frogel, J. A., Persson, S. E., Aaronson, M., and Matthews, K. 1978, *Ap. J.*, **220**, 75.
Frogel, J. A., Persson, S. E., and Cohen, J. G. 1981, *Ap. J.*, **246**, 842.
———. 1983, preprint.
Frogel, J. A., and Whitford, A. E. 1982, *Ap. J.* (*Letters*), **259**, L7.
Frogel, J. A., Whitford, A. E., and Rich, R. M. 1983, in preparation.
Glass, I. S., and Feast, M. W. 1982, *M.N.R.A.S.*, **198**, 199.
Griffin, R. F. 1968, *A Photometric Atlas of the Spectrum of Arcturus* (Cambridge: Cambridge Philosophical Society).
Gunn, J. E., Stryker, L. L., and Tinsley, B. M. 1981, *Ap. J.* **249**, 48 (GST).
Gustafsson, B., Kjaergaard, P., and Andersen, S. 1974, *Astr. Ap.*, **34**, 99.
Janes, K. A. 1977, *Ap. J.* (*Letters*), **212**, L59.
Johnson, H. L. 1966, *Comm. Lunar Planetary Lab.*, **4**, 99.
Kraft, R. P. 1980, in *Globular Clusters*, ed. D. Hanes and B. Madore (Cambridge: Cambridge University Press), p. 92.
Larson, R. B. 1974, *M.N.R.A.S.*, **166**, 585.
———. 1976, *M.N.R.A.S.*, **176**, 31.
Lee, T. A. 1970, *Ap. J.*, **162**, 217.
Leep, E. M., and Wallerstein, G. 1981, *M.N.R.A.S.*, **196**, 543.
McClure, R. D. 1969, *A.J.*, **74**, 50.
Mould, J. R. 1978, *Ap. J.*, **220**, 434.
O'Connell, R. W. 1976, *Ap. J.*, **206**, 370.
Peterson, R. C. 1976, *Ap. J. Suppl.*, **30**, 61.
Pilachowski, C. 1978, *Pub. A.S.P.*, **90**, 675.
Pilachowski, C., Sneden, C., and Wallerstein, G. 1983, *Ap. J. Suppl.*, **52**, 241.
Pritchet, C., and Campbell, B. 1980, *Ap. J.*, **240**, 768.
Renzini, A. 1977, in *Advanced Stages in Stellar Evolution*, ed. P. Bouvier and A. Maeder (Sauverny: Geneva Observatory), p. 224 ff.
Sandage, A. R. 1954, *A.J.*, **59**, 162.
Shectman, S. 1978, in *Annual Report of the Director of the Hale Observatories*, 1977–78.
Spinrad, H., and Taylor, B. J. 1969, *Ap. J.*, **157**, 1279.
———. 1971, *Ap. J. Suppl.*, **22**, 445.
Sweigart, A. V., and Gross, P. G. 1978, *Ap. J. Suppl.* **36**, 405.
Tinsley, B. M. 1972, *Ap. J.*, **178**, 319.
———. 1978, *Ap. J.*, **222**, 14.
Tinsley, B. M., and Gunn, J. E. 1976, *Ap. J.*, **203**, 52.
van den Bergh, S. 1971, *A.J.*, **76**, 1082.
van den Bergh, S., and Herbst, E. 1974, *A.J.*, **79**, 603.
Whitford, A. E. 1978, *Ap. J.*, **226**, 277.
Whitford, A. E., and Blanco, V. M. 1979, *Bull. AAS*, **11**, 675.
Williams, P. M. 1971, *M.N.R.A.S.*, **153**, 171.
Wu, C. C., Faber, S. M., Gallagher, J. S., Peck, M., and Tinsley, B. M. 1980, *Ap. J.*, **237**, 290.
Zinn, R. 1980, *Ap. J. Suppl.*, **42**, 19.

R. M. RICH: Astronomy Department 105-24, California Institute of Technology, Pasadena, CA 91125

A. E. WHITFORD: Lick Observatory, University of California, Santa Cruz, CA 95064

CHAPTER 2

ABUNDANCES OF 88 NUCLEAR BULGE K GIANTS

ABSTRACT

Spectroscopy and photometry has been obtained for 100 K giants in Baade's Window at $l = 1°, b = -4°$. For a galactocentric distance 7.5 kpc the line of sight passes 522 pc below the nucleus. Line strengths have been measured for 34 features. Abundances have been derived from the Fe λ 5270, 5328 Å, and Mg b features, using a technique which compares the Baade's Window giants to 45 local giants of known abundance. The abundance distribution of the nuclear bulge K giants has been derived. The abundances run from -1 to nearly $+1$ dex, with a peak at 0.3 dex, or twice the solar abundance. Of the 88 stars with derived abundances, 22% exceeded the abundance of the most metal rich local K giants; 50% exceeded the solar abundance, and 10% were metal poor (< -0.6 dex). We present evidence for high metal abundances in the nuclear bulge K giants based on a wide variety of features, including clumps of weak iron lines on the linear portion of the curve of growth.

I. Introduction

The population of stars in the galactic nuclear bulge is unique compared to other resolved populations which have been studied. The nearest similar population, the bulge of M31, is nearly 100 times as distant, so even the Hubble Space Telescope must study it under the handicap of an order of magnitude poorer resolution than is possible for ground-based studies of the Galaxy's bulge.

In this program, we have undertaken to determine the metal abundances of K giants in the direction of Baade's Window (BW), on a line of sight which passes 500 pc below the nucleus on the minor axis of the Galaxy. Although this study contains 5 times the program stars and twice the number of standards as Whitford and Rich (1983) (WR), the procedures used to derive metal abundances are the same. The bulge stars are compared with a grid of standard stars composed of local K giants with high dispersion abundances and globular cluster giants. A least-squares multiple regression analysis is used to find the dependence of abundance on equivalent widths of metal lines and IR color (temperature).

Although the most luminous members of the bulge population are M giants, the K giants were selected for the abundance study because every star, metal rich or poor, evolves through the K giant phase. Although M giants are found in relatively metal poor globular clusters such as 47 Tuc, the vast majority of M giants will have metal rich progenitors. If only the M giants are used, one loses information about the shape and range of the abundance distribution function.

The observations, which consist of spectroscopy and IR photometry, are discussed in §II. The method of measuring the equivalent widths is discussed in §III a. The formal errors in the equivalent widths are discussed in §III b. The method used to measure the abundances, which is to establish the dependence of abundance of standard stars on equivalent width and $(J-K)$ colors, is discussed in §III c and d.

The abundances of the Baade's Window K giants are derived in §IV b; the choice of reddening towards Baade's Window, which affects the derived abundances, is defended in §IV a.

Other spectral features such as the G band, Na, and CN are measured, and their behavior is summarized in §V and a series of figures. A summary is found in §VI.

II. Observations

a) Spectroscopy and the Sample

All the spectra were obtained using the intensified Reticon detector (Shectman, 1978) on the Cassegrain spectrograph of the 2.5m du Pont telescope of the Las Campanas Observatory. The observations were made between 1980 and 1984 during the May – July period. Seeing ranged from 1 $''$ – 2 $''$ with usual being about 1.5 $''$. Spectra had 3744 channels and a 3.5 channel resolution of 4.5 Å, and were obtained through two entrance apertures of $2'' \times 4''$ diameter separated by 27.4 $''$ (a star and sky aperture). Considerable care was required in positioning the sky aperture when working in Baade's Window, in order to avoid including faint stars in the sky aperture. The bulge also has a high surface brightness due to unresolved stars near the main sequence turnoff, and this background affected spectroscopy in much the way moonlight does. Arp (1965) found V=20.6 mag/arcsec^2 and $(B-V)$ =0.92; van den Bergh (1971) found V=20.8 mag/arcsec^2 and $(B-V)$ =1.22 for a "star free" aperture of about 10 $''$ diameter. Whitford (1977) found V=20.0 mag/arcsec^2 using a $50'' \times 80''$ aperture; $(B-V)$ was $\approx$ 0.8. The most appropriate estimate for the background contribution is probably van den Bergh's measurement. Hence, while the BW K giants were mostly brighter than V = 16.5, integration times of 2000 sec per star were usually required. For all but two of the stars observed, the 600 line grating blazed at 5000 Åwas used. In 1984, a 1200 line grating was used to obtain velocity data; this yielded a resolution of 2.2Å.

All of the stars but 10 were chosen from a region of a photographic $(R-I)$

,I color-magnitude diagram (Whitford and Blanco 1979) $0.5 < (R-I) < 1.0$ and $15.5 < I < 12.0$. The $(R-I)$ photometry was on the Cousins magnitude system (Bessell, 1979). This region contained a well defined clump and giant branch. Stars classified as M giants by Blanco, McCarthy, and Blanco (1984) were avoided. About ten stars were selected from CCD images of Baade's Window taken using a narrow band filter system which measures the absorption by MgH. These stars were chosen to sample the extremes of the abundance distribution. The least biased sample is the sample of stars with IR photometry (Frogel, Whitford, and Rich, 1984). The high abundance end of the distribution function may have been underestimated by excluding stars with strong TiO bands regardless of their colors. The bulge M giants are hotter at constant spectral type than their solar neighborhood counterparts (Frogel and Whitford , 1982); some stars with strong TiO bands have the colors of local K4 giants. Nonetheless, an unbiased sampling of less luminous K giants should uncover the progenitors of these stars. An experiment with the Bahcall and Soneira model, considering the extreme cases of M92 and 47-Tuc like stars, indicates that if the stars were sampled without bias in color, there would be no resulting bias in abundance for the sample. A rapid CCD survey of the bulge abundance distribution is underway, and should provide a complete, unbiased sample. Another concern is contamination of the sample from members of NGC 6522, the cluster on which Baade's Window is centered. Annular star counts indicated that the cluster was making a negligible contribution to the field beyond a radius of $2'$; the stars observed were $> 3'$ from the cluster. Another possible source of contamination is that of stars

from the disk closer than the bulge. Two populations show striking concentration in their spatial distribution. The M giants studied by Blanco, McCarthy, and Blanco (1984) and the RR Lyrae variables studied by Blanco (1984) both show peaked distributions in number as a function of apparent magnitude. This fact, combined with the selection of stars from a clump region on the color-magnitude diagram, supports membership in a central population.

The local standard stars are mainly drawn from the Cayrel catalog of [Fe/H] determinations (Cayrel de Strobel *et al.* 1980), and from Frogel *et al's* 1983 IR photometry of globular clusters. A total of 45 standard stars covering an abundance range of -2 to $+0.5$ dex were used, and are listed in Table 1.

b) Photometry

Because line strength depends on both temperature and abundance, it is necessary to have a system of measuring stellar temperatures which allows direct comparison of the standard stars (local stars of known abundance) with the unknowns (members of Baade's Window). Further, the gravities of stars in the two groups must be similar, although Faber *et al.* 1985 has demonstrated that the Fe 5270 and Fe 5328 Å lines are not gravity sensitive. In order to work within these constraints, local abundance standards were selected to be G5III – M0III and covered an abundance range from -2.3 to 0.5 dex. Many of these abundance standards, chosen to have high dispersion fine abundance determinations, lacked IR photometry, so JHK CO H_20 photometry was obtained at Las Campanas Observatory using

the Swope 1m telescope InSb system [1] . Some of the stars were too bright for the system, so the telescope aperture was masked to allow their colors to be measured. The observations were made between 28 May and 1 June 1981, and included CTIO/CIT system standards (Elias *et al.* 1982; Frogel *et al.* 1978). Some of the standards also had colors from Johnson (1966) and were transformed to the CIT system (Elias *et al.* 1985). The photometry of the giants in Baade's Window is from Frogel, Whitford, and Rich (1984) and Frogel (1985). The standard stars and Baade's Window giants then have a common temperature measurement, subject to the reddening in Baade's Window. This temperature measurement was chosen to be the $(J-K)$ index. This was chosen rather than $(V-K)$ or $(R-I)$ because it was thought that the J and K bandpasses would be less likely to be be affected by blanketing arising in stars of differing abundances, and also would suffer much less from spatial variations in the reddening in Baade's window. At the time this project was initiated, only photographic V data from Arp (1965) were available for these stars; these were inaccurate due to crowding in Baade's Window. Ultimately, $(V-K)$ may be a better temperature index for these purposes. However, there is an advantage to having the standards and program stars on the same system, measured with the same equipment. The new measurements determined $(J-K)$ on the CIT system to be ≈ 0.04 bluer than the $(J-K)$ quoted in WR. The effect of decreasing derived abundances of the BW stars slightly was compensated for by new reddening determinations which require a larger reddening than in WR (see § IVa).

[1] developed by E. Persson

Only about half the sample of 99 BW K giants has JHK photometry from Frogel, Whitford, and Rich 1984. For the other half, some means of measuring a pseudo $(J-K)$ had to be developed. For this purpose, frames were taken on the 5m telescope using the "4-shooter" CCD system (Gunn *et al.* 1984), kindly provided by J. Mould and E. Shaya. These data were obtained on the *griz* system (Schneider, Gunn, and Hoessel 1983). The $8' \times 8'$ frames covered the entirety of the Arp (1965) field of photometry in Baade's Window, allowing a plot of $(g-z)_{inst}$ vs $(J-K)$, using those stars in BW *with* IR photometry as standards. It was found that a 100s g frame and 1s z frame provided the best data; measurements were made using 6 pixel (1.8 $''$) apertures which are shown in Figure 1 and are tabulated in Table 2. The relationship allows estimation of $(J-K)$ from $(g-z)_{inst}$ with errors of less than 0.05 in $(J-K)$. In the work with pseudo-colors, no absolute photometry was necessary because $(J-K)$ was read off of a calibration curve, in the same sense that a photographic plate is calibrated with photometry. Another source of pseudo-colors were frames obtained at CTIO using the 4m PFCCD system. These data cover only a portion of BW and are through filters centered at 4900Å and 7000Å, each with 50Å bandpass. The narrow-band images are part of Rich's rapid survey of the bulge abundance distribution function, in which images were also obtained through a narrow-band filter centered at MgH, 5170Å. An instrumental $(49-70)$ index is plotted against $(J-K)$ in Figure 2. A few stars were also obtained from a plot of $(r-i)$ vs $(J-K)$ (not shown), although the correlation was poorer than the correlations used to obtain the majority of the pseudo colors. It was found that

$(i-z)$ correlated poorly with every other index; the i and z filters may have some overlap in wavelength. The tight correlation found between $(g-z)_{inst}$ and $(J-K)$ indicates that spatial variations in reddening across the window are $< E_{B-V} = 0.1$ and that blanketing does not have a serious effect on the broad band colors.

III. Calibration of Abundance Against Equivalent Width and Color

a) Measurement of Equivalent Widths

Equivalent widths were measured from flattened, wavelength calibrated but unfluxed data. The data were not fluxed because then the original Poisson statistics would be lost and a proper error analysis rendered harder. In addition, standard stars were observed through neutral density filters of different thicknesses and types over the years, and while these did not affect the measurement of equivalent widths, fluxing for each filter thickness would have been difficult and, as demonstrated below, unnecessary.

A computer program was written which measured the widths in a batch mode, producing a table of widths and plots of each feature as output. Radial velocities were determined for each star against a template, α Ser (BS5854), which was shifted to zero velocity. All observations of this star were summed, adjusted for velocity, so the resulting template had at least 5000 counts per channel. The program SCROSS was used to measure a radial velocity (it is based on Tonry's 1979 cross correlation method). [1] No heliocentric correction was made to arrive at the velocity used to adjust the bandpasses, for these were adjusted only to duplicate feature measurements from stars to star. The amount by which a feature could be affected would vary depending on how the bandpasses were set; in the case of Faber's (SMF)

[1] The program SCROSS is a part of the FIGARO system of reduction programs written by K. Shortridge on the Caltech VAX. For convenient use in a batch mode, other programs, such as the equivalent widths program, were written so as to be a part of Shortridge's system.

features, which have bandpasses bracketing the features, half the equivalent width could be lost. This could amount to a correction of 1-2Å in equivalent width. In addition, each equivalent width was converted to the rest velocity frame by division of $1 + z$; for galactic stars, this is a 1% adjustment, but was included in order for the program to yield correct, consistent results for extragalactic objects.

The equivalent width is defined to be as close as possible to the classical definition of an equivalent width, and the definition is identical to that used in WR. It differs from a true equivalent width only in that a pseudo-continuum, rather than the true continuum, is used. At this low resolution, there are no true continuum points in the spectrum. The continuum $I_c(\lambda)$ was a straight-line interpolation between the average intensity in two bandpasses bracketing the feature. If only a single side bandpass could be used, it was the average intensity (in counts) in this bandpass. The area of an absorption or emission line was the difference between the continuum and the data within the feature bandpass, and included all contributions, whether positive or negative. The following definition:

$$W_\lambda(\text{Å}) = \int_{-\infty}^{+\infty} \left(1 - \frac{I(\lambda)}{I_c(\lambda)}\right) d\lambda \tag{1}$$

was expressed for digital data as:

$$W = \sum_{i=1}^{n} \left(1 - \frac{I(\lambda)_i}{I_c(\lambda)_i}\right) \Delta\lambda_i; \qquad \Delta\lambda_i = \frac{(\lambda_2 - \lambda_1)}{\text{n bins}} \tag{2}$$

where the sum is over the data between two limits λ_1 and λ_2 which define the feature bandpass, and the calculation is done pixel-by-pixel. A computationally more efficient expression which gives the same answer may be found in equation

(4). A "line strength" , the flux of the spectrum in the bandpass compared with the continuum, can be measured in magnitudes:

$$m = -2.5 \log \left(\frac{\sum(\text{cont})}{\sum(\text{line})} \right) \quad (3)$$

which can be thought of as the net deficit or excess due to a feature. The continuum definition is the same as for the equivalent width.

A total of 34 features were measured and plotted; these are listed in Table 3 and plotted on a stellar spectrum in Figure 3. Not all of these features were actually analyzed for this work; some will be considered at a later time. Features designated "RMR" are from Whitford and Rich (1983), except for the Fe 4383Å bandpasses which were changed slightly. Features marked "SMF" in Table 3 are from Faber *et al.* 1985, with the bandpasses used without modification. Some features, particularly the G and Ca measurements, are from Stetson (1984); the Ca measurement derives originally from Suntzeff's 1980 widely used m_{HK} index, and his modification to measure H and K separately is more appropriate for unfluxed data. The last features, w1–8, are clumps of weak Fe lines on the linear portion of the curve of growth and local continuum regions selected from the Arcturus Atlas (Griffin 1968) emulating methods used by Gustafsson, Kjaergaard, and Anderson (1974), who derived Fe abundances for bright stars using a similar method. Unfortunately, this latter approach requires data with high signal to noise ratio (S/N) to be fully successful. Other features are possible dwarf/giant discriminators, such as Sr II 4077Å and Ca I 4227Å. Again, low counts in these spectral regions prevented their use for quantitative purposes. As discussed in WR, blends of Fe lines with different

excitation potentials, or blends of Fe lines with other metals were avoided for use as principal abundance indicators. For each feature, the following information was determined: an equivalent width in Å, an error in width, in Å, a line strength, in magnitudes, an error in line strength, in magnitudes, and S/N at the center of the feature.

In addition, each star had a header which included other information such as the velocity and airmass. A program was written to average repeat observations, and their errors were reduced by $\sqrt{N_{obs}}$. In all, there were over 500 observations, because stars were often observed in the following mode: Two apertures, star and sky, alternating between apertures and summing the result. Separate (star−sky) results were preserved, when observations were made in this mode. Sometimes, the data were not written to tape until both sides were summed, which loses the information from separate channels. Equivalent width measurements made on separate sides were in good agreement.

Measured widths and derived errors (§ IIIb) for a selection of features are listed for standard stars in Table 4, other non-bulge K giants in Table 5, and for members of Baade's Window in Table 6.

b) Error Analysis for Equivalent Widths

A major shortcoming of any quantitative approach to error analysis for these data is that one can reasonably only deal with errors due to Poisson statistics of counts in each channel. Actual errors in the data found from repeat measurements were about 1.5 times the errors due to counting statistics. Other contributors to errors could be flattening problems (due to flexure), variation in the thickness and type of neutral density filters used over the years (necessary to obtain a safe counting rate for the bright local standard stars), and instrumental sensitivity variations (unlikely).

The "neutral" density filters tended to heavily absorb in the blue, and this made measurements of features below 4200Å in the standard stars very uncertain. Nonetheless, the excellent fits given by the regressions, as well as an independent analysis by Faber *et al.* 1985 indicates that the neutral density filters did not contribute to excess scatter in measurements of features. However, Fe 4383Å, (feature 2), was adversely affected and was not used in the regressions, a departure from the procedure of Whitford and Rich 1983.

The errors mentioned above effectively place an upper limit on S/N for any data. A "fat zero" of 1% fractional error in equivalent width was added to all equivalent width error measurements. It has an effect only when the number of counts in a given spectrum is so large that unreasonably small errors would be derived which do not take into account the above problems.

For the faint bulge stars, errors are larger than indicated from counts because of the substantial "sky" background in Baade's Window due to the unresolved turnoff stars. For some stars in the blue, sky counts were half the object counts. However, by 5000Å, the sky contribution was down substantially; it should not affect the crucial Fe and Mg features.

To derive the errors in equivalent width, we begin by describing equation (2) in a more computationally efficient, but equivalent form:

$$W = W_\lambda(\text{Å}) = \sum_{i=1}^{n} \left(1 - \frac{y_i}{\bar{c}}\right) \Delta\lambda_i \tag{4}$$

where the sum is over n bins in the line, y_i are the data within the line bandpass, and $\bar{c}$ the mean continuum at the feature, defined as the central continuum point of the line drawn between the two bandpasses. The sum can be carried through and:

$$W = \Delta\lambda \left(n - \frac{N_l}{\bar{c}}\right) \tag{5}$$

where N_l is the total counts in the line bandpass (including negative counts, as always). Because these data are placed on a linear wavelength scale as a result of wavelength calibration, $\Delta\lambda = \Delta\lambda_i$. The mean continuum is:

$$\bar{c} = c_1(1 - w) + c_2 w \tag{6}$$

where

$$w = \frac{x_c - x_1}{x_2 - x_1} \tag{7}$$

and the coordinates of the lower, feature, and upper points are:

$$\begin{aligned} \text{lower}: &\quad x_1,\, c_1 \\ \text{feature}: &\quad x_c,\, \bar{c} \\ \text{upper}: &\quad x_2,\, c_2 \end{aligned} \tag{8}$$

The error in measuring the equivalent width arises from both error in placing the continuum and Poisson statistics. General propagation of errors, for the case of uncorrelated errors:

$$z = f(x_1, x_2, \ldots); \qquad \sigma(z)^2 = \left(\frac{\partial f}{\partial x_1}\right)^2 \sigma_{x_1}^2 + \left(\frac{\partial f}{\partial x_2}\right)^2 \sigma_{x_2}^2 + \cdots \tag{9}$$

Applying (9) to (5):

$$\sigma(W)^2 = \left(\frac{\Delta\lambda}{\bar{c}}\right)^2 \sigma^2(N_l) + \left(\frac{\Delta\lambda N_l}{\bar{c}}\right)^2 \sigma_{\bar{c}}^2 \tag{10}$$

Although $\sigma^2(N_l) = N_l$, we must derive the error in continuum placement, $\sigma_{\bar{c}}$ from propagation of errors:

$$\sigma_{\bar{c}}^2 = \frac{N_{LO}}{n_{LO}^2}(1-w)^2 + \frac{N_{HI}}{n_{HI}} w^2 \tag{11}$$

where N_{LO} and N_{HI} are the number of counts in the continuum, and n_{LO} and n_{HI} are the number of bins in the sidebands. The error in determining the position, in counts, of a continuum point is:

$$\sigma(c_1 \text{ or } c_2) = \frac{\sqrt{N(\text{counts in band})}}{n(\text{bins in band})} \tag{12}$$

from (10) and (11) it follows that the error in equivalent width due to counting statistics alone is :

$$\sigma(W) = \frac{\Delta\lambda N_l}{\bar{c}} \left[\frac{1}{N_l} + \left(\frac{\sigma_c}{\bar{c}}\right)^2\right]^{1/2} \tag{13}$$

where $\Delta\lambda$, is the dispersion, as defined previously. For the line strength,

$$m = -2.5 \log \left(\frac{N_l}{\bar{c}n} \right) \tag{14}$$

where n is the number of bins in the bandpass. and using a similar derivation as for the equivalent width:

$$\sigma(m) = (-2.5 \log_{10} e) \left[\frac{1}{N_l} + \frac{\sigma_{\bar{c}}^2}{(\bar{c}n)^2} \right]^{1/2} \tag{15}$$

and likewise for a single sideband case.

In order to test the accuracy of the derived errors, a high S/N spectrum of α Ser was degraded by adding gaussian noise with $\sigma = \sqrt{y(i)}$ where $y(i)$ is the initial spectrum. This simulates the addition of Poisson noise, which, by the central limit theorem, is gaussian when the number of counts is large. The effect on the measured width of Mg is illustrated in Figure 4 and the calculated error is in Figure 5. Different S/N was obtained by dividing the spectrum by an increasing constant and adding noise as previously described. It is interesting to note that the widths have very large errors below a S/N of about 8; this is the same level where radial velocity cross-correlation techniques begin to produce inaccurate answers as well (Tonry and Davis, 1979).

c) Dependence of Abundance on Equivalent Width and $(J - K)$

Ideally, it would be desirable to determine the abundances of the BW K giants from their spectra alone, using the IR colors to determine temperatures, and

a spectrum synthesis program to fit the spectra. At the current time, such an approach may just be becoming feasible. Few grids of model atmospheres extend into the metal rich domain, and there are many problems to be understood before low resolution spectra can be modelled. There are sources of missing opacity, and the complicated and ubiquitous red system of the CN molecule. Before low resolution spectra can be fit, model atmospheres will have to successfully fit *high* resolution spectra. It was decided that the best, most enduring comparison would be to observe a grid of local standard stars with abundances derived from high dispersion spectra. In addition, members of well studied globular clusters with abundances from Zinn and West (1984) were also observed. This method also permits a comparative study of the bulge population's properties independent of *any* model. The population is compared with the two best understood stellar populations: the disk and the galactic globular clusters.

For reasons described in WR, we adopt the abundances determined by Branch, Bonnell, and Tomkin (1978) for the metal rich stars, particularly μ Leo at +0.48 dex. This contention has recently been strengthened both by the high dispersion spectroscopy of Bond *et al.* 1985, in which the stars with strong lines at *low* dispersion also have enhanced *weak* lines on the linear portion of the curve of growth, and the work of Faber *et al.* 1985 which also found metal line enhancements in local K giants which had been classified as strong lined at low dispersion.

Faber *et al.* (1985) used the Fe 5270 and 5328Å lines, and used residuals from a line strength–temperature relationship as the abundance measure. We have chosen

not to use such a "$\delta - \delta$" method in spite of the obvious complexity of the relationship between equivalent width, temperature, and abundance. The mathematical regression technique which has been used preserves information about errors, and permits a genuine weighted fit. Different approaches can be easily tried. No measurements by hand or judgement decisions are involved; in particular, a freehand curve is *not* drawn through the data, as in the "$\delta - \delta$" method. If a different value of the reddening towards Baade's Window should be determined, the effect on the abundance distribution function can be calculated easily (§ IVb, Eq. 24). A drawback of the mathematical approach is that it requires one to assume a functional dependence in the relationship *i.e.*, it is a parametric approach; on the other hand, in working with residuals, one can easily deal with complex nonlinear relationships. We believe that the functional forms proposed below fit the data at least as well as Faber's approach.

The method used to calibrate the widths and colors is a multivariate least-squares approach. The heart of the method is J. Tonry's MINI program, a least-squares minimization program. This program is easy to use and handles virtually any expression, although it has some difficulty with greater than 4 parameters to vary. The basic method is to minimize the weighted least squares:

$$\chi^2 = \sum_{i=1}^{n} \left[\frac{([\mathrm{Fe/H}]_{i,obs} - [\mathrm{Fe/H}]_{i,pred})^2}{\sigma(y_i)^2} \right] \tag{16}$$

Because we seek to determine abundances for "unknowns" with widths and colors,

[Fe/H] is always the dependent variable. The full expression to be minimized is:

$$[\mathrm{Fe/H}]_{pred,i} = A_0 + A_1(J-K)_{r,i} + A_2 \log W_{r,i} + A_3(J-K)_{r,i}(\log W_{r,i}) + A_4(\log W_{r,i})^2 \tag{17}$$

where

$$\log W_{r,i} = \log W_i - \langle \log W \rangle$$
$$(\mathrm{J\text{-}K})_{r,i} = (J-K)_i - \langle (J-K) \rangle \tag{18}$$

where the r subscript indicates that the *average* color or width of the sample has been subtracted – amounting to a change of coordinates which causes the fit to be made centered on the data. The fits were made logarithmically in equivalent width because it improved the fit significantly, and one expects strong lines to grow roughly as the 0.5 power of the abundance; a power law is always a good local approximation to the curve of growth. For fits which covered the full 2.5 dex of abundance, all five of the above constants were necessary to achieve a fit. For restricted ranges of abundance, a fit linear in color and width was acceptable. The full χ^2 minimization of (16) also requires division by $\sigma(y_i)^2$, which is derived according to propagation of errors, equation (9):

$$\sigma(y_i)^2 = [A_1 + A_3 \log W_{r,i}]^2 \sigma(J-K)_i^2 + [A_2 + 2A_4 \log W_{r,i} + A_3(J-K)_{r,i}]^2 \sigma(\log W_i)^2 \tag{19}$$

Where

$$\sigma(\log W_i)^2 = \left[\log_{10} e \left(\frac{\sigma(W_i)}{W_i}\right)\right]^2 + (0.01 \log_{10} e)^2 \tag{20}$$

and $\sigma(J-K)$ is the statistical error from the finite number of 'deflections' taken in the IR photometry runs, and also from the photometric solution for the night on

which the star was observed. For members of Baade's Window, an additional 0.03 was added in quadrature to $(J-K)$, reflecting the reddening uncertainty discussed in § IVa. Equation (19) was the denominator of χ^2. To converge to a solution, MINI was allowed to vary the coefficients in the numerator, based on initial guesses. When these converged to a solution, the coefficients in the denominator were adjusted by hand to these values. This was repeated until the values of the coefficients did not change with an additional iteration. When both the denominator and numerator were allowed to vary, MINI frequently failed to converge.

d) Establishment of the Calibration

In minimizing equation (16), one can choose from among the 34 features listed in Table 3. In practice, many can be ruled out as good abundance indicators for various reasons. The two hydrogen lines obviously are not abundance sensitive. The Ca and Na lines both suffer from interstellar contributions because the line of sight to Baade's Window is heavily reddened (see § IVa). The effect of interstellar Na causes the BW members to scatter above the local giant relationship between Fe and Na line strengths in Figure 6. Because the total equivalent width of Ca H and K is so large, the interstellar contribution is less important. Previous experience in WR suggested that an index formed from Fe and Mg might well be best. In addition, Faber *et al.* 1985 found that Fe 5270Å + Fe 5328Å gave the best correlation with abundance. We decided to exclude the Fe 4383Å line this time; in addition to the reasons mentioned earlier in § IIIb, the bulge giants have less flux below 4500Å. For each candidate feature, a test regression was run using all the standards covering the full 2.5 dex abundance range, and again using the 31 standards which are "local" K giants, which range between -0.5 and +0.5 dex. Of the features, only Na correlated as well with abundance as the Fe+Mg index, but could not be applied to the bulge stars because of the interstellar contribution. The Faber indices, which measure the continuum very close to the feature, could be used to measure abundance over the full range, whereas the indices measured in WR were useful for the metal rich stars only. The WR sidebands were more distant from the feature, but were chosen to be relatively free of absorption lines. All of the Mg indices correlated well with

abundance, however, only the Mg b line feature was used because it is not as gravity sensitive as the molecular absorption. Three separate sets of features were used to calibrate the abundances of the bulge K giants:

(1) : SMF Fe 5270 + Fe 5328 + Mg b 5170; w 9,10,11

(2) : SMF Fe 5270 + Fe 5328

(3*a*) : SMF Fe 5270 + Fe 5328 + Mg b 5170; [Fe/H] < -0.5

(3*b*) : RMR Fe 5270 + Fe 5328 + Mg b 5170; w 3,4,2; [Fe/H] ≥ -0.5

The third method above will be called the "split" regression. Solutions (1) and (2) used 5 terms; methods 3a and b used 3 terms, and were linear in $(J-K)$ and $\log W$. The derived coefficients and rms residuals are listed in Table 7. The covariance matrix for Solution 1 is in Table 8. The solution for the metal rich stars was carried out using only the local K giant standards, while the solution for the metal poor stars used only globular cluster giants. It was hoped that by restricting the range of validity, a more precise comparison of stars with similar properties could be achieved. The regression using Fe alone was suggested by the finding in Faber et al. (1985) that Fe is the best abundance indicator and free from gravity effects. The fits used to determine the abundances of the Baade's Window stars had rms deviations of at most 0.2 dex over the full 2.5 dex; the difference between the high dispersion [Fe/H] and the calculated value has been plotted against [Fe/H] and $(J-K)$ in Figures 7 and 8 (for Solution 1) and in Figures 9 and 10 for Solution 2 and 3, respectively. All solutions tend to underestimate abundances at the *metal rich* end. The derived abundances for the standard stars for all solutions are in

Table 9.

If the gravities of the K giants in Baade's Window were systematically higher than those of the standard stars, it is conceivable that abundances could be overestimated if Mg is used in the determination. A test regression using just Mg found lower derived abundances, as illustrated in Figure 11. When abundances derived using Solution 1 are plotted against Solution 2 (the Fe only solution), a similar result follows, namely, that use of Fe only results in slightly *higher* derived abundances (Figure 12). Solution 3b, which uses only metal rich giants in the fit, derives the lowest abundances at the metal rich end, as illustrated in Figure 13. Not surprisingly, the split regression correlates the least well with abundances from Solution 1.

A further means of evaluating the validity of this technique is to determine abundances for K giants which are neither standards nor program stars. In the course of this program, a number of stars were observed in NGC 5927 and 6522, as well as some local K giants found to be metal rich by other investigations. The regression technique *never* found any abundances for local K giants which extended into the range of the bulge giants. A metal abundance of $[Fe/H] = -0.02 \pm 0.15$ was derived for NGC 5927, and -1.3 ± 0.56 dex for NGC 6522. Although the 5927 value is higher than the Zinn and West 1984 mean abundance, Cohen (1983) found this cluster to be 0.59 dex more metal rich than 47 Tuc, or about -0.10 dex on this scale. NGC 5927 has E_{B-V} =0.46 (Frogel, Persson, and Cohen, 1983) which is nearly the same as Baade's Window, making it a good independent population of

near solar abundance with which to compare the Baade's Window K giants.

IV. Abundances of the Bulge K Giants

a) Reddening in Baade's Window

As the abundance derived depends on both equivalent width and $(J-K)$, the zero-point of the abundance distribution function will depend on the adopted reddening E_{J-K} for Baade's Window. Spatial variations in the reddening across the window pose a potential source of error in abundance measurement for individual stars. Blanco *et al.* (1984) point out that E_{B-V} likely varies across the window, and some variation in absorption is obviously present when one inspects a blue photograph (Blanco *et al's* Plate 1). Blanco (1984, private communication) has used preliminary colors of RR Lyrae stars studied by Blanco and Blanco (1984) and E_{B-V} of M giants to map the reddening variations. He finds that a $3'$ circle centered on NGC 6522 has $E_{B-V} \approx 0.49$. For area A, as defined in Blanco *et al.* 1984, $E_{B-V} \approx 0.35$. For his area B, $E_{B-V} \approx 0.42$. For area C, south of the cluster, he suggested the linear approximation $E_{B-V} = 0.49 + 0.016\delta$ where δ is the arcmin south of the *northern* boundary of area C. If Elias *et al's* (1985) ratio of $E_{J-K}/E_{B-V} = 0.605$, Blanco suggests that variations by as much as 0.09 in E_{J-K} are present. Nonetheless, most of the program stars fall between $2'$ and $4'$ radius from the cluster, and could well be considered to fall within the cluster reddening domain. Because we do not know the reddening of individual stars with *certainty*, we have chosen to adopt a single value of reddening for the entirety of BW.

The methods used to determine reddening in Baade's Window all rely on a comparison of the colors of BW stars with nearby ones of the same type. Arp (1965)

used the UBV two-color diagram to deredden field star photoelectric standards, and based his reddening determination of E_{B-V} =0.46 largely on the colors of two luminosity class III stars estimated to lie 6 kpc distant. Arp also presumed that NGC 6522 and 47 Tuc had comparable abundances (NGC 6522 is actually metal poor, Zinn and West 1984), and obtained a lower reddening estimate for the cluster. Arp found the line of sight to leave the absorbing material 2 kpc from the sun, 140 pc above the plane. Funfschilling (1971) observed the BW in the UGR system, and again found the line of sight to leave reddening material about 2 kpc from the sun. Again, his final estimate relied on K giants. Van den Bergh (1971) redid Arp's work and improved upon the photometry. He found $E_{B-V} = 0.47$ from UBV colors of the late giants in the line of sight, and the red limit in $(B-V)$ of the BW M giants compared with local M giants. He also compared colors of M giants typed by Nassau and Blanco (1958) with local giants of the same spectral type (almost certainly an incorrect method, as discussed below). Glass and Feast (1982) measured the colors of Mira variables in BW and compared them to local Miras. The bulge Miras do fall in a similar location in the JHK color-color diagram as local giants. They found $E_{J-K} = 0.36$ for Miras of 150 – 400 day period, and $E_{J-K} = 0.32$ for Miras of 180 – 300 days. All of the above reddening methods rely on the colors of either K or M giants which are members of the bulge. Frogel and Whitford (1983) have demonstrated that many properties of these stars, particularly their colors at a given TiO band strength, differ radically from giants in the solar neighborhood. The BW M giants are too hot at a given spectral type and have a dip in the R band

not found in local M giants. WR and this work also find a substantial population of metal rich K giants which have no counterparts in the solar neighborhood. It is clear that the bulge population has enough peculiarities that the late giants should *not* be used for any reddening determination. Safe populations would be NGC 6522 and the metal poor RR Lyrae stars studied by Butler, Carbon, and Kraft (1976). These populations have well understood counterparts in unreddened systems.

The two most secure methods are:

(1) Use of Sturch's (1966) result that ab RR Lyrae stars have a constant color at minimum light which can be determined from their periods and [Fe/H] .

(2) Comparison of the integrated color and giant branch of NGC 6522 with a local cluster of the same [Fe/H] .

Walker and Mack (1985) have employed both of these methods and find the following:

$E(B-V) = 0.59$ 6 RR ab variables, Sturch's method

$E(B-V) = 0.55$ Comparison of giant branch of NGC 6522 with NGC 6752

$E(B-V) = 0.51$ Comparison of integrated color of NGC 6522 (Zinn 1980)

To use Sturch's method, six RR Lyraes were observed by Walker and Mack in B and V over their entire light curves. The actual E_{B-V} values determined for the RR Lyrae stars ranged from 0.53 to 0.64. While the sample was too small to look for any evidence of absorption variations, the full range in E_{B-V} was 0.07 for both of the two 6 arcmin^2 fields surveyed, and there was no systematic difference between

the fields. The mean of the three methods listed above is $E_{B-V}(B0) = 0.56$, which we believe to be the best reddening measurement in BW. We need to know E_{J-K}/E_{B-V}, and must calculate E_{J-K} for a K2III star. This may be done using using Walker and Mack's $A_v(B0) = 1.78$ and correct to K2 using Olson's (1975) finding that the ratio of total to selective absorption can be expressed as

$$R = 3.25 + 0.25(B-V)_0 + 0.05E_{B-V} \tag{21}$$

from which E_{B-V} (K2) = 0.49 . Elias et al. 1985 found E_{J-K} / E_{B-V} = 0.605 for M2 supergiants with $(B-V)_0 = 1.7$ (this ratio is 0.5 at A0 for the Whitford (1958) and van de Hulst reddening curves). Using slightly less than the Elias ratio, E_{J-K} for BW is found to 0.30 from the Walker and Mack measurement. Frogel, Whitford, and Rich (1983) used the more traditional value for BW of E_{B-V} (B0) = 0.50 to obtain E_{J-K} =0.26 . The Walker-Mack value is based on a more sound stellar population, but we must still consider Elias *et al.* 1985 large ratio of E_{J-K} / E_{B-V} . The best compromise was judged to be adopting $E_{J-K} = 0.28 \pm 0.03$, with the error due to spatial variations and uncertainty concerning the correct reddening value.

b) Abundances of the Bulge Giants and

The Distribution of Abundances in Baade's Window

With the reddening having been determined to be $E_{J-K} = 0.28$, the abundances of the giants in BW can be derived from their unreddened $(J-K)$ colors and measured equivalent widths, using the regression equations obtained in § IIIc. Errors in the abundances can be considered as due to a "systematic" error—the errors in the coefficients output by the regression solutions and "random" errors, due to the errors in $(J-K)$, the reddening, and $\log W$ which are associated in each star. The error $\sigma([\mathrm{Fe/H}])$ follows:

$$\sigma([\mathrm{Fe/H}])^2 = \sigma_r^2 + \sigma(y_i)^2 \tag{22}$$

where $\sigma(y_i)^2$ is defined in (19) and $\sigma(J-K)_i$ for the BW stars has the reddening error of 0.03 added in quadrature. The error due to the uncertainties in the derived coefficients, σ_r is, using (9):

$$\begin{aligned}\sigma_r^2 = \sigma_{a_0}^2 + (J-K)_{r,i}{}^2\sigma_{a_1} + \log W_{r,i}{}^2\sigma_{a_2} \\ + (J-K)_{r,i}{}^2\log W_{r,i}{}^2\sigma_{a_3}^2 + \log W_{r,i}{}^4\sigma_{a_4}^2\end{aligned} \tag{23}$$

The resulting errors of ≈ 0.15 dex for the BW stars would make a bin size of 0.25 dex appropriate for expressing the distribution function. Abundance histograms for solutions 1–3 are illustrated in Figures 14–16. Figure 14, for Solution 1, also illustrates separate histograms for those stars with and without IR photometry. These figures do not contain stars with $(J-K) < 0.45$ because these are more

blue than the bluest point on the M92 giant branch, reddened to Baade's Window, hence, it is not clear what these giants would be, if they were reddened by the foreground reddening sheet.

The following features are noteworthy:

1. All the distribution functions have a substantial number of stars ($\approx 10\%$) with abundances larger than 0.5 dex

2. The peak is near the solar abundance and the distribution function is not bimodal, as it was in WR.

3. The "split" regression has stars at lower abundances, however all the distributions have a tail toward -1 dex.

4. Those stars that had $(J-K)$ derived from $g-z$ colors have essentially the same distribution as those that had colors from IR photometry.

5. The tail towards low abundances is always more gentle than the fall off at high abundance.

6. The distribution function obtained from Fe lines alone extends to higher abundances than that obtained from Fe + Mg.

The bulge population could be generally characterized as having a mean solar abundance with $\sigma \approx 0.4$dex. Table 12 summarizes the properties of the distribution functions.

The effect of an error in E_{J-K} for Baade's window follows most simply from coefficient A_1 in Solution 3a, and is generally applicable to all the solutions:

$$\delta[\mathrm{Fe/H}] = 1.4\delta E_{J-K} \tag{24}$$

so a *decrease* in E_{J-K} of 0.1 would decrease the derived abundances by only 0.14 dex; *the conclusion that the bulge population contains very metal rich stars is consistent with all reddening determinations for Baade's Window that are quoted in the literature.*

In WR, it was thought that the bulge population might have a bimodal distribution of abundance. The larger sample of K giants does not show bimodality. The plot of $\sum$(Fe 5270 + Fe 5328 + Mg b) vs $(J-K)_0$, [1] We may also test whether the abundance distribution depends on the apparent luminosities of the stars. Figure 17 illustrates that, to some extent, it does. For V<16, there is an excess of metal poor stars and a deficiency of metal rich stars. This may be understood qualitatively in that the brighter metal rich stars are M giants, and were excluded. The fainter metal poor stars may be blue horizontal branch stars; with their strong Balmer lines, these objects were also excluded from abundance determination. As a result of these effects, the derived distribution function may have been somewhat deficient at both extremes. In figure 18, we see that while weak lined stars are present in BW, they are significantly hotter than the local comparison stars. In Figure 19, the globular cluster members are explicitly indicated, and again, while a number

[1] In this and all other figures, the Baade's window stars have been dereddened by $E_{J-K} = 0.28$, as discussed in §IVa.

of stars resembling members of 47 Tuc are present, the stars hotter than $(J-K)$ =0.5 are too hot to be analagous to giants in metal poor globular clusters. Such stars may have been judged to be too bright to be included in the sample, since the giant branch tips of the metal poor clusters would terminate at V=14 (Arp, 1965). When abundances are derived for the stars with $(J-K) < 0.5$, they differ significantly depending on whether the split regression or full regression is used. There were no standard stars which were both metal poor and had $(J-K) < 0.6$. A careful consideration of the completeness of this sample will be undertaken at a later time, when the distribution of abundances is related to the stellar population in the Galactic bulge.

Nearby dwarf stars are a possible contaminant at the metal rich end. There is also the possibility that the enhanced Mg of the dwarfs could give rise to a false population of metal rich stars. However, Frogel *et al.* 1978 tabulated colors for dwarfs which range from $(J-K)_0$ =0.43 for K0 to $(J-K)_0$ =0.81 for M2. The bluest *observed* color for stars with derived abundances was $(J-K)$ =0.73. If we adopt a linear reddening model for the extinction (Arp 1965), we could expect foreground dwarfs in the range $15 < V < 17$ to be reddened by up to 0.14 mag, assuming they lay at a distance of 1 kpc. This would mean that contaminating dwarfs could have observed colors as red as $(J-K)$ =0.87. A large fraction of the sample could be contaminating dwarfs, based on the colors. However, two points can be made against possible dwarf contamination.

1. We can modify the Bahcall-Soneira model and use a linear model for the

extinction. As the line of sight leaves the disk quickly, we would expect relatively few contaminating dwarfs relative to the spheroid. This is in fact found to be the case; all predicted dwarfs lie to the blue of $(B-V)$ =1.1, which is the blue limit of the program stars. Of these few dwarfs, contaminant stars must also come from a narrow color range. However, the Standard Galaxy model lacks a "central bulge" component which is required by the rotation curve of the Galaxy (Bahcall, Schmidt, and Soneira, 1983). If this component were present in the model, following their density law, the number of predicted central component giant stars would be 60% larger, rendering the dwarf contamination problem even less significant. In support of this, Mould's 1983 spectroscopy of the Blanco M giants contains no dwarfs out of 49 stars.

2. Eight bulge K giants have measured CO from Frogel, Whitford, and Rich (1984). These are plotted along with the abundance standards observed from Las Campanas in Figure 20. The CO of dwarfs never exceeds 0.04 mag over the range of the plot, but the bulge members are all well above the dwarf range. The metal rich bulge giants generally tend to lie on or above the upper envelope of the abundance standards. Not a single case occurred where a star of high derived abundance failed to have high CO.

The blue colors of the galactic bulge giants discussed in Frogel, Whitford, and Rich, 1983 remain a problem. Note particularly 1021 in Figure 20, with $(J-K)_0$ =0.46 and CO of 0.12.

Is there any other evidence, besides the abundances derived in the regression,

that some of the BW K giants are much more metal rich than any local giants? Figure 18 illustrates that the bulge giants extend to much higher (Fe + Mg) equivalent widths at constant color than do the local giants. Figure 21 illustrates the same point, using just the SMF Fe lines, most abundance sensitive, according to Faber *et al.* 1985. The RMR lines, with the continuum points chosen to be more distant from the feature and more appropriate for measurements in metal rich stars, also show the same effect (Figure 22). A slight change in the reddening of the BW stars would not change these conclusions. The sum of w1—8, features chosen to contain weak Fe lines, also extends well beyond the range of the local giants in a plot against $(J-K)_0$ (Figure 23). In a given stellar spectrum, it is difficult to tell that any of the weak features is present at all; it is surprising that such a positive result follows for the low S/N bulge giants. Figure 24 illustrates that sum of the weak features is well correlated with the (Fe + Mg) index; it also is correlated with the Fe lines alone. The TiO bands have been found to be abundance sensitive as well (Mould and McElroy, 1978). A plot of TiO2 (Feature 18) vs $(J-K)_0$ in Figure 25 shows the BW stars have TiO enhanced over local K giants even at hot $(J-K)$ (a significant excess over the standards appears at $(J-K)$ of 0.6, corresponding to K0).

The derived abundances could be spuriously high if the stars had higher gravity, and gravity-sensitive features were used in the abundance derivation. As mentioned earlier, Faber *et al.* 1985 found the Fe lines were not affected by changes in stellar gravity, but Mg was. They found that Mg_2 was the index most sensitive to gravity.

In Figure 26, Mg_2 is plotted against the RMR Fe indices for both the BW stars and standards. It does not appear to be systematically high in the BW stars. It is also clear from Figure 12 that the high derived abundances are not affected by the inclusion of Mg in the abundance index.

There is generally agreement to within 0.2 dex between abundances derived in this work and in WR; however, weak-lined stars such as 3106 are discrepant by up to 0.5 dex, because small changes in the measured equivalent width can lead to large changes in the abundances derived from weak absorption lines.

V. Other Spectral Features in the Bulge Giants

The features used for the abundance analysis are the strongest features and are located in regions of the spectrum with high S/N. Other features among the 34 measured were chosen for future study; a few were examined for this work.

Figure 6, which plots Na against the Fe + Mg abundance index, is noteworthy because although the interstellar contribution is well illustrated, there is also a suggestion of excess scatter in the Na equivalent width. High dispersion spectroscopy should help to answer whether there are significant star-to-star variations in Na. Further study of those stars with large Na widths would be particularly valuable.

The G band is well correlated with the Fe + Mg index in Figure 27; in Figure 28, when plotted against $(J-K)_0$, it follows the basic behavior of the other features. However, when plotted against the CN 4144Å feature in Figure 29, the Baade's Window stars appear to have systematically lower CN at a given G band strength. When CN is plotted against the Fe + Mg index in Figure 30, the standards define an upper envelope well above the bulge giants; again, the CN equivalent width is weak in the bulge stars.

Further study of the CN feature, perhaps using spectrum synthesis, would be worthwhile. Depression of the continuum due to many metal lines may also be artificially decreasing the CN width. Because CO is strong in the bulge stars, it may be that CN is weak because nitrogen is underabundant. The data are not sufficiently good to allow a conclusion at this time.

Efforts to study the Ca lines were disappointing because there is so little flux in the blue for both the bulge stars and the standards. No conclusive results were found for any other feature.

Future investigations should rely on high dispersion spectra to study the relative abundances of various species.

VI. Conclusions

Abundances have been derived for 88 K giants in the galactic nuclear bulge based on low dispersion spectra. The conclusion of Whitford and Rich (1983) that some stars in the bulge are extremely metal rich has been confirmed. The distribution of stellar abundances is, on average, solar with a dispersion of ± 0.4 dex, and is not bimodal, rather running from -1 dex to nearly 1 dex, with a more gentle tail toward low abundance. The CN molecule may be systematically weak in the bulge stars.

TABLE 1

ABUNDANCE STANDARD STARS

No. (1)	Name (2)	V_0 (3)	$(V-K)_0$ (4)	$(J-K)_0$ (5)	$\sigma(J-K)$ (6)	CO (7)	[Fe/H] (8)	Notes (9)
489.....	ν Psc	4.44	3.20	0.810	0.030	...	−0.30	J
1953.....	γ Men	5.19	3.97	0.620	0.030	...	0.35	J
3905.....	μ Leo	3.88	2.67	0.650	0.015	0.098	0.48	a
3994.....	λ Hya	3.61	2.20	0.500	0.020	0.018	0.10	
4287.....	α Crt	4.08	2.44	0.570	0.018	0.092	−0.12	
4365.....	73 Leo	5.32	2.84	0.700	0.015	0.044	−0.17	
4608.....	o Vir	4.12	2.23	0.520	0.010	0.058	−0.50	
4695.....	16 Vir	4.96	2.76	0.690	0.015	0.144	−0.11	
4932.....	ϵ Vir	2.83	2.06	0.490	0.020	0.056	0.00	
5089.....	...	3.88	2.57	0.600	0.015	0.103	−0.16	
5288.....	θ Cen	2.06	2.32	0.560	0.012	0.068	−0.19	
5340.....	α Boo	−0.04	2.96	0.750	0.030	...	−0.50	J
5370.....	20 Boo	4.86	2.72	0.660	0.022	0.098	0.35	b
5777.....	37 Lib	4.62	2.36	0.580	0.012	0.051	−0.14	
5824.....	42 Lib	4.96	2.92	0.690	0.018	0.088	−0.07	
5854.....	α Ser	2.65	2.56	0.600	0.016	0.096	0.23	a
6056.....	δ Oph	2.74	3.97	0.910	0.017	0.162	0.32	
6159.....	29 Her	4.84	3.62	0.870	0.017	0.165	−0.13	
6241.....	ϵ Sco	2.29	2.58	0.630	0.019	0.119	−0.31	
6299.....	κ Oph	3.20	2.56	0.610	0.014	0.049	0.00	
6603.....	β Oph	2.77	2.52	0.560	0.030	0.087	0.18	b
6973.....	α Scut	3.85	3.02	0.730	0.020	0.155	0.00	
7120.....	ν^2 Sgr	4.99	2.97	0.715	0.017	0.169	−0.40	
7317.....	...	6.06	3.50	0.840	0.021	...	−0.60	
HD 175674....	...	6.65	2.93	0.714	0.017	0.117	0.25	C
7429.....	μ Aql	4.45	2.66	0.630	0.015	0.107	0.27	
7754.....	α^2 Cap	3.57	2.09	0.540	0.030	...	0.11	J
7869.....	α Ind	3.11	2.26	0.540	0.019	0.047	0.25	
7900.....	ν Cap	5.10	4.32	0.990	0.014	0.209	0.10	
8852.....	γ Psc	3.69	2.24	0.530	0.030	0.019	−0.16	
2426.....	47 Tuc	11.98	3.50	0.900	0.020	0.110	−0.71	F;d
4415.....	47 Tuc	12.22	2.37	0.590	0.020	0.090	−0.33	F;c
5527.....	47 Tuc	13.48	2.61	0.660	0.020	...	−0.71	F;d
8517.....	47 Tuc	12.04	2.49	0.740	0.030	0.145	−0.71	F;d
8518.....	47 Tuc	12.98	2.58	0.690	0.020	0.090	−0.71	F;d
HD 165195....	...	6.50	2.45	0.650	0.050	0.010	−2.00	P
I-68	M5	12.30	3.24	0.850	0.020	0.105	−1.40	F;d
II-50	M5	13.92	2.73	0.680	0.020	...	−1.40	F;d
III-56.....	M5	13.26	2.52	0.640	0.020	0.005	−1.40	F;d
IV-28.....	M5	14.36	2.51	0.640	0.030	...	−1.40	F;d
IV-47.....	M5	12.27	3.28	0.880	0.030	0.090	−1.40	F;d
IV-81.....	M5	12.06	3.45	0.890	0.020	0.080	−1.40	F;d
I-12	M15	12.30	2.91	0.730	0.020	0.010	−2.15	F;d
II-29	M15	12.76	2.49	0.690	0.020	0.000	−2.15	F;d
II-64	M15	13.08	2.54	0.640	0.020	0.000	−2.15	F;d
S6	M15	13.09	2.72	0.650	0.020	0.020	−2.15	F;d

NOTES.—Col. (1) HR/HD/star number in cluster (Frogel *et al.* 1983 and references therein). Col. (2) V from Hoffleit and Jaschek (1982); not dereddened. Col. (3)–(7) K, $J - K$ from observations at Las Campanas (§IIb); unless otherwise noted in col. (9). Col. (8) Abundance of Fe relative to solar value (logarithmic) from Cayrel de Strobel *et al.* 1980 unless otherwise noted in col. (9).

Sources of magnitudes: (C) V from Cayrel de Strobel *et al.* (1980) (F) Dereddened IR magnitudes from Frogel, Persson, and Cohen 1983 and references therein. (J) V, J, and K from Johnson 1966. (P) Pilachowski 1978.

Sources of abundances: (a) Branch, Bonnel and Tomkin 1978. (b) Gustafsson, Kjaergaard, and Andersen 1974 (c) R. Gratton, 1983 (private communication); not a cluster member. (d) Zinn and West 1984.

TABLE 2

PSEUDO-INFRARED COLORS FROM CCD PHOTOMETRY

(1)	(2)	(3)	(4)	(5)	(6)	(1)	(2)	(4)	(5)	(1)	(2)	(4)	(5)
1012	−3.99	1.05	...	0.89	0.90	2018	−3.74	...	0.98	3141	−5.29	0.46	...
1016	...	1.23	1.00	...	...	2026	−3.65	...	1.01	3152	−3.85	0.97	...
1021	−4.30	0.80	0.74	...	...	2027	−3.28	1.04	...	3157	−3.67	1.02	...
1025	−3.92	1.00	0.90	...	...	2033	−3.80	0.95	...	3159	−4.07	...	0.86
1034	...	1.69	1.09	...	...	2040	−4.39	0.75	...	3160	−4.25	0.79	...
1039	−4.05	1.02	0.89	...	...	2041	−5.13	...	0.47	3164	−3.82	0.97	...
1041	−3.76	...	...	0.98	...	2042	−3.80	0.99	...	3169	−5.21	...	0.44
1043	...	0.88	1.21	...	...	2044	−3.62	...	1.02	3197	−3.97	...	0.89
1049	−4.42	0.73	0.70	...	...	2049	−4.30	0.77	...	3200	−4.63	0.76	...
1053	−4.61	0.66	0.68	...	...	2116	−3.77	0.96	...	3209	−3.65	0.96	...
1064	−3.83	1.25	1.05	...	...	2118	−3.89	...	0.94	3224	−3.88	...	0.94
1068	...	1.43	1.06	...	...	2119	−4.10	0.85	...	3244	−4.56	...	0.65
1073	...	1.45	1.08	...	...	2122	−3.26	1.13	...	3261	−4.65	...	0.63
1076	−3.69	...	1.00	...	...	2123	−2.20	1.24	...	4003	−3.97	0.84	...
1078	...	1.81	1.19	...	...	2136	−4.18	...	0.81	4011	−4.23	...	0.78
1083	−4.21	0.89	...	0.82	0.80	2139	−4.58	...	0.65	4022	−3.88	...	0.94
1093	−4.00	1.03	...	0.90	0.90	2145	−3.95	0.82	...	4025	−4.20	0.78	...
1102	−4.12	0.98	...	0.83	0.88	2146	−4.03	0.82	...	4063	−4.04	...	0.86
1129	−3.96	0.39	...	0.90	0.51	2147	−4.26	0.71	...	4065	−4.09	...	0.84
1140	−3.93	1.10	...	0.90	0.94	2151	−3.89	...	0.94	4071	−4.13	...	0.81
1141	−4.01	0.99	0.94	...	...	2154	−4.18	...	0.82	4072	−3.90	...	0.93
1144	−3.62	1.28	...	1.02	1.02	2166	−4.28	...	0.78	4146	−4.12	...	0.82
1145	−4.43	0.77	0.76	0.71	0.78	2167	−3.76	...	0.98	4148	−4.32	...	0.75
1151	−4.24	0.85	...	0.78	0.78	2171	−3.89	...	0.94	4164	−4.14	...	0.81
1153	−4.39	0.86	...	0.73	0.79	2173	−4.17	0.81	...	4165	−3.62	...	1.01
1155	−4.06	1.01	0.92	...	...	2174	−3.95	...	0.70	4167	−3.96	0.86	...
1156	−4.07	0.97	...	0.85	0.85	2197	−3.28	1.06	...	4203	−2.89	1.15	...
1158	−4.12	0.94	0.87	...	...	2199	−4.20	...	0.80	4285	−3.96	...	0.90
1161	−5.20	0.13	0.40	...	...	2200	−4.02	...	0.87	4312	−4.43	0.71	...
1164	−4.01	1.05	0.90	...	...	2201	−3.77	...	0.98	4315	−3.89	...	0.92
1174	−4.28	0.85	...	0.78	0.78	2206	−4.98	0.57	...	4316	−4.08	...	0.84
1181	−4.35	0.80	...	0.75	0.74	2215	−4.42	0.70	...	4325	−3.97	0.87	...
1194	−3.92	1.10	0.94	...	...	2216	−4.05	...	0.85	4329	−3.88	1.00	...
1196	−3.38	1.45	1.00	...	...	2240	−4.54	0.73	...	5060	...	...	...
1202	−3.90	1.07	0.90	...	...	2242	−4.39	...	0.74	5435	−4.00	...	0.88
1298	−3.19	...	1.16	...	...	2244	−3.71	1.01	...	5445	1.08[a]	...	0.92[a]
1308	−5.01	...	...	0.52	...	2245	−4.43	0.71	...	6192	−3.93	...	0.91
1319	−3.78	...	...	0.98	...	2252	−3.91	0.92	...	6322	−3.42	...	1.05
1322	−3.79	...	0.95	...	...	2261	−3.67	1.03	...	6406	−3.28	...	1.10
1329	−3.75	...	...	0.98	...	3079	−4.14	...	0.81				
1335	−3.84	...	...	0.95	...	3106	−4.32	0.78	...				
1368	...	−0.20	...	...	−0.20	3133	−3.96	...	0.89				

NOTES.—Cols. (1) Star number from Arp (1965) with roman numeral sector number converted to decimal. Stars beginning with a 5 or 6 were found using narrow-band CCD imaging photometry and will be identified in a later paper. Cols. (2) $(g-z)_{inst}$ color from 4-shooter CCD photometry. Col. (3) For stars in the first box, (49 − 70) color from narrow-band CCD images. Also for star 5445. Col. (4) *observed* $(J-K)$ from IR photometry. Col. (5) $(J-K)$ derived from $(g-z)_{inst}$ using calibration in Figure 1. Col. (6) $(J-K)$ derived from (49 − 70) using calibration of Figure 2.

[a] Color from (49-70) and $(J-K)$ derived from (49 − 70)

TABLE 3

WAVELENGTH INTERVALS FOR EQUIVALENT WIDTH MEASUREMENTS

No. (1)	Feature (2)	Lower Band (Å) (3)	Feature Band (Å) (4)	Upper Band (Å) (5)
1	RMR Fe I λ4383	4325.00—4335.00	4365.00—4415.00	4503.00—4510.00
2	RMR Mg I b.....	4940.00—4955.00	5157.00—5192.00	5355.00—5361.00
3	RMR Fe I λ5270	4940.00—4955.00	5255.00—5280.00	5355.00—5361.00
4	RMR Fe I λ5328	5055.00—5060.00	5315.00—5340.00	5355.00—5361.00
5	RMR Na I D.....	5820.00—5840.00	5877.00—5910.00	5960.00—5975.00
6	G band λ4300	4268.25—4283.25	4283.25—4317.00	4320.75—4335.75
7	PBS G band	4233.00—4267.00	4267.00—4319.00	4349.00—4381.00
8	MgH	4930.00—4980.00	5150.00—5210.00	5470.00—5530.00
9	SMF Mg I b	5144.50—5162.00	5162.00—5193.25	5193.25—5207.00
10	SMF Fe I λ5270	5235.50—5249.25	5248.00—5286.75	5288.00—5319.25
11	SMF Fe I λ5328	5307.25—5317.25	5314.75—5353.50	5356.00—5364.75
12	SMF Na I D	5863.00—5876.75	5879.25—5910.50	5924.50—5949.25
13	SMF Hβ	4829.50—4848.25	4849.50—4877.00	4878.25—4892.00
14	SMF CN λ4140	4082.00—4118.25	4144.00—4177.75	4246.00—4284.75
15	SMF Mg_1	4897.00—4958.25	5071.00—5134.75	5303.00—5366.75
16	SMF Mg_2	4897.00—4958.25	5156.00—5197.25	5303.00—5366.75
17	SMF TiO_1	5819.00—5850.25	5939.00—5995.25	6041.00—6104.75
18	SMF TiO_2	6069.00—6142.75	6192.00—6273.25	6375.00—6416.25
19	NBS m_{HK}	...	3910.00—4020.00	4020.00—4130.00
20	CN λ3880.....	...	3846.00—3883.00	3883.00—3916.00
21	Ca I λ4227	4210.00—4220.00	4223.00—4232.00	4240.00—4250.00
22	(Ca I +Fe I) λ6103	6066.00—6078.00	6157.00—6167.00	6201.00—6210.00
23	Hα.....	6520.00—6530.00	6558.00—6568.00	6615.00—6623.00
24	Sr II λ4077	4040.00—4070.00	4073.00—4081.00	...
25	PBS Ca II K	3892.00—3914.00	3914.00—3952.00	3986.00—4004.00
26	PBS Ca II H	3892.00—3914.00	3961.00—3982.00	3986.00—4004.00
27	w1	5799.00—5804.00	5804.00—5818.00	5818.00—5823.00
28	w2	5967.00—5975.00	5975.00—6030.00	6043.00—6053.00
29	w3	6066.00—6078.00	6078.00—6110.00	6201.00—6210.00
30	w4	6043.00—6053.00	6053.00—6066.00	6066.00—6078.00
31	w5	6201.00—6210.00	6213.00—6225.00	...
32	w6	6345.00—6353.00	6353.00—6370.00	6370.00—6390.00
33	w7	6440.00—6448.00	6452.00—6460.00	...
34	w8	...	6490.00—6505.00	6520.00—6530.00

NOTES.—Col. (1) Numerical order in analysis program. Col. (2) RMR–from Whitford and Rich, 1983; SMF–from Faber *et al.* 1985; NBS–from Suntzeff, 1980; PS–from Stetson, 1984. Features marked "w" are blends of weak metal (mostly Fe) lines. Col. (3)–(7) Blank entries are single sideband measures.

TABLE 4

EQUIVALENT WIDTHS OF STANDARD STARS

Name[a]	N[b]	$(J-K)_0$ [c]	2 Mg b	3 Fe 52	4 Fe 53	7 G ps	9 Mg b	10 Fe 52	11 Fe 53	12 Na 58	13 Hβ	14 CN	16 Mg_2	18 TiO_2	23 Hα	25 Ca K	26 Ca H	27 $\sum$w
489.....	1	0.81	10.01	4.60	2.62	10.26	3.66	3.39	3.75	3.92	1.10	4.91	9.60	7.04	1.34	18.20	12.72	6.87
		0.03	0.21	0.21	0.24	0.43	0.21	0.23	0.25	0.18	0.20	0.43	0.17	0.34	0.14	0.70	0.37	0.61
1953.....	2	0.62	12.22	6.07	3.02	9.65	5.16	4.52	3.92	4.28	1.35	8.20	11.57	3.33	1.66	17.93	10.66	7.75
		0.03	0.17	0.17	0.21	0.36	0.18	0.20	0.22	0.19	0.18	0.33	0.14	0.34	0.12	0.63	0.37	0.60
3905.....	9	0.65	11.43	5.87	3.23	11.44	4.75	4.86	4.43	4.99	1.25	12.84	10.53	1.45	1.17	15.56	12.62	9.90
		0.01	0.10	0.09	0.11	0.25	0.10	0.11	0.12	0.11	0.10	0.24	0.08	0.19	0.07	0.85	0.37	0.33
3994.....	1	0.50	7.33	4.45	1.99	8.21	3.04	4.09	2.83	2.80	1.85	9.76	6.72	−3.19	1.94	18.89	10.88	8.81
		0.02	0.24	0.22	0.27	0.39	0.22	0.24	0.29	0.28	0.19	0.34	0.19	0.51	0.17	0.72	0.41	0.84
4287.....	1	0.57	8.32	4.31	2.40	8.83	3.50	3.51	4.05	3.09	1.68	7.38	7.46	−2.26	1.40	17.58	12.14	8.77
		0.02	0.34	0.33	0.40	0.58	0.32	0.36	0.41	0.40	0.28	0.54	0.28	0.71	0.24	1.14	0.58	1.17
4365.....	1	0.70	9.96	5.33	3.45	6.37	3.88	3.73	3.98	3.16	1.21	4.88	8.69	3.81	1.52	12.67	10.80	9.98
		0.01	0.23	0.21	0.25	0.42	0.22	0.25	0.27	0.21	0.22	0.36	0.19	0.39	0.15	0.61	0.31	0.66
4608.....	2	0.52	4.96	2.84	1.70	7.79	2.20	2.61	1.76	1.35	1.77	3.49	4.09	−0.19	2.07	14.95	10.22	4.28
		0.01	0.23	0.21	0.25	0.34	0.19	0.22	0.26	0.24	0.17	0.31	0.17	0.41	0.13	0.57	0.31	0.71
4695.....	3	0.69	8.09	3.60	2.28	10.79	3.76	3.03	3.44	2.11	1.09	4.89	7.47	2.99	1.52	17.49	11.68	6.97
		0.01	0.16	0.15	0.17	0.28	0.14	0.16	0.18	0.16	0.14	0.28	0.12	0.28	0.10	0.48	0.26	0.48
4932.....	2	0.49	5.57	4.05	2.60	8.48	2.15	3.55	3.31	1.84	2.60	6.04	4.20	0.69	1.39	17.32	10.39	4.36
		0.02	0.24	0.21	0.25	0.37	0.21	0.23	0.27	0.24	0.18	0.34	0.19	0.43	0.16	0.65	0.39	0.75
5089.....	1	0.60	6.44	4.39	2.50	8.37	1.07	4.22	3.75	3.39	2.03	8.48	5.64	0.08	2.33	19.24	10.77	6.64
		0.01	0.38	0.34	0.41	0.64	0.36	0.37	0.43	0.41	0.30	0.59	0.30	0.71	0.23	1.24	0.73	1.23
5288.....	1	0.56	6.23	4.31	2.52	7.34	2.63	3.80	2.64	2.10	1.86	7.12	5.19	−1.95	1.48	17.51	10.48	4.75
		0.01	0.36	0.32	0.38	0.58	0.32	0.35	0.41	0.40	0.28	0.52	0.28	0.69	0.24	1.15	0.65	1.19
5340.....	2	0.75	9.34	4.06	2.53	9.64	3.55	2.86	3.20	2.11	1.11	5.59	8.78	1.96	1.53	21.04	13.09	5.50
		0.03	0.16	0.15	0.18	0.36	0.16	0.17	0.19	0.17	0.14	0.37	0.13	0.28	0.10	0.75	0.40	0.49
5370.....	2	0.66	11.07	5.95	3.19	9.64	4.10	4.49	3.83	3.87	1.50	9.65	9.91	2.01	1.21	17.43	11.42	8.14
		0.02	0.21	0.20	0.24	0.44	0.22	0.23	0.27	0.23	0.20	0.41	0.17	0.42	0.16	0.95	0.53	0.72
5777.....	2	0.58	8.77	4.43	2.75	8.71	4.03	3.95	3.36	2.88	1.45	4.34	7.90	1.99	1.30	15.81	11.44	6.82
		0.01	0.23	0.22	0.26	0.38	0.22	0.24	0.28	0.26	0.20	0.36	0.18	0.46	0.17	0.66	0.34	0.79
5824.....	1	0.69	10.37	6.11	3.15	10.85	3.82	4.48	3.09	4.54	1.30	11.05	9.53	−0.23	1.35	23.33	13.61	12.09
		0.02	0.35	0.33	0.41	0.70	0.36	0.39	0.45	0.41	0.33	0.65	0.29	0.74	0.26	1.24	0.69	1.22
5854.....	15	0.60	9.95	5.36	3.05	10.21	4.07	4.24	3.85	3.87	1.47	10.64	8.96	1.33	1.30	18.66	11.24	8.07
		0.02	0.07	0.06	0.08	0.13	0.07	0.07	0.08	0.07	0.06	0.12	0.06	0.13	0.05	0.27	0.16	0.23

TABLE 4

EQUIVALENT WIDTHS OF STANDARD STARS (CONTINUED)

Name[a]	N[b]	$(J-K)_0$ [c]	2 Mg b	3 Fe 52	4 Fe 53	7 G ps	9 Mg b	10 Fe 52	11 Fe 53	12 Na 58	13 Hβ	14 CN	16 Mg_2	18 TiO_2	23 Hα	25 Ca K	26 Ca H	27 $\sum$w
6056.....	1	0.91	14.73	6.80	3.98	8.52	5.79	4.26	4.13	4.63	0.34	4.75	14.41	19.30	1.34	22.19	13.35	10.92
		0.02	0.27	0.27	0.34	0.82	0.32	0.34	0.38	0.35	0.32	0.89	0.23	0.47	0.19	1.75	1.01	0.99
6159.....	2	0.87	11.45	4.97	2.52	9.87	4.56	3.38	3.09	2.95	0.73	6.08	11.06	6.41	1.33	19.11	11.43	8.49
		0.02	0.17	0.18	0.21	0.39	0.18	0.20	0.23	0.19	0.17	0.40	0.14	0.32	0.12	0.83	0.49	0.57
6241.....	1	0.63	9.93	5.18	2.57	8.92	3.66	3.67	3.13	3.34	1.62	9.55	8.74	−1.29	1.56	19.44	12.54	7.73
		0.02	0.34	0.33	0.40	0.69	0.34	0.38	0.43	0.39	0.31	0.62	0.28	0.70	0.23	1.39	0.73	1.18
6299.....	2	0.61	9.47	5.17	2.87	9.94	4.16	4.13	3.73	3.15	1.22	8.81	8.60	2.12	0.83	18.26	11.29	8.01
		0.01	0.22	0.21	0.25	0.44	0.21	0.23	0.26	0.24	0.20	0.41	0.18	0.42	0.16	0.90	0.54	0.72
6603.....	1	0.56	10.17	5.23	2.61	9.82	3.93	4.53	3.38	4.27	2.00	10.50	9.47	−1.11	1.18	20.00	11.51	8.70
		0.03	0.35	0.34	0.41	0.67	0.35	0.38	0.44	0.40	0.31	0.61	0.28	0.73	0.26	1.47	0.83	1.24
6973.....	1	0.73	10.94	4.37	2.25	8.75	4.54	4.40	3.30	3.92	0.33	10.63	10.86	0.85	1.57	22.16	11.88	10.39
		0.02	0.27	0.28	0.33	0.67	0.28	0.29	0.34	0.30	0.27	0.62	0.22	0.53	0.18	1.63	0.94	0.91
7120.....	1	0.71	10.47	4.98	2.64	9.70	4.27	3.94	3.71	2.89	0.74	10.28	9.54	6.23	0.89	15.24	12.41	7.47
		0.02	0.23	0.22	0.26	0.42	0.23	0.25	0.28	0.21	0.22	0.35	0.18	0.37	0.15	0.65	0.32	0.66
7317.....	1	0.84	11.55	4.10	2.42	8.70	4.16	3.39	4.03	3.42	0.84	7.90	11.44	2.83	1.34	21.69	12.69	10.91
		0.02	0.39	0.41	0.48	0.90	0.42	0.44	0.49	0.47	0.39	0.88	0.32	0.78	0.27	2.12	1.14	1.35
175674....	1	0.71	10.43	5.31	3.09	9.90	4.04	4.61	4.27	5.18	2.04	12.16	9.70	1.43	1.28	21.28	11.20	7.27
		0.02	0.42	0.40	0.48	0.74	0.42	0.45	0.51	0.50	0.37	0.60	0.34	1.03	0.45	0.90	0.58	1.75
7429.....	1	0.63	12.18	5.40	3.01	10.50	5.31	4.03	3.78	4.81	2.11	7.32	11.61	−1.12	1.11	21.15	13.27	8.27
		0.01	0.36	0.37	0.44	0.86	0.38	0.42	0.47	0.43	0.34	0.90	0.30	0.80	0.29	2.01	1.07	1.36
7754.....	1	0.54	6.62	4.34	2.14	7.36	2.96	3.23	2.55	1.86	1.92	6.59	5.83	−1.45	1.42	15.80	10.17	6.99
		0.03	0.31	0.28	0.34	0.48	0.27	0.31	0.36	0.37	0.23	0.43	0.24	0.63	0.22	0.97	0.53	1.07
7869.....	2	0.54	6.43	3.88	2.34	8.96	2.74	3.21	2.94	1.93	1.74	5.15	5.54	0.51	1.44	17.75	11.20	5.83
		0.02	0.20	0.18	0.21	0.32	0.17	0.19	0.23	0.21	0.16	0.30	0.15	0.36	0.13	0.53	0.30	0.61
7900.....	2	0.99	14.31	6.14	2.77	9.24	5.96	4.37	3.77	5.15	1.22	2.95	14.53	28.71	1.17	16.20	10.87	8.35
		0.01	0.17	0.18	0.22	0.47	0.20	0.21	0.23	0.21	0.20	0.52	0.14	0.25	0.12	1.27	0.68	0.61
8852.....	1	0.53	5.73	2.94	2.19	8.24	2.48	2.01	1.81	1.21	1.27	3.70	5.02	−1.05	1.60	16.86	9.96	3.18
		0.03	0.32	0.30	0.34	0.49	0.27	0.32	0.37	0.37	0.24	0.47	0.24	0.63	0.22	0.96	0.55	1.09
47-2426 ...	1	0.90	10.79	3.90	1.70	7.33	4.18	3.16	2.83	3.62	0.82	5.75	10.75	7.33	0.99	22.43	11.10	5.70
		0.02	0.30	0.30	0.36	0.56	0.30	0.33	0.37	0.24	0.30	0.51	0.24	0.36	0.13	0.66	0.46	0.69
47-4415 ...	2	0.59	6.99	3.44	1.57	9.29	3.08	2.56	2.39	1.92	1.09	2.81	6.59	1.46	1.35	15.61	10.84	5.77
		0.02	0.18	0.17	0.20	0.22	0.16	0.18	0.21	0.17	0.14	0.19	0.14	0.31	0.11	0.23	0.13	0.53

TABLE 4

EQUIVALENT WIDTHS OF STANDARD STARS (CONTINUED)

Name[a]	N[b]	$(J-K)_0$ [c]	2 Mg b	3 Fe 52	4 Fe 53	7 G ps	9 Mg b	10 Fe 52	11 Fe 53	12 Na 58	13 Hβ	14 CN	16 Mg_2	18 TiO_2	23 Hα	25 Ca K	26 Ca H	27 $\sum$w
47-5527 ...	1	0.66	3.84	1.40	0.87	8.05	2.53	2.48	2.12	0.89	1.34	0.48	3.25	1.93	1.24	16.61	9.61	3.86
		0.02	0.43	0.41	0.46	0.61	0.34	0.39	0.46	0.43	0.32	0.57	0.32	0.79	0.34	0.71	0.45	1.37
47-8517 ...	2	0.74	7.18	3.19	1.70	9.64	3.24	3.23	2.63	1.99	0.89	2.43	6.65	3.82	1.41	18.36	12.09	6.42
		0.03	0.16	0.15	0.17	0.24	0.14	0.16	0.18	0.16	0.14	0.23	0.12	0.27	0.10	0.27	0.15	0.47
47-8518 ...	1	0.69	3.77	1.54	1.61	10.30	2.64	1.99	2.43	0.85	1.50	0.57	2.67	1.28	1.82	16.43	10.67	4.27
		0.02	0.37	0.35	0.38	0.51	0.29	0.34	0.40	0.38	0.28	0.50	0.28	0.69	0.28	0.64	0.38	1.19
165195....	1	0.65	3.20	2.05	1.09	3.19	1.13	1.46	1.13	0.81	4.07	−2.72	2.43	0.94	2.72	8.88	7.66	−2.68
		0.05	0.28	0.26	0.31	0.24	0.23	0.27	0.33	0.29	0.18	0.20	0.21	0.51	0.17	0.21	0.13	0.93
5-1068....	1	0.85	6.25	2.90	1.58	7.93	2.05	2.18	1.88	1.54	1.14	1.73	5.82	2.82	1.34	17.82	10.71	6.19
		0.02	0.23	0.22	0.25	0.30	0.21	0.23	0.27	0.21	0.19	0.27	0.18	0.36	0.13	0.32	0.20	0.64
5-2050....	1	0.68	1.76	0.83	0.23	9.06	0.88	1.74	1.19	0.58	1.10	1.26	1.32	1.58	1.21	14.89	10.52	2.65
		0.02	0.42	0.38	0.43	0.48	0.33	0.37	0.44	0.42	0.30	0.44	0.31	0.77	0.33	0.55	0.32	1.35
5-3056....	1	0.64	1.32	0.42	0.34	6.25	0.71	1.13	1.13	0.98	1.42	1.48	0.94	1.49	1.67	14.93	10.69	0.88
		0.02	0.42	0.38	0.43	0.49	0.32	0.37	0.44	0.41	0.29	0.43	0.30	0.75	0.31	0.54	0.31	1.34
5-4028....	1	0.64	3.56	2.27	1.59	7.92	1.40	1.44	1.51	1.47	2.10	1.34	2.75	1.69	1.07	13.71	9.87	3.48
		0.03	0.32	0.29	0.33	0.28	0.26	0.30	0.36	0.31	0.21	0.23	0.24	0.55	0.21	0.24	0.15	0.98
5-4047....	1	0.88	5.62	3.12	2.00	7.13	2.05	2.69	1.96	1.94	0.53	2.34	4.94	1.76	1.06	17.52	11.67	3.87
		0.03	0.26	0.24	0.27	0.33	0.23	0.25	0.29	0.20	0.22	0.29	0.20	0.32	0.11	0.34	0.20	0.59
5-4081....	1	0.89	8.07	4.10	2.67	8.53	2.46	2.75	2.67	1.79	1.44	2.15	7.01	1.88	1.05	19.51	10.72	6.28
		0.02	0.25	0.24	0.27	0.37	0.24	0.26	0.30	0.21	0.23	0.34	0.20	0.33	0.11	0.38	0.25	0.59
15-1012 ...	1	0.73	1.81	0.90	0.83	4.55	0.08	0.60	1.03	1.80	0.55	0.91	1.29	−0.03	0.93	13.20	7.16	−0.11
		0.02	0.31	0.28	0.30	0.37	0.25	0.27	0.32	0.24	0.23	0.32	0.22	0.42	0.15	0.42	0.28	0.75
15-2029 ...	1	0.69	0.11	−0.08	0.45	7.60	0.80	1.15	1.13	1.40	1.70	−0.34	−0.33	−1.48	1.06	10.20	7.04	1.68
		0.02	0.42	0.38	0.41	0.52	0.30	0.35	0.41	0.37	0.28	0.50	0.30	0.70	0.30	0.72	0.44	1.20
15-2064 ...	1	0.64	1.86	1.18	1.34	3.99	0.54	0.41	1.03	1.75	0.78	−0.42	0.97	0.47	0.86	11.05	7.33	1.65
		0.02	0.30	0.26	0.29	0.32	0.23	0.27	0.31	0.25	0.21	0.27	0.22	0.43	0.16	0.32	0.20	0.76
15-S6.....	1	0.65	−1.45	−1.48	−0.15	4.66	0.71	0.50	0.73	1.41	1.07	0.31	−1.14	−0.27	1.01	11.34	7.39	−0.92
		0.02	0.48	0.44	0.46	0.59	0.33	0.39	0.46	0.41	0.31	0.53	0.33	0.76	0.33	0.73	0.45	1.34

NOTES— Equivalent widths and errors in Å (derived in § III). Errors are listed underneath each measurement, including $(J-K)_0$. Feature names and numbers are from Table 3.

[a] Name, BS or HD. Cluster members indicated with hyphenated cluster name and roman number converted to decimal. *e.g.* M5 I-68 is 5-1068. 47 Tuc numbers are from Lee, 1970. (See also notes to Table 1.)

[b] Number of separate observations, which were averaged, and errors reduced by $\sqrt{N}$.

[c] $(J-K)_0$ color, and error. Sources of observations in Table 1.

TABLE 5

EQUIVALENT WIDTHS OF NON-BULGE K GIANTS

Name[a]	N[b]	$(J-K)_0$ [c]	2 Mg b	3 Fe 52	4 Fe 53	7 G ps	9 Mg b	10 Fe 52	11 Fe 53	12 Na 58	13 Hβ	14 CN	16 Mg_2	18 TiO_2	23 Hα	25 Ca K	26 Ca H	27 $\sum w$
224.....	1	...	13.48	5.49	3.33	12.49	4.41	3.67	4.17	4.84	0.92	4.35	13.13	12.04	1.09	17.67	12.31	8.90
		...	0.19	0.20	0.24	0.47	0.22	0.23	0.25	0.18	0.22	0.51	0.16	0.30	0.13	0.85	0.45	0.57
3369.....	1	...	4.67	3.14	2.07	8.63	2.62	3.72	2.13	2.70	2.25	9.58	3.41	−1.51	1.33	19.43	12.07	4.68
		...	0.40	0.35	0.39	0.79	0.32	0.35	0.42	0.37	0.32	0.72	0.30	0.69	0.27	1.43	0.78	1.17
4894.....	1	...	8.12	5.09	3.29	7.05	3.33	3.93	4.20	3.25	2.68	9.35	6.71	0.21	2.24	15.06	10.51	7.82
		...	0.35	0.32	0.37	0.61	0.32	0.35	0.40	0.40	0.29	0.51	0.28	0.68	0.19	1.21	0.63	1.20
6104.....	1	0.55	5.89	3.16	2.06	9.39	2.45	2.95	2.56	2.41	1.51	5.50	5.19	3.82	1.68	15.64	10.42	5.73
		0.02	0.24	0.22	0.25	0.34	0.20	0.22	0.26	0.20	0.19	0.30	0.18	0.36	0.14	0.45	0.26	0.63
6171.....	1	...	10.93	4.94	2.64	8.19	6.10	3.68	2.92	3.10	2.46	−0.55	10.36	−1.98	1.82	17.08	9.60	3.94
		...	0.51	0.51	0.61	0.81	0.48	0.57	0.66	0.67	0.44	0.79	0.42	1.19	0.35	1.20	0.72	2.04
6746.....	1	0.60	5.84	3.77	2.28	9.31	2.62	2.75	2.74	1.43	1.76	4.18	4.67	2.58	1.41	14.97	10.63	4.68
		0.02	0.21	0.19	0.22	0.29	0.18	0.21	0.24	0.19	0.17	0.26	0.17	0.32	0.12	0.37	0.21	0.57
8413.....	2	0.77	14.11	6.58	4.04	11.34	5.06	5.11	5.12	5.56	1.03	7.90	13.70	11.13	1.38	19.32	12.47	11.83
		0.02	0.15	0.15	0.18	0.37	0.18	0.18	0.19	0.14	0.17	0.36	0.13	0.24	0.10	0.63	0.35	0.44
8795.....	1	0.90	14.01	6.58	4.14	8.75	4.96	3.48	4.89	6.29	0.34	3.03	13.41	22.64	0.95	19.55	7.30	9.53
		0.02	0.19	0.19	0.23	0.51	0.23	0.24	0.26	0.19	0.24	0.54	0.17	0.27	0.13	0.87	0.69	0.57
8924.....	1	0.59	10.96	4.93	2.52	11.22	5.32	4.67	4.88	5.07	1.28	9.17	10.53	5.79	1.13	15.27	9.88	7.97
		0.02	0.21	0.21	0.25	0.35	0.20	0.22	0.25	0.19	0.20	0.31	0.17	0.38	0.16	0.53	0.31	0.65
175164....	1	...	10.40	4.92	2.19	8.87	3.90	4.36	3.64	4.68	1.38	12.81	9.65	1.63	0.88	16.16	9.77	8.80
		...	0.32	0.30	0.37	0.73	0.32	0.33	0.38	0.32	0.31	0.60	0.25	0.59	0.24	1.27	0.75	1.02
232078....	1	...	7.44	3.51	1.76	8.83	2.66	3.08	2.52	1.68	0.57	1.72	7.17	8.18	−0.10	18.72	10.09	4.70
		...	0.25	0.23	0.25	0.68	0.23	0.23	0.26	0.18	0.26	0.74	0.19	0.27	0.11	1.18	0.75	0.52
1377947[d]	2	...	13.72	6.44	3.63	10.48	4.87	4.37	4.68	5.13	1.36	5.14	13.42	17.27	1.29	20.69	11.44	10.69
		...	0.19	0.19	0.23	0.50	0.22	0.23	0.25	0.22	0.21	0.54	0.16	0.31	0.12	1.14	0.70	0.65
59-23.....	1	0.76	11.87	4.14	2.85	8.17	5.78	3.39	3.95	5.63	0.35	1.84	12.09	12.51	1.04	19.66	13.17	10.62
		0.02	0.41	0.42	0.47	0.88	0.41	0.45	0.49	0.38	0.47	0.84	0.33	0.64	0.26	0.94	0.51	1.20
59-157....	1	0.78	12.72	4.88	2.09	13.70	5.47	3.32	3.75	4.84	0.86	3.27	11.99	10.06	0.87	22.40	7.67	4.87
		0.02	0.45	0.46	0.55	0.92	0.47	0.52	0.56	0.45	0.53	0.90	0.37	0.77	0.30	0.84	0.76	1.45
59-563....	1	0.68	9.04	4.95	3.05	11.39	3.12	3.21	3.70	5.31	0.77	7.61	7.98	5.78	0.26	20.19	9.82	6.68
		0.02	0.42	0.38	0.43	0.71	0.40	0.43	0.46	0.36	0.42	0.61	0.33	0.68	0.27	0.75	0.52	1.21

TABLE 5

EQUIVALENT WIDTHS OF NON-BULGE K GIANTS (CONTINUED)

Name[a]	N[b]	$(J-K)_0$ [c]	2 Mg b	3 Fe 52	4 Fe 53	7 G ps	9 Mg b	10 Fe 52	11 Fe 53	12 Na 58	13 Hβ	14 CN	16 Mg_2	18 TiO_2	23 Hα	25 Ca K	26 Ca H	27 $\sum$w
59-587	1	0.64	11.08	4.98	3.15	10.00	4.13	3.68	3.33	4.85	0.93	6.21	9.12	3.08	0.33	16.70	12.71	5.31
		0.02	0.43	0.43	0.50	0.93	0.45	0.48	0.55	0.44	0.45	0.85	0.37	0.86	0.39	1.29	0.65	1.50
59-622	2	0.85	13.26	5.45	3.09	10.54	5.26	3.80	3.97	7.43	0.44	4.97	12.89	17.70	1.10	17.49	8.33	8.12
		0.02	0.22	0.22	0.26	0.52	0.24	0.25	0.27	0.20	0.27	0.48	0.18	0.33	0.13	0.75	0.51	0.68
59-857	1	0.74	8.68	3.17	1.65	13.30	3.56	3.85	3.75	7.09	1.08	6.20	8.98	3.55	1.34	20.83	13.66	5.02
		0.02	0.57	0.55	0.63	0.93	0.53	0.55	0.62	0.45	0.55	0.88	0.43	0.92	0.33	1.03	0.54	1.62
65-15	1	0.83	5.69	3.07	2.20	11.33	2.88	2.04	1.71	3.75	1.14	4.52	4.13	2.19	0.98	18.41	11.18	7.77
		0.05	0.42	0.37	0.41	0.73	0.35	0.39	0.45	0.35	0.36	0.74	0.32	0.65	0.28	1.01	0.61	1.12
65-46	1	0.58	2.05	1.77	0.29	9.73	2.57	2.46	−0.52	3.43	1.47	2.80	1.66	1.19	2.14	12.97	8.37	6.50
		0.05	0.69	0.60	0.69	0.84	0.50	0.58	0.74	0.58	0.50	0.77	0.49	1.10	0.42	1.03	0.63	1.91
65-60	1	0.78	5.10	5.34	5.84	0.14	2.76	5.39	5.96	0.97	−0.38	2.20	−0.56	10.29	2.43	15.78	−25.39	0.58
		0.05	1.96	1.57	1.63	4.71	1.60	1.68	1.92	1.90	1.77	3.63	1.66	2.98	1.22	5.36	11.13	5.95
65-120	1	0.88	3.50	2.27	1.17	5.53	1.21	1.55	2.41	2.56	0.63	−4.10	2.87	2.76	1.31	9.65	8.59	1.32
		0.05	0.61	0.54	0.60	0.92	0.50	0.55	0.61	0.52	0.51	0.83	0.45	0.90	0.34	0.92	0.53	1.64
65-153	1	0.91	6.74	3.96	1.74	9.48	1.99	4.20	3.27	3.77	0.18	8.76	6.25	3.78	1.13	27.77	15.48	5.98
		0.05	0.48	0.42	0.48	0.96	0.43	0.43	0.48	0.38	0.46	0.85	0.36	0.67	0.24	0.78	0.50	1.20

NOTES— Equivalent widths and errors in Å (derived in § III). Errors are listed underneath each measurement, including $(J-K)_0$. Feature names and numbers are from Table 3.

[a] Name, BS or HD. Cluster members: 59=NGC 5927; star numbers from Menzies, 1974; 65=NGC 6522; star numbers from Arp, 1965. (See also notes to Table 2.)

[b] Number of separate observations, which were averaged, and errors reduced by $\sqrt{N}$.

[c] $(J-K)_0$ color, and error. Sources of observations in Table 2. For members of NGC 6522, $(J-K)_0$ was derived from a plot of $(J-K)$ vs $(B-V)$ for members of M13 from Frogel *et al.* 1983.

[d] HD 1377947 a very metal rich star; Gunn, 1981, private communication.

TABLE 6

EQUIVALENT WIDTHS OF BULGE K GIANTS

Name[a]	N[b]	$(J-K)$ [c]	2 Mg b	3 Fe 52	4 Fe 53	7 G ps	9 Mg b	10 Fe 52	11 Fe 53	12 Na 58	13 Hβ	14 CN	16 Mg_2	18 TiO_2	23 Hα	25 Ca K	26 Ca H	27 $\sum$w
BL212 ..	1	...	13.25	5.94	2.76	7.16	9.41	3.51	1.10	5.14	3.92	−1.87	12.95	39.93	0.42	17.45	10.53	1.24
		...	0.40	0.41	0.52	1.02	0.39	0.50	0.59	0.56	0.48	1.03	0.34	0.52	0.34	1.16	0.71	1.63
1012....	1	0.95	9.10	3.48	1.52	9.93	4.00	2.75	3.30	6.03	1.19	5.74	8.37	2.16	1.96	19.73	12.33	6.24
		0.03	0.44	0.43	0.51	0.80	0.41	0.46	0.51	0.39	0.41	0.73	0.35	0.81	0.32	0.96	0.56	1.40
1021[d] ..	1	0.74	10.31	5.68	3.36	12.42	5.15	5.72	3.87	...	2.08	11.02	9.10	...	...	...	...	...
		0.03	0.37	0.35	0.42	0.73	0.36	0.39	0.46	...	0.34	0.71	0.31	...	...	...	...	...
1025....	2	0.90	12.73	6.73	3.52	11.41	4.63	5.12	5.00	8.42	1.47	11.18	11.43	6.10	0.58	17.61	13.01	12.25
		0.03	0.35	0.33	0.41	0.65	0.39	0.40	0.44	0.32	0.37	0.53	0.30	0.66	0.28	0.83	0.41	1.14
1039....	2	0.89	13.60	6.72	4.24	10.93	5.87	5.29	6.07	8.40	1.70	8.88	12.64	5.86	1.00	20.66	6.79	11.81
		0.03	0.30	0.30	0.35	0.63	0.33	0.35	0.37	0.28	0.34	0.55	0.26	0.59	0.25	0.76	0.65	1.02
1053....	1	0.68	4.01	2.19	1.10	8.07	1.19	1.58	1.20	3.78	0.52	0.70	3.54	2.57	1.40	12.68	9.56	3.65
		0.03	0.54	0.49	0.55	0.59	0.45	0.50	0.59	0.44	0.42	0.50	0.40	0.81	0.30	0.57	0.34	1.44
1064....	1	1.05	14.84	6.74	4.06	7.61	4.66	4.19	5.28	6.95	0.38	0.05	14.32	14.56	1.14	6.88	20.93	9.49
		0.04	0.39	0.40	0.48	1.08	0.49	0.49	0.51	0.36	0.51	1.03	0.34	0.60	0.24	1.57	0.12	1.17
1076....	1	1.00	14.56	6.73	3.80	11.48	4.73	5.18	5.76	7.30	0.90	8.33	14.00	11.75	1.06	18.76	12.84	10.92
		0.03	0.31	0.32	0.39	0.64	0.38	0.39	0.41	0.29	0.38	0.57	0.27	0.50	0.19	0.87	0.45	0.95
1083....	1	0.82	12.29	6.22	3.41	10.21	5.19	3.77	5.33	7.85	0.47	9.47	10.30	5.14	1.99	17.16	10.33	8.05
		0.05	0.43	0.41	0.51	0.85	0.45	0.50	0.53	0.43	0.47	0.73	0.37	0.90	0.37	1.11	0.69	1.59
1093....	1	0.89	10.54	3.42	1.94	10.29	5.21	3.82	3.63	5.83	0.94	5.42	10.19	5.64	1.09	15.04	11.67	6.42
		0.05	0.30	0.31	0.35	0.56	0.28	0.31	0.35	0.29	0.31	0.50	0.24	0.56	0.21	0.66	0.35	1.00
1102....	1	0.83	9.23	3.27	2.70	7.81	3.75	3.07	3.47	4.69	0.33	1.78	8.49	3.68	1.36	18.19	8.99	6.83
		0.05	0.42	0.41	0.45	0.74	0.40	0.42	0.48	0.39	0.42	0.66	0.33	0.72	0.26	0.70	0.50	1.25
1129....	1	0.90	12.22	6.24	2.97	8.14	5.00	6.61	4.88	9.57	−0.44	10.21	11.65	7.42	1.98	15.70	9.64	9.10
		0.05	0.46	0.44	0.54	0.97	0.49	0.48	0.54	0.39	0.55	0.74	0.38	0.81	0.28	1.16	0.74	1.45
1140....	1	0.95	8.97	3.36	2.04	10.72	4.09	2.63	3.41	4.38	0.44	3.14	8.20	3.30	1.28	16.41	12.74	7.87
		0.03	0.34	0.33	0.38	0.62	0.32	0.35	0.39	0.32	0.33	0.61	0.27	0.61	0.25	0.88	0.45	1.05
1141....	1	0.94	9.55	3.34	1.55	11.09	5.55	3.17	3.51	3.75	1.24	3.83	9.35	2.64	1.69	19.82	12.93	6.77
		0.03	0.43	0.43	0.50	0.78	0.38	0.44	0.50	0.42	0.40	0.76	0.33	0.80	0.32	0.90	0.52	1.38
1144....	1	1.01	12.72	5.37	2.25	11.13	5.59	4.91	5.33	6.61	0.33	4.17	12.31	13.91	0.47	21.75	9.16	8.53
		0.03	0.40	0.41	0.50	0.90	0.42	0.44	0.48	0.39	0.45	0.90	0.33	0.70	0.34	1.07	0.84	1.36
1145....	2	0.76	2.73	2.23	1.36	8.53	1.64	1.88	1.24	3.80	1.22	0.09	1.75	0.88	1.71	13.41	10.03	4.15
		0.03	0.29	0.25	0.28	0.34	0.22	0.25	0.30	0.23	0.21	0.31	0.21	0.45	0.17	0.38	0.22	0.78
1151....	1	0.78	5.11	2.03	1.00	9.98	2.78	1.93	2.03	3.34	2.11	2.51	4.76	1.16	0.55	15.20	10.10	−0.15
		0.05	0.45	0.41	0.47	0.64	0.37	0.42	0.48	0.40	0.34	0.60	0.33	0.77	0.35	0.80	0.47	1.38

TABLE 6

EQUIVALENT WIDTHS OF BULGE K GIANTS (CONTINUED)

Name[a]	N[b]	$(J-K)$ [c]	2 Mg b	3 Fe 52	4 Fe 53	7 G ps	9 Mg b	10 Fe 52	11 Fe 53	12 Na 58	13 Hβ	14 CN	16 Mg_2	18 TiO_2	23 Hα	25 Ca K	26 Ca H	27 $\sum$w
1153....	1	0.73	6.70	2.54	1.18	8.51	4.06	3.89	2.41	5.63	1.23	5.78	6.12	2.70	1.08	13.77	11.45	5.21
		0.05	0.52	0.50	0.58	0.81	0.44	0.49	0.59	0.47	0.44	0.68	0.40	0.96	0.43	1.00	0.52	1.68
1155....	1	0.92	11.70	4.59	3.06	11.19	5.06	4.10	4.76	6.23	1.54	9.62	10.82	3.56	0.88	20.59	11.53	10.76
		0.03	0.36	0.37	0.43	0.73	0.38	0.40	0.45	0.37	0.38	0.63	0.30	0.75	0.33	0.84	0.54	1.27
1156....	1	0.85	6.43	3.46	2.09	9.11	2.61	3.17	2.70	4.96	1.67	1.68	4.77	3.38	1.25	17.46	13.02	1.51
		0.05	0.49	0.45	0.51	0.81	0.43	0.47	0.54	0.44	0.41	0.77	0.38	0.85	0.37	0.95	0.50	1.55
1164....	1	0.90	9.03	3.24	1.35	9.18	3.70	2.67	2.47	5.46	−0.87	5.20	8.59	2.86	0.94	18.47	11.41	5.53
		0.03	0.38	0.38	0.45	0.71	0.36	0.40	0.46	0.35	0.38	0.64	0.30	0.71	0.31	0.83	0.49	1.24
1174....	1	0.78	5.01	2.77	0.80	7.01	2.90	3.24	1.87	3.86	−0.26	3.85	4.17	2.60	1.18	16.39	10.83	6.35
		0.05	0.50	0.46	0.54	0.77	0.41	0.46	0.55	0.46	0.43	0.66	0.38	0.89	0.37	0.84	0.49	1.53
1181....	1	0.75	6.52	2.76	0.92	9.14	4.39	3.75	1.92	4.68	2.06	4.02	6.20	4.32	1.08	17.36	9.95	3.89
		0.05	0.55	0.53	0.62	0.87	0.46	0.52	0.63	0.50	0.45	0.78	0.42	0.98	0.43	0.99	0.62	1.77
1194....	1	0.94	11.08	4.12	2.16	11.48	5.73	4.31	3.55	5.56	1.23	3.02	11.08	5.48	1.05	15.95	8.83	8.66
		0.03	0.41	0.42	0.49	0.84	0.39	0.43	0.50	0.39	0.41	0.86	0.33	0.76	0.33	1.38	0.90	1.35
1196....	1	1.00	14.71	6.37	4.14	13.69	5.70	4.71	6.33	8.99	0.93	6.54	14.26	19.52	1.02	11.71	13.94	11.25
		0.03	0.31	0.32	0.38	0.82	0.37	0.38	0.39	0.31	0.40	0.89	0.27	0.54	0.26	1.79	0.73	1.10
1202....	1	0.90	12.96	6.35	3.81	10.35	4.58	4.54	4.95	8.73	0.60	5.29	12.33	7.58	0.81	10.36	3.56	8.76
		0.03	0.51	0.50	0.60	0.91	0.57	0.59	0.64	0.42	0.56	0.81	0.43	0.82	0.31	1.30	0.93	1.49
1304....	1	0.56	10.38	4.54	3.09	11.16	5.51	5.09	4.20	5.94	−0.03	8.89	9.60	4.69	1.12	13.90	11.40	7.47
		0.05	0.45	0.44	0.50	0.81	0.42	0.46	0.53	0.43	0.46	0.71	0.36	0.86	0.38	1.29	0.65	1.52
1308....	1	0.48	5.37	2.70	0.94	5.49	3.37	2.02	0.58	2.83	3.14	−1.88	4.74	2.36	1.73	9.02	8.32	2.16
		0.05	0.46	0.43	0.51	0.47	0.37	0.45	0.54	0.44	0.33	0.40	0.35	0.82	0.30	0.45	0.26	1.46
1319....	1	0.98	11.09	4.25	3.06	9.09	5.57	3.92	5.07	5.58	1.58	−0.76	10.39	14.26	0.70	12.55	9.98	4.56
		0.05	0.43	0.44	0.50	0.83	0.42	0.47	0.51	0.44	0.43	0.82	0.35	0.76	0.38	1.04	0.58	1.53
1320....	1	0.91	13.61	7.29	5.63	5.71	1.54	2.20	5.65	8.09	0.84	−22.17	12.81	25.99	1.28	−4.40	19.79	6.63
		0.03	1.10	1.04	1.19	3.02	1.46	1.42	1.40	0.97	1.38	5.36	0.95	1.32	0.54	5.35	0.56	3.17
1322....	1	0.95	11.82	5.51	2.96	11.25	4.39	3.96	3.94	4.55	1.58	3.36	11.05	5.61	0.99	13.28	13.58	6.35
		0.03	0.30	0.29	0.34	0.64	0.31	0.33	0.36	0.26	0.32	0.66	0.25	0.44	0.16	1.11	0.47	0.81
1329....	1	0.98	12.00	5.67	2.66	10.68	5.73	4.42	3.66	5.71	0.53	8.50	11.56	5.70	1.72	20.99	15.61	10.26
		0.05	0.46	0.45	0.55	1.01	0.47	0.51	0.58	0.45	0.50	0.87	0.38	0.87	0.36	1.29	0.61	1.50
1335....	1	0.95	10.53	4.78	2.49	14.65	4.60	4.40	2.97	5.31	0.49	9.58	10.11	4.66	1.72	21.51	11.03	10.75
		0.05	0.40	0.38	0.45	0.69	0.39	0.41	0.48	0.38	0.42	0.61	0.32	0.71	0.24	0.79	0.54	1.21
1368....	1	0.20	2.33	1.70	0.33	1.17	1.17	1.22	0.19	0.84	5.15	−4.20	1.94	0.56	3.35	4.54	7.08	1.01
		0.05	0.30	0.28	0.33	0.24	0.24	0.29	0.35	0.27	0.19	0.20	0.22	0.44	0.13	0.21	0.12	0.79

TABLE 6

EQUIVALENT WIDTHS OF BULGE K GIANTS (CONTINUED)

Name[a]	N[b]	$(J-K)$ [c]	2 Mg b	3 Fe 52	4 Fe 53	7 G ps	9 Mg b	10 Fe 52	11 Fe 53	12 Na 58	13 Hβ	14 CN	16 Mg_2	18 TiO_2	23 Hα	25 Ca K	26 Ca H	27 $\sum$w
2018....	1	0.98	9.86	4.99	2.78	6.33	3.86	4.13	2.60	5.61	0.75	3.73	9.73	3.08	1.46	17.13	9.50	6.38
		0.05	0.52	0.49	0.57	0.87	0.50	0.54	0.62	0.37	0.51	0.72	0.40	0.64	0.22	0.79	0.52	1.16
2026....	1	1.01	12.48	6.33	3.90	10.91	4.70	4.79	5.06	6.21	0.45	4.51	10.88	6.95	1.34	19.59	12.13	10.56
		0.05	0.35	0.34	0.40	0.80	0.38	0.40	0.44	0.35	0.40	0.80	0.30	0.67	0.29	1.06	0.62	1.18
2027....	1	1.04	14.63	6.90	3.73	10.77	5.39	4.92	4.55	6.46	2.34	5.67	14.23	18.76	1.54	16.53	9.88	11.86
		0.02	0.34	0.35	0.43	0.72	0.41	0.42	0.46	0.29	0.41	0.67	0.29	0.41	0.15	0.91	0.57	0.86
2033....	1	0.95	4.84	1.19	0.51	11.67	3.06	3.07	2.26	...	1.46	3.18	5.80	...	...	...	...	...
		0.03	0.61	0.59	0.66	1.10	0.50	0.55	0.66	...	0.47	1.21	0.44	...	...	...	...	...
2040....	1	0.75	3.47	0.31	−0.49	9.90	3.27	1.84	2.44	3.62	0.78	1.66	2.94	2.06	2.43	15.62	9.60	7.07
		0.03	0.53	0.51	0.58	0.67	0.40	0.47	0.54	0.47	0.41	0.62	0.39	0.91	0.34	0.73	0.46	1.55
2041....	1	0.47	3.07	3.75	2.80	1.17	−0.46	3.22	2.40	2.13	6.48	−4.80	2.15	1.70	3.39	−0.28	6.20	2.81
		0.05	0.40	0.34	0.39	0.38	0.35	0.36	0.43	0.37	0.25	0.33	0.30	0.68	0.21	0.42	0.22	1.20
2042....	1	0.99	9.31	3.46	2.04	8.41	4.07	3.07	2.65	3.70	1.02	3.09	8.30	3.98	1.58	16.98	13.90	6.88
		0.03	0.45	0.44	0.51	0.86	0.42	0.46	0.54	0.44	0.43	0.80	0.36	0.81	0.34	1.10	0.53	1.43
2044....	1	1.02	10.96	4.25	3.21	5.67	3.59	1.40	3.33	5.04	−0.17	1.97	10.66	12.73	1.19	12.78	9.95	8.96
		0.05	0.44	0.45	0.50	0.71	0.47	0.51	0.55	0.35	0.47	0.59	0.36	0.52	0.19	0.70	0.40	1.03
2049....	1	0.77	5.56	3.69	2.09	9.85	2.90	3.28	2.73	3.26	1.55	2.89	3.97	1.09	1.46	13.40	11.13	2.96
		0.03	0.43	0.38	0.43	0.58	0.36	0.39	0.46	0.40	0.36	0.51	0.33	0.74	0.26	0.61	0.32	1.30
2110....	1	1.20	14.72	7.42	4.12	12.44	7.53	4.76	4.51	5.71	4.16	0.77	14.21	34.68	0.68	27.44	7.51	4.02
		0.03	0.68	0.68	0.85	1.39	0.75	0.87	0.93	0.74	0.79	1.54	0.59	0.80	0.40	1.34	1.67	2.21
2116....	1	0.96	15.15	7.81	3.33	13.46	5.69	7.77	5.39	6.37	3.00	25.99	14.81	3.53	0.36	...	...	7.78
		0.02	0.53	0.52	0.68	1.17	0.65	0.60	0.70	0.43	0.61	0.61	0.46	0.76	0.28	...	...	1.35
2118....	1	0.94	9.55	3.80	2.25	10.35	5.40	3.03	3.47	2.89	0.51	4.51	8.60	4.28	1.57	21.43	12.61	8.86
		0.05	0.43	0.42	0.49	0.84	0.39	0.45	0.50	0.43	0.43	0.81	0.34	0.77	0.32	0.97	0.61	1.34
2119....	1	0.85	1.77	1.38	1.09	9.10	1.60	1.70	1.83	3.26	−0.04	0.01	0.86	1.59	1.37	14.32	10.68	3.33
		0.03	0.47	0.41	0.45	0.62	0.35	0.40	0.47	0.40	0.36	0.59	0.34	0.75	0.32	0.71	0.40	1.31
2122....	1	1.13	11.99	4.54	2.23	9.04	5.18	3.57	3.73	4.93	0.92	3.35	12.10	14.29	0.97	18.58	11.98	7.09
		0.03	0.21	0.22	0.26	0.39	0.22	0.24	0.27	0.19	0.23	0.37	0.17	0.29	0.12	0.45	0.27	0.58
2123....	1	1.24	16.16	6.66	3.08	7.93	10.76	1.77	2.63	5.12	2.99	−1.20	16.13	39.98	0.83	16.53	10.30	3.91
		0.02	0.30	0.33	0.42	0.74	0.32	0.44	0.47	0.36	0.43	0.75	0.27	0.30	0.15	0.97	0.57	0.94
2136....	1	0.81	0.65	0.44	0.83	6.56	0.75	1.35	1.71	4.20	0.11	1.18	0.09	−0.24	1.60	13.03	8.95	−0.06
		0.05	0.48	0.42	0.45	0.61	0.35	0.39	0.46	0.37	0.35	0.53	0.34	0.74	0.30	0.67	0.41	1.30
2139....	2	0.65	4.89	2.46	2.06	8.43	2.82	2.12	3.23	3.65	2.00	1.93	3.59	1.84	1.18	10.53	8.14	3.78
		0.05	0.26	0.24	0.27	0.34	0.21	0.24	0.28	0.25	0.20	0.31	0.20	0.49	0.22	0.41	0.24	0.86

TABLE 6

EQUIVALENT WIDTHS OF BULGE K GIANTS (CONTINUED)

Name[a]	N[b]	$(J-K)$ [c]	2 Mg b	3 Fe 52	4 Fe 53	7 G ps	9 Mg b	10 Fe 52	11 Fe 53	12 Na 58	13 Hβ	14 CN	16 Mg_2	18 TiO_2	23 Hα	25 Ca K	26 Ca H	27 $\sum$w
2145....	1	0.82	11.37	5.55	2.67	11.67	5.14	6.47	4.48	7.14	1.72	7.96	10.23	2.81	0.96	8.50	6.60	11.98
		0.03	0.47	0.46	0.55	0.91	0.47	0.48	0.57	0.45	0.47	0.81	0.39	0.95	0.42	1.73	1.05	1.57
2146....	1	0.82	8.06	4.84	2.28	9.77	4.42	4.51	3.54	6.46	1.42	8.11	7.35	4.10	1.16	14.70	11.61	7.24
		0.03	0.38	0.34	0.41	0.52	0.33	0.37	0.42	0.29	0.34	0.43	0.30	0.57	0.21	0.63	0.35	1.00
2147....	1	0.71	1.95	1.02	1.06	8.50	1.13	1.23	0.24	4.28	2.71	−4.04	1.08	1.50	0.97	14.14	9.38	2.85
		0.02	0.73	0.65	0.71	0.93	0.56	0.63	0.77	0.60	0.51	0.95	0.53	1.20	0.52	1.06	0.64	2.12
2151....	1	0.94	8.50	3.02	1.20	9.21	4.15	2.63	2.11	3.64	1.53	4.44	7.86	3.22	1.24	15.95	12.08	7.42
		0.05	0.43	0.43	0.50	0.78	0.39	0.44	0.51	0.41	0.39	0.71	0.34	0.78	0.32	0.98	0.51	1.35
2154....	1	0.82	3.37	2.05	1.53	8.80	2.07	2.02	1.55	4.01	0.84	−1.52	2.15	3.45	1.44	14.25	9.65	2.05
		0.05	0.54	0.48	0.53	0.77	0.43	0.48	0.57	0.46	0.43	0.78	0.40	0.88	0.38	0.96	0.57	1.62
2166....	1	0.78	−0.05	0.01	0.00	4.48	0.35	1.42	−0.41	...	1.40	2.44	−0.01	...	...	...	...	...
		0.05	0.78	0.71	0.79	1.07	0.58	0.66	0.83	...	0.51	0.98	0.55	...	...	...	...	...
2167....	1	0.98	12.84	6.47	4.60	11.69	5.07	4.76	5.85	7.58	1.30	14.90	11.31	6.13	0.92	11.16	19.53	10.63
		0.05	0.49	0.47	0.55	1.14	0.53	0.56	0.60	0.47	0.56	0.91	0.42	0.95	0.42	2.56	0.44	1.67
2171....	1	0.94	10.07	3.90	2.97	8.93	4.58	3.03	4.08	6.92	1.81	5.70	8.42	6.00	1.40	12.24	13.64	4.33
		0.05	0.48	0.48	0.53	0.94	0.46	0.51	0.57	0.44	0.46	0.82	0.40	0.90	0.39	1.32	0.57	1.65
2173....	1	0.81	2.94	−0.16	0.28	5.68	2.89	1.33	1.80	3.29	1.35	0.78	2.59	0.03	1.38	15.38	10.75	−3.81
		0.03	0.60	0.57	0.62	0.86	0.45	0.53	0.61	0.52	0.45	0.77	0.43	1.00	0.40	0.94	0.53	1.79
2174....	1	0.70	2.06	0.86	1.72	9.40	2.55	2.27	2.37	2.76	0.78	−0.67	1.00	0.10	1.76	15.49	9.48	0.11
		0.05	0.68	0.61	0.64	0.89	0.49	0.57	0.66	0.56	0.50	0.88	0.49	1.03	0.40	1.03	0.65	1.82
2199....	1	0.80	9.77	4.53	2.22	10.19	4.11	3.78	3.44	3.79	1.22	4.32	9.36	4.10	0.73	16.16	10.46	2.89
		0.05	0.31	0.30	0.36	0.46	0.30	0.32	0.37	0.29	0.29	0.41	0.25	0.51	0.19	0.52	0.31	0.93
2201....	1	0.98	12.07	4.69	4.02	13.25	4.96	2.67	5.58	6.24	2.14	6.02	10.25	4.88	1.21	6.75	10.93	9.11
		0.05	0.48	0.49	0.55	0.98	0.51	0.57	0.59	0.48	0.50	0.97	0.42	0.95	0.41	1.95	0.86	1.66
2206....	1	0.57	7.35	3.36	2.99	7.90	3.76	1.19	3.11	3.55	2.98	−1.40	5.78	2.22	2.50	10.51	8.39	1.79
		0.06	0.53	0.51	0.57	0.54	0.46	0.56	0.62	0.51	0.40	0.47	0.42	0.97	0.31	0.51	0.30	1.70
2215....	2	0.70	1.98	0.97	0.44	8.74	2.20	2.31	1.51	1.49	1.38	−0.61	1.27	1.30	1.35	13.53	9.62	3.70
		0.03	0.32	0.29	0.32	0.41	0.24	0.27	0.33	0.29	0.23	0.40	0.23	0.54	0.23	0.52	0.30	0.94
2216....	1	0.85	2.39	2.34	0.68	10.35	1.47	3.47	1.70	4.58	1.53	0.84	1.66	2.35	1.54	12.73	10.79	0.85
		0.05	0.55	0.47	0.54	0.74	0.42	0.45	0.55	0.43	0.41	0.72	0.40	0.85	0.36	1.00	0.52	1.52
2238....	1	−5.00	14.78	6.91	3.08	−6.92	13.86	−3.42	−1.43	8.92	11.12	3.86	13.41	41.74	0.13	−4.21	16.11	−7.41
		−5.00	1.24	1.30	1.72	4.27	0.97	1.98	2.12	1.46	1.47	2.43	1.12	1.42	0.83	5.45	1.25	4.85
2240....	1	0.73	9.63	4.30	2.47	10.12	3.90	3.80	2.86	3.56	1.93	3.07	8.90	1.69	1.00	14.97	10.30	7.75
		0.03	0.33	0.32	0.38	0.40	0.32	0.35	0.41	0.32	0.28	0.34	0.26	0.59	0.22	0.39	0.23	1.01

TABLE 6

EQUIVALENT WIDTHS OF BULGE K GIANTS (CONTINUED)

Name[a]	N[b]	$(J-K)$ [c]	2 Mg b	3 Fe 52	4 Fe 53	7 G ps	9 Mg b	10 Fe 52	11 Fe 53	12 Na 58	13 Hβ	14 CN	16 Mg_2	18 TiO_2	23 Hα	25 Ca K	26 Ca H	27 $\sum$w
2242....	1	0.74	2.41	1.72	1.04	−0.37	0.44	0.10	0.30	0.18	9.06	−10.83	1.92	1.15	4.11	−9.46	8.91	−2.66
		0.05	0.32	0.30	0.35	0.25	0.27	0.32	0.38	0.35	0.17	0.24	0.24	0.61	0.18	0.29	0.11	1.11
2244....	1	1.01	10.72	4.72	2.82	8.95	4.16	3.22	3.41	5.00	1.35	7.55	9.74	2.91	1.21	15.16	8.55	5.01
		0.02	0.49	0.48	0.55	0.83	0.50	0.54	0.59	0.36	0.50	0.68	0.40	0.61	0.21	1.02	0.71	1.14
2252....	1	0.92	5.19	1.98	1.00	9.22	2.91	2.87	2.93	4.18	0.45	−2.33	4.63	1.59	2.14	19.12	11.62	1.90
		0.03	0.51	0.48	0.54	0.81	0.42	0.46	0.53	0.44	0.43	0.84	0.38	0.85	0.33	0.90	0.54	1.50
2261....	1	1.03	9.81	3.63	2.24	10.57	4.01	3.98	3.43	4.98	1.03	4.94	9.46	5.79	1.55	21.35	12.11	6.70
		0.03	0.39	0.39	0.44	0.75	0.38	0.40	0.46	0.36	0.39	0.72	0.31	0.69	0.29	0.92	0.58	1.24
3106....	2	0.78	4.95	1.71	0.58	8.95	3.06	2.20	2.21	3.74	1.36	−0.68	4.15	1.80	0.73	13.07	10.08	3.99
		0.03	0.40	0.38	0.44	0.50	0.33	0.37	0.44	0.35	0.31	0.47	0.30	0.64	0.26	0.55	0.31	1.13
3133....	1	0.89	3.14	2.48	1.48	1.03	0.18	1.66	1.22	1.34	6.02	−5.24	2.58	1.28	3.36	2.72	6.86	0.77
		0.05	0.33	0.30	0.35	0.30	0.28	0.32	0.38	0.33	0.20	0.26	0.25	0.58	0.18	0.29	0.16	1.04
3141....	1	0.46	4.23	1.18	0.47	6.63	3.08	0.64	0.71	2.37	2.68	−2.35	3.76	0.80	2.04	10.84	8.77	2.73
		0.03	0.41	0.40	0.46	0.36	0.33	0.41	0.48	0.35	0.29	0.31	0.31	0.60	0.20	0.30	0.18	1.07
3152....	1	0.97	9.27	3.08	1.61	8.42	5.04	2.92	2.94	5.53	0.76	2.89	9.01	4.52	0.99	18.94	12.26	6.18
		0.03	0.40	0.40	0.46	0.81	0.36	0.41	0.46	0.36	0.39	0.79	0.31	0.70	0.31	1.10	0.63	1.26
3157....	1	1.02	11.52	4.64	2.79	11.32	5.26	4.67	4.85	6.48	0.80	8.12	10.64	10.43	1.53	19.63	11.16	7.17
		0.03	0.40	0.40	0.46	0.87	0.40	0.42	0.47	0.37	0.43	0.81	0.33	0.69	0.31	1.26	0.81	1.30
3159....	1	0.86	11.14	5.30	2.85	10.43	5.67	4.87	3.34	5.12	1.17	6.37	9.31	1.11	1.11	10.98	9.92	8.99
		0.05	0.45	0.44	0.52	0.87	0.43	0.48	0.57	0.45	0.46	0.82	0.38	0.92	0.39	1.41	0.72	1.53
3160....	1	0.79	5.32	2.52	1.54	8.65	3.65	2.14	2.61	5.94	1.19	3.98	4.00	3.35	1.06	15.73	11.21	2.35
		0.03	0.46	0.43	0.49	0.70	0.37	0.44	0.50	0.39	0.38	0.63	0.36	0.78	0.34	0.86	0.48	1.40
3164....	1	0.97	12.16	5.26	3.10	9.78	5.10	3.95	4.49	4.39	1.24	4.69	11.49	5.00	0.87	18.48	12.45	7.65
		0.03	0.28	0.29	0.34	0.47	0.30	0.32	0.35	0.27	0.29	0.41	0.24	0.47	0.18	0.48	0.27	0.85
3169....	1	0.44	2.88	2.22	1.27	1.18	1.15	1.20	1.09	0.68	5.90	−5.24	2.19	1.00	2.88	0.71	6.93	−0.90
		0.05	0.31	0.28	0.33	0.25	0.25	0.30	0.35	0.31	0.19	0.22	0.23	0.53	0.17	0.25	0.13	0.97
3197....	1	0.89	11.95	4.46	2.97	11.07	5.99	3.57	5.14	7.10	0.99	8.21	11.25	4.67	0.41	13.54	13.40	11.26
		0.05	0.48	0.50	0.56	0.94	0.48	0.53	0.57	0.46	0.51	0.87	0.40	0.96	0.46	1.54	0.69	1.65
3200....	1	0.76	−0.10	−0.60	−0.10	−0.20	−0.09	0.29	0.24	3.42	5.58	−7.63	−0.57	−0.35	1.73	−3.96	8.64	5.06
		0.03	0.62	0.57	0.63	0.69	0.47	0.54	0.65	0.55	0.38	0.67	0.45	1.09	0.45	0.95	0.39	1.85
3209....	1	0.96	13.76	7.03	4.00	10.24	5.40	5.78	5.31	8.25	1.92	7.25	13.32	8.57	1.36	4.18	9.10	7.18
		0.03	0.38	0.37	0.45	0.75	0.43	0.43	0.48	0.33	0.42	0.67	0.32	0.62	0.22	1.53	0.70	1.15
3224....	1	0.94	9.94	3.66	1.94	10.21	4.93	4.45	2.10	3.82	1.82	7.53	9.68	3.62	1.31	15.84	9.63	9.76
		0.05	0.51	0.51	0.59	0.96	0.48	0.51	0.62	0.49	0.48	0.84	0.40	0.91	0.38	1.31	0.80	1.57

TABLE 6

EQUIVALENT WIDTHS OF BULGE K GIANTS (CONTINUED)

Name[a]	N[b]	$(J-K)$ [c]	2 Mg b	3 Fe 52	4 Fe 53	7 G ps	9 Mg b	10 Fe 52	11 Fe 53	12 Na 58	13 Hβ	14 CN	16 Mg_2	18 TiO_2	23 Hα	25 Ca K	26 Ca H	27 $\sum$w
4003....	2	0.84	2.60	2.08	0.81	9.82	1.01	2.21	1.51	3.93	1.30	−0.83	1.98	−0.22	1.29	16.69	9.50	4.95
		0.03	0.30	0.26	0.29	0.38	0.23	0.26	0.30	0.22	0.22	0.37	0.21	0.41	0.15	0.42	0.28	0.70
4011....	1	0.78	10.13	6.38	3.15	10.41	3.59	4.27	4.76	6.76	1.55	7.94	8.90	2.24	1.11	16.74	10.80	7.38
		0.05	0.45	0.41	0.51	0.62	0.46	0.50	0.54	0.39	0.43	0.52	0.38	0.78	0.29	0.61	0.37	1.35
4022....	1	0.94	13.11	6.16	3.81	14.16	5.14	4.78	5.60	9.70	1.69	7.63	11.95	7.01	1.48	14.74	11.61	7.45
		0.05	0.35	0.35	0.42	0.73	0.39	0.40	0.44	0.32	0.39	0.73	0.30	0.71	0.30	1.23	0.62	1.28
4025....	1	0.78	11.79	4.68	2.38	11.95	5.19	4.38	4.52	5.38	1.59	10.41	11.98	1.32	1.84	14.70	11.09	11.55
		0.03	0.45	0.47	0.56	0.66	0.47	0.50	0.56	0.43	0.44	0.52	0.37	0.82	0.27	0.76	0.41	1.36
4063....	1	0.86	12.79	5.96	3.09	13.78	6.43	5.72	4.76	7.19	2.38	13.92	11.83	5.19	1.69	6.44	15.90	11.34
		0.05	0.44	0.44	0.53	0.90	0.45	0.49	0.56	0.44	0.46	0.77	0.38	0.90	0.38	2.05	0.60	1.54
4065....	1	0.84	11.95	4.45	2.37	9.29	6.38	3.53	4.00	4.80	0.14	4.73	11.30	3.91	1.22	18.80	9.27	9.46
		0.05	0.57	0.60	0.71	0.93	0.57	0.66	0.74	0.54	0.61	0.76	0.48	0.98	0.36	0.91	0.64	1.69
4071....	1	0.81	7.07	2.31	1.29	10.71	3.95	3.18	2.44	3.96	1.58	1.17	6.82	1.83	1.22	14.66	12.12	5.09
		0.05	0.44	0.43	0.49	0.67	0.38	0.42	0.49	0.41	0.38	0.67	0.33	0.79	0.34	0.85	0.44	1.37
4072....	1	0.93	13.52	5.60	3.78	10.75	5.56	5.32	5.92	7.47	0.96	7.76	12.69	7.56	0.98	15.10	11.72	9.31
		0.05	0.39	0.41	0.47	0.88	0.44	0.45	0.49	0.39	0.45	0.81	0.34	0.80	0.37	1.29	0.67	1.43
4146....	1	0.82	9.68	5.10	2.36	10.50	4.33	4.01	3.58	5.32	−0.27	7.02	8.04	1.32	1.26	19.10	11.18	4.61
		0.05	0.46	0.43	0.52	0.85	0.44	0.48	0.55	0.45	0.47	0.75	0.38	0.92	0.39	0.96	0.60	1.59
4148....	1	0.75	3.44	1.31	2.02	7.40	2.85	1.69	2.45	3.64	1.67	1.16	2.63	3.08	0.81	16.49	10.79	4.12
		0.05	0.50	0.45	0.47	0.78	0.38	0.43	0.49	0.42	0.40	0.69	0.37	0.76	0.29	0.80	0.48	1.37
4164....	1	0.81	11.16	4.49	2.48	9.71	5.36	4.58	3.45	7.55	2.42	5.54	10.71	4.44	1.67	14.32	7.98	14.81
		0.05	0.51	0.51	0.60	0.73	0.50	0.54	0.63	0.43	0.46	0.64	0.41	0.84	0.29	0.80	0.52	1.43
4165....	1	1.01	11.43	3.62	1.00	7.83	4.08	3.04	2.85	5.73	1.16	5.18	11.87	6.56	1.25	20.34	11.84	9.58
		0.02	0.46	0.49	0.58	1.07	0.49	0.51	0.58	0.43	0.49	0.99	0.37	0.83	0.35	1.27	0.80	1.46
4167....	1	0.86	13.11	6.78	3.90	15.55	6.07	6.18	5.38	9.32	2.32	7.66	12.19	4.88	0.67	16.71	12.65	10.16
		0.03	0.49	0.47	0.56	1.03	0.51	0.54	0.60	0.45	0.54	1.08	0.41	0.99	0.44	1.98	1.02	1.72
4203....	1	1.15	8.30	4.17	2.23	10.69	2.80	2.78	2.95	3.69	0.83	3.41	7.55	4.19	0.80	16.69	9.79	4.04
		0.05	0.23	0.21	0.25	0.38	0.22	0.24	0.26	0.18	0.22	0.37	0.18	0.30	0.11	0.52	0.34	0.54
4285....	1	0.90	11.90	5.62	3.60	12.89	4.05	4.45	4.87	7.76	0.22	9.73	10.87	4.23	1.63	19.88	16.56	8.15
		0.05	0.42	0.41	0.48	0.86	0.45	0.46	0.51	0.39	0.46	0.81	0.35	0.83	0.34	1.29	0.53	1.46
4297....	1	0.85	10.13	5.23	3.82	8.01	3.78	4.88	4.76	5.33	0.78	4.37	8.44	4.44	0.96	13.26	9.94	3.57
		0.05	0.44	0.42	0.47	0.91	0.44	0.45	0.51	0.43	0.45	0.84	0.37	0.82	0.37	1.28	0.72	1.50
4312....	1	0.71	1.39	0.37	0.14	7.64	2.38	1.79	0.92	4.10	1.22	−2.30	1.89	1.14	0.59	13.70	9.60	−1.89
		0.03	0.53	0.48	0.53	0.65	0.38	0.44	0.53	0.43	0.37	0.63	0.37	0.85	0.39	0.74	0.44	1.54

TABLE 6

EQUIVALENT WIDTHS OF BULGE K GIANTS (CONTINUED)

Name[a]	N[b]	$(J-K)$ [c]	2 Mg b	3 Fe 52	4 Fe 53	7 G ps	9 Mg b	10 Fe 52	11 Fe 53	12 Na 58	13 Hβ	14 CN	16 Mg_2	18 TiO_2	23 Hα	25 Ca K	26 Ca H	27 $\sum$w
4315....	1	0.92	9.38	4.24	2.54	10.64	4.40	2.77	3.15	3.39	0.55	−1.12	7.52	3.62	0.09	11.65	9.00	5.29
		0.05	0.56	0.53	0.62	0.97	0.52	0.59	0.66	0.55	0.54	1.04	0.46	1.05	0.50	1.33	0.78	1.85
4325....	1	0.87	11.35	6.21	3.88	11.56	2.76	5.41	5.43	7.84	2.15	10.98	10.50	6.87	0.67	16.91	9.72	5.22
		0.03	0.57	0.54	0.64	0.87	0.64	0.61	0.67	0.48	0.55	0.69	0.47	0.91	0.37	1.03	0.66	1.71
4329....	2	1.00	6.47	2.97	1.26	9.43	2.64	2.88	2.59	4.07	1.15	1.03	6.24	1.91	1.48	17.43	12.19	4.84
		0.03	0.25	0.23	0.27	0.37	0.22	0.24	0.28	0.21	0.22	0.36	0.19	0.39	0.15	0.44	0.25	0.69
5006....	1	0.80	0.64	0.50	0.60	6.08	0.14	1.26	1.06	...	1.16	−0.84	0.05	...	...	...	...	...
		0.05	0.37	0.34	0.38	0.54	0.29	0.32	0.39	...	0.25	0.54	0.27	...	...	...	...	...
5006[e]...	1	0.80	−0.90	0.50	−0.80	8.37	−0.50	0.65	−0.07	4.04	0.04	−2.15	−0.47	2.37	1.63	9.53	7.63	4.96
		0.05	0.78	0.65	0.74	0.90	0.56	0.62	0.73	0.56	0.56	0.85	0.53	1.03	0.36	0.97	0.57	1.80
5017....	1	...	0.53	1.33	0.56	2.51	1.11	1.83	1.07	...	5.66	−2.13	0.93	...	...	...	...	...
		...	0.76	0.68	0.79	0.90	0.56	0.67	0.82	...	0.42	0.88	0.54	...	...	...	...	...
5024....	1	0.91	14.24	6.57	4.99	10.31	6.15	3.77	6.11	3.88	1.75	20.81	12.24	2.63	0.62	...	...	8.96
		0.05	0.85	0.86	0.98	2.10	0.93	1.06	1.07	0.95	1.01	1.22	0.76	1.66	0.60	...	...	2.83
5060....	1	0.88	8.20	3.19	0.30	9.91	5.10	3.07	2.17	4.90	0.70	2.04	7.86	2.57	1.01	15.79	11.64	2.53
		0.92	0.52	0.50	0.59	0.86	0.44	0.51	0.58	0.46	0.49	0.78	0.40	0.86	0.31	0.91	0.49	1.55
5445....	1	0.92	9.95	4.17	2.93	11.34	4.39	2.69	4.17	3.91	0.56	7.78	9.29	3.70	0.88	17.50	11.79	7.97
		0.05	0.53	0.51	0.57	0.99	0.50	0.55	0.59	0.50	0.56	0.86	0.42	0.90	0.33	1.21	0.68	1.57
6192....	1	0.91	4.12	1.38	1.99	8.05	1.89	1.27	2.72	4.05	1.17	0.92	2.95	3.63	0.64	16.21	10.13	4.41
		0.05	0.39	0.35	0.37	0.59	0.31	0.35	0.39	0.34	0.32	0.53	0.29	0.61	0.23	0.60	0.37	1.10
6322....	1	1.05	11.27	5.16	2.35	15.89	6.73	5.51	4.84	8.52	−1.46	10.77	10.63	1.53	1.44	20.62	16.55	13.95
		0.05	0.56	0.54	0.65	1.03	0.51	0.56	0.64	0.49	0.67	0.94	0.45	1.10	0.37	1.18	0.50	1.78
6406....	1	1.10	13.16	5.82	3.02	11.84	4.59	5.13	5.11	8.06	2.01	7.18	11.86	7.94	0.96	10.40	11.39	10.05
		0.05	0.46	0.46	0.55	0.92	0.51	0.51	0.56	0.42	0.52	0.85	0.39	0.83	0.31	1.48	0.64	1.48

NOTES— Equivalent widths and errors in Å (derived in § III). Errors are listed underneath each measurement, including $(J-K)$. Feature names and numbers are from Table 3.

[a] Name from Arp (1965) with roman numeral sector numbers converted to decimal *e.g.* 3056 = III-56. Stars with numbers beginning with 5 and 6 were selected using unpublished narrow-band CCD photometry by Author (see § II in text).

[b] Number of separate observations, which were averaged, and errors reduced by $\sqrt{N}$.

[c] $(J-K)$ color, and error; all entries with errors of 0.05 were derived from CCD colors (see Table 2).

[d] Some stars were observed at 1.5Å resolution which covered only λλ4000-5800Å.

[e] 5006 was observed at both high and low dispersion. No radial velocity correction was possible at low dispersion, so a zero velocity was used. The high dispersion widths should be considered most reliable.

TABLE 7

REGRESSION SOLUTIONS

Solution (1)	N (2)	⟨log W⟩ (3)	⟨(J − K)⟩ (4)	A_0 (5)	A_1 (6)	A_2 (7)	A_3 (8)	A_4 (9)	σ_{rms} (10)	Notes (11)
1.....	46	0.907	0.681	−0.601	−2.659	3.620	7.582	1.693	0.21	SMF Fe 5270 + 5328 + Mg b
				±0.051	±0.362	±0.221	±2.183	±0.662		
2.....	46	0.732	0.681	−0.555	−2.398	3.849	11.228	1.437	0.22	SMF Fe 5270 + 5328
				±0.056	±0.408	±0.282	±3.157	±0.920		
3a.....	15	0.650	0.729	−1.506	−2.485	2.871			0.25	SMF Fe 5270 + 5328 + Mg b
				±0.075	±0.578	±0.352				metal poor[a]
3b	31	1.215	0.658	−0.019	−1.385	2.800			0.21	RMR Fe 5270 + 5328 + Mg b
				±0.039	±0.381	±0.544				metal rich[b]

NOTES.—Col. (1) Regression solution (§ IIId). Col. (2) Number of stars used in regression solution. Col. (3) Average logarithm of equivalent widths of stars used in regression. Col. (4) Average $(J - K)$ colors of stars used in regression. For role in regression equations, see § IIIc. Col. (5) – (9) Regression coefficients (Eqn. 17, § IIIc). Col. (10) σ_{rms} in dex from observed−predicted Fe abundance. Col. (11) Equivalent widths used; conditions on the sample.

[a](See Table 1) All members of globular clusters and HD 165195 , *except* 47 Tuc 4415, which is metal rich.

[b](See Table 1) Local K giants not in the metal poor group, mostly more metal rich than [Fe/H] = −0.5

TABLE 8

COVARIANCE MATRIX FOR SOLUTION 1

	A_0	A_1	A_2	A_3	A_4
A_0	0.0242	0.4798	−0.7436	−0.3011	−0.6440
A_1	0.4798	0.1730	−0.3638	−0.7272	−0.2352
A_2	−0.7436	−0.3638	0.1054	0.3154	0.3422
A_3	−0.3011	−0.7272	0.3154	1.0429	0.1276
A_4	−0.6440	−0.2352	0.3422	0.1276	0.3164

NOTES.—Col. (1)-(4) covariance between two terms of Equation (17) §III c (Solution 1). Individual entries are covariance terms A_{ij}.

TABLE 9

DERIVED ABUNDANCES FOR STANDARD STARS

		log W				[Fe/H] DERIVED			SOLUTION 1		
No. (1)	$(J-K)_0$ (2)	1 (3)	2 (4)	3a, b (5)	[Fe/H] (6)	1 (7)	2 (8)	3a, b (9)	σ_r (10)	$\sigma(y_i)$ (11)	$\sigma[\mathrm{Fe/H}]_1$ (12)
489.....	0.81	1.03	0.85	1.24	−0.30	−0.33	−0.20	−0.17	0.08	0.10	0.13
1953.....	0.62	1.13	0.93	1.33	0.35	0.36	0.26	0.35	0.09	0.05	0.10
3905.....	0.65	1.15	0.97	1.31	0.48	0.39	0.43	0.26	0.09	0.03	0.09
3994.....	0.50	1.00	0.84	1.14	0.10	0.10	0.09	−0.01	0.09	0.06	0.11
4287.....	0.57	1.04	0.88	1.18	−0.12	0.11	0.12	0.00	0.08	0.09	0.12
4365.....	0.70	1.06	0.89	1.27	−0.17	−0.02	0.06	0.08	0.06	0.07	0.10
4608.....	0.52	0.82	0.64	0.98	−0.50	−0.37	−0.34	−0.49	0.09	0.06	0.11
4695.....	0.69	1.01	0.81	1.15	−0.11	−0.23	−0.26	−0.26	0.06	0.06	0.08
4932.....	0.49	0.95	0.84	1.09	0.00	0.02	0.10	−0.14	0.09	0.07	0.11
5089.....	0.60	0.96	0.90	1.12	−0.16	−0.23	0.18	−0.19	0.06	0.11	0.12
5288.....	0.56	0.96	0.81	1.12	−0.19	−0.14	−0.07	−0.16	0.07	0.09	0.11
5340.....	0.75	0.98	0.78	1.20	−0.50	−0.46	−0.48	−0.18	0.06	0.09	0.11
5370.....	0.66	1.09	0.92	1.31	0.35	0.16	0.23	0.23	0.07	0.07	0.10
5777.....	0.58	1.05	0.86	1.20	−0.14	0.13	0.07	0.05	0.08	0.06	0.10
5824.....	0.69	1.06	0.88	1.29	−0.07	−0.03	0.04	0.15	0.06	0.12	0.13
5854.....	0.60	1.08	0.91	1.26	0.23	0.20	0.20	0.20	0.08	0.03	0.09
6056.....	0.91	1.15	0.92	1.41	0.32	0.20	0.18	0.17	0.17	0.12	0.21
6159.....	0.87	1.04	0.81	1.28	−0.13	−0.39	−0.53	−0.14	0.11	0.08	0.14
6241.....	0.63	1.02	0.83	1.25	−0.31	−0.08	−0.09	0.11	0.06	0.11	0.12
6299.....	0.61	1.08	0.90	1.24	0.00	0.17	0.15	0.13	0.08	0.06	0.10
6603.....	0.56	1.07	0.90	1.26	0.18	0.22	0.19	0.23	0.09	0.09	0.13
6973.....	0.73	1.09	0.89	1.24	0.00	0.05	0.04	−0.04	0.07	0.09	0.12
7120.....	0.71	1.08	0.88	1.26	−0.40	0.02	0.04	0.02	0.07	0.08	0.10
7317.....	0.84	1.06	0.87	1.26	−0.60	−0.22	−0.13	−0.15	0.10	0.16	0.19
175674.....	0.71	1.11	0.95	1.27	0.25	0.17	0.35	0.07	0.08	0.13	0.15
7429.....	0.63	1.12	0.89	1.31	0.27	0.29	0.13	0.30	0.08	0.10	0.13
7754.....	0.54	0.94	0.76	1.12	0.11	−0.14	−0.15	−0.13	0.07	0.10	0.13
7869.....	0.54	0.95	0.79	1.10	0.25	−0.12	−0.08	−0.17	0.07	0.06	0.10
7900.....	0.99	1.15	0.91	1.37	0.10	0.12	0.06	−0.06	0.22	0.08	0.23
8852.....	0.53	0.80	0.58	1.04	−0.16	−0.45	−0.48	−0.34	0.09	0.13	0.16
47-2426....	0.90	1.01	0.78	1.01	−0.71	−0.63	−0.79	−0.91	0.11	0.15	0.18
47-4415....	0.59	0.90	0.69	1.08	−0.33	−0.36	−0.44	−0.31	0.06	0.07	0.10
47-5527....	0.66	0.85	0.66	0.85	−0.71	−0.73	−0.75	−0.75	0.05	0.15	0.16
47-8517....	0.74	0.96	0.77	0.96	−0.71	−0.54	−0.53	−0.65	0.06	0.09	0.11
47-8518....	0.69	0.85	0.65	0.85	−0.71	−0.83	−0.91	−0.84	0.05	0.14	0.15
165195.....	0.65	0.57	0.41	0.57	−2.00	−1.47	−1.45	−1.54	0.12	0.29	0.31
M5 I-68....	0.85	0.79	0.61	0.79	−1.40	−1.62	−1.65	−1.42	0.10	0.15	0.18
M5 II-50...	0.68	0.58	0.47	0.58	−1.40	−1.60	−1.47	−1.58	0.11	0.22	0.24
M5 III-56..	0.64	0.47	0.35	0.47	−1.40	−1.61	−1.53	−1.79	0.17	0.21	0.27
M5 IV-28..	0.64	0.64	0.47	0.64	−1.40	−1.26	−1.25	−1.32	0.10	0.19	0.21
M5 IV-47..	0.88	0.83	0.67	0.83	−1.40	−1.53	−1.42	−1.38	0.10	0.17	0.20
M5 IV-81..	0.89	0.90	0.73	0.90	−1.40	−1.21	−1.04	−1.20	0.09	0.14	0.17
M15 S6....	0.65	0.29	0.09	0.29	−2.15	−1.97	−2.14	−2.35	0.30	0.25	0.39
M15 I-12...	0.73	0.23	0.21	0.23	−2.15	−2.65	−2.57	−2.71	0.35	0.26	0.44
M15 II-29..	0.69	0.49	0.36	0.49	−2.15	−1.87	−1.85	−1.87	0.16	0.23	0.28
M15 II-64..	0.64	0.30	0.16	0.30	−2.15	−1.88	−1.93	−2.30	0.29	0.19	0.35

NOTES.—Col. (1) Star number; see notes to Table 1. HD 165195 and members of globular clusters *except* 47-4415 were used in the metal poor solution 3b; this and Solutions 1 and 2 are described in § IIId. Col. (2) $(J-K)_0$, as in Table 1. Col. (3) $\log \sum$(SMF Fe 5270 + Fe 5328 + Mg b). Col. (4) $\log \sum$(SMF Fe 5270 + Fe 5328) *only*. Col. (5) For metal poor regression stars, same as col. (3); for metal rich stars, RMR Fe + Mg indices summed. Col. (6) [Fe/H] from catalog (see Table 1 for sources). Col. (7) Derived [Fe/H] using Solution 1 (§ IIId). Col. (8) Derived [Fe/H] using Solution 2. Col. (9) Derived [Fe/H] using Solutions 3a and b. Col. 10 Error due to uncertainties in coefficients (eqn. 23, § IVa). Col. 11 Errors due to error in observed equivalent widths and colors for each star (eqn. 19, § IIIc). Col. (12) $\sigma[\mathrm{Fe/H}]_1 = \sqrt{\sigma_r^2 + \sigma(y_i)^2}$

TABLE 10

NON-BULGE K GIANTS

No. (1)	Name (2)	V_0 (3)	$(V-K)_0$ (4)	$(J-K)_0$ (5)	$\sigma(J-K)$ (6)	CO (7)	[Fe/H] (8)	$[Fe/H]_1$ (9)	$[Fe/H]_2$ (10)	$\sigma[Fe/H]_1$ (11)	Notes (12)
6104...	ψ Oph	4.50	2.32	0.550	0.019	0.073	...	−0.27	−0.22	0.10	
6746...	γ Sgr	2.99	2.35	0.596	0.019	0.061	...	−0.37	−0.33	0.10	
8413...	*νPeg*	4.84	3.27	0.775	0.019	0.158	≈ 0.5	0.48	0.69	0.13	a
8795...	55 Peg	4.52	3.90	0.900	0.020	...	...	0.05	0.18	0.18	
8924...	...	6.25	2.39	0.590	0.020	0.039	+0.55	0.54	0.45	0.12	b
23.....	NGC 5927	13.86	2.97	0.760	0.020	...	−0.30	0.16	−0.09	0.16	F;c
157....	NGC 5927	14.16	3.09	0.780	0.020	0.170	−0.30	0.04	−0.19	0.18	F;c
563....	NGC 5927	14.46	2.74	0.680	0.020	...	−0.30	−0.24	−0.12	0.14	F;c
587....	NGC 5927	14.54	2.70	0.640	0.020	...	−0.30	0.01	−0.05	0.15	F;c
622....	NGC 5927	13.37	3.45	0.850	0.020	0.120	−0.30	0.04	−0.01	0.15	F;c
857....	NGC 5927	14.25	2.94	0.740	0.020	...	−0.30	−0.15	0.01	0.19	F;c
60.....	NGC 6522	14.21	...	0.780	0.050	...	−1.44	0.30	−0.20	0.49	A;c
15.....	NGC 6522	14.02	...	0.830	0.050	...	−1.44	−1.39	−1.26	0.27	A;c
46.....	NGC 6522	16.04	...	0.580	0.050	...	−1.44	−0.95	−1.12	0.33	A;c
153....	NGC 6522	13.97	...	0.910	0.050	...	−1.44	−0.83	−1.02	0.25	A;c
120....	NGC 6522	15.19	...	0.880	0.050	...	−1.44	−2.06	−1.70	0.44	A;c

NOTES.—Col. (1) HR/HD/star number in cluster; NGC 5927 from Frogel *et al.* 1983; NGC 6522 from Arp (1965). Col. (2) V (not dereddened) from Hoffleit and Jaschek (1982); dereddened V for members of NGC 5927 from Frogel *et al.* 1983 and *observed* V for 6522 (Arp, 1965). Col. (3)–(7) K, $J-K$ from observations at Las Campanas (§ IIb); unless otherwise noted in col. (12). Col. (8) Abundance of Fe relative to solar value (logarithmic); sources noted in col. (12). Col. (9) [Fe/H] from regression using Faber Fe+Mg (method 1, § IIId). Col. (10) [Fe/H] from regression using Faber Fe only (method 3), *except* for members of NGC 6522, where [Fe/H] was derived using Faber Fe+Mg, but only metal poor stars in the regression (method 2b). Col. (11) Error in [Fe/H] (col. 9); derived using methods in § IVb.

Sources of magnitudes: (F) Dereddened IR magnitudes from Frogel, Persson, and Cohen 1983 and references therein. (A) Dereddened IR colors from plot of $(J-K)$ vs. $(B-V)$ using data in Frogel *et al.* 1983; these colors derived from $(B-V)$ of Arp 1965 which was dereddened using $E_{B-V} = 0.50$.

Sources of abundances: (a) Faber *et al.* (1985). (b) Gustafsson, Kjaergaard, and Andersen 1974 (c) Zinn and West 1984.

TABLE 11

DERIVED ABUNDANCES FOR BULGE STARS

No. (1)	$(J-K)_0$ (2)	log W 1 (3)	log W 2 (4)	log W 3 (5)	[Fe/H] DERIVED 1 (6)	[Fe/H] DERIVED 2 (7)	[Fe/H] DERIVED 3 (8)	SOLUTION 1 σ_r (9)	SOLUTION 1 $\sigma(y_i)$ (10)	SOLUTION 1 $\sigma[\mathrm{Fe/H}]_1$ (11)
1012	0.67	1.00	0.78	1.15	−0.22	−0.34	−0.22	0.06	0.16	0.17
1021	0.46	1.17	0.98	1.29	0.61	0.41	0.46	0.17	0.07	0.19
1025	0.62	1.17	1.01	1.36	0.51	0.56	0.44	0.10	0.09	0.13
1039	0.61	1.24	1.06	1.39	0.79	0.75	0.54	0.13	0.07	0.14
1053	0.40	0.60	0.44	0.60[a]	−0.15	0.04	−0.84[a]	0.24	0.22	0.32
1064	0.77	1.15	0.98	1.41	0.31	0.50	0.37	0.10	0.14	0.18
1076	0.72	1.20	1.04	1.40	0.57	0.80	0.41	0.10	0.10	0.14
1083	0.54[1]	1.16	0.96	1.34	0.51	0.37	0.50	0.13	0.10	0.16
1093	0.61[1]	1.10	0.87	1.20	0.26	0.07	0.01	0.08	0.10	0.13
1102	0.55[1]	1.01	0.82	1.18	0.04	−0.03	0.04	0.08	0.14	0.16
1129	0.62[1]	1.22	1.06	1.33	0.71	0.79	0.36	0.12	0.10	0.15
1140	0.67	1.01	0.78	1.16	−0.21	−0.34	−0.20	0.06	0.13	0.14
1141	0.66	1.09	0.82	1.16	0.14	−0.16	−0.18	0.07	0.12	0.14
1144	0.73	1.20	1.01	1.31	0.58	0.66	0.14	0.11	0.11	0.15
1145	0.48	0.68	0.49	0.68[a]	−0.46	−0.37	−0.81[a]	0.15	0.19	0.24
1151	0.50[1]	0.83	0.60	0.83[a]	−0.29	−0.34	−0.42[a]	0.09	0.21	0.23
1153	0.45[1]	1.02	0.80	1.02	0.24	0.09	−0.28	0.12	0.14	0.18
1155	0.64	1.14	0.95	1.29	0.39	0.34	0.21	0.09	0.10	0.13
1156	0.57[1]	0.93	0.77	1.08	−0.24	−0.19	−0.28	0.07	0.19	0.20
1164	0.62	0.95	0.71	1.13	−0.31	−0.48	−0.19	0.06	0.15	0.16
1174	0.50[1]	0.90	0.71	0.93	−0.13	−0.16	−0.59	0.08	0.19	0.20
1181	0.47[1]	1.00	0.75	1.01	0.17	−0.02	−0.34	0.10	0.15	0.18
1194	0.66	1.13	0.90	1.24	0.33	0.12	0.05	0.08	0.11	0.14
1196	0.72	1.22	1.04	1.40	0.71	0.82	0.42	0.11	0.09	0.14
1202	0.62	1.15	0.98	1.36	0.42	0.45	0.45	0.09	0.13	0.16
1304	0.28[1]	1.17	0.97	1.26	0.74	0.33	0.62	0.29	0.05	0.29
1308	0.20[1]	0.78	0.41	0.95	0.71	1.23	−0.11	0.23	0.21	0.31
1319	0.70[1]	1.16	0.95	1.26	0.43	0.37	0.06	0.09	0.12	0.15
1322	0.67	1.09	0.90	1.31	0.13	0.13	0.22	0.07	0.10	0.12
1329	0.70[1]	1.14	0.91	1.31	0.32	0.16	0.18	0.08	0.14	0.16
1335	0.67[1]	1.08	0.87	1.25	0.08	0.00	0.06	0.07	0.14	0.15
2018	0.70[1]	1.02	0.83	1.25	−0.18	−0.20	0.01	0.06	0.19	0.20
2026	0.73[1]	1.16	0.99	1.36	0.40	0.58	0.28	0.09	0.11	0.15
2027	0.76	1.17	0.98	1.40	0.43	0.50	0.36	0.11	0.12	0.16
2033	0.67	0.92	0.73	0.92[a]	−0.51	−0.55	−0.57[a]	0.05	0.21	0.22
2040	0.47	0.88	0.63	0.88[a]	−0.10	−0.18	−0.21[a]	0.09	0.15	0.18
2041	0.19[1]	0.71	0.75	0.98	0.79	0.59	−0.02	0.28	0.24	0.37
2042	0.71	0.99	0.76	1.17	−0.34	−0.52	−0.22	0.06	0.17	0.18
2044	0.74[1]	0.92	0.67	0.92[a]	−0.70	−0.95	−0.76[a]	0.06	0.24	0.25
2049	0.49	0.95	0.78	1.05	0.00	−0.01	−0.24	0.09	0.13	0.15
2116	0.68	1.28	1.12	1.42	0.96	1.15	0.52	0.13	0.13	0.18
2118	0.66[1]	1.08	0.81	1.19	0.09	−0.20	−0.08	0.07	0.14	0.16
2119	0.57	0.71	0.55	0.71[a]	−0.79	−0.72	−0.94[a]	0.09	0.22	0.24
2122	0.85	1.10	0.86	1.10[a]	−0.06	−0.18	−0.53[a]	0.12	0.10	0.15
2136	0.53[1]	0.58	0.49	0.58[a]	−0.83	−0.64	−1.21[a]	0.16	0.32	0.36
2139	0.37[1]	0.91	0.73	0.97	0.23	0.19	−0.30	0.12	0.16	0.20
2145	0.54	1.21	1.04	1.29	0.69	0.62	0.36	0.15	0.09	0.17

No. (1)	$(J-K)_0$ (2)	log W 1 (3)	log W 2 (4)	log W 3 (5)	[Fe/H] Derived 1 (6)	[Fe/H] Derived 2 (7)	[Fe/H] Derived 3 (8)	Solution 1 σ_r (9)	Solution 1 $\sigma(y_i)$ (10)	Solution 1 $\sigma[\mathrm{Fe/H}]_1$ (11)
2146.....	0.54	1.10	0.91	1.18	0.32	0.22	0.05	0.10	0.09	0.14
2147.....	0.43	0.41	0.17	0.41[a]	−0.37	−0.08	−1.44[a]	0.35	0.23	0.42
2151.....	0.66[1]	0.95	0.68	1.10	−0.40	−0.70	−0.33	0.05	0.19	0.20
2154.....	0.54[1]	0.75	0.55	0.75[a]	−0.58	−0.58	−0.75[a]	0.09	0.26	0.28
2166.....	0.50[1]	0.13	0.00	0.13[a]	−0.85	−0.68	−2.42[a]	0.53	0.52	0.74
2167.....	0.70[1]	1.20	1.03	1.38	0.58	0.72	0.38	0.10	0.13	0.17
2171.....	0.66[1]	1.07	0.85	1.23	0.06	−0.05	0.02	0.07	0.16	0.17
2173.....	0.53	0.78	0.50	0.78[a]	−0.49	−0.62	−0.64[a]	0.09	0.21	0.22
2174.....	0.42[1]	0.86	0.67	0.86[a]	0.01	0.02	−0.14[a]	0.11	0.20	0.23
2199.....	0.52[1]	1.05	0.86	1.22	0.22	0.11	0.18	0.10	0.11	0.15
2201.....	0.70[1]	1.12	0.92	1.32	0.23	0.20	0.21	0.08	0.16	0.17
2206.....	0.29	0.91	0.63	1.14	0.44	0.45	0.27	0.15	0.18	0.24
2215.....	0.42	0.78	0.58	0.78[a]	−0.09	−0.04	−0.37[a]	0.13	0.16	0.21
2216.....	0.57[1]	0.82	0.71	0.82[a]	−0.53	−0.34	−0.62[a]	0.07	0.23	0.25
2240.....	0.45	1.02	0.82	1.21	0.25	0.13	0.27	0.12	0.10	0.15
2244.....	0.73	1.03	0.82	1.26	−0.20	−0.27	0.01	0.06	0.18	0.19
2252.....	0.64	0.94	0.76	0.94[a]	−0.38	−0.35	−0.45[a]	0.05	0.17	0.18
2261.....	0.75	1.06	0.87	1.20	−0.12	−0.06	−0.20	0.07	0.14	0.16
3106_____	0.50	0.87	0.64	0.87[a]	−0.19	−0.27	−0.30[a]	0.08	0.15	0.17
3152.....	0.69	1.04	0.77	1.14	−0.11	−0.43	−0.26	0.06	0.14	0.15
3157.....	0.74	1.17	0.98	1.28	0.43	0.50	0.04	0.10	0.11	0.15
3159.....	0.58[1]	1.14	0.91	1.29	0.43	0.23	0.29	0.10	0.11	0.15
3160.....	0.51	0.92	0.68	0.97	−0.11	−0.25	−0.49	0.08	0.14	0.16
3164.....	0.69	1.13	0.93	1.31	0.29	0.25	0.21	0.08	0.09	0.12
3197.....	0.61[1]	1.17	0.94	1.29	0.51	0.31	0.25	0.10	0.12	0.15
3209.....	0.68	1.22	1.04	1.39	0.69	0.79	0.45	0.11	0.10	0.14
3224.....	0.66[1]	1.06	0.82	1.19	0.03	−0.19	−0.09	0.06	0.17	0.18
4003_____	0.56	0.67	0.57	0.67[a]	−0.82	−0.63	−1.01[a]	0.11	0.20	0.23
4011.....	0.50[1]	1.10	0.96	1.29	0.38	0.36	0.42	0.12	0.11	0.17
4022.....	0.66[1]	1.19	1.02	1.36	0.58	0.64	0.39	0.10	0.09	0.14
4025.....	0.50	1.15	0.95	1.28	0.52	0.34	0.37	0.14	0.09	0.17
4063.....	0.58[1]	1.23	1.02	1.34	0.76	0.59	0.44	0.14	0.09	0.16
4065.....	0.56[1]	1.14	0.88	1.27	0.46	0.13	0.28	0.11	0.14	0.18
4071.....	0.53[1]	0.98	0.75	1.03	−0.01	−0.15	−0.36	0.08	0.15	0.17
4072.....	0.65[1]	1.23	1.05	1.36	0.73	0.78	0.40	0.11	0.09	0.15
4146.....	0.54[1]	1.08	0.88	1.23	0.26	0.15	0.20	0.10	0.13	0.16
4148.....	0.47[1]	0.84	0.62	0.84[a]	−0.16	−0.20	−0.30[a]	0.10	0.20	0.22
4164.....	0.53[1]	1.13	0.90	1.26	0.43	0.22	0.28	0.12	0.12	0.17
4165.....	0.73[1]	1.00	0.77	1.21	−0.35	−0.50	−0.15	0.06	0.19	0.20
4167.....	0.58	1.25	1.06	1.38	0.83	0.74	0.54	0.14	0.10	0.17
4203.....	0.87	0.93	0.76	1.17	−0.98	−0.85	−0.45	0.09	0.18	0.20
4285.....	0.62[1]	1.13	0.97	1.32	0.34	0.42	0.34	0.09	0.12	0.15
4297.....	0.57[1]	1.13	0.98	1.28	0.39	0.46	0.29	0.10	0.11	0.15
4312.....	0.43	0.71	0.43	0.71[a]	−0.21	−0.13	−0.60[a]	0.16	0.19	0.25
4315.....	0.64[1]	1.01	0.77	1.21	−0.12	−0.32	−0.01	0.06	0.19	0.20
4325.....	0.59	1.13	1.04	1.33	0.39	0.65	0.40	0.10	0.14	0.17
4329.....	0.72	0.91	0.74	0.91[a]	−0.70	−0.62	−0.74[a]	0.05	0.14	0.15
5006_____	0.52[1]	0.39	0.37	0.39[a]	−0.96	−0.73	−1.73[a]	0.29	0.39	0.48
5060.....	0.60[1]	1.01	0.72	1.07	−0.04	−0.40	−0.35	0.07	1.70	1.70
5445.....	0.64[1]	1.05	0.84	1.23	0.02	−0.09	0.05	0.06	0.17	0.18
6192.....	0.63[1]	0.77	0.60	0.77[a]	−0.88	−0.84	−0.92[a]	0.07	0.25	0.26
6322.....	0.77[1]	1.23	1.01	1.27	0.74	0.72	−0.01	0.13	0.14	0.19
6406.....	0.82[1]	1.17	1.01	1.34	0.38	0.73	0.11	0.13	0.16	0.20

NOTES.—Col. (1) Star number from Arp (1965) with sector number converted to first decimal. Numbers beginning with 5 and 6 are from unpublished narrow-band photometry by author. Col. (2) $(J-K)_0$, dereddened by E_{J-K} =0.28 (§ IV). Entries marked with [1] are pseudo-infrared colors (see Table 2 and § II). Stars hotter than $(J-K)_0$ =0.45 were not included in abundance distribution function. Col. (3) log $\sum$(SMF Fe 5270 + Fe 5328 + Mg b). Col. (4) log $\sum$(SMF Fe 5270 + Fe 5328) *only*. Col. (5) For metal poor regression stars (marked with [a], same as col. (3); for metal rich stars, RMR Fe + Mg indices summed. (6) Derived [Fe/H] using Solution 1 (§ IIId). Col. (7) Derived [Fe/H] using Solution 2. Col. (8) Derived [Fe/H] using Solutions 3a and b. Numbers marked with [a] use the metal poor solution a. All others derived from metal rich solution b. Col. 9 Error due to uncertainties in coefficients (eqn. 23, § IVa). Col. 10 Errors due to error in observed equivalent widths and colors for each star (eqn. 19, § IIIc). Col. (11) $\sigma[\mathrm{Fe/H}]_1 = \sqrt{\sigma_r^2 + \sigma(y_i)^2}$

[1] $(J-K)$ is a pseudo-infrared color derived from CCD photometry (§ IIb, Table 2).

[a] Solution 3a (metal poor stars only) used to derive [Fe/H] ; log W for this solution used SMF Fe+Mg.

TABLE 12

PROPERTIES OF THE ABUNDANCE DISTRIBTION FUNCTIONS

No.	IR Sample	N	⟨[Fe/H]⟩	σ[Fe/H]
(1)	(2)	(3)	(4)	(5)
Solution 1.....	$(J-K)_0 > 0.45$[a]	42	0.094	0.402
Solution 1.....	$(J-K)_0 > 0.45$	88	0.082	0.391
Solution 1.....	$(J-K)_0 > 0.40$	94	0.075	0.385
Solution 2.....	$(J-K)_0 > 0.45$	88	0.042	0.450
Solution 3.....	$(J-K)_0 > 0.45$	88	−0.085	0.602

NOTES.—Mean and dispersion in [Fe/H] of abundance distribution functions of galactic bulge K giants. Col. (1) Solution used (see Table 7 and § IIId). Col. (2) Restrictions on the $(J-K)_0$ color of the sample, and the source of the photometry. Only 42 stars had IR photometry; the rest had IR colors from CCD colors (see Table 2). Col. (3) Number of stars in distribution function. Col. (4) Mean [Fe/H] . Col. (5) Standard deviation of distribution function in dex.

[a] Stars with IR photometry only.

TABLE 13

STEM AND LEAF TABLE FOR SOLUTION 1

−0.9	−0.8	−0.7	−0.6	−0.5	−0.4	−0.3	−0.2	−0.1	−0.0	0.0	0.1	0.2	0.3	0.4	0.5	0.6	0.7	0.8	0.9
													1155 9						
								2040 0					4297 9						
								3160 1					4325 9	4065 6	4022 8				
								3152 1		2218 9			6406 8	4164 3	2167 8				
								4315 2		1335 8			4011 8	3157 3	1144 8		1039 9		
							2244 0	2261 2		2171 6		3164 9	4285 4	1319 3	1076 7		4063 6		
	4003 2					1164 1	1140 1	1174 3		1102 4		4146 6	1194 3	3159 3	4025 2		6322 4		
	2136 3	2044 0		2033 1	2151 0	2042 4	1012 2	4148 6	4071 1	3224 3	1181 7	1093 6	2146 2	2027 3	3197 1	3209 9	4072 3		
5006 6	2166 5	4329 0		2216 3	1145 6	4165 5	1156 4	2018 8	5060 4	5445 2	1141 4	2201 3	1329 2	1202 2	1025 1	2145 9	1196 1		
4203 8	6192 8	2119 9		2154 8	2173 9	2252 8	1151 9	3106 9	2122 6	2049 0	1322 3	2199 2	1064 1	2026 0	1083 1	1021 1	1129 1	4167 3	2116 6

NOTES.— Stem and leaf diagram for abundances of 88 bulge K giants derived using Solution 1. The numbers are from Arp, 1965 with roman numeral sector numbers converted to decimal. Stars beginning with 5 and 6 are from unpublished narrow-band photometry by the author. Abundances are listed in upper column headings, with last significant digit following the star name; *e.g.* I-21 = 1021 has an abundance of [Fe/H] =0.61.

TABLE 14

BAADE'S WINDOW STARS OMITTED FROM ABUNDANCE DETERMINATION

No. (1)	$(J-K)$ (2)	Spectrum (3)
2123	1.24	TiO
3141	0.46	H
2110	1.20	TiO
1320	0.91	TiO
3200[a]	0.76	H
B212[b]	...	TiO
1368	0.20[c]	H
3133	0.89[c]	H
2242	0.74[c]	H
3169	0.44[c]	H

NOTES.—These stars were excluded from the abundance distribution function because their spectra were not those of K giants. Either hydrogen lines or TiO bands dominated these spectra. Col. (1) Star number in Baade's Window, from Arp (1965) with roman numeral converted to decimal. Col. (2) $(J-K)$ *observed*; see note c also. Col. (3) Reason the star was excluded; either strong TiO or H lines.

[a] Star 3200 has strong hydrogen lines and strong Na (indicating it is in the bulge); it may be a horizontal branch star in the bulge.

[b] B212 is an M giant from Blanco, McCarthy, and Blanco 1984.

[c] These $(J-K)$ colors are from CCD photometry (see notes to Table 2 and § II).

References

Arp, H. C. 1965, *Ap. J.*, **141**, 43.

Bessll, M. 1979, *P.A.S.P.*, **91**, 589.

Blanco, V. M., McCarthy, S. J., and Blanco, B. M. 1984, *A. J.*, **89**, 636.

Bond, H. E., Burstein, D., Faber, S. M., Luck, R. E. 1985, *A. J.*, **90**, 1349.

Branch, D. Bonnell, J., and Tomkin, J. 1978 , *Ap. J.*, **225**, 902.

Butler, D., Carbon, D. F., Kraft, R. P. 1976 , *Ap. J.*, **210**, 120.

Cayrel de Strobel, G., Bentolila, C., Hauck, B., and Curchod, A. 1980 , *Astr. Astrophys. Suppl.*, **41**, 405.

Cohen, J. G. 1983 , *Ap. J.*, **270**, 654.

Elias, J. H., Frogel, J. A., Humphreys, R. M. 1985 , *Ap. J. Suppl. Ser.*, **57**, 91.

Elias, J. H., Frogel, J. A., Matthews, K., Neugebauer, G. 1982, *A. J.*, **87**, 1029.

Faber, S. M., Friel, E. D., Burstein, D., Gaskell, C. M. 1985, *Ap. J. Suppl*, **57**, 711.

Frogel, J. A., Whitford, A. E., and Rich, R. M. 1984, *A. J.*, **89**, 1536.

Frogel, J. A., Persson, S. E., Aaronson, M., Matthews, K. 1978, *Ap. J.*, **220**, 442.

Frogel, J. A. and Whitford, A. E. 1982, *Ap.J. (Letters)*, **259**, L7.

Frogel, J. A., Persson, S. E., and Cohen, J. G. 1983, *Ap.J. Suppl. Ser.*, **53**, 713.

Frogel, J. A. 1985 Private Communication .

Funfschilling, H. 1971, *Astr. Ap.*, **13**, 454.

Glass, I.S., and Feast, M.J. 1982, *M.N.R.A.S.*, **198**, 199.

Griffin, R. F. 1968 *A Photometric Atlas of the Spectrum of Arcturus* (Cambridge: Cambridge Philosophical Society) .

Gunn, J. E., Carr, M., Chang, J., Danielson, G. E. A., Lorenz, E. O., Lucinio, R., Nenow, V. E., Smith, O. J., Westphal, J. A., and Zimmerman, B. A. 1984, *Bull. A.A.S.*, **16**, 447.

Gustafsson, B., Kjaergaard, P., and Andersen, S. 1974, *Astr. Ap.*, **34**, 99.

Hoffleit, D. and Jaschek, C. 1982 *The Bright Star Catalog* (New Haven: Yale University Observatory).

Johnson, H. L. 1966 , *Comm. Lunar Planetary Lab.*, **4**, 99.

Lee, S.-W. 1977, *Astr.Ap.Suppl.*, **27**, 381.

Menzies, J. 1974, *M.N.R.A.S.*, **169**, 79.

Mould, J. R., and Mc Elroy, D. 1978 , *Ap. J.*, **221**, 580.

Nassau, J. J., and Blanco, V. M. 1958, *Ap. J.*, **128**, 46.

Olson, B.I. 1975 , *Pub. A.S.P.*, **87**, 349.

Pilachowski, C. 1978 , *Publ. A.S.P.*, **90**, 675.

Schneider, D. P., Gunn, J. E., Hoessel, J. G. 1983, *Ap.J.*, **264**, 337.

Shectman, S. 1978, in *Annual Report of the Director of the Hale Observatories*, 1977-78 .

Stetson, P. B. 1984, *Pub. A.S.P.*, **96**, 128.

Sturch, C. 1966, *Ap. J.*, **143**, 774.

Suntzeff, N. B. 1980 , *A. J.*, **85**, 408.

Tonry, J., and Davis, M. 1979 , *A.J.*, **84**, 1511.

van den Bergh, S. 1971, *A. J.*, **76**, 1082.

Walker, A. R., and Mack, P. 1985, Preprint .

Whitford, A. E. and Blanco, V. M. 1979 , *Bull. AAS*, **11**, 675.

Whitford, A. E. 1977, *Ap. J.*, **211**, 527.

Whitford, A. E., and Rich, R. M. 1983 *Ap. J.* **274** 723 (WR).

Whitford, A.E. 1958, *A. J.*, **63**, 201.

Zinn, R., and West, R. J. 1984, *Ap. J. Suppl.*, **55**, 45.

Figure Captions

Figure 1— $(g-z)_{inst}$ from 4-shooter data vs *observed* $(J-K)$. The g exposure was 100s long and the z was 1s long; stars were measured through 6 pixel apertures and sky measured through a 6–26 pixel annulus.

Figure 2— $(49-70)_{inst}$ from 4m RCA CCD vs *observed* $(J-K)$ for a portion of Baade's Window. The 49 and 70 exposures were 700 seconds long.

Figure 3— Feature bandpasses from Table 3 illustrated using α Ser, a K giant standard. Flattened counts are plotted as a function of wavelength. The continua are drawn in as lines connecting the bandpasses.

Figure 4— The effect of adding noise to a spectrum and measuring the equivalent width (Å) of Mgb. Signal to noise ratio plotted as abscissa.

Figure 5— Error in Mgb, in Å, as a function of signal to noise ratio.

Figure 6— SMF Na in Å as a function of $\sum$(Fe 5270 + Fe 5328 + Mg b). All equivalent width measurements in this and subsequent plots in Å.

Figure 7— Difference between derived and cataloged abundance as a function of cataloged abundance. [Fe/H] is the log of the ratio of the stellar metal abundance to the solar abundance. Solution 1 is defined in § IIId.

Figure 8— As in Figure 7, except vs $(J-K)_0$.

Figure 9— As in Figure 7, for Solution 2

Figure 10— As in Figure 7, for Solution 3. "×" symbols are metal poor stars.

Figure 11— Derived [Fe/H] using regressions for Fe lines only and Mg b only. The SMF indices were used for this test.

Figure 12— Derived [Fe/H] from Solution 1 vs Solution 2, for BW stars only. The circles have IR photometry; "×" have pseudo-colors. This convention is used on all following plots with BW stars.

Figure 13— As in Figure 12, with Solution 3.

Figure 14— Number of stars at a given abundance in 0.25 dex bins. The dashed line histogram is for those stars *with* IR colors; the dotted line histogram is for those stars with pseudo-colors.

Figure 15— As in Figure 14, for Solution 2.

Figure 16— As in Figure 14, for Solution 3.

Figure 17— Abundance distribution for Solution 1 divided according to apparent V magnitude.

Figure 18— $\sum$(Fe 5270 + Fe 5328 + Mg b) in Åvs $(J-K)_0$. Unless otherwise stated, all $(J-K)$ colors are dereddened by 0.28 for the BW stars. Symbols: open circles: BW stars with IR photometry. Crosses: BW stars with pseudo-IR colors. Filled circles: metal rich standards. Filled triangles: metal poor standards. Boxes: Non-BW K giants, not standards (Table 2). This convention is used throughout.

Figure 19— As in Figure 17, with globular cluster members explicitly identified. 5–M5; 15–M15; 47–47 Tuc; 59–NGC 5927; 65–NGC 6522

Figure 20— CO index in mags vs $(J-K)_0$. BW stars are illustrated using Arp (1965) numbers with roman numerals converted to decimal. Actual symbol positions indicated with open circles. The BW photometry is from Frogel, Whitford, and Rich 1984. The filled circles are local K giant standards observed from Las Campanas and tabulated in Table 1. Globular cluster stars indicated with numbers as in Figure 18. Their CO measurements from Frogel *et al.* 1983.

Figure 21— Sum of Fe 5270 and Fe 5335 (Faber indices) vs $(J-K)_0$. Symbols: see Figure 17. In this and subsequent figures, the enhanced line strengths at similar colors are apparent for the bulge stars.

Figure 22— As in Figure 21, with Rich indices.

Figure 23— Sum of 8 weak Fe features (w 27—34) vs $(J-K)_0$. Symbols as in Figure 17.

Figure 24— Sum of 8 weak Fe features vs sum of Fe 5270, 5335, Mgb (Faber indices).

Figure 25— Faber TiO 2 index vs $(J-K)_0$. Note enhanced TiO at constant color for the bulge stars

Figure 26— Gravity-sensitive Faber Mg 2 index vs abundance-sensitive Fe 5270 + Fe 5335 Rich indices.

Figure 27— Stetson's G band index vs Fe 5270 + 5335 + Mg b (Faber indices).

Figure 28— Stetson's G band index vs $(J-K)_0$.

Figure 29— CN λ4200Å vs Stetson's G band index.

Figure 30— CN λ4200Å vs Fe 5270 + 5335 + Mgb (Faber indices)

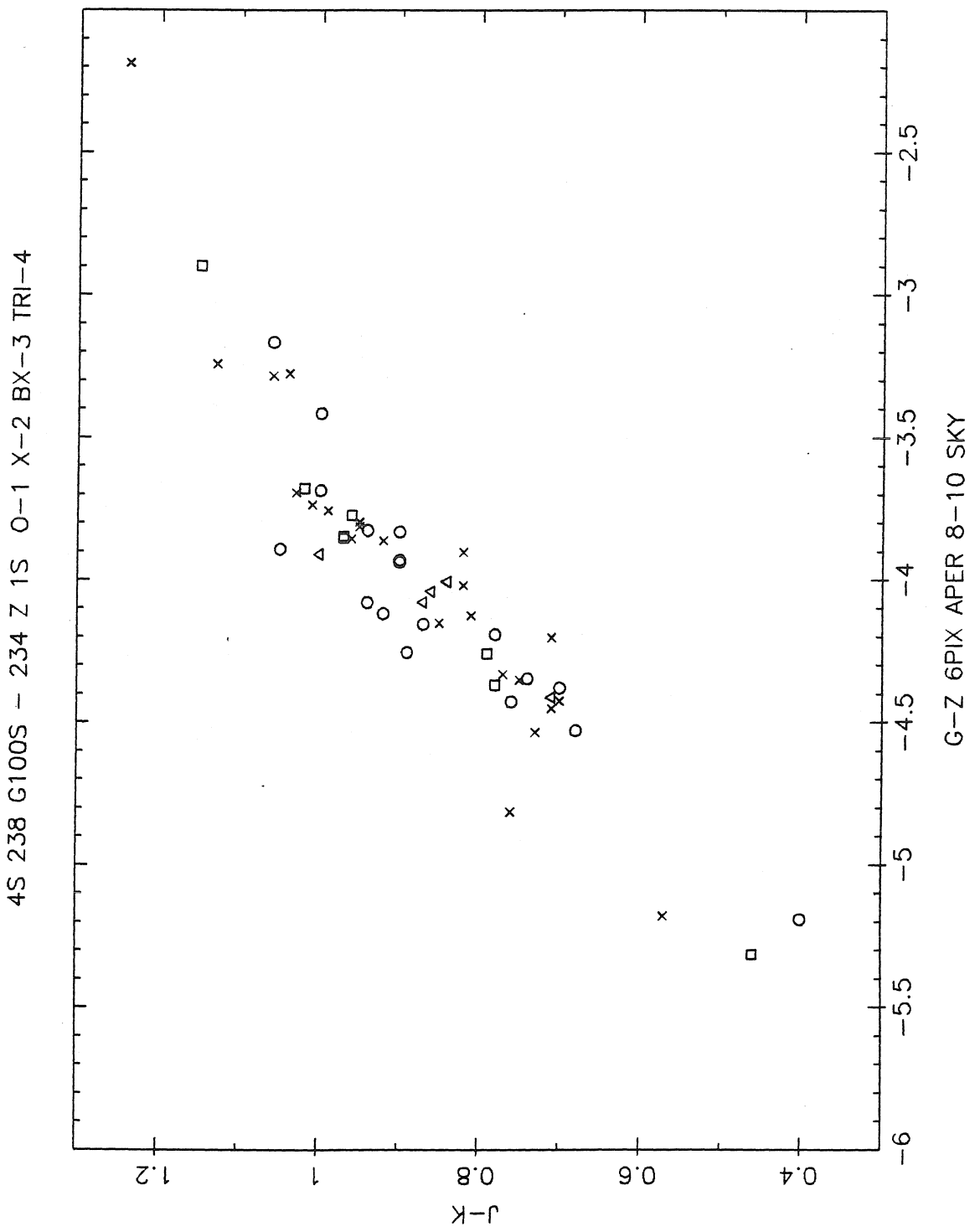
4S 238 G100S - 234 Z 1S O-1 X-2 BX-3 TRI-4
G-Z 6PIX APER 8-10 SKY
J-K
0.4
0.6
0.8
1
1.2
-2.5
-3
-3.5
-4
-4.5
-5
-5.5
-6

Figure 1

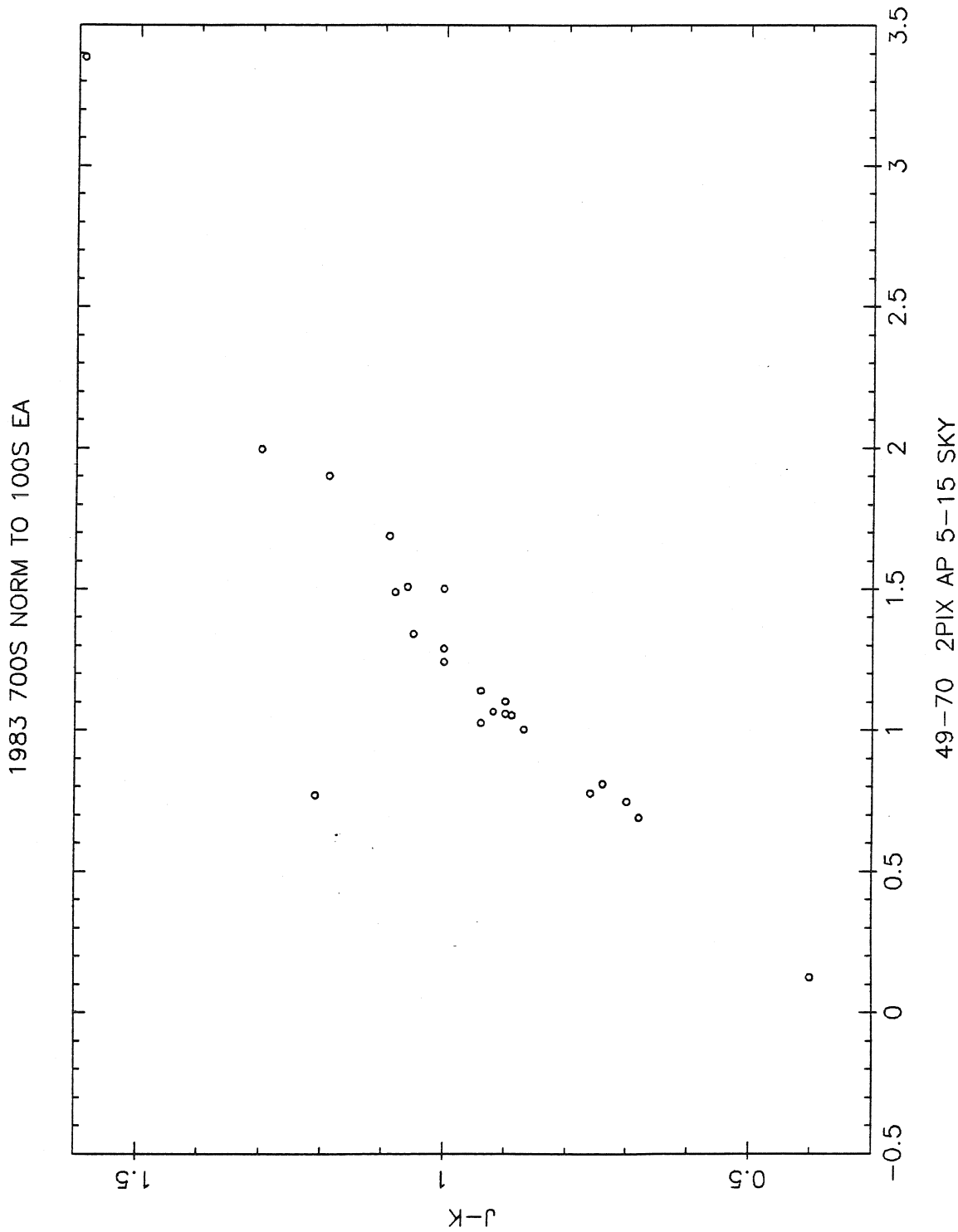
1983 700S NORM TO 100S EA
49-70 2PIX AP 5-15 SKY
J-K
0.5
1
1.5
-0.5
0
0.5
1
1.5
2
2.5
3
3.5

Figure 2

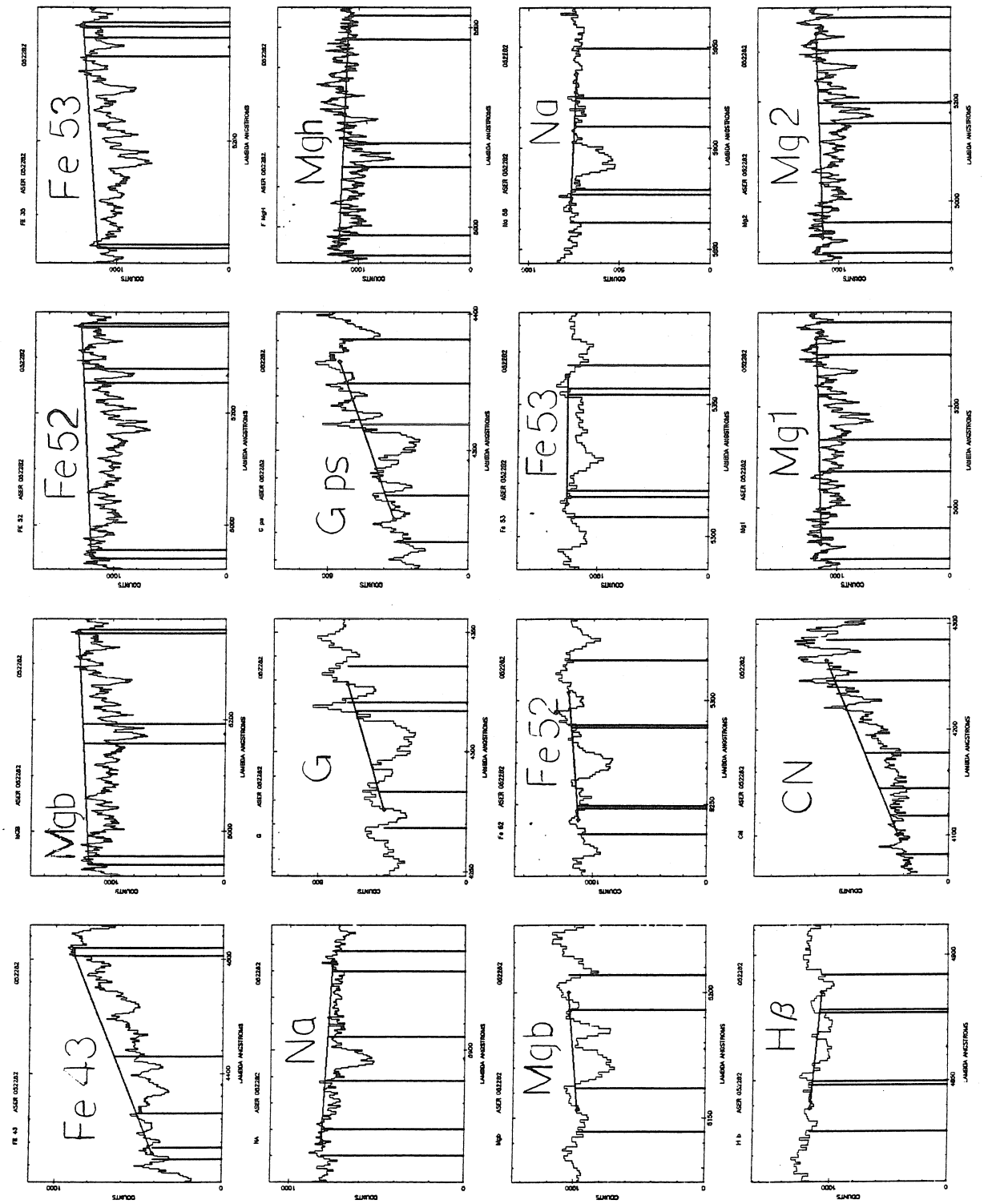

Figure 3

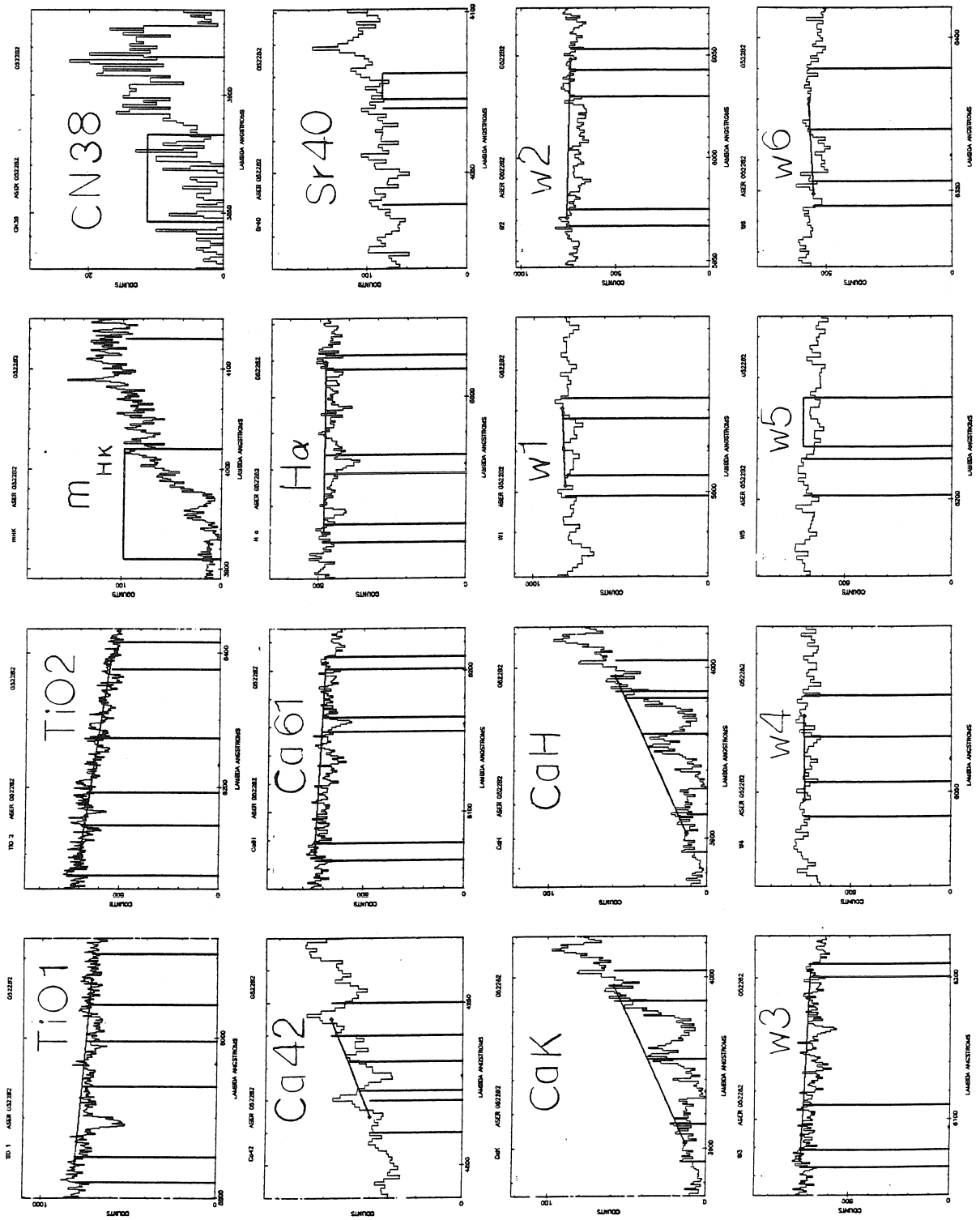

Figure 3 (Cont'd)

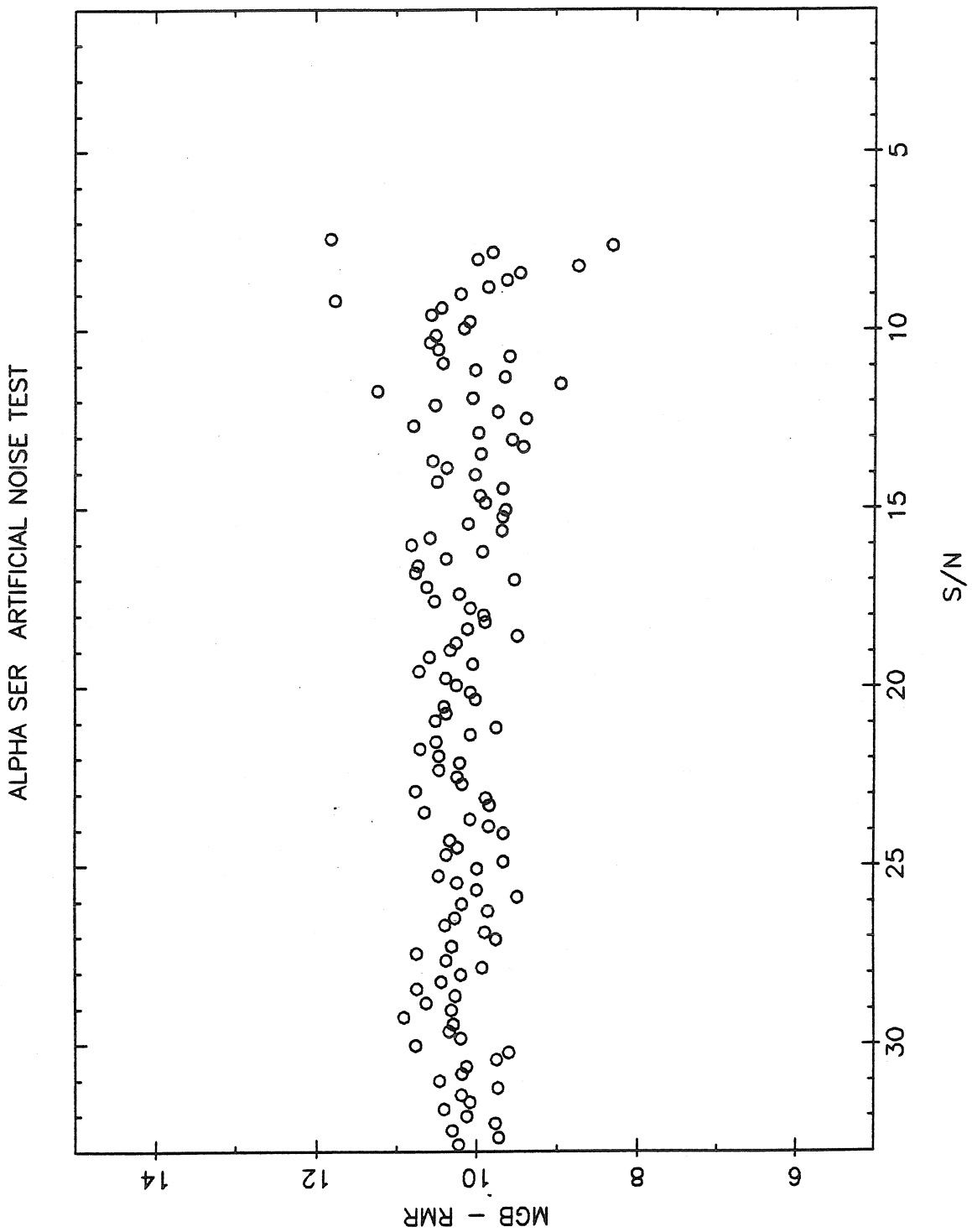
ALPHA SER ARTIFICIAL NOISE TEST
MGB - RMR
14
12
10
8
6
S/N
5
10
15
20
25
30

Figure 4

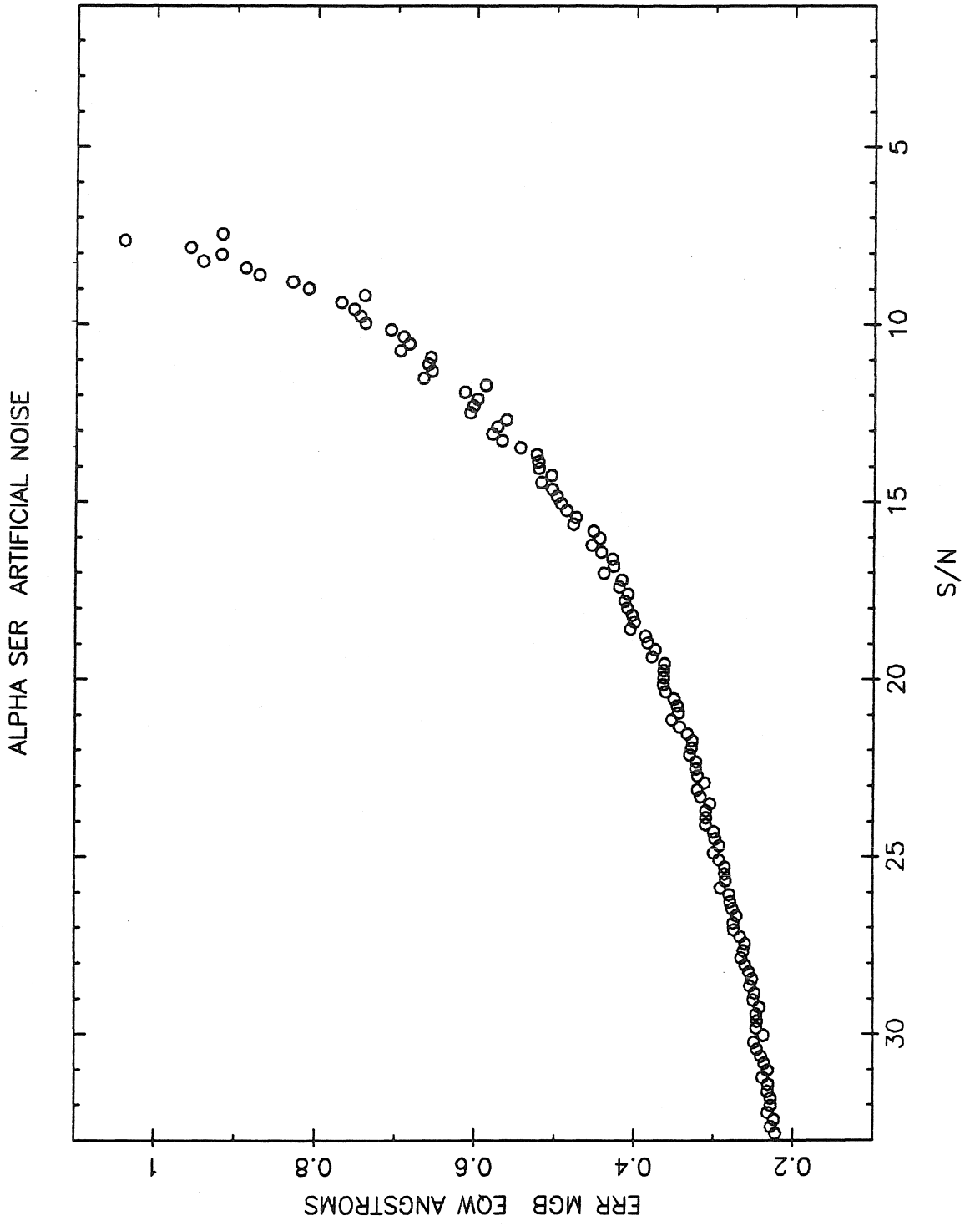
ALPHA SER ARTIFICIAL NOISE
ERR MGB EQW ANGSTROMS
0.2
0.4
0.6
0.8
1
5
10
15
20
25
30
S/N

Figure 5

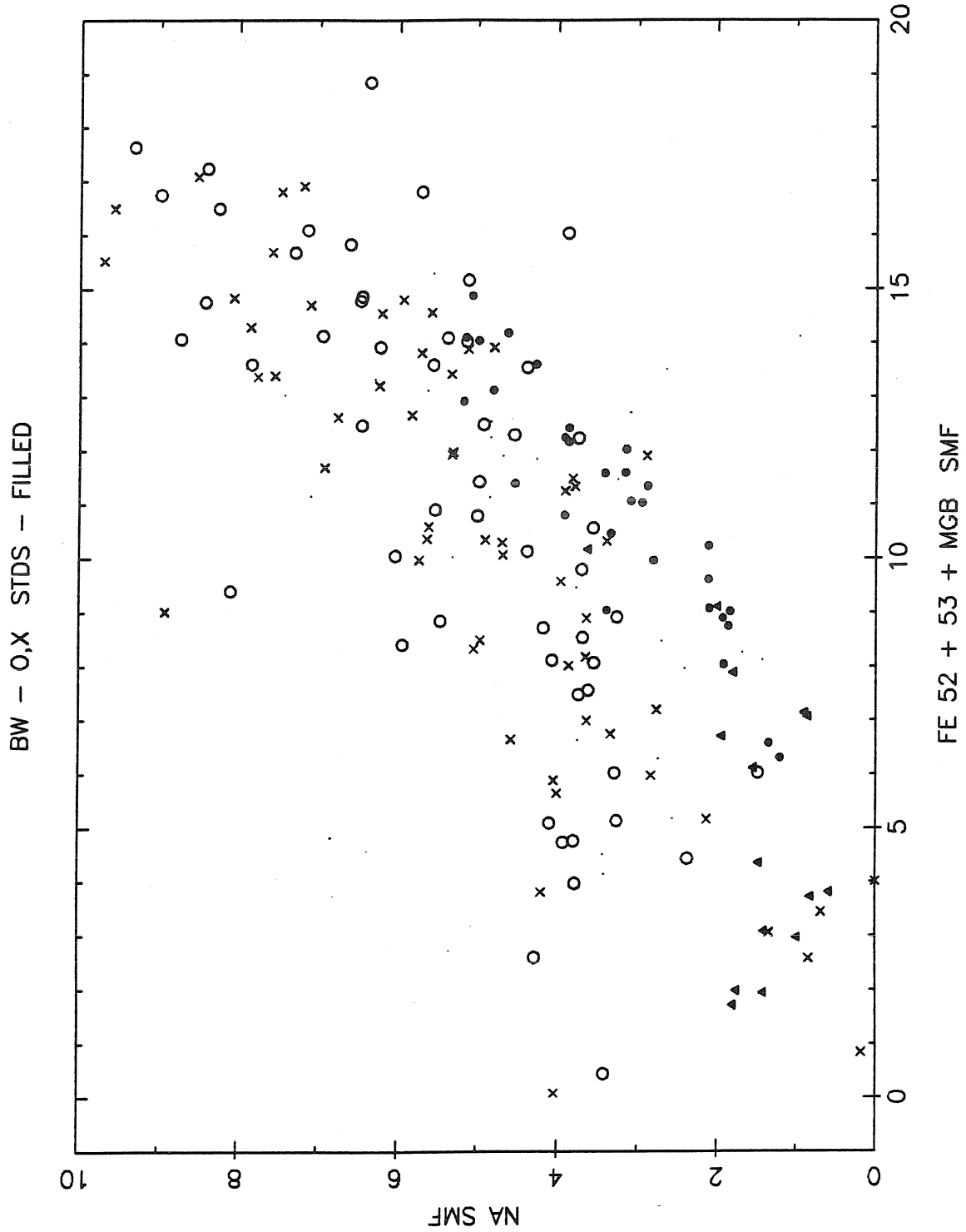

Figure 6

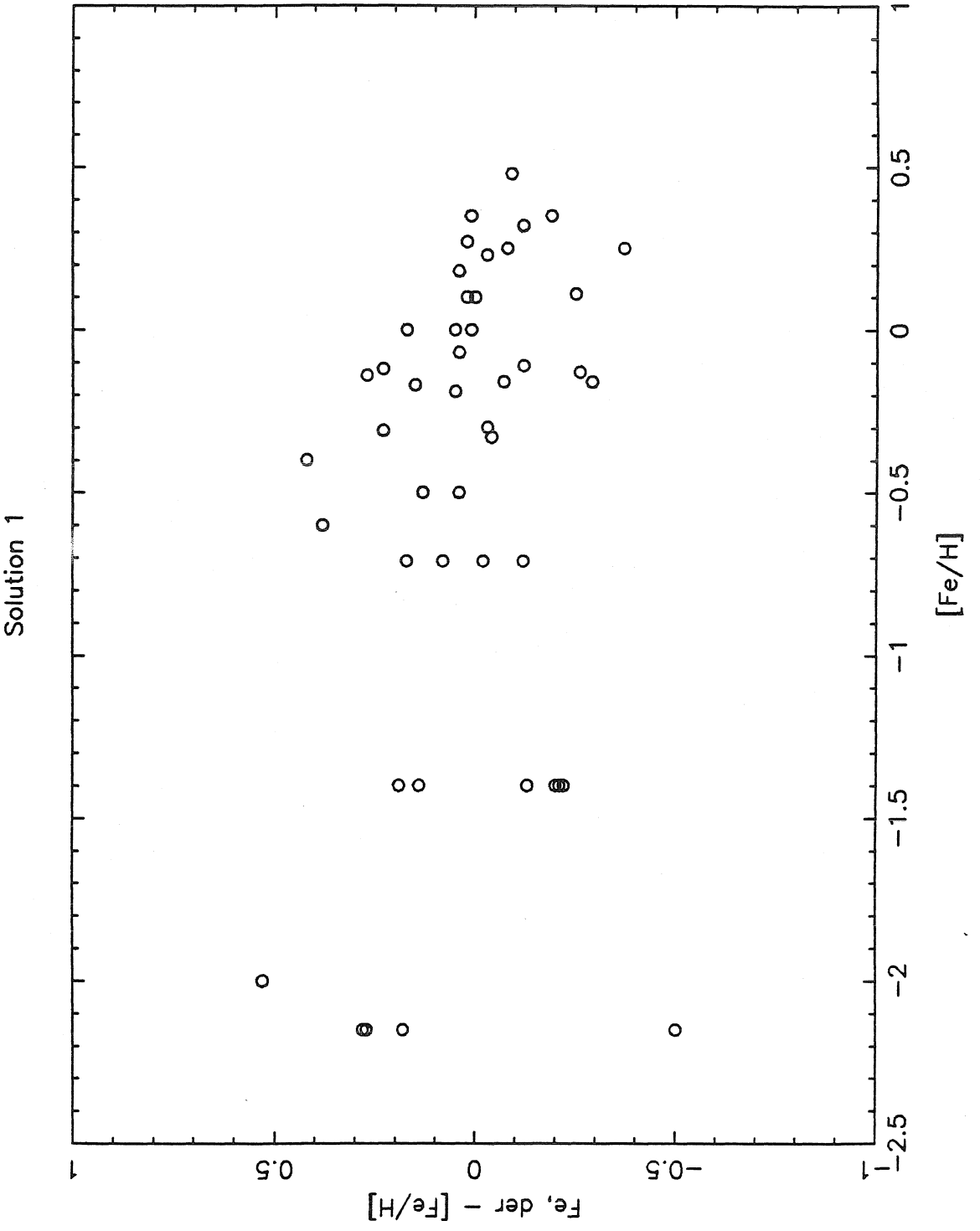

Figure 7

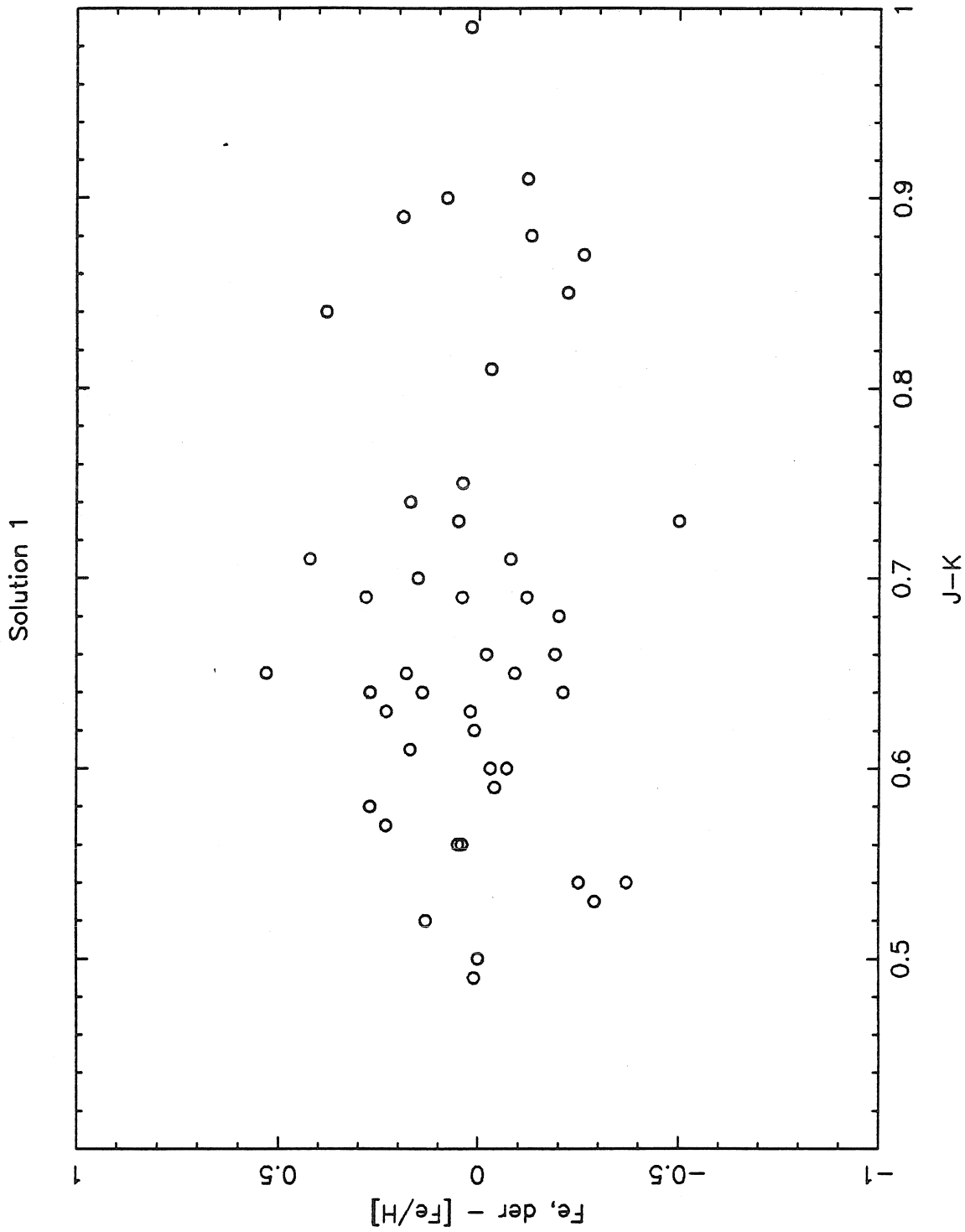

Figure 8

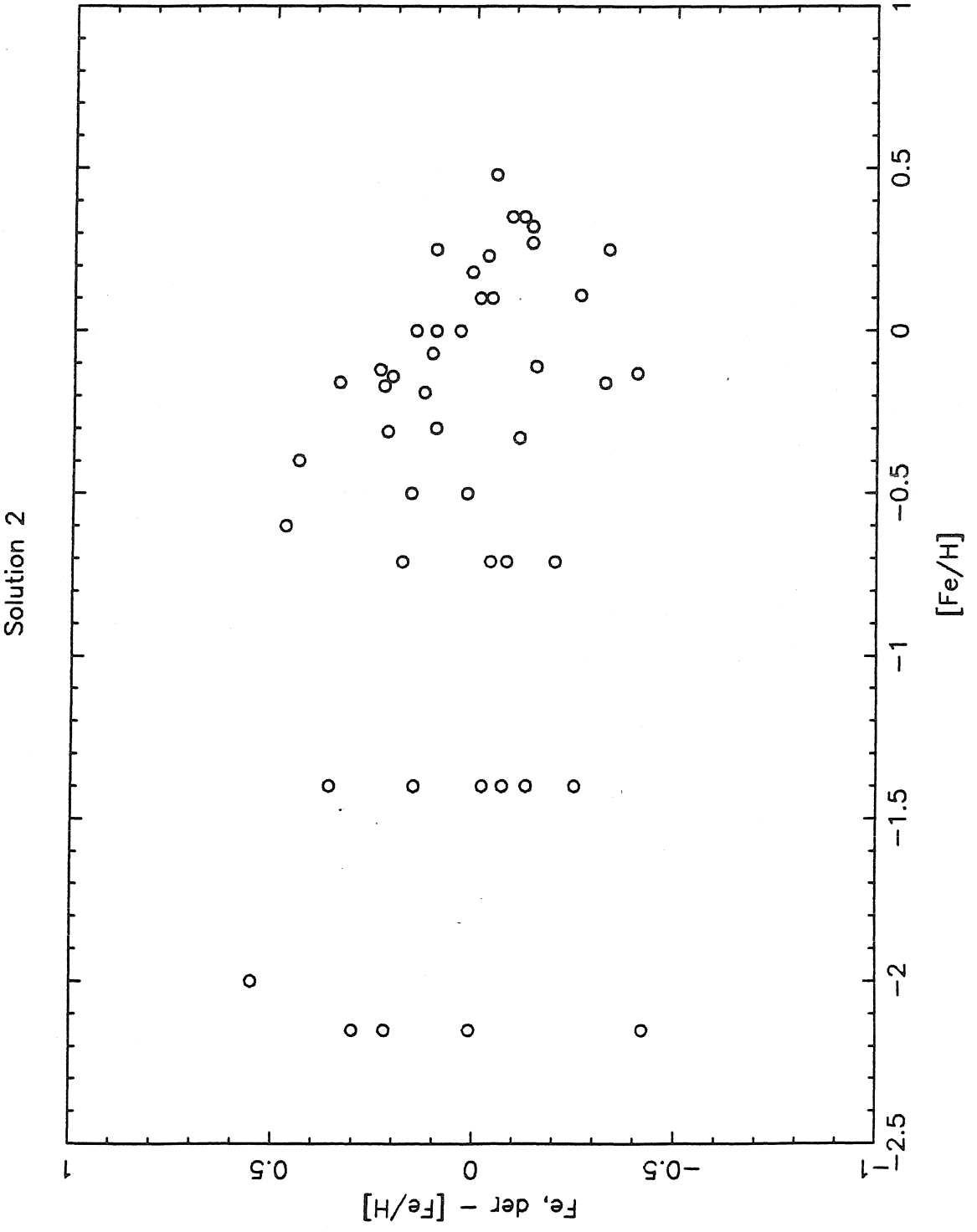

Figure 9

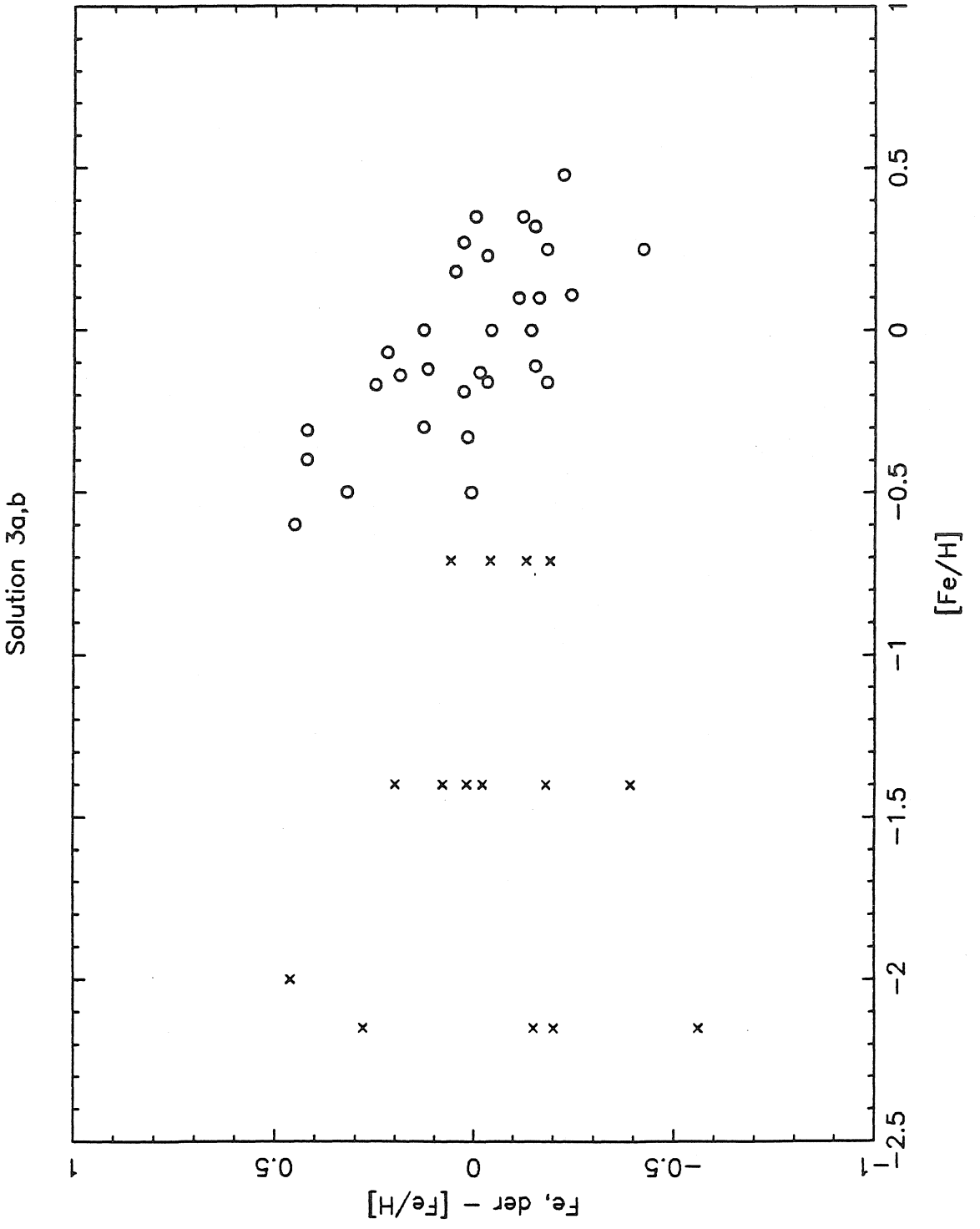

Figure 10

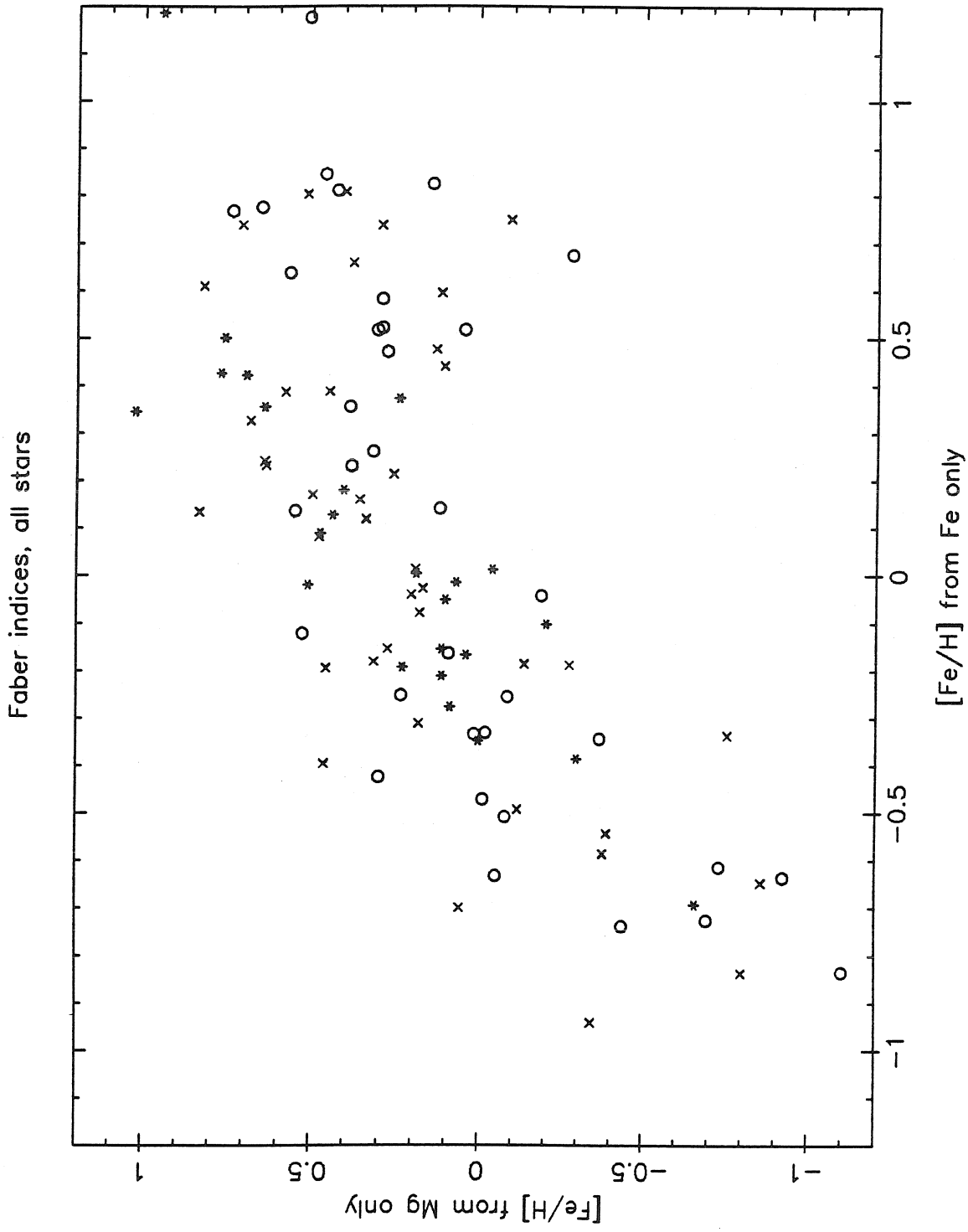
Faber indices, all stars
[Fe/H] from Mg only
[Fe/H] from Fe only
1
0.5
0
−0.5
−1
1
0.5
0
−0.5
−1

Figure 11

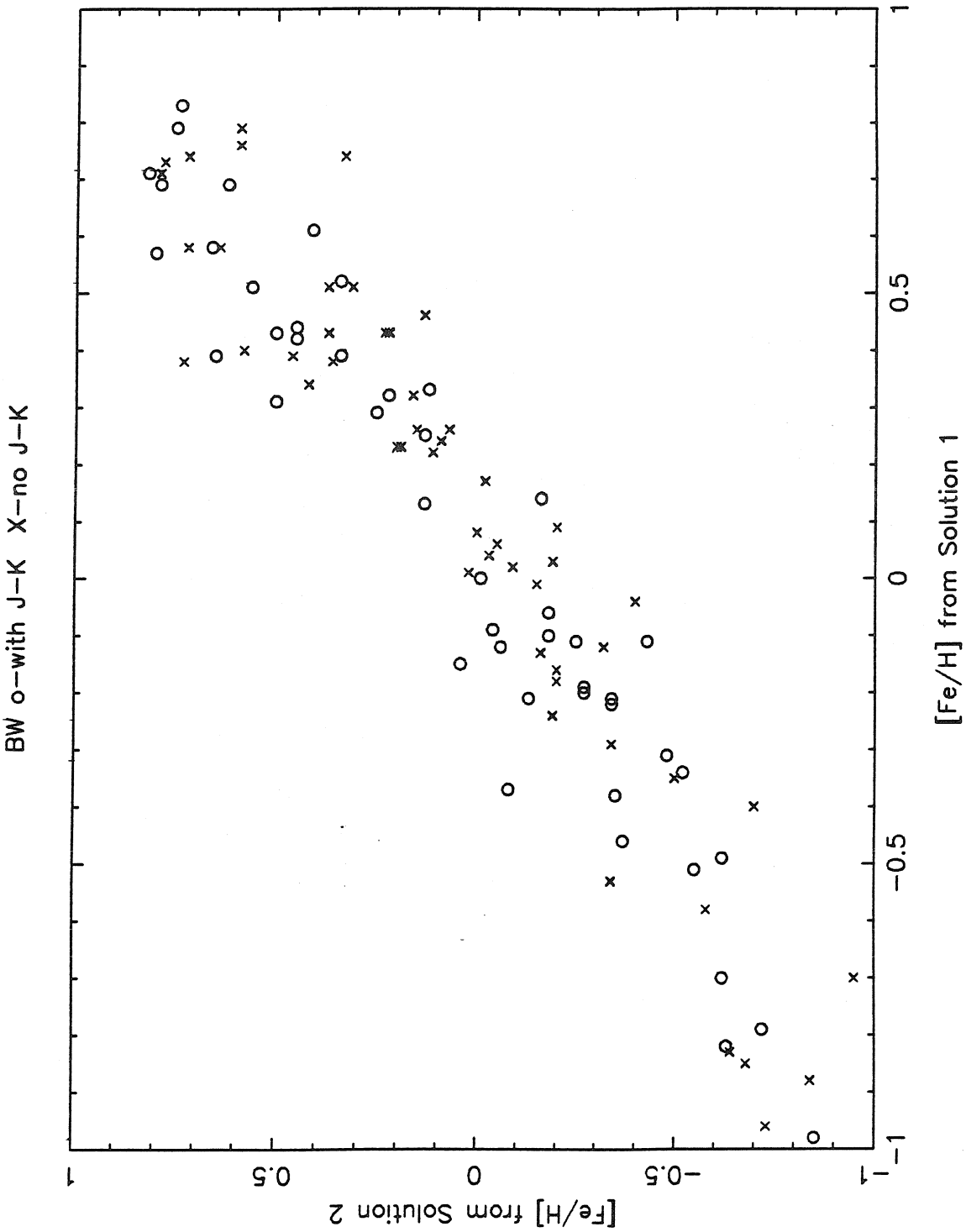
BW o-with J-K X-no J-K
[Fe/H] from Solution 2
[Fe/H] from Solution 1
1
0.5
0
−0.5
−1

Figure 12

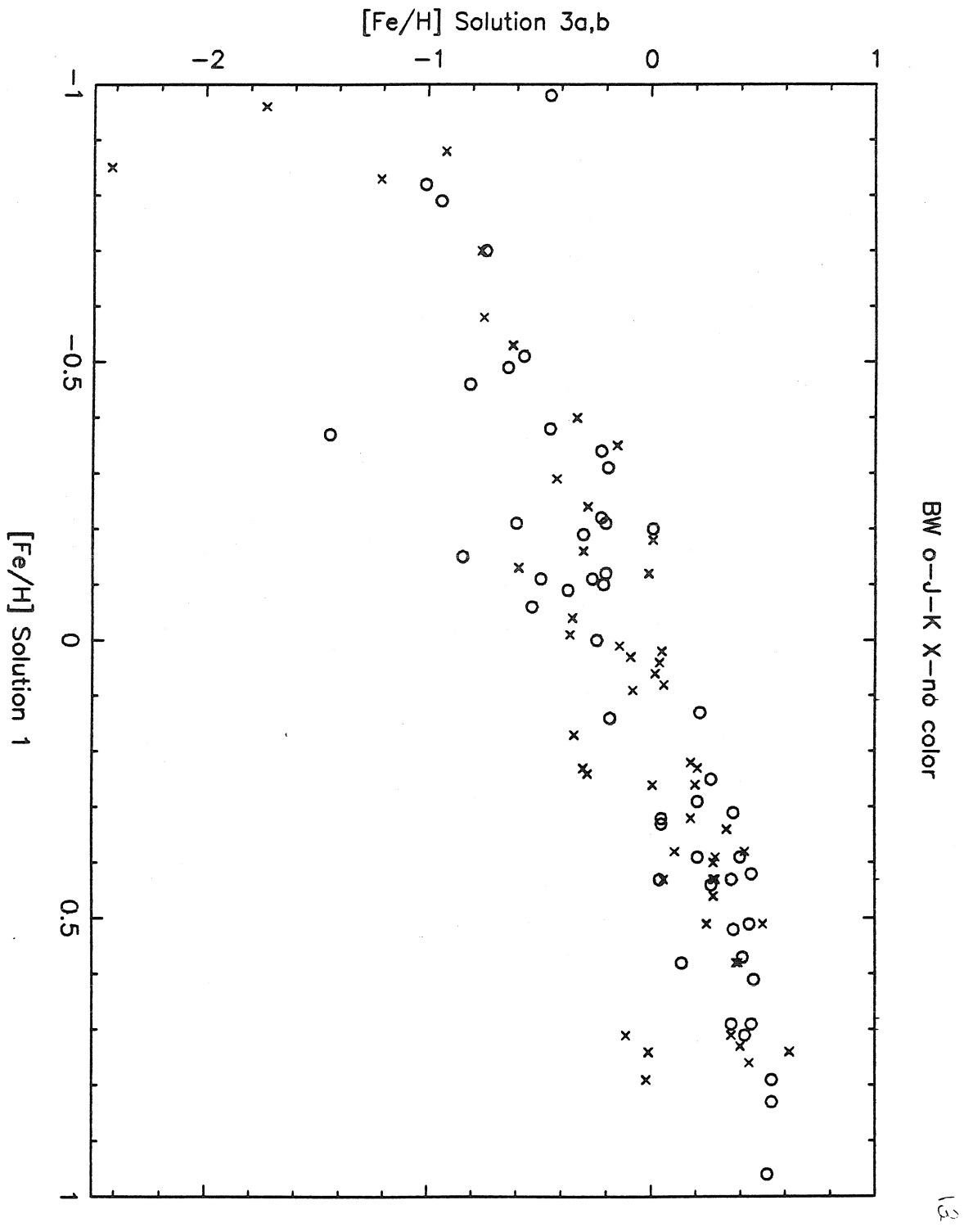
[Fe/H] Solution 3a,b
−2
−1
0
1
−1
−0.5
0
0.5
1
[Fe/H] Solution 1
BW o−J−K X−nó color

Figure 13

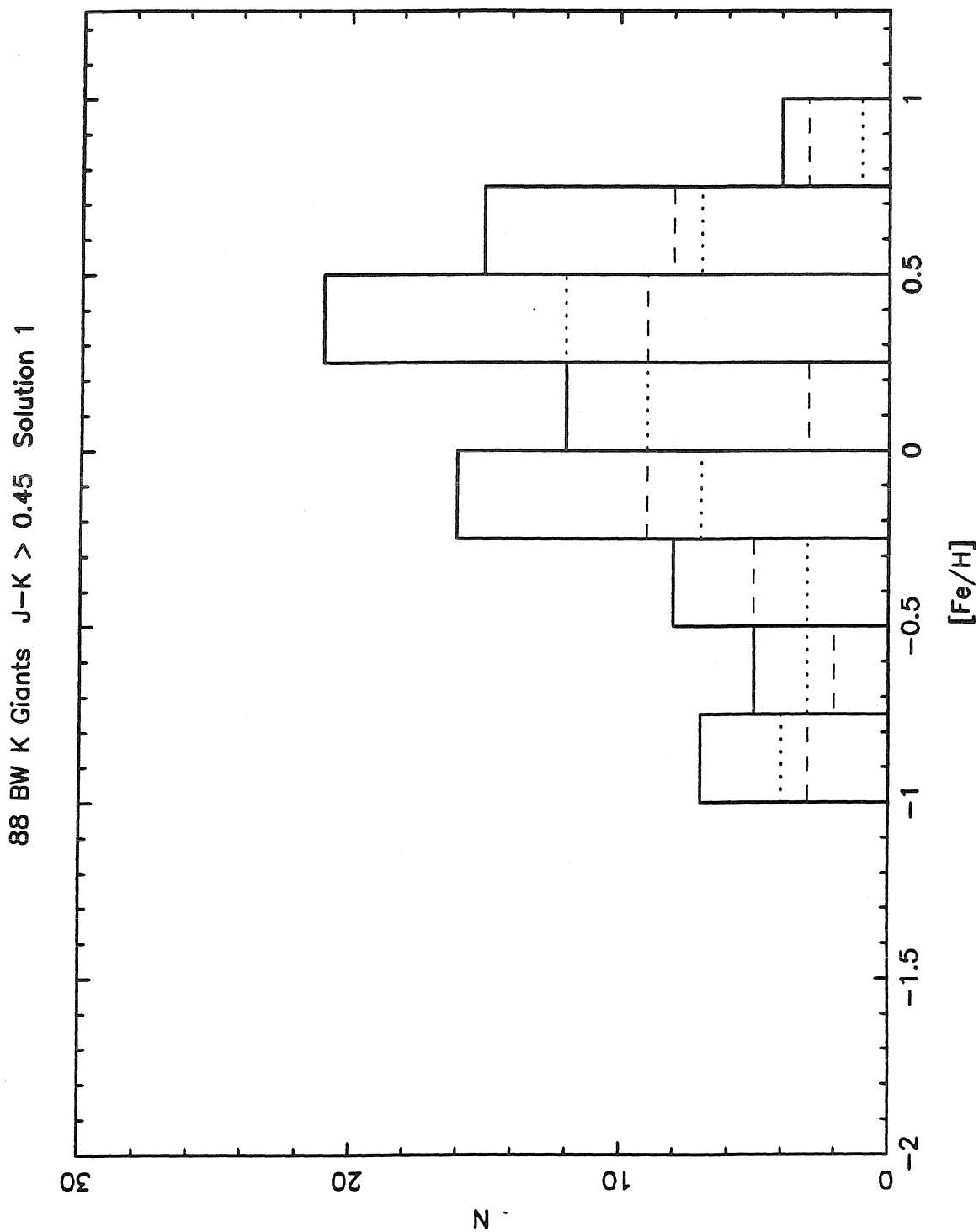

Figure 14

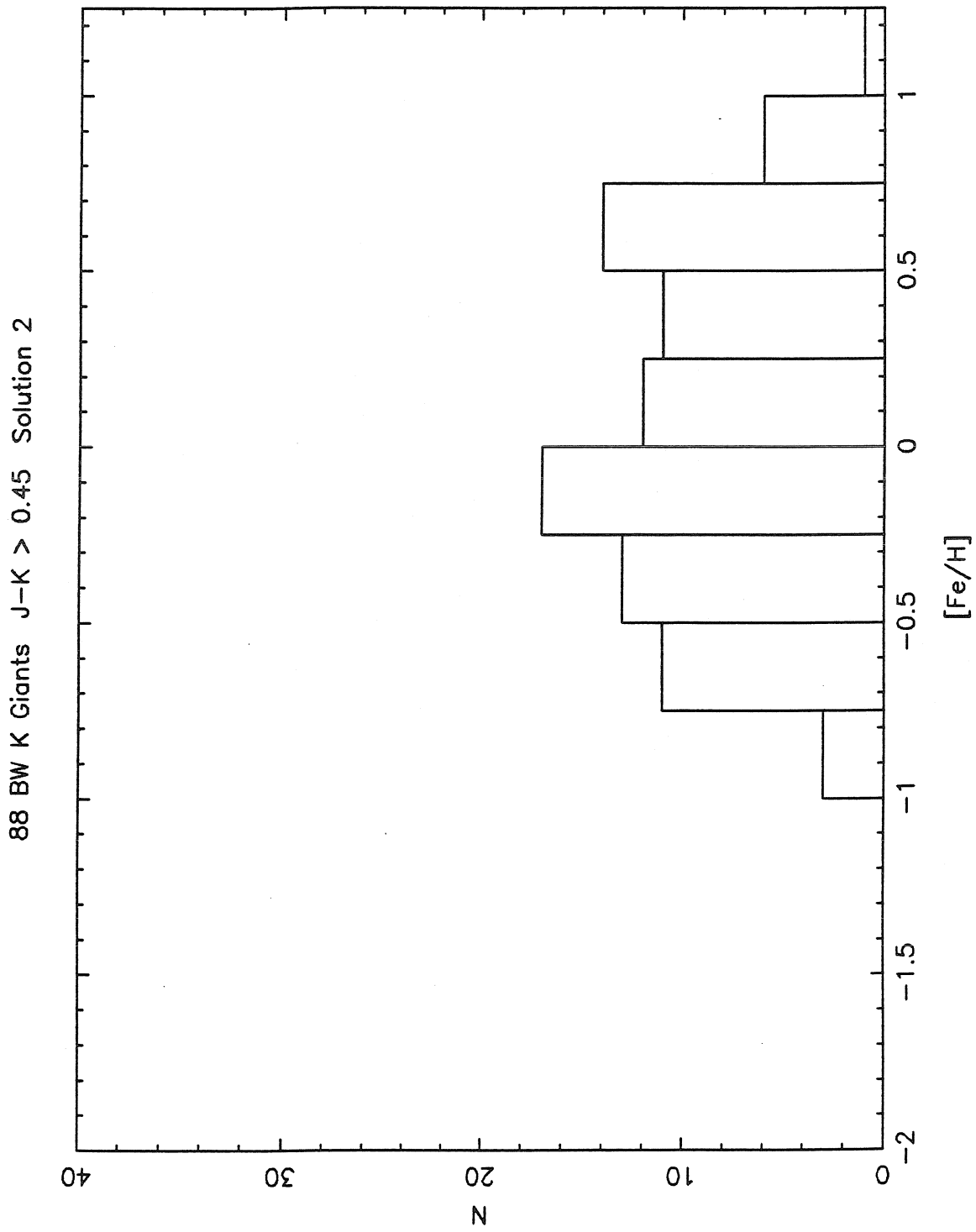

Figure 15

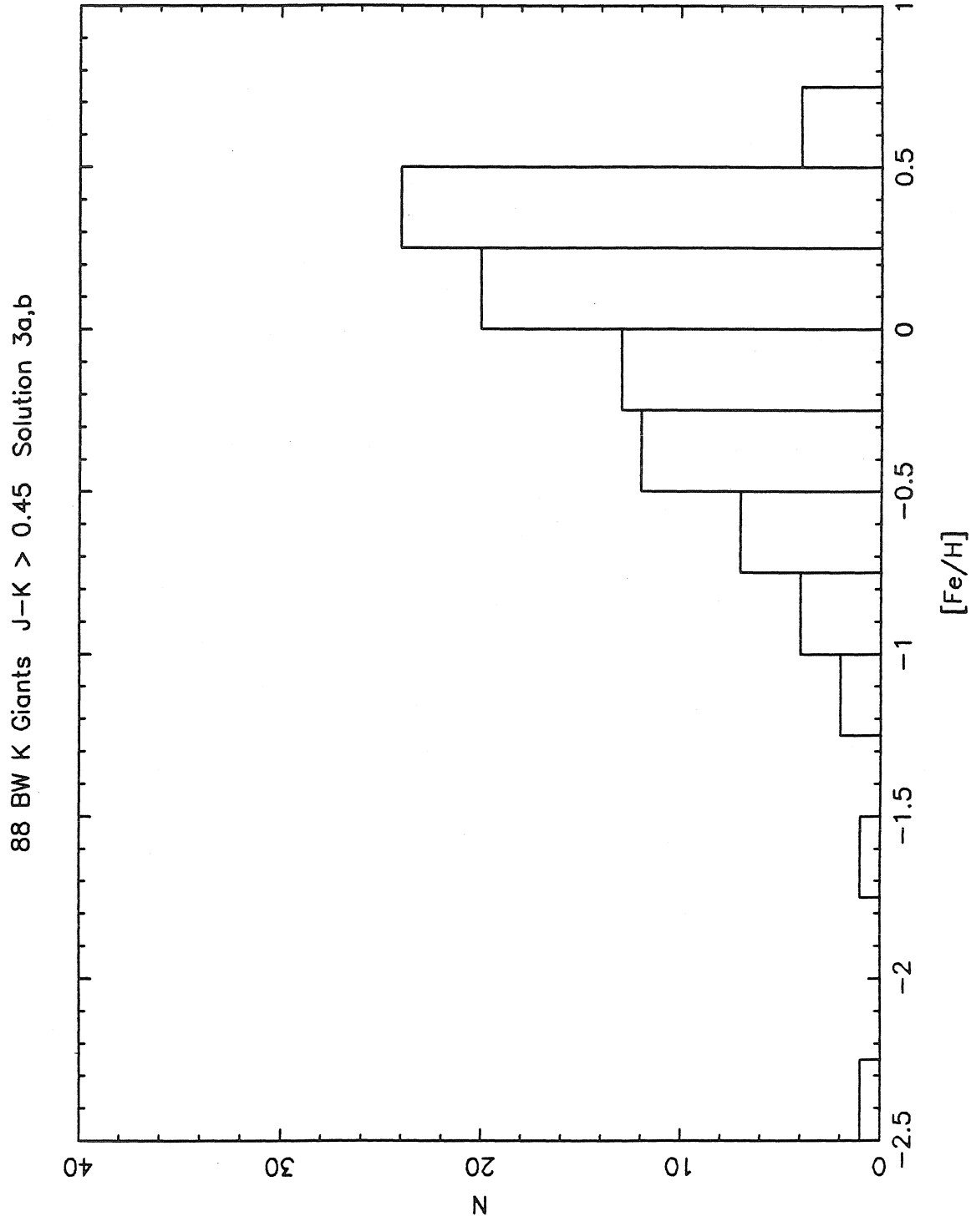
88 BW K Giants J−K > 0.45 Solution 3a,b
N
0
10
20
30
40
[Fe/H]
1
0.5
0
−0.5
−1
−1.5
−2
−2.5

Figure 16

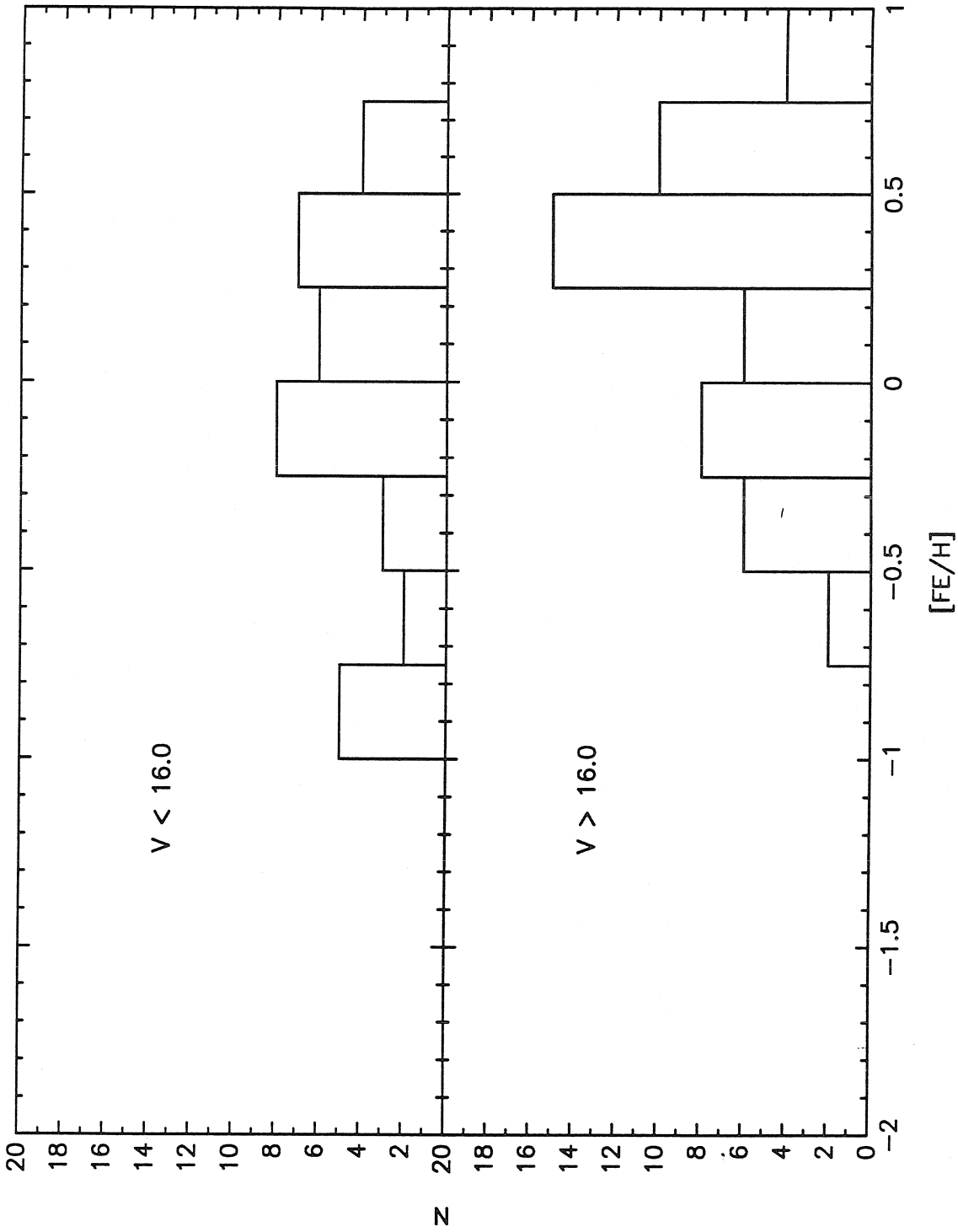

Figure 17

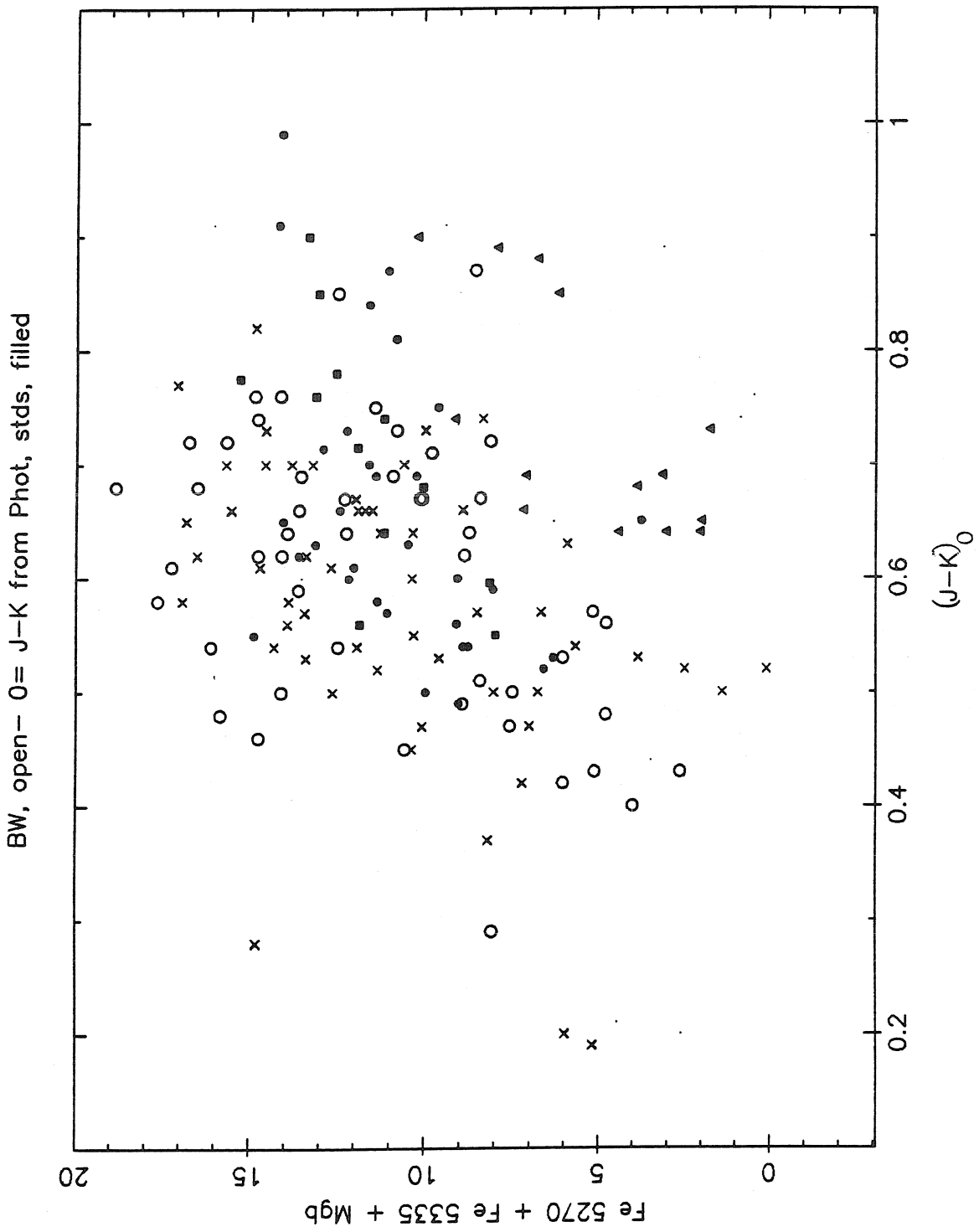
BW, open- O= J-K from Phot, stds, filled
Fe 5270 + Fe 5335 + Mgb
0
5
10
15
20
0.2
0.4
0.6
0.8
1
$(J-K)_0$

Figure 18

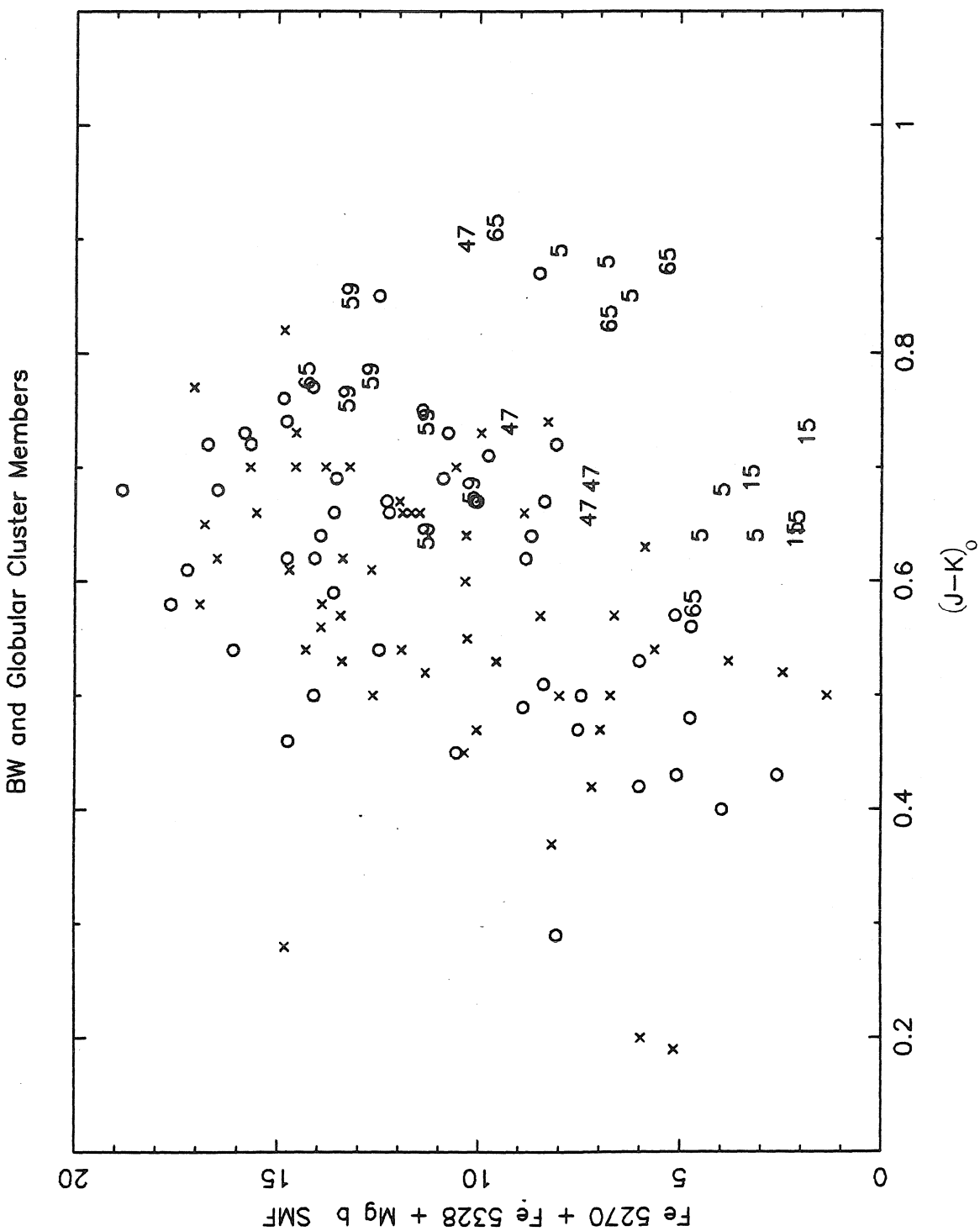
BW and Globular Cluster Members
Fe 5270 + Fe 5328 + Mg b SMF
0
5
10
15
20
0.2
0.4
0.6
0.8
1
(J-K)o

Figure 19

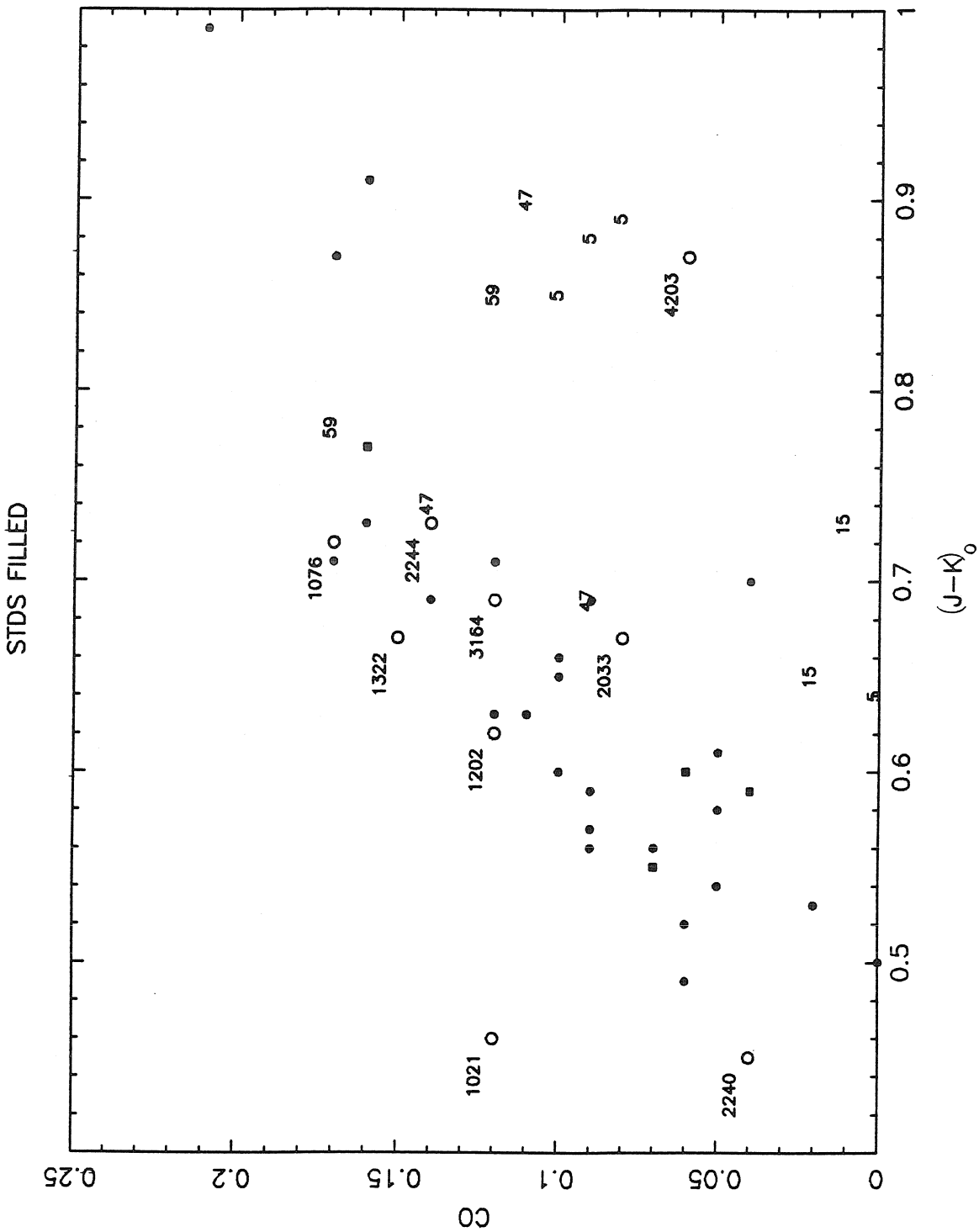
STDS FILLED
CO
0
0.05
0.1
0.15
0.2
0.25
0.5
0.6
0.7
0.8
0.9
1
$(J-K)_o$
1076
59
1322
2244
47
3164
1202
1021
2033
47
15
5
59
5
5
4203
47
15
2240

Figure 20

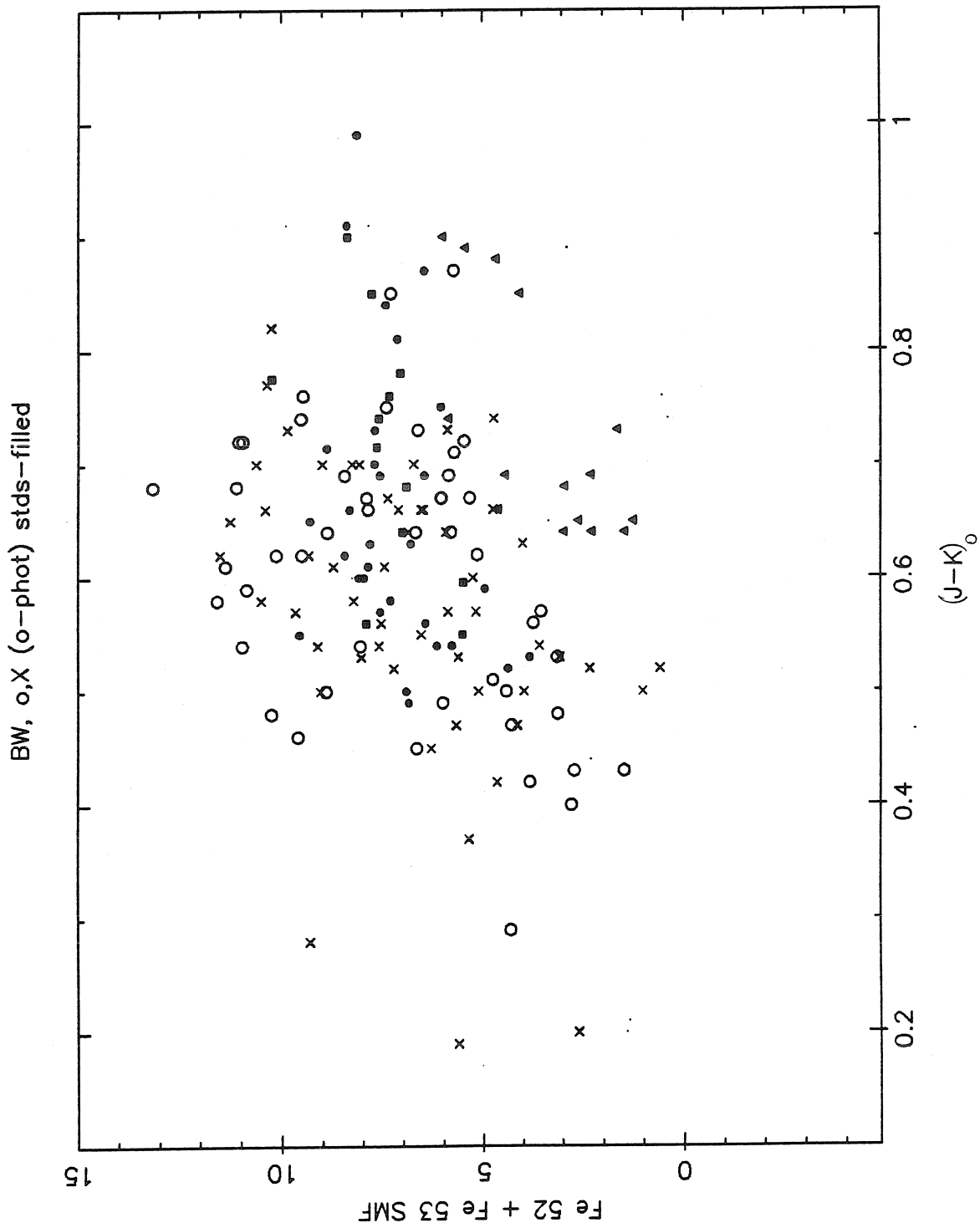

Figure 21

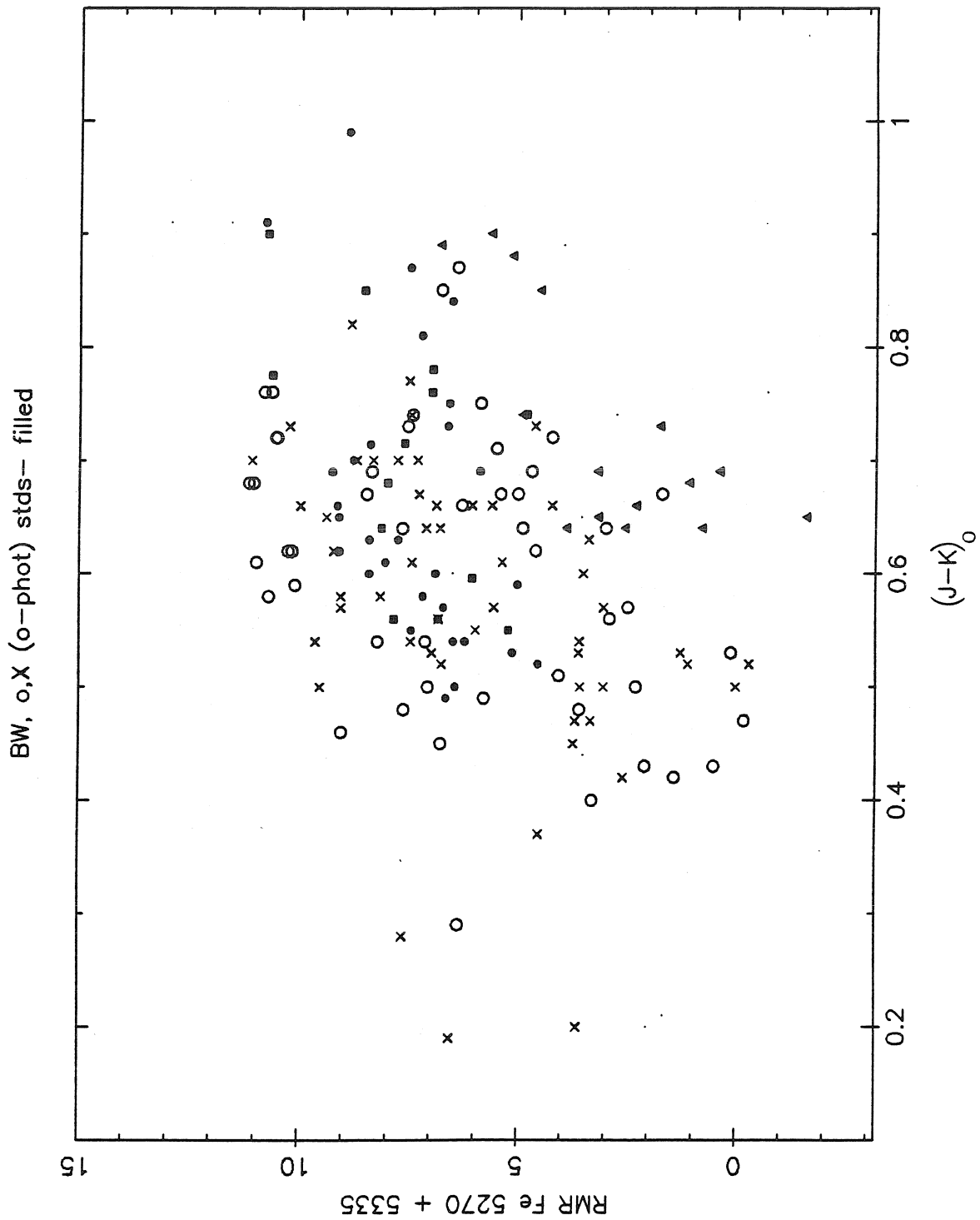
BW, o,X (o-phot) stds- filled
RMR Fe 5270 + 5335
15
10
5
0
0.2
0.4
0.6
0.8
1
$(J-K)_o$

Figure 22

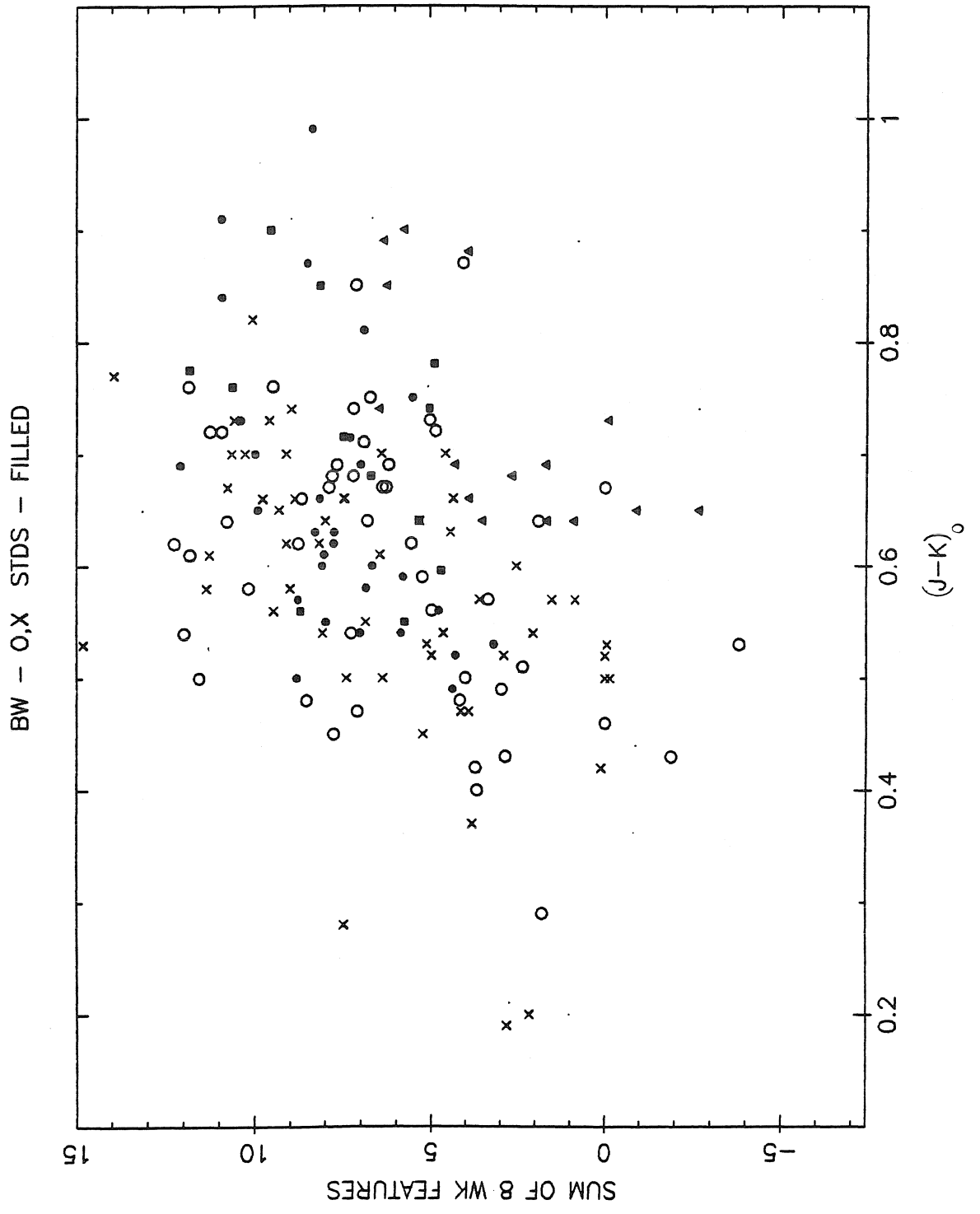

Figure 23

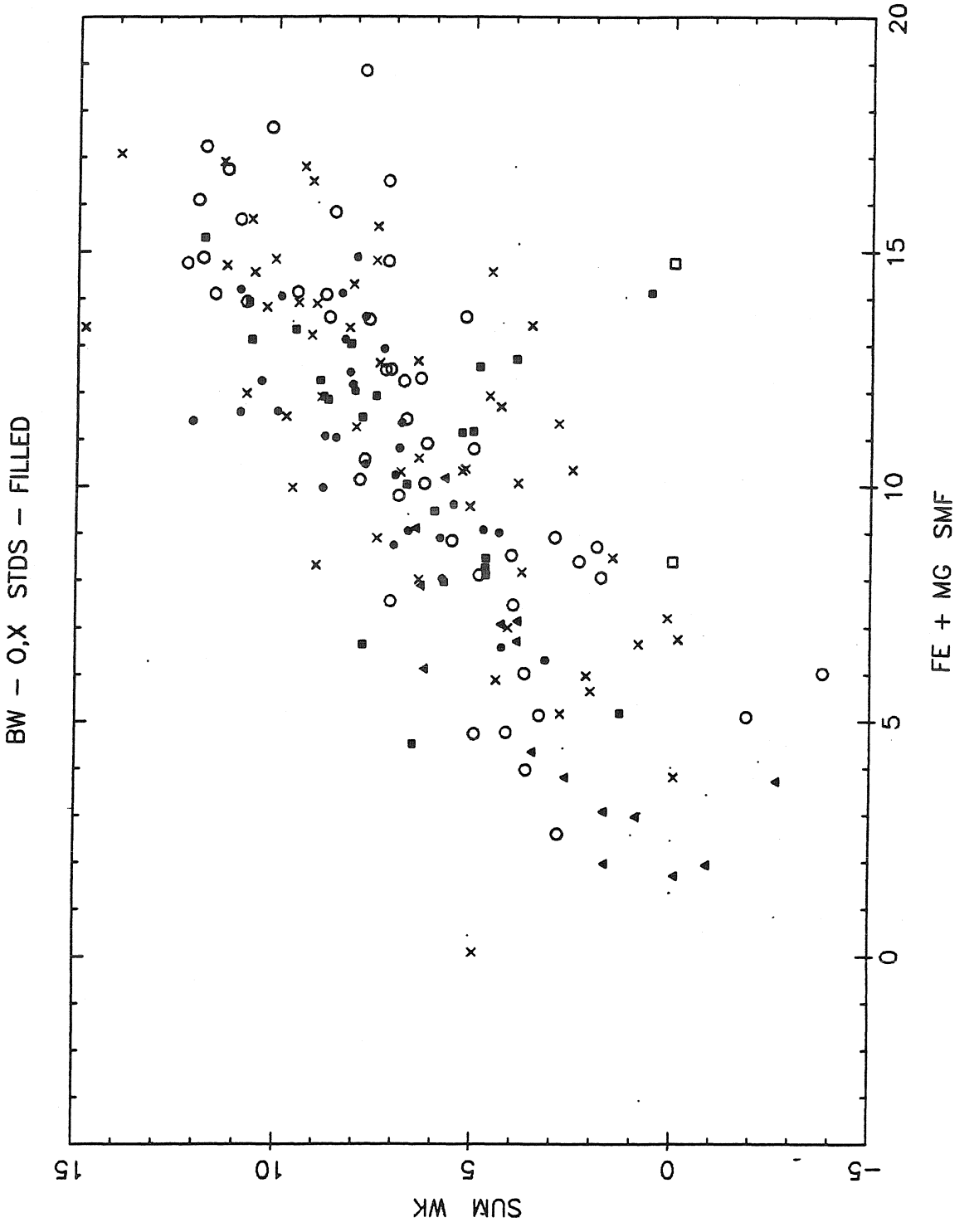

Figure 24

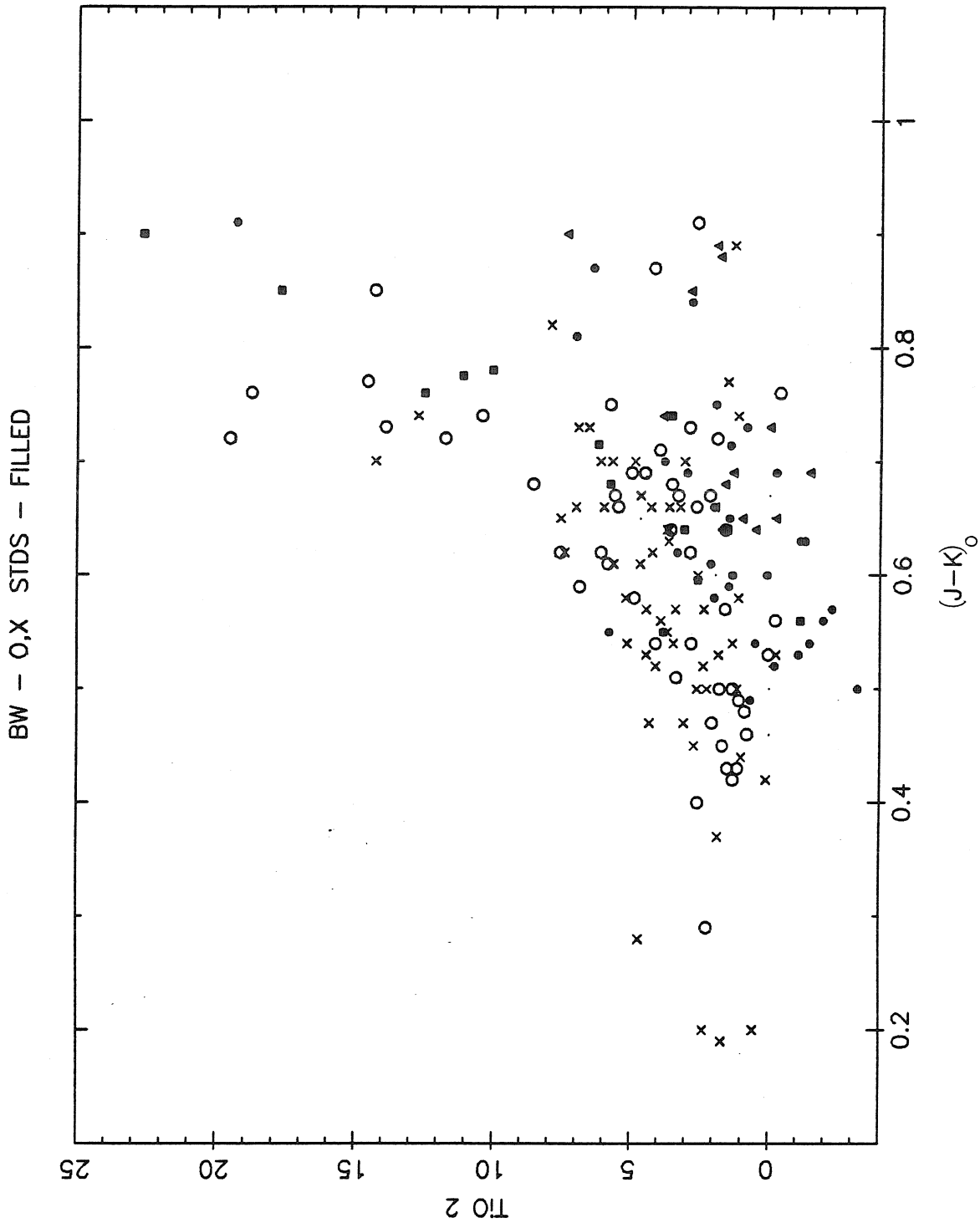

Figure 25

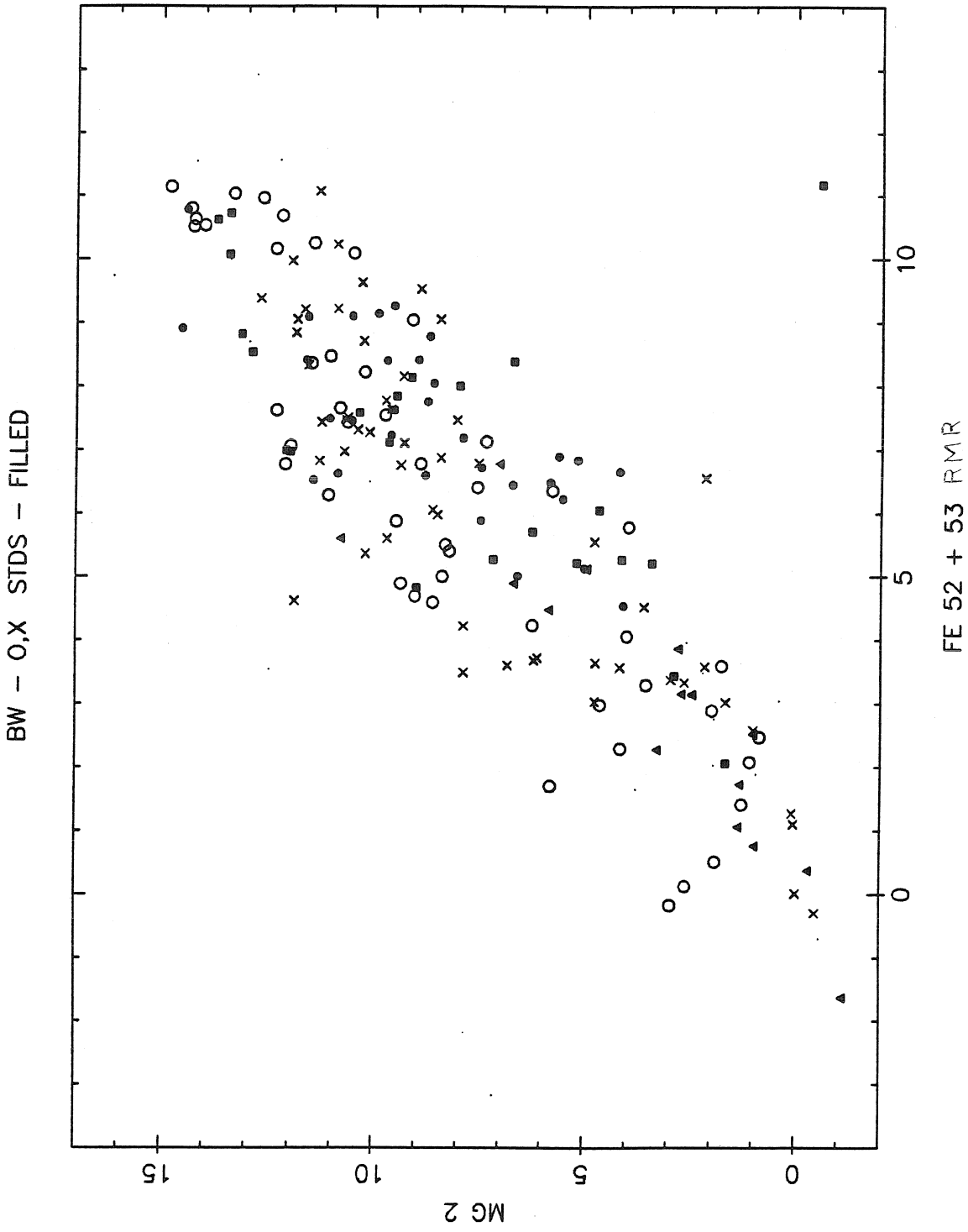

Figure 26

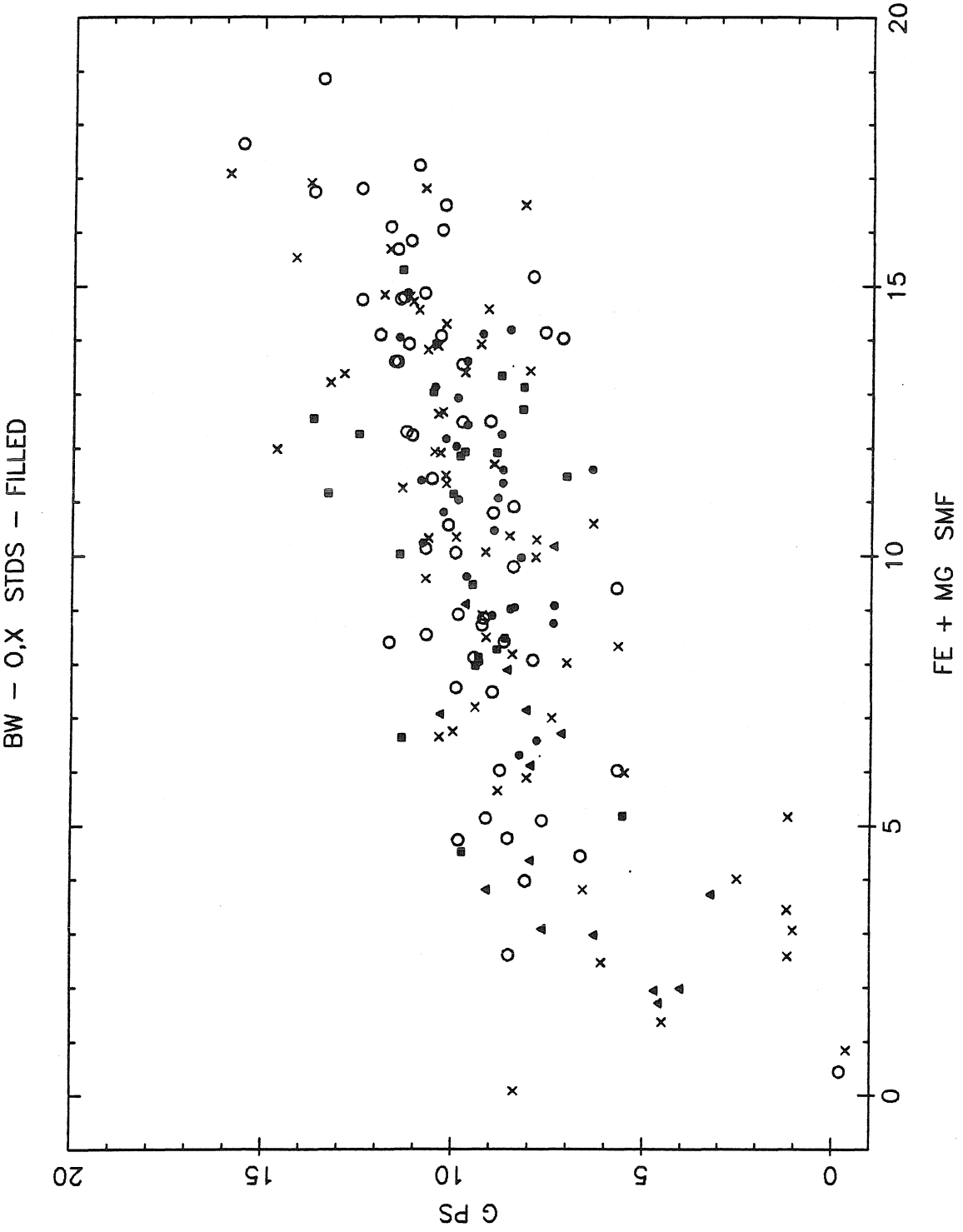

Figure 27

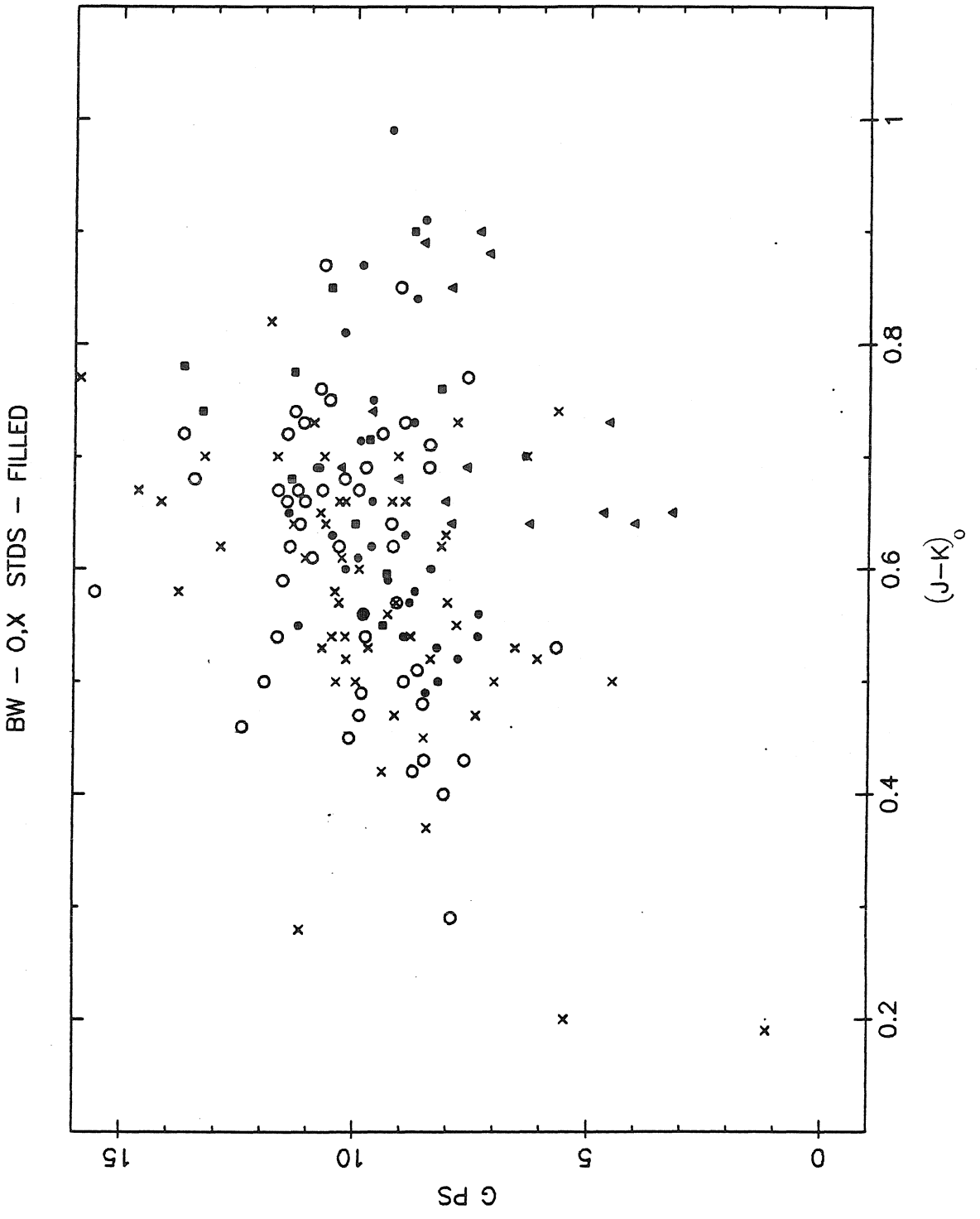

Figure 28

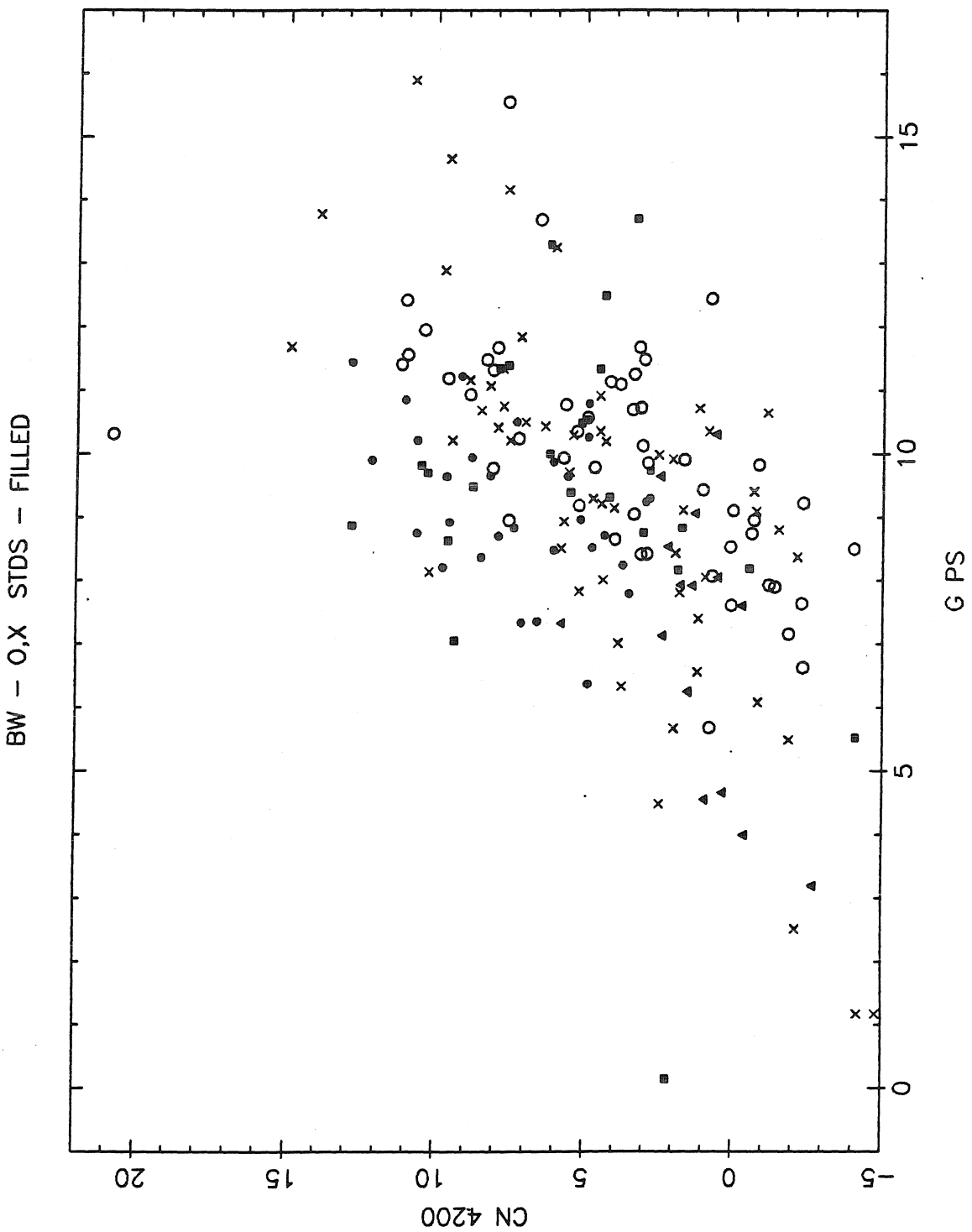

Figure 29

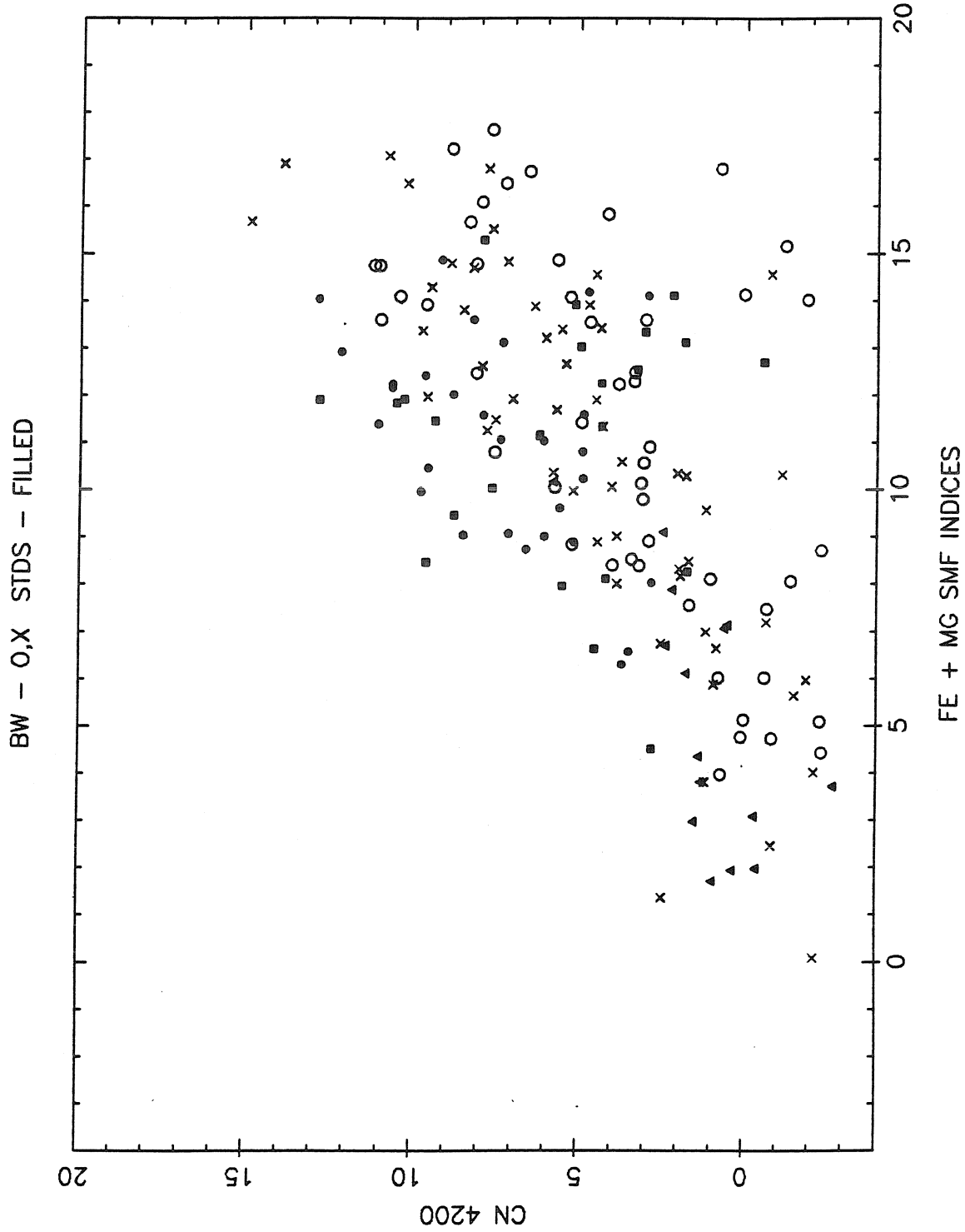
BW – O,X STDS – FILLED
FE + MG SMF INDICES
CN 4200
20
15
10
5
0
20
15
10
5
0

Figure 30

CHAPTER 3

ABUNDANCES AND KINEMATICS OF K GIANTS IN THE GALACTIC NUCLEAR BULGE

ABSTRACT

Spectroscopy and photometry has been obtained for 100 K giants in Baade's Window at $l = 1°, b = -4°$. For a galactocentric distance 7.5 kpc the line of sight passes 522 pc below the nucleus. Line strengths have been measured for 34 features. Abundances have been derived from the Fe λ 5270, 5328 Å, and Mg b features, using a technique which compares the Baade's Window giants to 45 local giants of known abundance. The abundance distribution of the nuclear bulge K giants has been derived. The abundances run from -1 to nearly $+1$ dex, with a peak at 0.3 dex, or twice the solar abundance. Of the 88 stars with derived abundances, 22% exceeded the abundance of the most metal rich local K giants; 50% exceeded the solar abundance, and 10% were metal poor (< -0.6 dex). We present evidence for high metal abundances in the nuclear bulge K giants based on a wide variety of features, including clumps of weak iron lines on the linear portion of the curve of growth.

I. Introduction

Given the derived abundances of bulge K giants in chapter 1, it would be interesting to know their kinematics. The line of sight towards Baade's Window is ideal for using radial velocities to distinguish between circular orbits (with only small components in the line of sight) and radial orbits, which statistically would have larger components in the line of sight. Measurement of velocity dispersion would help to place the K giants among the other populations in the bulge, and any change in the dispersion which depended on metal abundance could preserve a record of the enrichment history and formation of the stellar population.

II. Observations

Spectra of a total of 88 K giants were obtained using the 2.5m du Pont telescope of the Las Campanas Observatory and the Shectman (1978) photon-counting Reticon detector (Shectograph) was used every year but 1985. In 1985, this instrument was replaced by a 2 dimensional photon counter designed by Shectman known as the 2D-Frutti (2DF).

Observations in 1980, 1982, and 1983 were made with the Shectograph and the 600 line grating blazed at 5000Å and were used primarily to derive abundances. In 1984 and 1985, for reasons described in §III, the 1200 line grating blazed at 5000 Å was employed. Spectra obtained at low resolution had 3650 bins from $\lambda\lambda$3500 to 7000Å with a dispersion of 1.04Å per channel. In this mode, one resolution element was 5Å. In the high resolution mode, the spectra had 0.55Å per channel, covered 3900 - 5800 Å, and one resolution element was 2.7Å. The 2DF has 3040 channels,

and only the 1200 line grating was used with it. This resulted in 0.69Å per channel, and a wavelength range of 3900 to 5800 Å. Exposure times for these red V=15.5-17 mag giants were from 2000 to 4000 sec. Arc exposures were obtained every 1000s. In 1984 and 1985, at least 3 radial velocity standard stars were observed every night. When possible, an exposure of the morning twilight sky was also obtained.

Observations using the 2DF were made with 3040 channels in the dispersion direction and 256 rows in the spatial direction (only about 130 of which fell on a usable portion of the detector). When the 1200 line grating was used, the spectra had a full width at half maximum of 4 rows in the *spatial* direction, a focus of 8 $''$; this increased the noise in the object due to sky.

The reduction package LOLITA, written by Peter Young, was used to reduce the one dimensional shectograph data; the following steps prepared the spectra for cross correlation:

1. Division by a tungsten flat field exposure, the sum of beginning and end of night flat fields.

2. A wavelength calibration using 40 to 45 He, Ar, Ne, and hollow cathode arc lines. The initial step was to fit a polynomial of order 5 to a long arc exposure taken at the beginning of the night. The A and B side were fit independently.

3. To solve for the wavelength scale for individual objects, the fit of the long arc exposure was perturbed up to terms of order 3. The highest order terms were presumed not to vary during the night. These "shift corrections" were usually about

1 - 3 channels for the high resolution mode. Shifts in the wavelength polynomial of up to 1.5 channels occurred at random times. Channel shifts also increased with increasing hour angle, as was found by Mould, 1983, and when large moves of the telescope were executed. The largest observed shifts were about 5 channels.

4. The background was subtracted and the A and B channel observations were summed. Although separate wavelength solutions were made for the A and B sides, subtraction of sky in B from a star observed in A (or vice versa) resulted in a clearly imperfect sky subtraction. The λ5577 Å night sky line had the appearance of a "P Cygni" profile line. As sky counts frequently amounted to as much as 40% of the counts in the blue, spectra from just the A or B sides were unacceptable for radial velocity measurement. Only summed spectra with a cancelled night sky line were considered suitable for radial velocity measurement; the A and B sides were on velocity systems which differed by 50 km/s. This was verified for spectra independent of the data reduction programs used. A spectrum reduced as above was ready for logarithmic rebinning and cross correlation, as described in §III.

For the 2DF spectra, data were reduced using the Figaro reduction package written by K. Shortridge, and the following steps resulted in a spectrum ready for cross correlation:

1. A flat field frame was prepared from beginning and end of night exposures. The frame was collapsed perpendicular to the dispersion, and a smooth polynomial spline-fitted to the result. The flat field was divided by this, resulting in data numbers over the frame near unity.

2. The frames were trimmed to contain only usable data, the channels were reversed so that blue and red were in the proper sense, and divided by the flat field.

3. Two dimensional data obtained using photon counters behind image tube chains have large distortions which cause a straight stellar spectrum to appear noticeably curved. Every few nights, a flat field exposure was obtained through nine equally spaced apertures. This exposure of nine curved spectra was the basis for a distortion correction (re-binning) which was applied to all the spectra. After this step, the nine initially curved "spectra" were rendered straight.

Steps 1-3 were performed automatically by a "macro" program, so a tape could be mounted and the process proceeded without need for intervention.

4. Although most of the visible distortion was removed using the distortion correction, the arc spectra were noticeably tilted across the slit, and a two dimensional arc fitting procedure was required. Initially, 20 rows of spectrum were extracted and added perpendicular to the spatial direction. A wavelength calibration was performed on this single high signal to noise ratio arc spectrum. 40-45 lines were fit to a 5th order polynomail and the resulting fit had an rms residual of 0.12 to 0.20 Å.

5. The fit was applied to a full arc frame. Only the 30 strongest lines were used, and were supplemented by weak lines in the sparse 5000 - 5500 Å region. Rows were summed in groups of five and the entire frame was split into regions which were fit with their own wavelength polynomials. Program spectra bracketed by arc observations were rebinned onto a linear wavelength scale following this prescription.

After this step, the strong night sky line λ5577 Å would subtract nearly perfectly from spectra when sky >> star. The procedure used by FIGARO could be improved by taking the shift-correction approach of LOLITA (this holds the high-order terms of the wavelength polynomial constant) and requiring some continuity across the frame (currently, each row is treated as an independent spectrum). There was not enough signal in the arc lines to get an excellent fit, and the residuals climbed to 0.25 Å. This would likely not be a problem if the Neon spectrum were used, because of its brighter arc lines.

6. The frames, now flattened and fully rectified, were ready for extraction of the objects. The frame was collapsed to a one dimensional plot of total counts as a function of row number, so a star appeared as a peak. From this, clean sky regions were selected, and subtracted from the extracted star spectrum.

At this point, the Shectograph and 2DF spectra were ready for velocity measurement, as described below.

III. Velocities

The cross correlation method of Tonry (1983) was employed to measure radial velocities. This procedure uses a high signal to noise ratio template and produces a spectrum with a peak centered near the central channel and a background of some noise. Several examples are illustrated in Figure 1. Figure 1 d is apparently an optical double, as its 450 km/s separation did not change over a period of 3 nights. The peak can have a maximum height of 1.0, and can be completely absent if there is no correlation. The height of the peak can be reduced by a mismatch between the template and the object, or (as more commonly occurred) by a low signal to noise ratio in the object spectrum (however, Tonry and Davis (1979) show that the error does not decrease appreciably for $S/N > 8$). As a rule, an attempt was made to get a minimum of 300,000 counts in the object spectrum. The procedure benefits if the template has very high signal to noise ratio . As the template was observed every night of a run, each nightly template was shifted and co-added to produce a single template with about 10,000 counts per channel. Every object, including individual template observations, was cross-correlated with this grand sum template.

In preparation for cross correlation, the wavelength scale was rendered logarithmic into 2048 channels from 4300 to 5800 Å for all of the shectograph data, and into 1024 channels from 4700 to 5700 Å for the 2DF data. This resulted in 43.8 and 56.5 km/s per channel, respectively.

The original method of observing, used in the 1980 observing season, was to obtain spectra using two 2 " X 4 " apertures, A, and B, as star and sky. Arcs

were obtained every other object when working in the same field. Ultimately, it actually proved necessary to obtain arcs no less frequently than once per 1000s and to bracket each exposure with them. Several unexpected difficulties occurred in the course of obtaining radial velocities for the nuclear bulge K giants.

1. The sky aperture was frequently contaminated by a faint star, and it was necessary to rotate the spectrograph in order to locate a true sky patch. This rotation frequently exceeded 90°, and caused several channel ($\sim$ 2Å) shifts in the arc lines.

2. For K giants, the region $\lambda\lambda 4900 - 5500$Å contains the all-important MgH region and many other important atomic features, such as Fe I λ5270 which contribute power to the cross correlation. This region has a lack of strong arc lines and is inevitably poorly fit by any arc fit.

3. The weak lined K giants required a high dispersion spectrum to get a good correlation peak (> 0.2) for the velocity determination. The weak lines were not resolved at lower dispersion.

The best observations were made in 1984 and 1985, when the 1200 line grating was employed. When possible, the observations were made through a 1 $''$ slit. Three or four radial velocity standards and the twilight sky were observed each night. The following standards were used:

1. Members of 47 Tuc with from Mayor *et al.* 1983, measured to 1 km/s accuracy with a radial velocity machine which used a physical template.

2. Members of M3 measured the same way by Griffin and Gunn 1981.

3. Standards from Tonry (1984)

4. The twilight sky.

5. Two members of the globular cluster NGC 6522, with radial velocities measured from high resolution CCD spectra.

These were measured from data kindly obtained by Dr. J. A. Graham using the CTIO 4m telescope and RC spectrograph with a GEC CCD detector. The wavelength range was 6394 to 6735 Å and a resolution element was 1.8 Å. The more stable CCD detector yielded very accurate radial velocities. NGC 6522 star 9 (Arp 1965) was measured to have a heliocentric velocity of -24.1 ± 1 km/s and star 70 has -27.1 ± 1 km/s. Webbink *et al.* (1981) list $< v_r >$ for NGC 6522 as 8 km/s, however the most modern measurement, using Hα Fabry-Perot interferometry, was -25 km/s (Smith, Hesser, and Shawl, 1976).

Cross correlation against a grand template yielded radial velocities for every object, including observations of the template star. Standard objects for each night were corrected for heliocentric velocity and then differenced with their catalog values. The mean of these differences provided a zero point for the night, to be added to all measured velocities. These zero points were determined to $\pm 10 - 20$ km/s each night. There was some evidence for zero point shifts from night to night at the 10 km/s level, but not at a level of significance which called for nightly corrections. For both the 2DF and Shectograph, a grand average of the standards

was ultimately used to set the zero point. As a result of the numerous repeats of standards, the formal error on the zero points was 2 km/s for both instruments (sigma of the mean). The best procedure for obtaining accurate radial velocities is to obtain several standards during the night, even though there was no strong evidence for a zero point shift during these particular runs.

Analysis of 26 repeat observations of program stars from 1984 and 1985 found the error of a single measurement to be $\sigma = 15$ km/s. Frequently, repeat observations were identical to within 10 km/s, and no repeat was different by more than 40 km/s (save for one measurement of 2119, which was so discrepant it was rejected).

Since it is well known that weak lined stars produce low-amplitude, hence low accuracy correlation peaks, special emphasis was placed on repeat observations of these stars. As a group, they repeated as well as strong lined stars (in the high dispersion mode). Star 5006 did not yield a correlation peak in the low dispersion mode, yet did have a well defined peak when observed at high dispersion.

The 1982 data, obtained in the low resolution mode, had several problems. Bright stars were used as radial velocity standards, but had to be observed using a post-slit neutral density filter. This procedure was reported to yield accurate velocities, but did not do so in this case. The error of $\sigma = 70$ km/s was unacceptable. The 1982 had 33 bulge stars in common with the higher accuracy 1984-5 measurements, which allowed an accurate zero-point to be determined. The mean offset was used to correct the 1982 velocities to the 1985 system. The lower accuracy 1982 stars had $\sigma = 118$ km/s, while the same set of stars observed in 1984-5 had

σ = 113 km/s; the larger dispersion can be accounted for by an error of 34 km/s present in the 1982/3 data added in quadrature. The difference between the 1982 data and the 1984-5 data, based on 33 program stars, had a σ = 35 km/s, and the zero-point correction was determined to $\pm$5 km/s. No repeat observations of program stars were made in 1982, although agreement with the 1984-5 high quality data is encouraging.

When the sample was split by apparent magnitude, the fainter half (fainter than V=16.0 mag) was found to have a dispersion of 109 km/s. This indicates that the fainter magnitudes did not increase errors substantially, nor are those stars at a different spatial location.

In Figure 2, the zero point corrections are illustrated for each set of data. The high resolution observations exhibit, by far, the tightest distributions. Figure 2c is the distribution of velocity differences between bulge stars observed in 1984/5 and 1982/3 and illustrates the much larger errors associated with the 1982/3 season, errors which would appear to be due to causes other than the decrease in resolution.

IV. Discussion

The most reliable data, those obtained at high resolution with sufficient standardization, were those of 1984 and 1985. These results are found in Table 1 and the less reliable 1982/3 data are listed in Table 2. The data set of 1984/5 is to be preferred for the reasons stated in §II. Repeat observations of program stars in different years and with different instruments also lends support to the belief that these data are sound, with errors no larger than 15 km/s.

In Table 3 and in Figures 3 and 6, one sees that the metal rich K giants have a dispersion smaller than the metal poor stars by 30-40 km/s. This effect even appears to hold for Mould's (1983) late M giants, which can be separated into groups according to temperature. The coolest M giants are the most luminous (Frogel and Whitford, 1982) and statistically have metal rich progenitors. One might speculate that the hotter giants may correspond to the giant population observed in the "metal rich" globular clusters such as 47 Tuc Based on this, the M giants also seem to show an effect, as illustrated in Figure 4.

While the results of Table 3 are intriguing, their statistical significance was found to be only marginal. The Kolmogorov-Smirnov 2 sample test found no significant differences between the metal rich and metal poor K giant velocity distributions, and was unable to reject the null hypothesis that the distributions are identical, except at the 50% significance level. This result repeated itself on other samples and other subsets, such as comparison of stars of abundance greater and less than solar. A running boxcar average of velocity and dispersion appeared to

indicate a change in the popultion at greater than -0.2 dex, but it was found not to be significant.

The next step was to verify if the velocity dispersions were in fact drawn from gaussian distribution functions. Because the gaussian parameters are estimated from the population, the Kolmogorov-Smirnov test must be modified (Lilliefors, 1974). This modified test never showed any deviation from a gaussian distribution in any subset of the velocity sample. An illustration of the cumulative counts compared with the error function is illustrated in Figure 5.

Having verified that the velocities were drawn from gaussian distributions, one can estimate the mean and sigma following the usual procedures. Application of the F test to compare two dispersions confirmed that the metal rich objects of the 1984/5 data have a smaller dispersion at the 90% confidence level. The t test showed, at the 95% confidence level, that the mean velocity of -38 km/s for the metal rich stars was significantly less than the 2 km/s of the metal poor stars. As an alternative approach, a Monte Carlo simulation determined that only 5% of the time may one randomly select two samples of size 20 from a Gaussian distribution with $\sigma = 110$ km/s and estimate dispersions at least as extreme as the metal rich and metal poor samples.

Another concern is that the difference in dispersions may arise only because both the means and dispersions are estimated for the two samples. However, if we estimate the dispersions using the full sample mean of -19 km/s, we find dispersions of 128 and 94 km/s for the metal poor and metal rich stars respectively. If we use

the solar Π velocity of -10 km/s, the dispersions are little altered, to 127 and 97 km/s. We may also remove the most extreme positive velocity star, 2252, from the metal poor sample. This star was observed twice, however, and the mean is 271.7 km/s. Nonetheless, removing 2252 reduces the metal poor dispersion to 107 km/s.

The above tests essentially illustrate only that it is unlikely that the metal rich and metal poor stars have identical gaussian distributions. In Figure 4, where the dispersions are plotted, it is noticeable that the metal rich velocities appear to have a smaller dispersion, and also a smaller full range. The plot of measured velocity against abundance for each star also appears to show such an effect (Figure 6). Unfortunately, a statistically solid conclusion must await a sample larger by a factor of 4 or 5, or confirmation with a different set of velocity probes.

V. Interpretation

a) Comparison With Previous Work

Two major results have emerged from the previous chapters:

1. The abundance distribution of the nuclear bulge K giants has been derived. The abundances run from -1 to nearly $+1$ dex, with a peak at .3 dex, or twice the solar abundance. Of the 88 stars with derived abundances, 22% exceeded the abundance of the most metal rich local K giants; 50% exceeded the solar abundance, and 10% were metal poor (< -0.6 dex).

2. The velocity dispersion of 53 K giants with derived abundances is 104 km/sec. The mean velocity is -19 ± 14 km/sec; within 1σ of Delhaye's 1965 value for the solar Π velocity of -10 km/sec. When this sample is divided into 3 subsets based on the abundances, the subset of 21 stars > 0.3 dex has $\sigma = 92 \pm 14$ km/sec and the metal poor subset of 16 stars < -0.3 dex has $\sigma = 126 \pm 22$ km/sec. An intermediate set of 16 stars has $\sigma = 97 \pm 17$km/sec. The most metal rich stars may have a bulk velocity of -38 ± 14 km/sec, 1σ less than the -19 km/sec of the metal poor stars.

The two best studied bulge populations with abundance information are the globular cluster system (Frenk and White, 1980) and the sample of K giants in this work. The K giant dispersion is within 1σ of the dispersions of other nuclear bulge populations studied, which include M giants, planetaries, and Miras, all of which have dispersions of $\approx$ 110 km/sec (Feast and Jones, 1985). The K giants and the

globular clusters have in common the property that metal rich subsets have a 1σ smaller velocity dispersion than the metal poor subsets. The metal rich G class clusters have $\sigma = 95$ km/sec, and the metal poor F class clusters have $\sigma = 124$ km/sec. These numbers are fortuitously close to the K giants, although the cluster system encompasses the entire galactic halo. Frenk and White also found that the metal rich clusters had a significantly larger rotation velocity than the metal poor clusters. Zinn (1980) found the metal rich clusters to be more spatially concentrated, in a disk-shaped subsystem of dimension 9 kpc.

Although the difference in dispersions between the metal rich and metal poor K giants is only 1σ, it is interesting to explore the implications of the difference, should it be confirmed in a larger sample, as well as to look for any other evidence that may support the difference in dispersions. We now consider several models which are consistent with the foregoing results.

b) Pure Bulge Kinematics

The bulge population is clearly not a pure extension of the metal poor spheroid, even though the velocity dispersion is consistent with that of spheroid populations such as the globular clusters (Frenk and White, 1980) and the RR Lyrae stars (Saha, 1985). Independent evidence for a wide abundance range comes from the evolved stellar population. RR Lyrae stars of abundance -0.6 dex are present (Butler, Carbon, and Kraft, 1976, Blanco, 1985), and occupy the same volume of space as the late, luminous M7-9 giants of Blanco, McCarthy, and Blanco (1984), which

are not found in any globular clusters (Frogel and Whitford, 1982, Frogel, 1983). Further evidence that the RR Lyraes and M giants occupy the same spatial volume comes from their sharply peaked apparent magnitude distributions (Blanco, 1984 for the RR Lyraes, and Blanco, McCarthy, and Blanco (1984) for the M giants.) As mentioned earlier, the metal rich population is more than an order of magnitude more metal rich than Zinn's "disk" globular cluster system; in fact, a majority of the stars are more metal rich than NGC 5927, the most metal rich cluster in Zinn and West's 1984 compilation.

An initial approach in modeling the bulge population employed the Bahcall-Soneira "export" galaxy model which was modified to include the appropriate extinction in the calculation. It also was used with the option of the "globular cluster feature" (horizontal branch). This decision was made based on the uncalibrated color magnitude diagram in Figure 7, which was made with narrow-band filters, and shows a clear horizontal branch clump. Walker and Mack's 1986 value of $A_V = 1.78$ was adopted, and a linear model of the reddening such that $A_V = 0.875$mag/kpc, such a model being supported by Arp (1965) and van den Bergh (1971). If we adopt 100pc as the scale height of absorbing material in the disk, (Belfort and Crovisier 1984) then the line of sight leaves the dust at 2kpc from the sun. The result of modifying the model is shown in Figure 8. All but 3 stars lie in the range of $15 < V < 17$; all are more red than $(B - V)$ =1.0. The model predicts equal numbers of disk and bulge giants, when the M67 giant branch is used for both the disk and bulge. At face value, we would expect disk giants to comprise half of the

Baade Window population. However, the galactic rotation curve demands addition of a central bulge component (Bahcall, Schmidt, and Soneira, 1982) of the form

$$\rho = 7.6 \times 10^5 \mathrm{M}_\odot \alpha^{-1.8} \exp(-R/1kpc)^3 \quad M_\odot pc^{-3} \tag{1}$$

where $\alpha^2 = (x^2 + 6.25z^2)(x, z \text{ in pc})$ which was derived by Sanders and Lowinger (1972) from Becklin and Neugebauer's 1968 infrared map, except for the exponential, which cuts off the population at 1kpc. Using the disk, spheroid, and central density laws and normalizations provided by Bahcall (1986), the ratio at the position of Baade's Window (x=100 pc, z=500 pc) is central:spheroid:disk is 6.6:1:1; if we use the Sanders and Lowinger central component, the ratio climbs to 8.6:1:1. If we use the Bahcall, Schmidt, and Soneira (1983) mass model of the Galaxy, in which the rotation curve of the Galaxy is supported, we find the importance of the central component to be great. Between 750 and 500 pc, assuming identical mass to light ratios for all components, the star density central:spheroid:disk is 25:1:1.7. The dominance of the central component based on the rotation curve is illustrated in Figure 9, where the enclosed mass at a given radius is found from the Bahcall, Schmidt, and Soneira (1983) rotation curve where $M(r) = rv(r)^2/G$. Within 1 kpc, nearly all of the mass enclosed is due to the central bulge component *not* found in the Bahcall-Soneira model. Sellwood (1985) points out that a bulge component would stabilize the disk against bar modes; but this fact does not require a bulge, because a hot disk also stabilizes against bar modes. If these density laws hold (and the central component is probably least certain) then we could expect 10-20% of the stars in Baade's window to be members of the disk.

Can we find evidence for this pure central bulge component in the kinematics ? If we assume rough spherical symmetry, we may follow Hartwick and Sargent 1978, and express the first moment of the Boltzmann equation in observable quantities:

$$\frac{GM(r)}{r} = v_c^2 = < v_r^2 > \left[-\frac{d\ln \nu_c}{d\ln r} - \frac{d\ln < v_r^2 >}{d\ln r} + (\lambda - 2) + \frac{\bar{v}_{rot}^2}{< v_r^2 >} \right] \qquad (2)$$

where r is the radius, $M(r)$ is the mass enclosed at that radius, $< v_r^2 >= \sigma^2$ for an isotropic velocity ellipsoid, v_c is the circular velocity at that radius, $\bar{v}_{rot}$ is the rotation velocity of the population, $\lambda = 0$ for radial orbits and $\lambda = 2$ for isotropic orbits.

The first term in (1) is the exponent of a density law ν_c^{-n}.

The second term is negligible if the velocity dispersion of the population does not change with galactocentric distance. Saha (1985) found no change in dispersion with galactocentric distance for halo RR Lyrae stars. This result was confirmed for a sample of halo K giants by Ratnatunga and Freeman (1985). Frenk and White (1980) separated the globular clusters in two groups; those with $R < 7.7$kpc had $\sigma = 96$ km/sec and those with $R > 7.7$kpc had $\sigma = 132$ km/sec. If we use their values as an upper limit, this term could be as large as 0.5.

The third term depends on the orbits being isotropic or radial. Frenk and White were not able to draw a specific conclusion for the globular cluster system. We assume isotropic orbits; if the orbits are radial, n is increased by 2.

The final term in (1) expresses the degree of rotation support. For a nearly spherical population b/a = 0.8, this term is also small. Frenk and White found

significant rotation velocities for the metal rich and metal poor globular cluster systems. Based on their results, a "mean" value for this term would be 0.5; this just cancels the second term. Equation (2) then reduces to:

$$v_c^2 = \sigma^2 [n + (\lambda - 2)] \tag{3}$$

Baade's window is located $\approx 500pc$ from the nucleus. Using the BSS potential, based on the enclosed mass, corresponds to $v_c = 250$ km/s. For $\sigma = 130$km/s and isotropic orbits, $n = 3.7 \pm 1.4$, close to the power law of 3.5 for the globular cluster system (de Vaucouleurs and Pence, 1978) and the halo stars (Saha, 1985). For $\sigma = 92$ km/s, n $= 7.4 \pm 2.2$. Both exponents increase by 2 for the case of radial orbits. Alternatively, (2) may be recast as a ratio of two populations occupying the same spatial location. If the metal poor stars corresponded to the n=3.5 globular cluster system, then

$$n_2/n_1 = \sigma_1^2/\sigma_2^2 \tag{4}$$

from which n for the metal rich system is 7.0, again for isotropic orbits. A power law decline of $\nu_c \sim r^{-7}$ would produce an extremely spatially concentrated population. It would be reasonable to conclude that the high abundance, and smaller velocity dispersion, would be characteristic of the central bulge component required by the dynamics. The spatial concentration would also be consistent with this interpretation. Are there any other populations which could also trace the central component?

Blanco and Blanco (1986) found many late M giants in windows in the bulge which run from $-3°$to $-12°$ galactic latitude. The number of the stars falls as

$r^{-5.7}$ in surface density, or $r^{-6.7}$ in space density. The population disappears by 12°latitude, roughly 1.5kpc. This steep decline in surface density could simply be caused by a decline in the metal abundance at increasing galactic latitude, with the giant branch tip becoming too hot for M giants as the abundance decreases. Most likely, the decline is caused by a combination of number density and abundance decrease. Mould (1983) found a dispersion of 113 km/sec for the M giants, making them consistent with the spheroid dispersion and density law. In the previous chapter, Mould's M giants were segregated by possible abundance classes and showed the same effect as the K giants; definitive results can come from obtaining the dispersion of a large number of the latest M giants and comparing it with the spheroid dispersion.

The metal rich stars found in Baade's Window at $b = -4°$ may not be present in the window at $b = -8°$ (van den Bergh and Herbst, 1974). The metal rich stars may also be part of the special central bulge component. If this is so, then the stars in Sgr I, at $b = -3.6°$ should be nearly pure central bulge stars. It would be interesting to test whether the cutoff at 1kpc incorporated into the bulge mass model actually occurrs.

Another possible group of tracers for the central component are the IRAS bulge sources (Habing *et al.* 1985). These luminous evolved giants may well be, at first glance, a subset of Blanco's M giants. While they are centrally concentrated (r_e=5°or $\sim$ 750 pc) , as opposed to the r_e of 2.7 kpc of the globular cluster system, their numbers fit an r^{-3} spatial density law. The IRAS bulge sources decline by a

factor of 25 between 2°and 10°galactic latitude. In the same range, Blanco's late M giants decline by a factor of 10^3. While both the M giants and IRAS sources are spatially more concentrated than the spheroid, they appear to be fundamentally different from one another. However, Frogel (1985) has observed some 20 IRAS bulge sources and found that they are late giants with TiO bands. So it would appear that only a fraction of the late giants were detected by IRAS, and it may be that there is a bias against the *latest* giants. A considerably larger sample will have to be studied to settle the question.

The IRAS sources may be OH/IR stars; if so, Isaacman and Oort (1981) have found that these sources fit an $r^{-1.8}$ mass model, similar to the Sanders and Lowinger expression im (1). Isaacman (1981) also found that the planetary nebulae fit a bulge mass model with the form of (1). It would appear that the reality of a distinct bulge component, required by the rotation curve and various tracers, is secure. In Baade's Window, the stellar population would be dominated by the bulge component; the spheroid population, with its more metal poor stars, would begin to dominate beyond 1 kpc.

c) Disk or Bulge Stars ?

Although disk objects probably comprise at most 20% of the population, we would like to find means to distinguish true bulge from disk population.

If we are to distinguish disk from bulge stars using kinematics, we can look for differences in either rotation or velocity dispersion. Van der Kruit and Searle

(1982) sec.6 point out that for a constant vertical scale height exponential disk, $\sqrt{v_r^2} \propto e^{-R/2h}$, where R is the galactocentric distance and h is the scale length of the disk. For R_o = 7kpc (Blanco, 1985), h=3.5kpc (Bahcall, 1986) and $\sqrt{v_r^2}$ in the solar neighborhood = 40 km/s (Wielen, 1974), one expects σ = 108 km/s as the central disk velocity dispersion; velocity dispersion makes a poor discriminant between disk and bulge for this population. Wood and Bessell (1983) have suggested stars as young as 1 Gyr populate the bulge, based on Mira pulsation masses. 1 Gyr old stars have a solar neighborhood dispersion of $\sqrt{< u^2 >}$ = 20 km/s (Wielen, 1974), leading to the prediction of 54 km/s dispersion, should such a population originate in the disk. Such a low dispersion has never been observed for any set of objects in the direction of the galactic center, particularly not for the Miras, (Feast, Robertson, and Black, 1980). This line of reasoning then suggests that if there are 1 Gyr old objects in the nuclear bulge, their formation history is different from the solar neighborhood, and fortuitously endows them with a velocity dispersion in agreement with the spheroid. However, if it can be convincingly demonstrated that a disk population can produce objects with the proper kinematics, the 20% disk component could be young, or intermediate age.

Assuming the disk is in rotation, we would expect large numbers of stars with velocities $\sim$ 200 km/s , the rotation velocity of OH/IR stars observed by Habing *et al.* within $\pm 1°$ of the nucleus, also the rotation velocity given by Oort (1977) at this distance. The rotation velocity near the nucleus rises rapidly because of the large amount of mass concentrated in a small volume there. However, neither in

Mould's 1983 velocity dispersion, nor in this study, is there a group of stars at large positive velocity. The samples actually show the opposite tendency: to have a mean negative velocity.

d) Interpretation of the Abundance Distribution

We can compare the observed abundance distribution with models of chemical evolution. The "simple" one-zone model of chemical evolution (Searle and Sargent 1972) is a good point of departure.

$$z = p \ln \mu^{-1} \tag{5}$$

where μ is the fraction of gas remaining. It can be shown (Pagel and Patchett 1975) that in the limit of complete gas consumption, the yield p tends towards $< z >$ and

$$f(z) = \frac{1}{< z >} exp\left(\frac{-z}{< z >}\right) \tag{6}$$

then the cumulative ditribution (Hartwick, 1976) is:

$$F(z) = 1 - exp\left(\frac{-z}{< z >}\right). \tag{7}$$

In Figure 10, we compare the cumulative abundance distribution with the simple model. The fit is good, and not lacking at the metal poor end. Searle and Zinn (1978) also find a similar good fit for the Galactic globular clusters, although for that system, their yield is $0.04z_{\odot}$. For the bulge stars, the yield is $\approx 2z_{\odot}$. The true yield probably does not vary this much (Edmunds and Pagel, 1983). The bulge value reflects the yield in the case where gas is conserved, and is the true yield unless

the gas was enriched before stars formed. In the case of the globular cluster system, there may well have been both inflow and outflow of gas during the formation; a decreased effective yield results.

The abundance distribution can be compared with the solar neighborhood G dwarf abundance distribution (Pagel and Patchett, 1975) shifted towards higher abundance to reflect Shaver *et al's* 1983 abundance gradient in the disk of -0.07 ± 0.015 dex/kpc. For a distance of 7 kpc, we expect a gradient of 0.5 dex, so the G dwarf distribution of mean -0.36 and $\sigma = 0.26$ is shifted to a new mean of 0.14. This cumulative lognormal distribution is also plotted, and falls short of the data in the metal poor regime. One might postulate a two-component model for the distribution function consisting of mildly metal poor stars (spheroid) and the metal rich disk. The abundance distribution would then consist of a metal rich component due to the disk, and a metal poor component, due to the spheroid. In any case, the disk contamination is likely to be only about 20% at most, as discussed earlier.

Dissipative models of galaxy formation (Larson, 1974, 1976, Carlberg, 1984) predict metal abundance gradients; (Carlberg's models predict a gradient of 0.5 dex over a galactic radius) and progressive flattening of more metal rich stellar populations within the Galaxy. The central component may then be identified with the metal rich population of stars, and would be the final stage of the collapse of the Galaxy. The gas enriched by previous generations of star formation would flow into this region; the large gravitational potential would prevent outflow, hence the high observed abundances.

If the bulge has an age-metallicity relation, Carlberg's (1985) models predict the existence of an intermediate age population, perhaps 2 Gyr younger than the oldest populations.

The metal rich stars are not members of the spheroid, based on their low velocity dispersion and exceptionally high abundances. They also do not appear to be members of the disk, because they do not have disk kinematics. Considered as a whole, the entire population appears to satisfy the simple, single zone model of chemical evolution, with conservation of gas flow. The metal rich stars may in fact be slightly younger than the oldest stellar populations in the Galaxy; they would be the final remnant of the Galaxy's dissipative collapse.

VI. Future Research

Further observations will be required before the foregoing conclusions can be confirmed or modified. The following questions should be answered:

(1) Are the high derived abundances for the K giants correct ?

(2) Are the kinematic differences between the metal rich and metal poor stars real ?

(3) What is the age, and age range for the bulge ? Is there an age-metallicity relationship ?

(4) How do standard galaxy models compare with observations in the bulge ?

(5) Is there an abundance gradient, and if so, is it a decline in mean abundance, or decline in a high abundance component ?

(6) Does the bulge rotate ?

The abundances derived in Chapter 1 using Solution 1 place some stars at 10 times the solar Fe abundance. The high abundances must be verified by measuring Fe lines on the linear portion of the curve of growth. These weak lines ($\approx$ 20mÅ) can only be measured at high dispersion (coude or echelle resolution). The high abundances for local metal rich K giants were confirmed by Branch, Bonnell, and Tomkin (1978) in this way. A preliminary analysis of a spectrum obtained at the 5m coude shows such weak lines are enhanced in at least one bulge giant, 1202. A project to obtain echelle spectra of several metal rich bulge giants is in progress.

Should these high abundances be verified, there will be a need for isochrones and evolution models for very metal rich stars; these do not currently exist.

The first investigation of metal rich vs metal poor kinematics suffered from small sample sizes. Both samples will have to be increased by factor of 4, or 100 stars in each group, for the differences to be confirmed or refuted at a statistically significant level. However, there is a ready sample of old, metal poor objects in the Baade's Window: the RR Lyrae stars studied by Blanco (1985). These stars will be an indpendent set of kinematic probes of the metal poor population; a project is underway to measure their velocity dispersion.

Another approach to studying the kinematics is to measure the number of metal rich stars as a function of galactic latitude. Data have been taken through narrow-band filters which are designed to measure the MgH feature. These data exist for several latitudes from $-3°$to $-8°$. The decline in numbers of metal rich giants can be compared with the decline in the number of M giants from Blanco's work. In §IV b, it was shown that the velocity dispersion data predicts a steep power law decline in the number of metal rich stars as a function of increasing galactic latitude. The narrow-band data will make it possible to distinguish between a multi-component model and a gradual abundance gradient.

An exciting development is the possibility of measuring proper motions from plates taken of Baade's Window. A. Spaenhauer is currently undertaking this task. When it is finished, we will have space velocities and abundances for stars in the bulge. This may ultimately be the only way to distinguish disk stars from bulge

stars, and to distinguish radial from isotropic orbits; a rotation-supported population would tend to have most velocity components perpendicular to the line of sight.

Two approaches can be taken in gauging the age of the bulge. The AGB can be studied, or deep photometry can find a young turnoff.

Study of the AGB has pointed toward a component as young as 1 Gyr (Wood and Bessell, 1983). Frogel and Whitford (1981) point out that the high AGB luminosities could result from normal evolution of old, metal rich stars. Carbon stars have recently been found as well (Azzopardi *et al.* 1985) but these are not the red, luminous type which are identified with intermediate-age populations in the Magellanic clouds. Photometry of these stars will settle the issue of age, and a measurement of their velocity dispersion should help to place them among the bulge populations. Comparison of observed luminosity functions with theoretical predictions should help to settle the issue.

The approach of obtaining color-magnitude diagrams for bulge fields is yet another means of searching for an intermediate age component. Van den Bergh (1974) found a turnoff population in a field at $-8°$latitude. Terndrup, Rich, and Whitford (1984) confirmed this result. Rich (1985) found that the number of possible main sequence progenitors was 10-100 times too small to explain the AGB as a 1 Gyr old population. This is particularly true in Baade's Window. Whitford (1977) found no evidence for a young component in the integrated light of Baade's Window. More broad-band CCD pictures will have to be obtained before any final conclusions are

drawn. In addition, the turnoff population will have to be modeled and compared with observations. The best current data are Terndrup's CCD color-magnitude diagrams, and one cannot rule out ages as young as 5 Gyr based on these data. In fact, some intermediate-age stars may well be present.

A final approach to the age question is to determine stellar masses directly for the eclipsing binaries found by Blanco (1985). Any direct measurement of stellar mases would help resolve the issue.

Ultimately, when multi-fiber spectrographs become available, it may be possible to derived the age-metallicity relation from the turnoff stars.

The Bahcall-Soneira model lacks a central component, as mentioned earlier. The same CCD data used to obtain ages could also be applied to testing and improving the standard model to include a central bulge component. The problem here is deciding which is the best tracer of the bulge component–the IRAS sources, M giants or metal rich K giants.

The question of bulge rotation also leads naturally to questions of disk vs. bulge populations. Many M giants have been identified in fields at $\pm 10°$galactic longitude, and at low enough galactic latitudes so they are likely members of the bulge; a study of the bulge rotation curve using these stars as kinematic probes is underway.

The bulge will also be studied by Space Telescope, with the hope that the slope of the initial mass function can be measured from stars at and below the turnoff.

This number figures prominently in models of color and luminosity evolution of galaxies with redshift.

One hopes that the bulge population can be applied as a general model for the (presumably) old and metal rich populations found in other galaxies. If the AGB of the bulge is found to be similar to the bulge population of M31, it may be possible to make such a comparison. If , however, the bulge population is significantly contaminated by a young component from the disk, or is intermediate age, the generalization would be invalid. The possiblity of studying nucleosynthesis and the formation of the Galaxy by observing the bulge is an exciting prospect. However, if the bulge population proves too complicated, we may find ourselves in a more confused state. Each component of the population likely has its own story to tell. The prize yet to be won is a convincing explanation for all of the bulge's features to the point where we can, in fact, use the information to learn how the Galaxy formed.

TABLE 1

VELOCITIES OF BULGE GIANTS MEASURED USING HIGH RESOLUTION

Star (1)	Mean RV (km s^{-1}) (2)	RV (km s^{-1}) (3)	Date (4)	$[Fe/H]_1$ dex (5)
1021.....	−113.2	−117.6	1984 Jun 10	0.61
		−108.7	1985 Jul 26	
1025.....	−54.3[a]	−80.5	1985 Jul 26	0.51
		−66.8	1985 Jul 26	
		−35.0	1984 Jun 9	
1034.....	−111.0		1985 Jul 18	
1039.....	61.9	65.2	1984 Jun 3	0.79
		58.6	1985 Jul 26	
1064.....	−58.7	−70.4	1985 Jul 18	0.31
		−47.0	1985 Jul 15	
1076.....	−34.2	−35.2[b]	1984 Jun 12	0.57
		−33.1	1985 Jul 15	
1083.....	−131.3		1985 Jul 18	0.51
1140.....	8.8		1984 Jun 10	−0.21
1141.....	−83.7		1984 Jun 10	0.14
1145.....	−78.5	−83.7	1984 Jun 10	−0.46
		−73.2	1984 Jun 11	
1151.....	92.5		1984 Jun 10	−0.29
1153.....	109.9		1984 Jun 3	0.24
1155.....	−70.2		1984 Jun 10	0.39
1158.....	−203.6	−209.9	1984 Jun 3	0.25
		−197.2	1985 Jul 26	
1194.....	−178.9		1984 Jun 3	0.33
1196.....	27.0		1985 Jul 15	0.71
1202.....	−97.2[c]	−123.6	1985 Jul 15	0.42
		−97.2[c]	1985 May 27	
1322.....	−73.6		1984 Jun 11	0.13
2026.....	−30.5	−24.0	1985 Jul 20	0.40
		−37.9	1984 Jun 11	
2027.....	174.9		1985 Jul 20	0.43
2033.....	20.8		1984 Jun 11	−0.51
2040.....	137.5	144.3	1984 Jun 1	−0.10
		118.7	1984 May 30	
		149.5	1985 Jul 20	
2042.....	−21.9		1984 Jun 1	−0.34
2116.....	1.5		1985 Jul 19	0.96
2119.....	−217.7[e]	−185.0	1985 Jul 20	−0.79
		−225.3	1984 Jun 1	
		−242.9	1984 May 31	
		−8.3	1985 Jul 18	
2122.....	114.8	118.8	1985 Jul 26	−0.06
		110.8[b]	1984 Jun 12	
2136.....	84.2	104.4	1985 Jul 26	−0.83
		63.9	1985 Jul 18	
2139.....	−0.3		1984 Jun 11	0.23
2145.....	44.3	48.7	1985 Jul 18	0.69
		38.8	1985 Jul 19	

TABLE 1

VELOCITIES OF BULGE GIANTS (CONTINUED)

Star (1)	Mean RV (km s^{-1}) (2)	RV (km s^{-1}) (3)	Date (4)	$[Fe/H]_1$ dex (5)
2147.....	115.3		1985 Jul 18	−0.37
2154.....	−48.2		1985 Jul 18	−0.58
2166.....	32.8		1984 May 31	−0.85
2167.....	−234.6		1984 May 31	0.58
2173.....	−9.2		1984 May 30	−0.49
2174.....	−121.2		1984 Jun 2	0.01
2199.....	−60.4		1985 Jul 26	0.22
2200.....	16.0		1985 Jul 26	
2215.....	−21.1	−25.3	1984 Jun 5	−0.09
		−12.0	1985 Jul 14	
		−16.9	1985 Jul 14	
2216.....	−89.2		1984 Jun 1	−0.53
2240.....	36.2	33.8	1985 Jul 14	0.25
		38.6	1985 Jul 15	
2252.....	271.7	282.5	1984 Jun 2	−0.38
		260.9	1985 Jul 20	
3106.....	−121.6	−118.6	1984 May 30	−0.19
		−124.6	1984 Jun 2	
3160.....	188.5[d]	188.1	1984 Jun 2	−0.11
		188.9	1984 May 30	
3209.....	−55.2	−54.0	1985 Jul 14	0.69
		−56.3	1985 Jul 15	
4003.....	208.4	204.9	1984 Jun 3	−0.82
		211.9	1984 May 31	
4022.....	78.0	79.8	1984 Jun 9	0.58
		76.1	1985 Jul 26	
4025.....	36.8		1984 Jun 9	0.52
4072.....	−103.0		1984 Jun 9	0.73
4148.....	0.2		1984 Jun 2	−0.16
4167.....	−15.9		1984 Jun 9	0.83
4203.....	−7.5		1984 Jun 11	−0.98
4312.....	−58.7		1984 Jun 1	−0.21
4325.....	−49.2	−39.5	1984 Jun 9	0.39
		−58.8	1985 Jul 26	
4329.....	−51.5	−31.3	1985 Jul 26	−0.70
		−63.0	1984 Jun 5	
		−61.1	1984 Jun 10	
		−50.5	1984 Jun 9	
5006.....	−181.2	−194.1	1984 Jun 1	−0.96
		−161.9	1985 Jul 18	
		−187.7	1984 Jun 3	
6192.....	7.4	23.5	1984 Jun 11	−0.88
		−8.7	1984 Jun 10	

NOTES.—Col. (1) Star name from Arp (1965) with roman numeral converted to decimal *e.g.* IV-25 = 4025. 5006 and 6192 from an unpublished study by the author. Col. (2) Mean radial velocity in km s^{-1}. All measurements made in 1985 used the "2D-Frutti" detector and the 1200 line 5000Åblaze grating (except those noted below). Measurements made in 1984 used the same grating with the one-dimensional shectograph detector. Col. (3) Individual radial velocity measurements. Col. 4 Date is U.T. date - 1. Col. (5) [Fe/H] from Rich and Whitford 1986, solution 1.

[a] Observations on the same night are averaged and treated as one number.

[b] On 1984 Jun 12, the 7500 line 7500 Åblaze grating was used.

[c] On 27 May 1985, 1202 was observed with the Palomar 5m coude and CCD with 0.5Å resolution; the resulting higher accuracy radial velocity is preferred.

[d] This star had a double peaked correlation peak in 1982 and 1984; no reliable velocity was obtained.

[e] Errant velocity of July 18 not included in average.

TABLE 2

VELOCITIES OF BULGE GIANTS MEASURED USING LOW RESOLUTION

Star (1)	Radial Velocity (km s^{-1}) (2)	Date (3)	$[Fe/H]_1$ dex (4)
1012.....	−270.6	1982 May 30	−0.22
1025.....	−38.3	1982 May 23	0.51
1039.....	81.0	1982 May 22	0.79
1083.....	−127.9	1982 May 29	0.51
1093.....	−81.9	1983 May 15	0.26
1102.....	−34.6	1983 May 21	0.04
1129.....	185.0	1983 May 19	0.71
1140.....	1.3	1982 May 24	−0.21
1141.....	31.3	1982 May 22	0.14
1144.....	55.1	1982 May 24	0.58
1145.....	−95.2	1982 May 30	−0.46
1151.....	80.5	1982 May 29	−0.29
1153.....	129.1	1982 May 28	0.24
1155.....	−55.7	1982 May 23	0.39
1156.....	−134.8	1982 May 26	−0.24
1158.....	−195.0	1982 May 23	0.25
1164.....	−196.6	1982 May 23	−0.31
1174.....	27.0	1982 May 26	−0.13
1181.....	172.3	1982 May 27	0.17
1194.....	−219.9	1982 May 29	0.33
1196.....	9.7	1982 May 24	0.71
1304[a].....	−139.6	1982 May 25	0.74
1319.....	8.6	1982 May 28	0.43
1329.....	143.6	1982 May 27	0.32
1335.....	256.6	1982 May 28	0.08
2026.....	−33.3	1982 May 27	0.40
2040.....	88.3	1982 May 24	−0.10
2042.....	−13.0	1982 May 24	−0.34
2049.....	−62.9	1982 May 24	0.00
2118.....	−34.2	1982 May 26	0.09
2119.....	−232.4	1982 May 23	−0.79
2136.....	139.7	1982 May 26	−0.83
2139.....	−43.0[b]	1982 May 28	0.23
	−39.9	1982 May 28	
	−46.0	1982 May 28	
2145.....	85.6	1982 May 23	0.69
2147.....	93.5	1982 May 23	−0.37
2151.....	−74.4	1982 May 29	−0.40
2154.....	−39.5	1982 May 25	−0.58
2167.....	−211.7	1982 May 26	0.58
2171.....	185.7	1982 May 29	0.06
2173.....	47.7	1982 May 22	−0.49
2174.....	21.7	1982 May 27	0.01

TABLE 2

VELOCITIES OF BULGE GIANTS (CONTINUED)

Star (1)	Radial Velocity (km s^{-1}) (2)	Date (3)	$[Fe/H]_1$ dex (4)
2201.....	39.0	1982 May 28	0.23
2215.....	−3.4	1982 May 26	−0.09
2216.....	−66.2	1982 May 26	−0.53
2252.....	282.5	1982 May 24	−0.38
2261.....	102.7	1982 May 25	−0.12
3106.....	−188.0	1982 May 28	−0.19
3152.....	−293.7	1982 May 25	−0.11
3157.....	−129.8	1982 May 25	0.43
3159.....	27.9	1982 May 26	0.43
3160.....	64.1[c]	1982 May 25	−0.11
3197.....	−4.8	1982 May 25	0.51
3200.....	−225.1[d]	1982 May 25	
3224.....	0.4	1982 May 29	0.03
4003.....	222.8	1982 May 30	−0.82
4022.....	90.3	1982 May 29	0.58
4063.....	45.0	1982 May 27	0.76
4071.....	−79.8	1982 May 27	−0.01
4072.....	−83.4	1982 May 26	0.73
4146.....	−70.3	1982 May 27	0.26
4148.....	17.8	1983 May 15	−0.16
4165.....	−82.7	1982 May 29	−0.35
4167.....	−15.8	1982 May 24	0.83
4285.....	56.7	1982 May 29	0.35
4297.....	75.5	1982 May 27	0.39
4312.....	−47.1	1982 May 22	−0.21
4315.....	−34.7	1982 May 30	−0.12
4316.....	−26.2	1982 May 27	0.35
4329.....	−53.4	1982 May 29	−0.70
5024.....	89.8	1983 May 21	
5060.....	−12.2	1983 May 22	−0.04
5445.....	76.2	1983 May 22	0.02
6192.....	47.6	1983 May 15	−0.88
6322.....	−68.2	1983 May 15	0.74
6406.....	105.2[b]	1983 May 21	0.38
	107.6	1983 May 21	0.38
	104.1	1983 May 19	
	101.4	1983 May 19	

NOTES. Col. (1) Star, as in Table 1. Col. (2) Radial velocity in km s^{-1}. All observations made using the 600 line 5000Å blaze grating. Col. (4) [Fe/H] from Solution 1 of Rich and Whitford 1986.

[a] Not included in abundance discussion because $(J-K)_0$ =0.28

[b] Average of velocities listed below.

[c] Double peaked correlation peak; velocity unreliable.

[d] Balmer lines; velocity may be unreliable.

TABLE 3

KINEMATICS OF BULGE GIANT POPULATIONS

Population	Number	Mean Velocity (km/s)	Velocity Dispersion (km/s)
(1)	(2)	(3)	(4)
All 1984/5	53	-19 ± 14	104 ± 10
1984/5 [Fe/H] < -0.3	16	2 ± 31	126 ± 22
1984/5 $-0.3 \leq$ [Fe/H] < 0.3 ..	16	-15 ± 24	97 ± 17
1984/5 [Fe/H] ≥ 0.3	21	-38 ± 20	92 ± 14
All 1982/3	71	-6 ± 14	119 ± 10
1982/3 [Fe/H] < -0.3	15	-1 ± 37	142 ± 26
1982/3 $-0.3 \leq$ [Fe/H] < 0.3 ..	32	-12 ± 22	122 ± 15
1982/3 [Fe/H] > 0.3	24	-1 ± 21	104 ± 15
Merged 1982-5 [a]	88	-13 ± 12	111 ± 8
Merged [Fe/H] < -0.3	19	-17 ± 29	126 ± 19
Merged [Fe/H] > 0.3	33	-9 ± 17	97 ± 10
Mould (1983) M Giants	49	-10 ± 16	113 ± 11
"hot [b]" M Giants	15	10 ± 34	131 ± 24
"intermediate" M Giants	17	-22 ± 26	109 ± 19
"cool" M Giants	18	-17 ± 24	100 ± 17
M7, M8, M9	9	45 ± 31	92 ± 22

NOTES.—Col. (1) Sample of bulge stars. The best data are those of 1984/5. Abundances are from Solution 1 in Chapter 1. Col. (2) Number of stars in the sample. Col. (3) Mean radial velocity; error is $\sigma/\sqrt{N}$. Col. (4) Velocity dispersion; error is $\sigma/\sqrt{2N}$.

[a] Merger of data from 1982-5, but 1984-5 observations supersede duplications observed in 1982-3. Net result ist to add 33 stars not observed in 1984/5.

[b] Rough temperature classification based on Mould's 1983 index [5320]-[7540]. "Hot" $(53-75) < 3.5$; "Cool" $(53-75) > 4.0$ or large TiO for given color. Many stars in the cool class are later than M6. Spectral types are from Blanco (1984).

References

Arp, H. 1965, *Ap. J.*, **141**, 45.

Azzopardi, M., Lequeux, J., and Rebeirot, E. 1985, *Astron. Astrophys.(Letters)*, **145**, L4.

Bahcall, J. N. 1986 *Ann. Rev. Astr. Ap.* **24** (Submitted).

Bahcall, J. N., Schmidt, M., and Soneira, R. M. 1982, *Ap. J. (Letters)*, **258**, L23.

Bahcall, J. N., Schmidt, M., and Soneira, R. M. 1983, *Ap. J.*, **265**, 730.

Becklin, E. E., and Neugebauer, G. 1968, *Ap. J.*, **151**, 145.

Blanco, B. M. 1984, *A. J.*, **89**, 1836.

Blanco, V. M., and Blanco, B. M. 1986 *Astrophys. and Space Science* **118** 365.

Blanco, V. M., M. F. McCarthy, S. J., and Blanco, B. M. 1984 *A. J.* **89** 636 .

Branch, D., Bonnell, J., and Tomkin, J. 1978, *Ap. J.*, **225**, 902.

Butler, D., Carbon, D., and Kraft, R. P. 1976 *Ap. J.* **210** 120.

Carlberg, R. G. 1985 in IAU Symposium 106 *The Milky Way Galaxy* H. van Woerden et al. ed. (Dordrecht:Reidel) p.615.

Delhaye,J. 1965, in *Stars and Stellar Systems*, Vol. **5**, *Galactic Structure*, ed. A. Blaauw and M. Schmidt (Chicago: University of Chicago Press), p. 1.

Edmunds, M. G., and Pagel, B. E. J., 1983 in *Stellar Nucleosynthesis* Ed. C. Chiosi and A. Renzini (Dordrecht:Reidel).

Feast, M. W., and Jones, J. H. S. 1985, Preprint.

Feast, M. W., Robertson, B. S. C., and Black, C. 1980, *M.N.R.A.S.*, **190**, 227.

Frenk, C. S., and White, S. D. M. 1980, *M.N.R.A.S.*, **193**, 295.

Frogel, J. A., and Whitford, A. E. 1982, *Ap. J. (Letters)*, **259**, L7.

Frogel, J. A. 1983, *Ap. J.*, **272**, 167.

Habing, H. J., Olnon, F. M., Winnberg, A., Matthews, H. E., Baud, B. 1983, *Astr. Ap.*, **128**, 230.

Habing, H. J., Olnon, F. M., Chester, T., Gillett, F., Rowan-Robinson, M., and Neugebauer, G. 1985 *Astron. Astrophys. (Letters)* **152** L1.

Hartwick, F. D. A. 1976, *Ap. J.*, **209**, 418.

Hartwick, F. D. A., and Sargent, W. L. W. 1978, *Ap. J.*, **221**, 512.

Isaacman, R. 1981, *Astr. Ap.*, **95**, 46.

Isaacman, R., and Oort, M. J. A., 1981, *Astr. Ap.*, **102**, 347.

Larson, R. B. 1974, *M.N.R.A.S.*, **166**, 585.

Larson, R. B. 1976, *M.N.R.A.S.*, **176**, 31.

Lilliefors, H. W. 1967, *J. Amer. Statist Assn.*, **62**, 399.

Mould, J. R. 1983, *Ap. J.*, **266**, 255.

Oort, J. 1977, *Ann. Rev. Astr. Ap.*, **15**, 295.

Pagel, B. E. J., and Patchett, B. E. 1975, *M.N.R.A.S.*, **172**, 13.

Ratnatunga, K. U., and Freeman, K., *Ap. J.*, **291**, 260.

Rich, R. M. 1985 (1984 Vulcano Conference: Population II Variables), *Mem. S.A.It.*, **56**, 23.

Saha, A. 1985, *Ap. J.*, **289**, 310.

Sanders, R. H., and Lowinger, T. 1972, *A. J.*, **77**, 292.

Searle, L., and Sargent, W. L. W. 1972, *Ap. J.*, **173**, 25.

Searle, L., and Zinn, R. 1978, *Ap. J.*, **225**, 357.

Sellwood, J. A. 1985, *M.N.R.A.S.*, **217**, 127.

Shaver, P. A., McGee, R. A., Danks, A. C., and Pottasch, S. R. 1983, *M.N.R.A.S.*, **204**, 53.

Shectman, S. 1978 in *Annual Report of the Director of the Hale Observatories*, 1977-78.

Smith, M. G., Hesser, J. E., and Shawl, S. J. 1976, *Ap. J.*, **206**, 66.

Terndrup, D., Rich, R. M., Whitford, A. E. 1984, *P.A.S.P.*, **96**, 796.

Tonry, J., and Davis, M. 1979, *A. J.*, **84**, 1511.

Walker, A. R., and Mack, P. R. 1985 Preprint.

Wielen, R. 1974 in *Highlights of Astronomy*, Vol. 3 XVth General Assembly of the IAU, G. Contopoulos (ed.) (Dordrecht:Reidel).

Wood, P. R., and Bessell, M. S., *Ap. J.*, **265**, 748.

Webbink, R. F., *Ap. J. Suppl.*, **45**, 259.

van der Kruit, P. A., and Searle, L. 1982, *Astr. Ap.*, **110**, 61.

van den Bergh, S. 1974, *Ap. J.(Letters)*, **188**, L9.

van den Bergh, S., 1971, *A. J.*, **76**, 1082.

van den Bergh, S., and Herbst, E. 1974, *A. J.*, **79**, 603.

de Vaucouleurs, G., and Pence, W. D. 1978, *A. J.*, **83**, 1163.

Zinn, R. 1980, *Ap. J.*, **241**, 602.

Captions

Figure 1. Correlation peaks used to determine radial velocities following the method of Tonry (1983). A) Spectrum of the template star, NGC 6522 star 9, logarithmically binned into 1024 bins. The peak illustrated is a nearly ideal peak. Ordinate is channel number. B) A star in Baade's Window, BW 1196. Because this star is strong lined, it is a good match with the template and the peak is at 0.6. C) A weak lined star in Baade's Window, BW 2136. The peak has a height of 0.25, and is well defined. This is one of the weakest correlations in the program. D) The peculiar double peak of BW 3160 with separation 450 km/s. This star is almost certainly an optical double, as the peak separation did not change over a 3 night period.

Figure 2. A) Residuals of standard star observations against the template for 1985 2DF data. The mean velocity was added to each observation to place it on the standard system. B) As in (A), for 1984 Shectograph data. C) Absolute value of velocity differences of repeat observations in 1984 and 1985. The rms value for these data is 20.5 km/s, so $\sigma = 14.5$ km/s. D) Distribution of differences between 1984-5 and 1982-3 data, for stars in common between those years.

Figure 3. Distribution of heliocentric radial velocities for K giants observed in the 1984-5 season, and separated into abundance groups.

Figure 4. Heliocentric radial velocities for Mould's (1983) M giants. Temperature classes are explained in §III in the text. The hot M giants may be metal poor

and correspond to 47 Tuc abundance. The coolest M giants include many stars of spectral type M7 and later, which may have metal rich stars as their progenitors.

Figure 5. Cumulative distribution of K giant radial velocities obtained during the 1984-5 season compared with the error function with σ and mean estimated from the distribution. (See Table 3) There is no significant deviation from normality.

Figure 6. Radial velocity plotted against [Fe/H] using Solution 1 from Chapter 1. Only the high resolution 1984-5 data are illustrated.

Figure 7. Color-magnitude diagram using instrumental colors from a narrow-band system. $\lambda 4900\text{Å} - \lambda 7000\text{Å}$ color agains a $\lambda 7000\text{Å}$ magnitude. A giant branch and clump is visible. The clump justifies use of the "globular cluster feature" in the Bahcall-Soneira model. Blue stars are probably foreground disk dwarfs.

Figure 8. The results of the Bahcall-Soneira model, modified to include reddening towards Baade's Window. Roughly equal numbers of disk and spheroid stars are predicted. The model lacks a dynamically necessary central bulge component, as discussed in the text.

Figure 9. Mass enclosed within a given radius from the Bahcall, Schmidt, and Soneira (1983) rotation curve where $M(r) = rv(r)^2/G$. Density laws for the various components may be found in Bahcall, Schmidt, and Soneira (1982). Note the dominance of the central bulge component within 1 kpc.

Figure 10. Chemical evolution models compared with cumulative abundance distribution from Solution 1 (Chapter 1). Solid line: Simple model, evolved to

complete gas consumption. Dotted line: Simple model, with no consumption of gas. Dashed line: local disk lognormal G dwarf abundance distribution, shifted by Shaver *et al's* abundance gradient to [Fe/H]=0.14, with $\sigma = 0.36$.

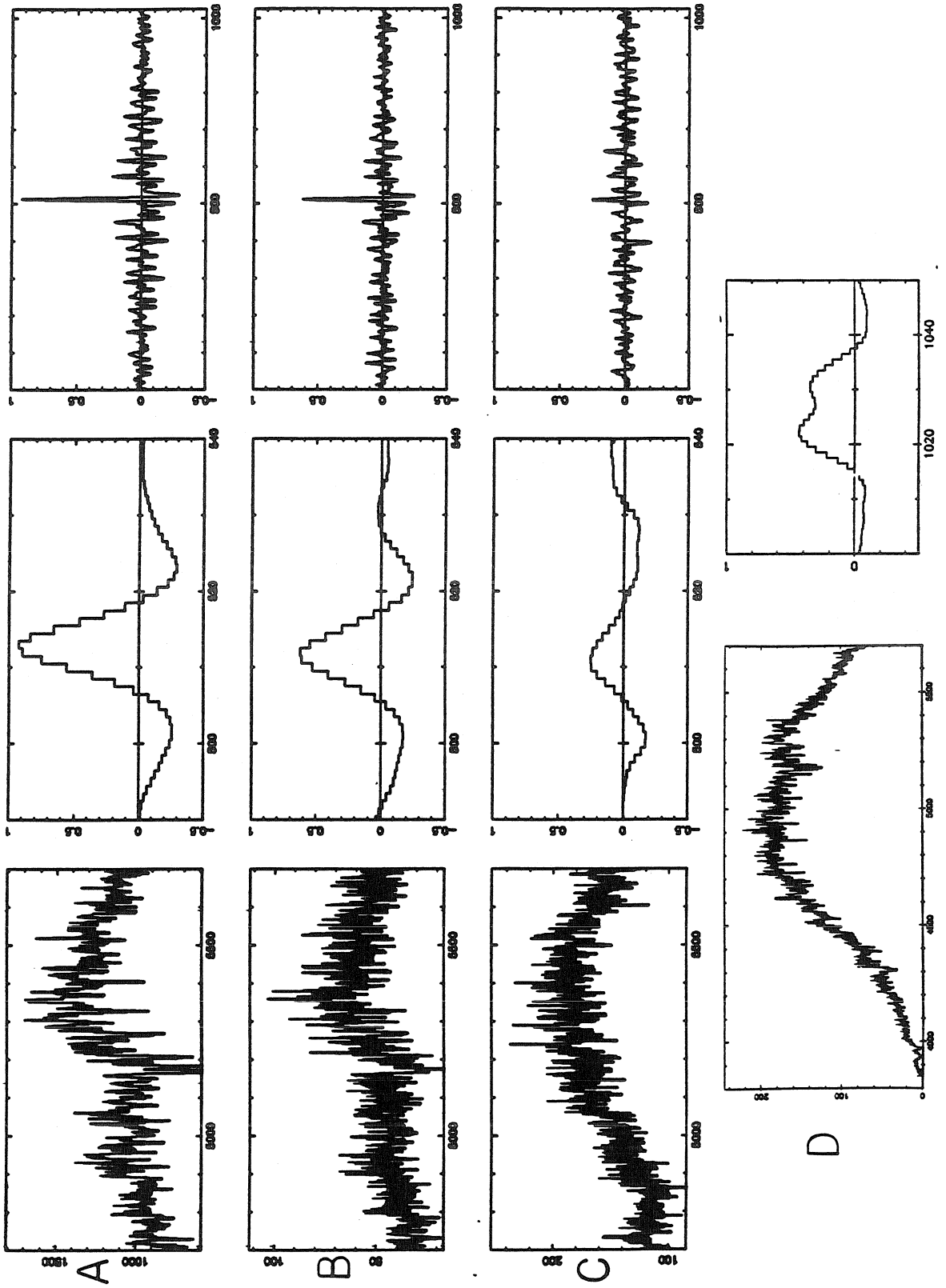

Figure 1

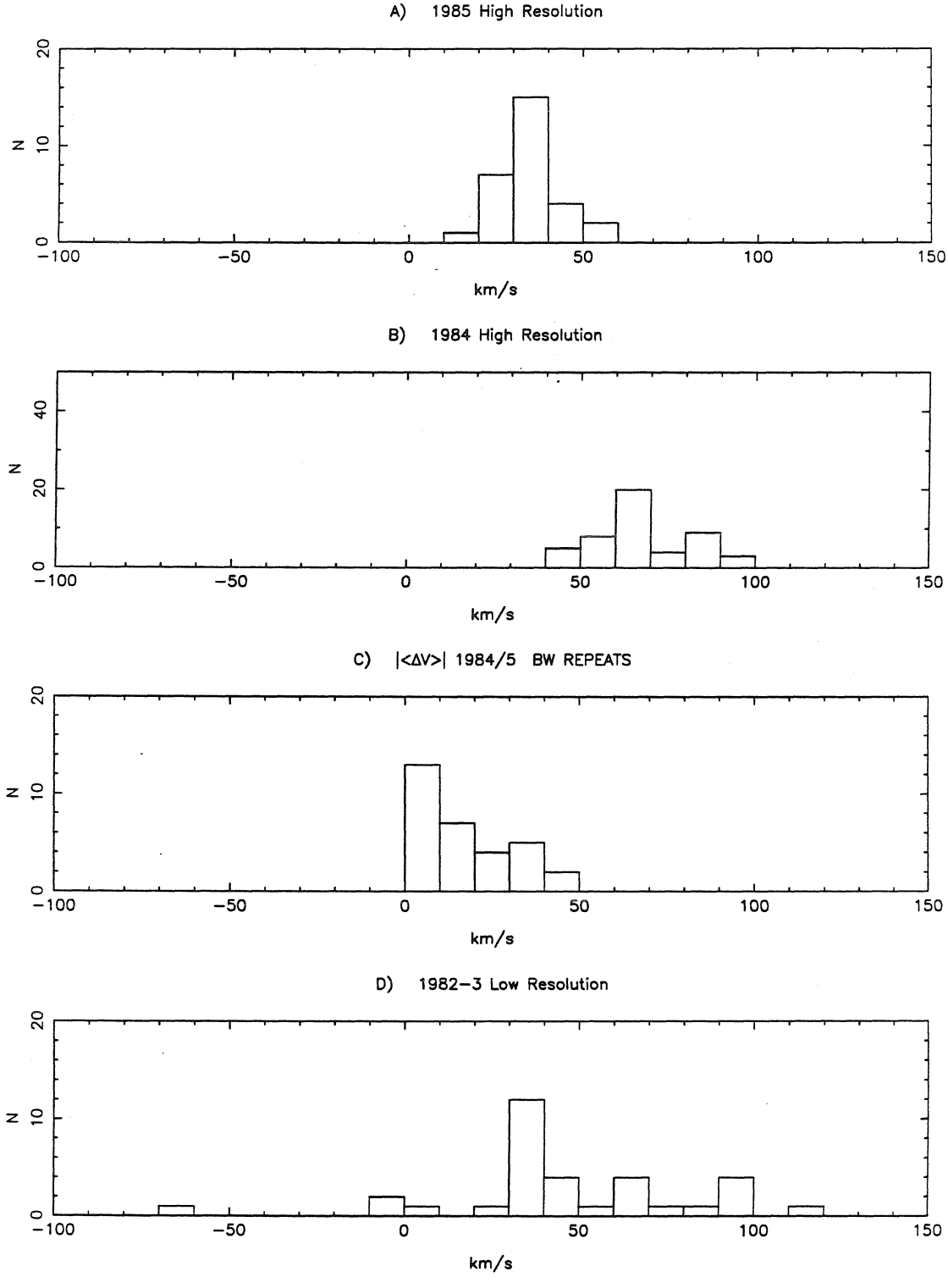
A) 1985 High Resolution
N
0
10
20
−100
−50
0
50
100
150
km/s
B) 1984 High Resolution
N
0
20
40
−100
−50
0
50
100
150
km/s
C) |<ΔV>| 1984/5 BW REPEATS
N
0
10
20
−100
−50
0
50
100
150
km/s
D) 1982−3 Low Resolution
N
0
10
20
−100
−50
0
50
100
150
km/s

Figure 2

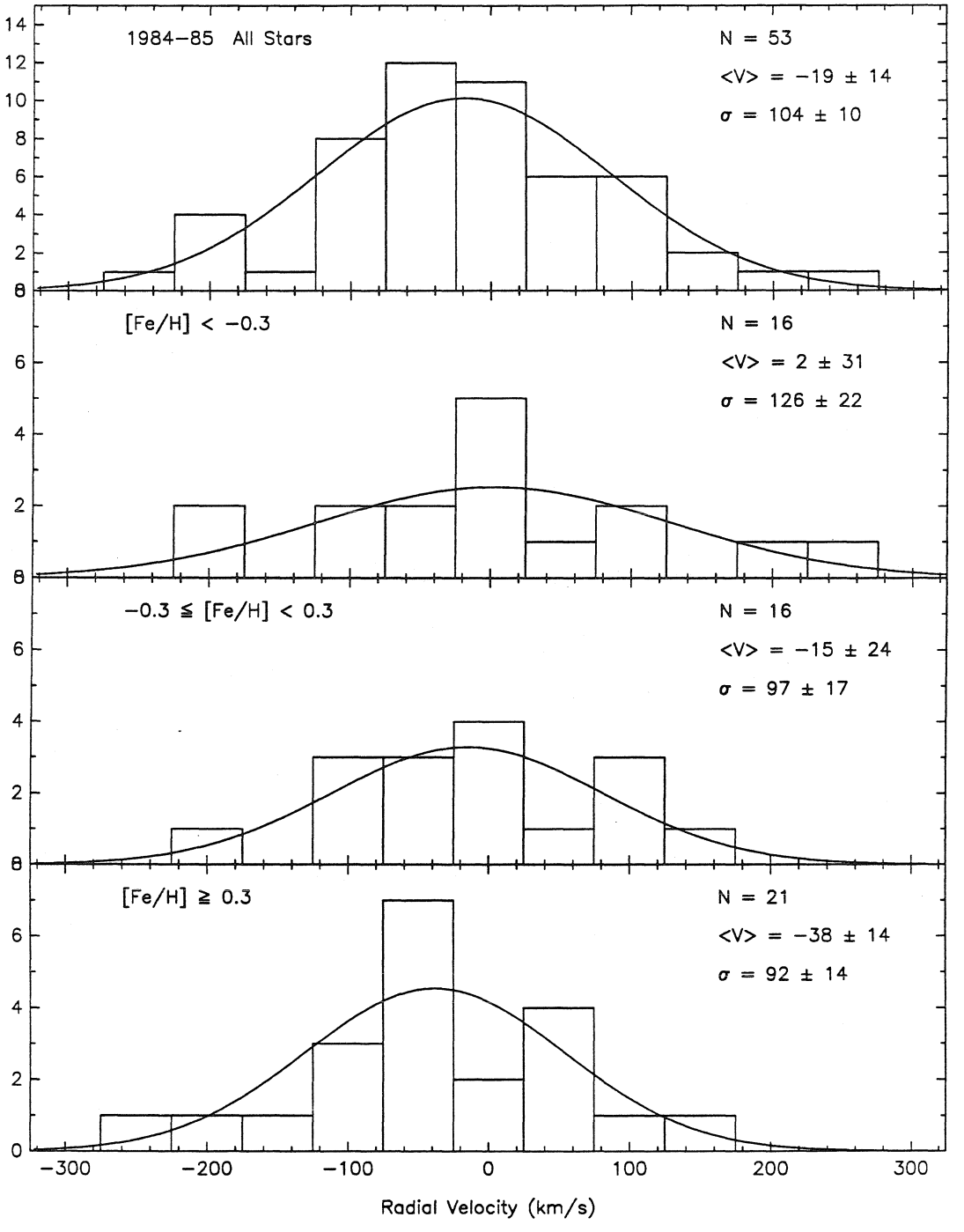
1984–85 All Stars
N = 53
<V> = −19 ± 14
σ = 104 ± 10
[Fe/H] < −0.3
N = 16
<V> = 2 ± 31
σ = 126 ± 22
−0.3 ≦ [Fe/H] < 0.3
N = 16
<V> = −15 ± 24
σ = 97 ± 17
[Fe/H] ≧ 0.3
N = 21
<V> = −38 ± 14
σ = 92 ± 14
−300
−200
−100
0
100
200
300
Radial Velocity (km/s)

Figure 3

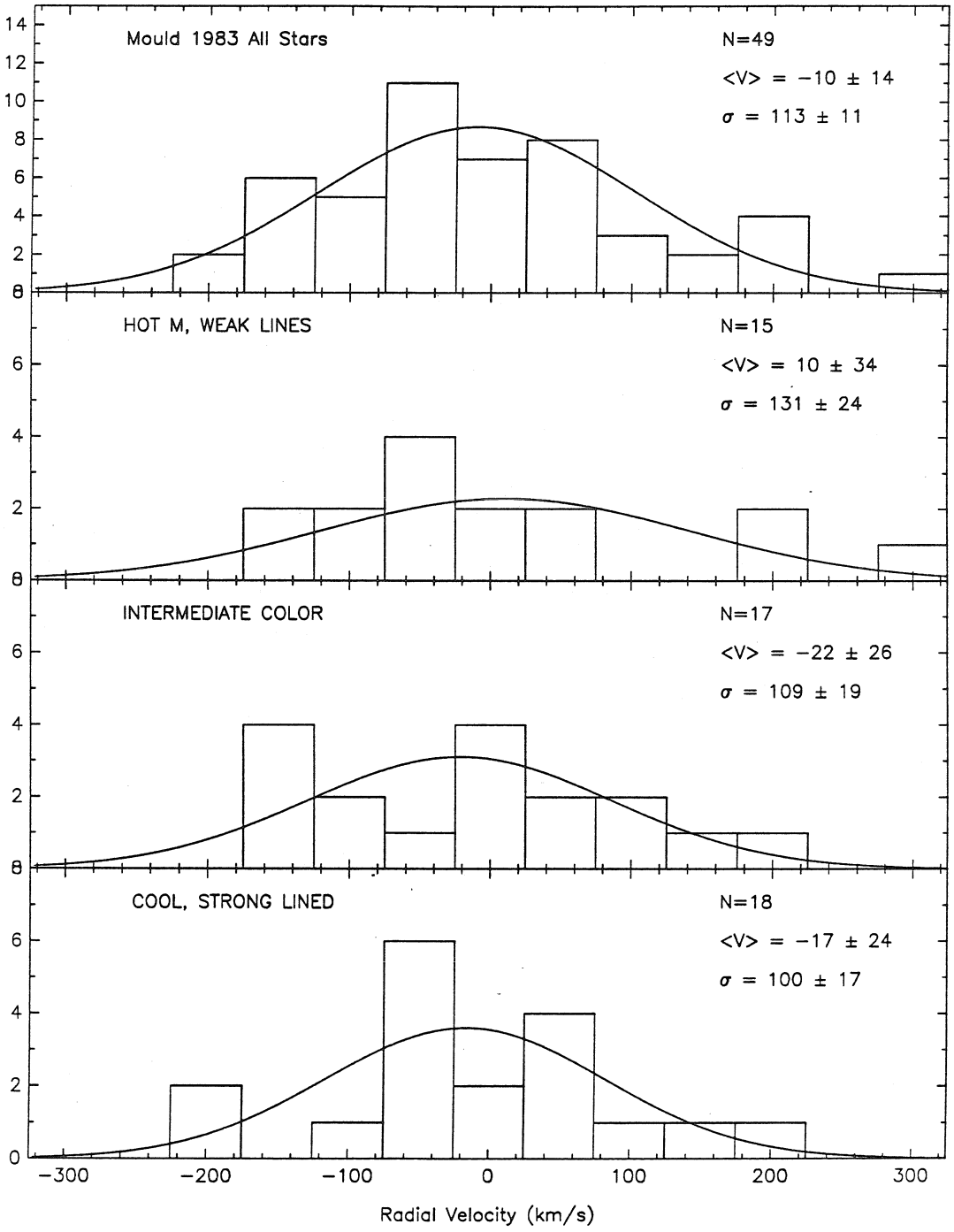
Mould 1983 All Stars
N=49
<V> = −10 ± 14
σ = 113 ± 11
HOT M, WEAK LINES
N=15
<V> = 10 ± 34
σ = 131 ± 24
INTERMEDIATE COLOR
N=17
<V> = −22 ± 26
σ = 109 ± 19
COOL, STRONG LINED
N=18
<V> = −17 ± 24
σ = 100 ± 17
−300
−200
−100
0
100
200
300
Radial Velocity (km/s)

Figure 4

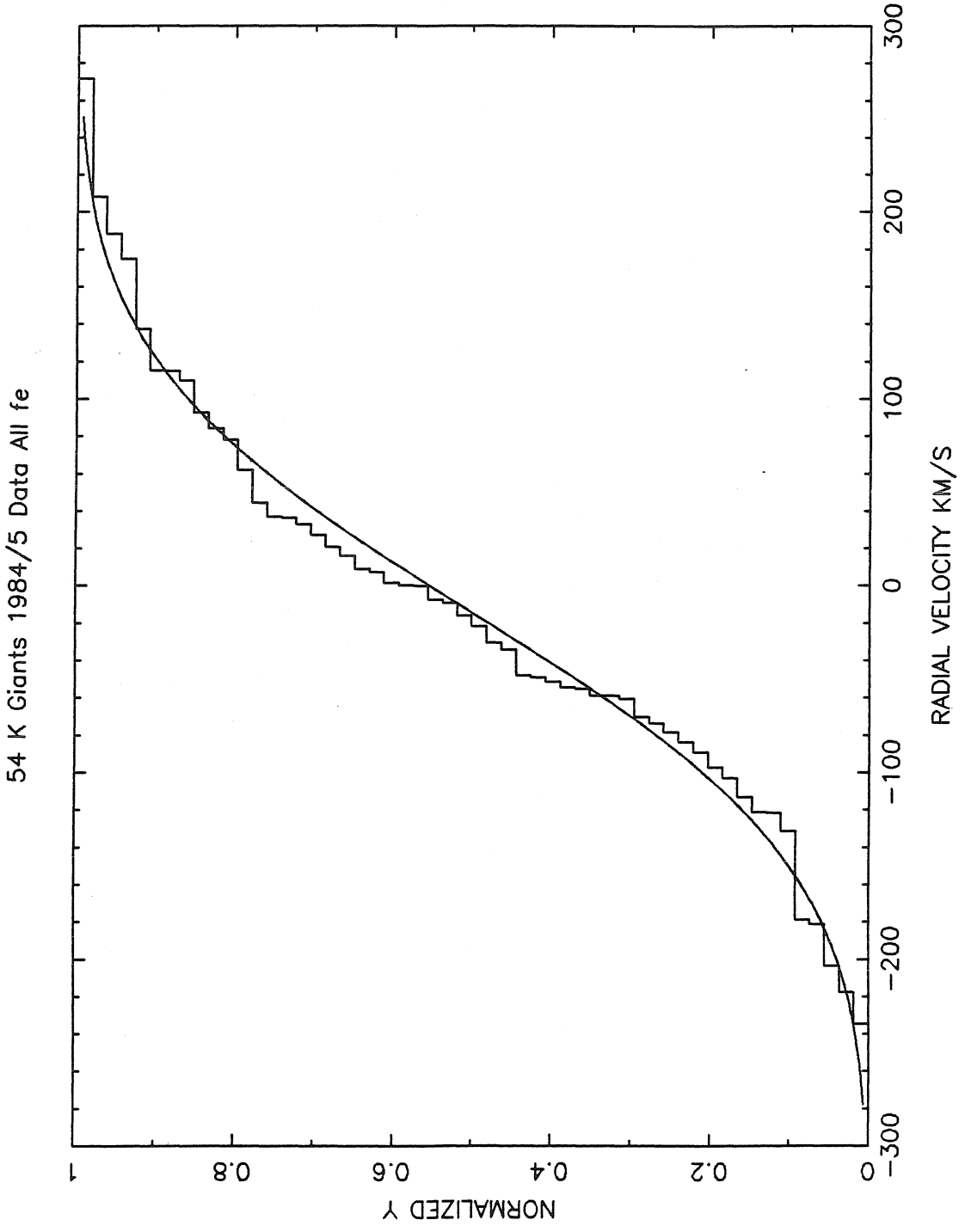
54 K Giants 1984/5 Data All fe
NORMALIZED Y
0
0.2
0.4
0.6
0.8
1
RADIAL VELOCITY KM/S
300
200
100
0
-100
-200
-300

Figure 5

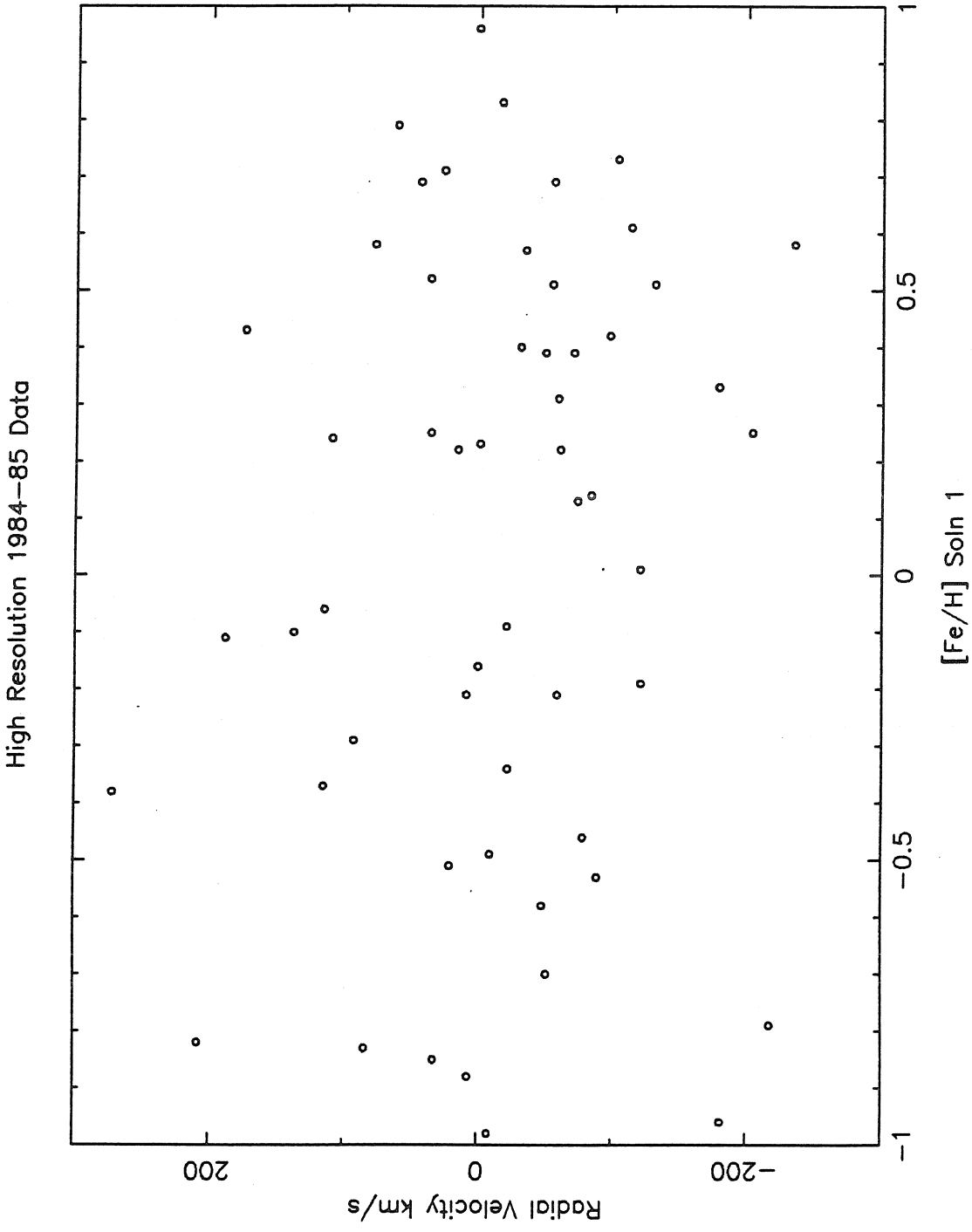
High Resolution 1984-85 Data
Radial Velocity km/s
-200
0
200
[Fe/H] Soln 1
-1
-0.5
0
0.5
1

Figure 6

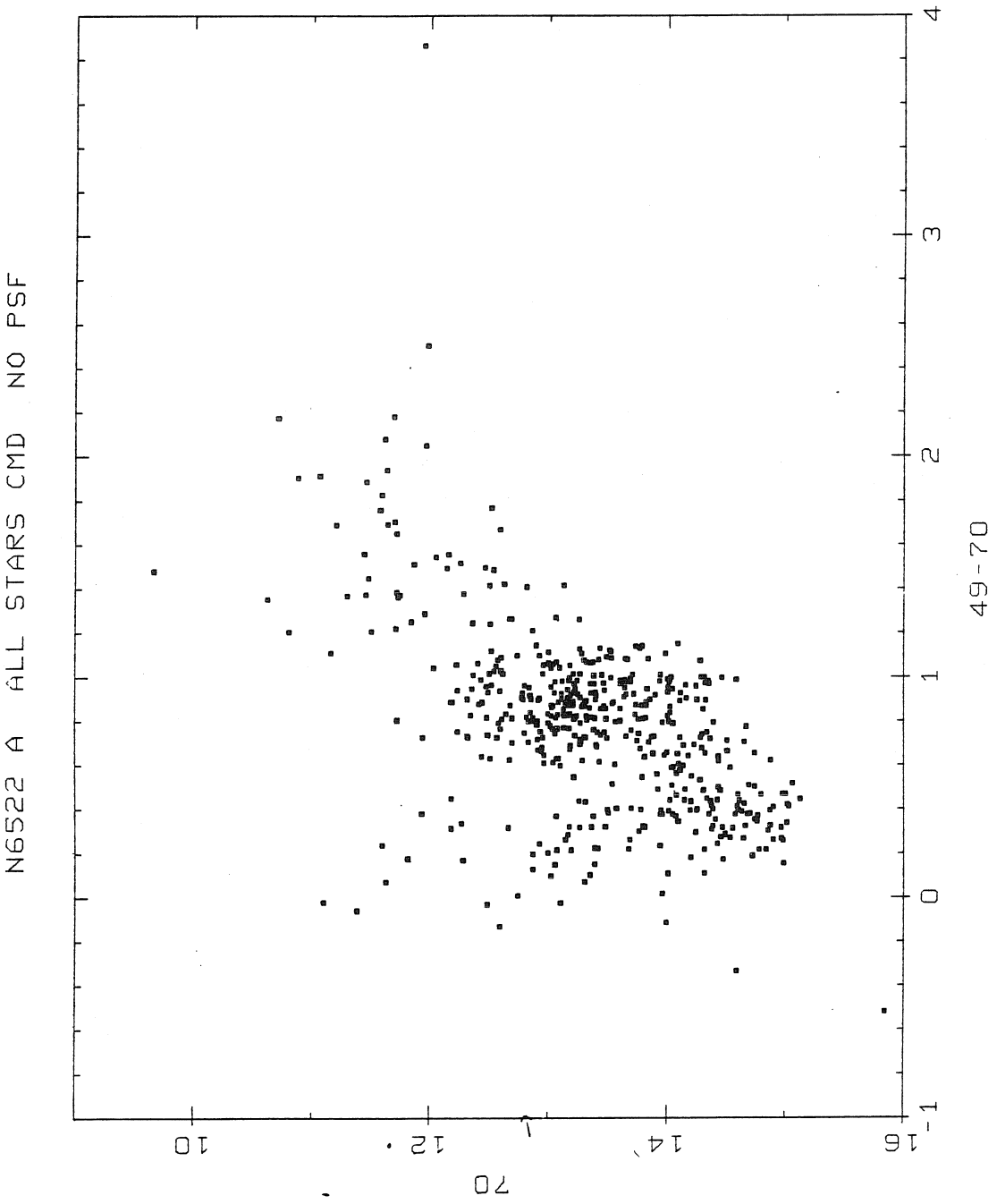

Figure 7

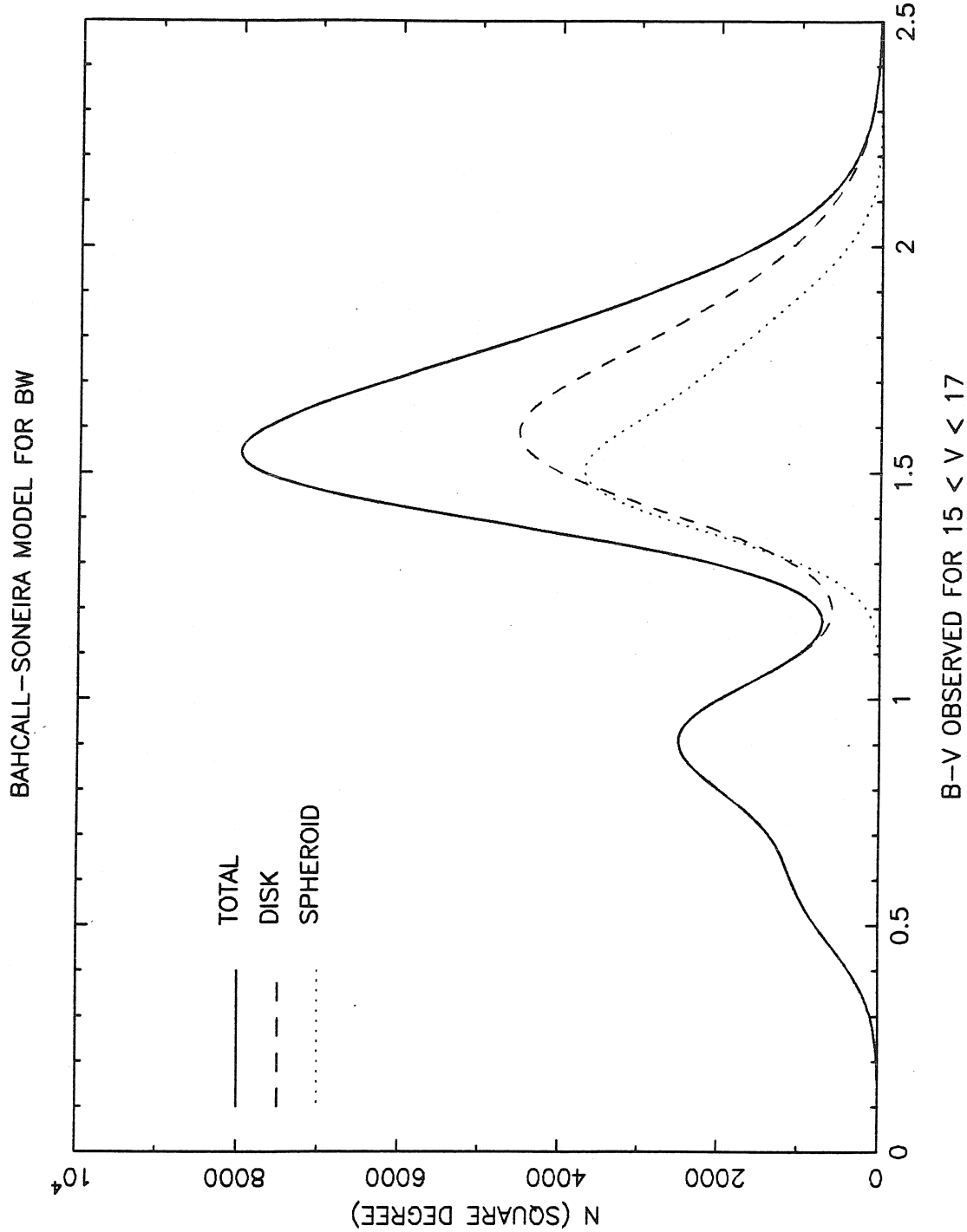
BAHCALL-SONEIRA MODEL FOR BW
TOTAL
DISK
SPHEROID
N (SQUARE DEGREE)
10^4
8000
6000
4000
2000
0
0
0.5
1
1.5
2
2.5
B-V OBSERVED FOR 15 < V < 17

Figure 8

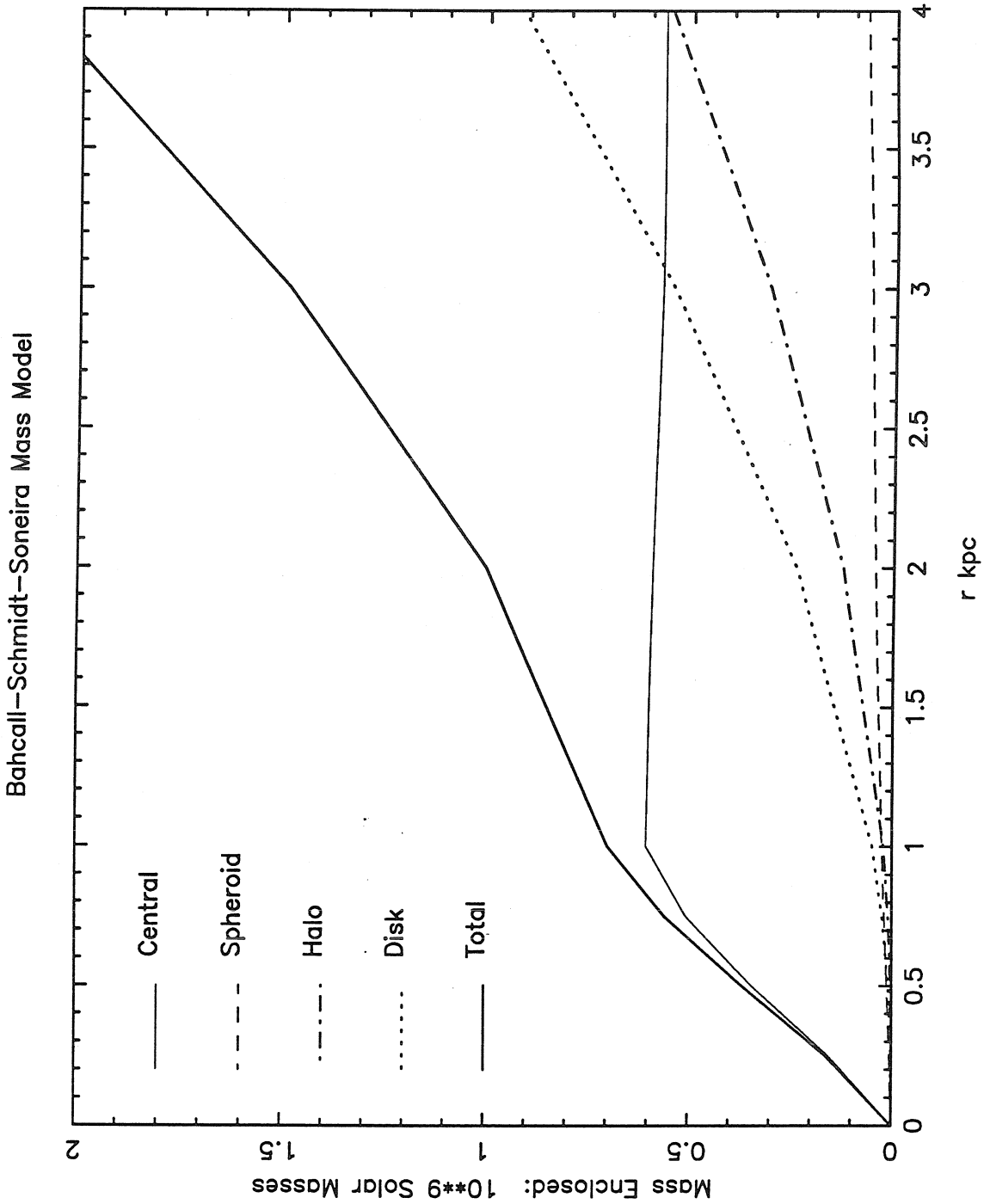
Bahcall-Schmidt-Soneira Mass Model
Central
Spheroid
Halo
Disk
Total
Mass Enclosed: 10**9 Solar Masses
r kpc
0
0.5
1
1.5
2
2.5
3
3.5
4

Figure 9

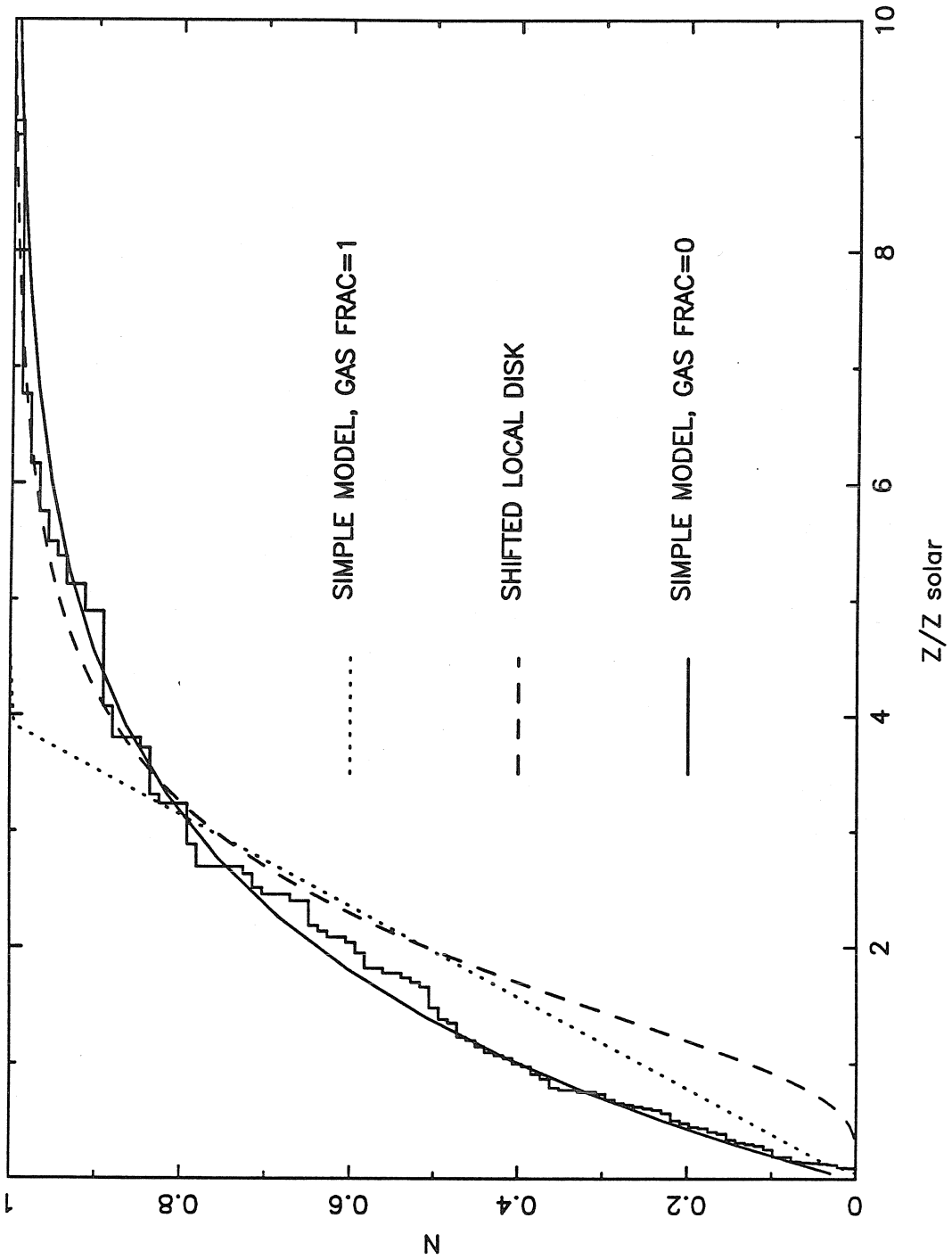
SIMPLE MODEL, GAS FRAC=1
SHIFTED LOCAL DISK
SIMPLE MODEL, GAS FRAC=0
N
Z/Z solar
0
0.2
0.4
0.6
0.8
1
2
4
6
8
10

Figure 10

APPENDIX 1

PHOTOMETRY OF K GIANTS IN THE NUCLEAR BULGE OF THE GALAXY

J. A. Frogel, A. E. Whitford, and R. M. Rich

Reprinted from the *Astronomical Journal* (1984, 89 1536–1542).

THE ASTRONOMICAL JOURNAL VOLUME 89, NUMBER 10 OCTOBER 1984

PHOTOMETRY OF K GIANTS IN THE NUCLEAR BULGE OF THE GALAXY

JAY A. FROGEL
Cerro Tololo Inter-American Observatory,[a] National Optical Astronomy Observatories, Casilla 603, La Serena, Chile

A. E. WHITFORD[b]
Lick Observatory, Board of Studies in Astronomy and Astrophysics, University of California at Santa Cruz, Santa Cruz, California 95064

R. M. RICH[b]
Astronomy Department 105-24, California Institute of Technology, Pasadena, California 91125
Received 4 June 1984; revised 11 July 1984

ABSTRACT

For 52 K and early-M giants in Baade's Window at a galactic latitude of $-3°.9$, we present *RIJHK* photometry. The location of these galactic bulge giants on various color-color plots is markedly different from both globular cluster and solar neighborhood giants. However, their locations in infrared color-magnitude diagrams are not obviously consistent with the interpretation that they are old and metal rich. We tentatively conclude that blanketing by an as yet unidentified source (or sources) has a significant effect on the energy distributions of these stars which spectroscopically have been shown to be metal rich.

I. INTRODUCTION

In principle, it should be possible to learn a great deal about the stellar content of the spheroidal component of galaxies by an examination of the giants in the nuclear bulge of the Milky Way. Morgan (1959) showed qualitatively, and Whitford (1978) quantitatively, that features in spectra of the integrated light from the Galactic nuclear bulge are quite similar to those seen in other galaxies.

Arp (1965) and van den Bergh (1971) obtained color-magnitude diagrams for stars in Baade's Window (galactic latitude $-3°.9$) around the globular cluster NGC 6522 (Baade 1963). They concluded that their CM diagrams were dominated by old giants with a range in metallicity extending from M3 (van den Bergh) or 47 Tuc (Arp) to that of NGC 188. The spectral surveys of Nassau and Blanco (1958), Blanco, Blanco, and McCarthy (1978), and Blanco, McCarthy, and Blanco (1984) have shown that Baade's Window (BW) contains a large number of M6–9 giants. Because of severe blanketing in the visible region of their spectra, many of the latest and bolometrically most luminous of the M giants are fainter at V than the faintest stars included in Arp's and van den Bergh's photometry (Frogel, Whitford, and Blanco 1984).

Whitford and Rich (1983) have investigated the metallicity distribution of a sample of K giants from the list of Arp (1965). Among their reasons for choosing the K giants for study is the fact that stars of all metallicities have to go through a K-giant phase at some point after leaving the main sequence, whether or not they go on to become a late-M giant. They find that a majority of stars in their sample are super-metal-rich (SMR) with a mean [Fe/H] = 0.3 and an upper extreme of nearly 1.0.

The present paper presents *RIJHK* photometry for a selection of Arp's (1965) stars in BW, most of which should be K giants. These data can be compared with similar data for Galactic globular clusters for which ages and metallicities are known. It is not our purpose at present to analyze the data for the BW stars in any detail. Rather, the comparison with globular cluster and solar neighborhood giants will define some of the problems to be encountered in a study of a complete sample of bulge giants (Frogel, Whitford, and Blanco 1984) and, we hope, encourage those whose research is concerned with model atmospheres to examine anew the effects of supermetallicity on stellar energy distributions. Also, these data will be used in subsequent papers as an aid in modeling the integrated light from the Galactic bulge.

II. THE DATA

Selection criteria for stars from the list of Arp (1965) are those enumerated by Whitford and Rich (1983). Late-M giants were specifically avoided by a comparison of Arp's identifications with those of Blanco and his collaborators. The final list of stars with infrared photometry is given in Table I. A few of these are of types M0–2 (Blanco, unpublished) as indicated in column 2. The remainder are most likely no later than M0. Four of the stars are in Frogel, Whitford, and Blanco's (1984) unbiased sample of early-M stars and are included here as well, since Whitford and Rich (1983) obtained spectra for them.

The infrared observations were made between 1980 May and 1981 June on the CTIO 4-m reflector with the D3 InSb system and the $f/30$ chopping secondary. The infrared data are on the CTIO/CIT system (Elias *et al.* 1982; Frogel *et al.* 1978). The focal-plane iris diaphragm was set at diameters between 3.5 and 7.2 arcsec. Crowding and contamination of the two sky positions used for each star were the main difficulties encountered in making the measurements. Long integrations with the acquisition TV allowed adjustment of the chopper throw for each star so as to minimize the latter problem. Nonetheless, we can not rule out errors in the K magnitudes 0.05 to 0.10 mag greater than those quoted in Table I for some of the stars, on account of crowding and contamination. Additional sources of errors in the colors should be significantly less important.

The V magnitudes are from Arp (1965), adjusted according to the recommendation of Blanco and Blanco (1984). The

[a] The Cerro Tololo Inter-American Observatory is operated by the Association of Universities for Research in Astronomy, Inc., under contract with the National Science Foundation.
[b] Visiting Astronomer at Cerro Tololo Inter-American Observatory.

 0004-6256/84/101536-07$00.90

TABLE I. Photometry[a] of nuclear bulge giants.

Star	Type	K	V-K	V-R	R-I	J-K	H-K	H_2O	CO
I-21	M0	11.63	3.65	.98	.63	.74	.18		.120
I-25		12.67(4)	4.03	.86	.71	.90	.21		
I-39		12.81(5)	3.89	.68	.75	.89	.23		
I-49		12.96(4)	3.17	.82	.93	.70	.12		
I-53		13.57(4)	3.18	.69	.75	.68	.11		
I-64	M1	11.51(4)	4.73	.99	.91	1.05(4)	.23(4)		
I-76	M1	11.08	4.42	.59	1.06	1.00	.23		.165
I-141		11.81	3.97	.58	.86	.92	.17		
I-145	M0	11.69	3.56	.79	.64	.76	.16		
I-155		12.31	4.20	1.20:	.70:	.92	.20		
I-158		12.48	4.03	1.04	.62	.87	.20		
I-161		12.71	1.83	.08	.65	.40	.10		-.020(4)
I-164		12.14	4.14	.99	.85	.90	.16		
I-194		11.75(4)	4.45	1.12	.73	.94	.18		
I-196	M2	11.22	4.85	.92	1.06	1.00	.26		
I-202	M0	11.63	4.14	.69	.97	.90	.21		.120
I-298	M2	10.79	5.05	.93	1.16	1.06	.26		
I-322		10.08	4.14	.56	.92	.95	.20	.030(3)	.150
II-33	M1	11.30	4.13	.73	.90	.95	.18		.075
II-40		13.18	3.57	.80	.76	.75	.17		
II-42		12.16	4.40	.92	.87	.99	.21		
II-49		12.42	3.61	.74	.66	.77	.16		
II-116		12.90(4)	4.12	.86	.77	.96	.20		
II-119		11.81	3.86	.83	.76	.85	.18		
II-122	M2	9.48	4.80	.76	1.08	1.13	.23	.070	.160
II-145		12.87	4.09	.95	.68	.82	.19		
II-146		11.69	3.91	.64	.87	.82	.20		
II-147		13.71(4)	3.37	.82	.65	.71	.12		
II-173		12.83	3.87	.92	.64	.81	.17		
II-197		12.23	4.54	.76	.97	1.06	.24		
II-206		14.14(7)	2.71	.56	.55	.57(6)	.17(5)		
II-215		11.51	3.26	.42	.77	.70	.12		
II-240		12.27	3.25	.48	.78	.73	.17		.040
II-244		11.56	4.66	.94	.93	1.01	.19		.135
II-245		13.15(4)	3.64	.85	.63	.71	.13		
II-252		12.37	4.23	.78	.89	.92	.16		
II-261	M1	11.46	4.46	.69	1.00	1.03	.20		
III-106		12.85(4)	3.96	1.11	.66	.78	.14		
III-141		13.02(4)	2.23	.34	.61	.46	.08		
III-152	M1	11.66	4.43	.89	.94	.97	.19		
III-157		11.79	4.70	.96	1.01	1.02	.24		
III-160		12.61	4.09	1.00	.82	.79	.19		
III-164		10.72	4.37	.86	.92	.97	.20		.120
III-200		12.92(4)	3.49	.71	.76	.76	.16		
III-209	M1	11.98(4)	4.51	.89	.94	.96	.20		
IV-3		11.20	3.84	.70	.82	.84	.15		
IV-25		12.50	3.53	.62	.73	.78	.17		
IV-167		12.72	4.09	.70	.92	.86	.19		
IV-203	M0	8.93	4.92	.95	1.00	1.15	.22	.040	.065
IV-312		12.82	3.46	.66	.69	.71	.12		
IV-325		12.76	3.88	.80	.78	.87	.17		
IV-329		10.92	4.17	.70	.97	1.00	.20		
Corrections[b]		0.14	1.40	0.33	0.25	0.26	0.09	0.025	-0.015

Notes:

a. Uncertainties in the K magnitudes and JHK colors are given in units of hundredths of a magnitude when greater than 0.03. For the H_2O and CO indices they are given when greater than 0.02.

b. These reddening corrections are based on a value of E(B-V)=0.48 for an A0 star as discussed in the text.

transformation they find for Arp's data is similar to that found by van den Bergh (1971).

The *RI* colors are from iris photometry of a pair of plates obtained by Blanco (Whitford and Blanco 1979). Magnitudes on the Cousins system (Bessell 1979) were determined relative to those stars in a photoelectric sequence in Baade's Window (Blanco, Blanco, and McCarthy 1979). Although the *R* and *I* plates were taken six months apart, this should not introduce appreciable error in the colors, since the spectral classes involved do not include late-M giants where variability is common. The photometric accuracy was undoubtedly affected by the uneven background of unresolved turnoff stars. The fit of standard stars on the calibrated curve suggests errors of 0.03–0.05 mag. In the one case where a faint companion was seen in the iris, the doubtful magnitude in Table I is followed by a colon.

Reddening and extinction values are noted at the bottom of Table I. For an A0 star in BW, $E(B-V)$ was taken to be 0.48 mag based on the work of Arp (1965) and van den Bergh (1971), and on Zinn's (1980) study of NGC 6522. For a K giant, this is equivalent to an $E(B-V)$ of 0.43 [Dean, Warren, and Cousins (1978)]. The remainder of the values are based on the reddening law given by Elias, Frogel, and Humphreys (1985) for M supergiants.* The value of $E(J-K)$ is somewhat larger than that used by Whitford and Rich (1983) to derive abundances. As they point out, the use of a larger value for the excess at $J-K$ will result in slightly higher abundances. Bolometric corrections were calculated by integrating under the stellar energy distributions.

III. COLOR-MAGNITUDE DIAGRAMS

Figures 1 and 2 illustrate two color-magnitude arrays for the stars of Table I. In these and succeeding plots, those giants with measured abundances from Whitford and Rich (1983) are distinguished from the remainder of the stars and are divided, at [Fe/H] = 0.0 from column 12 of their Table 2, into high- and low-metallicity groups.

In addition to the spread in colors to be expected from the range in metallicities, there is also a dispersion in magnitude arising from the variations in distance as the line of sight passes from the near to the far side of the bulge. Glass and Feast (1982) note that, for both the Mira variables and the RR Lyrae variables seen in the bulge windows, the one-sigma dispersion in the distance modulus is about 0.2 mag. If the bulge K giants here considered are assumed to have the same space distribution as these variables, the magnitude dispersion should be much less important than the color dispersion insofar as Figs. 1 and 2 are concerned.

In Fig. 1, the $K, (V-K)$ plot, it is clear that the sample of BW giants scatter between the M67 and M92 giant branches. The magnitude of the scatter in $(J-K)$ (Fig. 2) with respect to the separation between cluster giant branches is similar to that in $(V-K)$, but on the $(J-K)$ plot the stars are displaced somewhat blueward relative to their distribution in $(V-K)$. Given Whitford and Rich's (1983) mean [Fe/H] of 0.3 and the usual assumption that the BW K giants are comparable in age to globular clusters, it is noteworthy that in neither Fig. 1 nor Fig. 2 is there any sizable population of stars redward of the M67 or 47 Tuc giant branches, respectively. Unfortunately, the slope of the line which gives Arp's (1965) faintest V magnitude limit is nearly parallel to the giant branch of M67. While this could lead to the exclusion of very red stars from our sample, the high-metallicity stars in both figures should, in any case, lie far to the red of where they are located (Frogel, Persson, and Cohen 1983).

In their discussion of ω Centauri, Persson *et al.* (1980) defined a quantity $R(V-K)$ that measures the relative location of a star on a $V, (V-K)$ plot with respect to the M92 and the M71 giant branches. In a stellar system of uniform age, this quantity should be proportional to a star's metallicity.

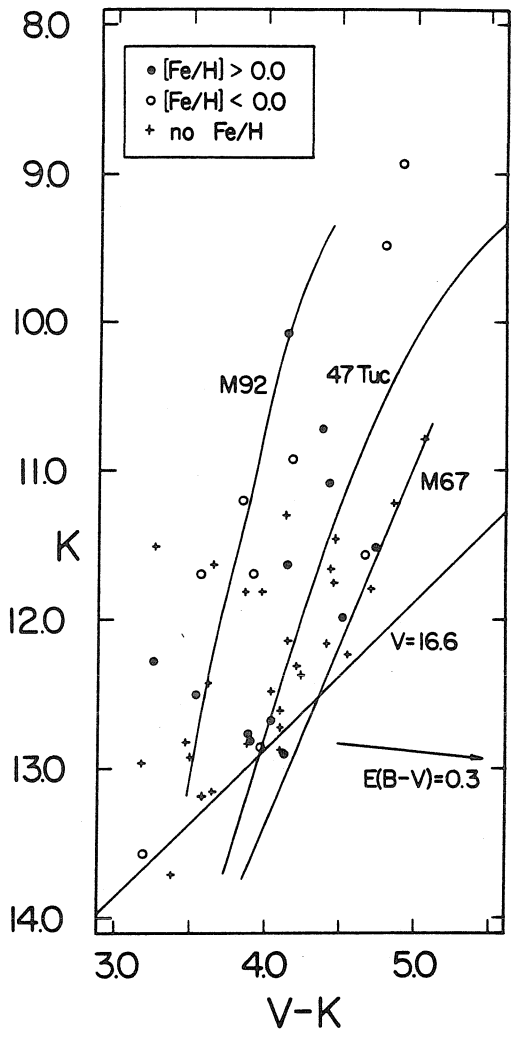

FIG. 1. On this and succeeding figures, the *observed* colors and magnitudes for all stars from Table I are plotted with the three bluest stars—I-161, II-206, and III-141 omitted. The fiducial cluster giant branches are from Cohen, Frogel, and Persson (1978) and Frogel, Persson, and Cohen (1981), shifted by the differences in apparent moduli and differential absorption implied by an adopted true distance modulus of 14.8 and the absorption values at the end of Table I. The metallicities are from column 12 of Table 2 in Whitford and Rich (1983). The V magnitude limit of Arp's (1965) survey, transformed according to the prescription of Blanco and Blanco (1984), is shown by the line labeled $V = 16.6$.

*These values will differ from those which would result from the application of Lee's (1970) reddening because of systematic errors in the spectral types used by Lee, and significant biases in the selection of stars available to him as discussed by Elias *et al.*

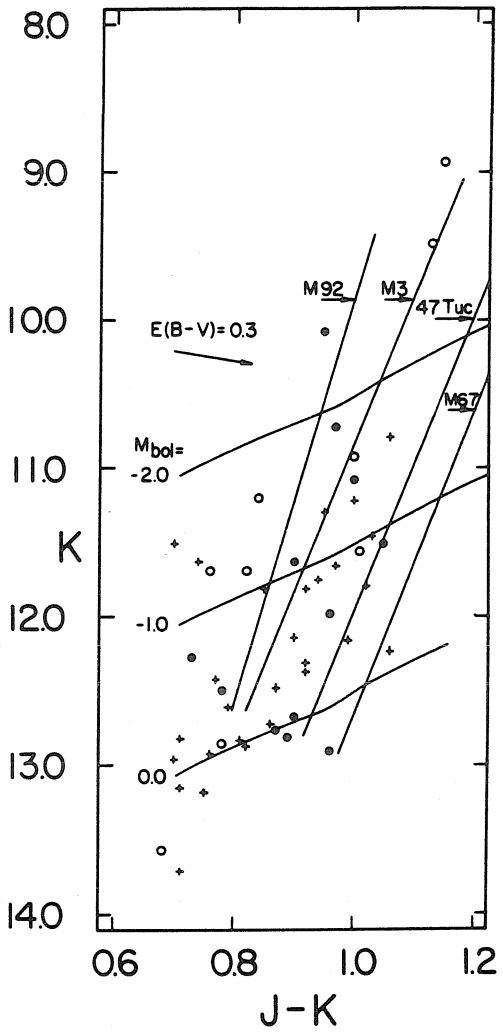

FIG. 2. Similar to Fig. 1 except $J-K$ replaces $V-K$. Lines of constant bolometric magnitude are shown.

Since the giant branches of M71 and 47 Tuc coincide (Frogel, Persson, and Cohen 1981), the calculation of R values for our sample of bulge stars may use the 47 Tuc giant branch as a reference line. The resulting distribution for the stars in Fig. 1 that have [Fe/H] values from Whitford and Rich (1983) is shown in Fig. 3. The mean values of $R\,(V-K)$ for the high- and low-Z groups are 0.51 and 0.21, respectively, with a one-sigma dispersion of 0.16 in both cases. Errors of 0.1–0.2 mag in V are expected to contribute significantly to the lack of detailed correlation between R and [Fe/H]. Variable reddening would contribute further, although there is at best only a weak correlation between Blanco, McCarthy, and Blanco's (1984) reddening values and a star's position in Figs. 1 and 3. Thus, although the overall distribution of stars in Fig. 1 is considerably bluer than would be expected from Whitford and Rich's (1983) metallicity values, Fig. 3 shows that the *relative* distribution of the high- and low-metallicity stars is qualitatively correct.

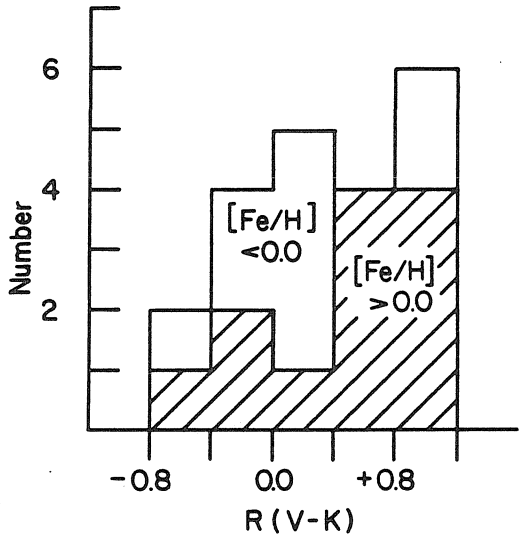

FIG. 3. For stars in BW with values of [Fe/H] from Whitford and Rich (1983), the distribution of the metallicity parameter $R\,(V-K)$ is shown.

IV. COLOR-COLOR DIAGRAMS

a) (J−K), (V−K)

At a given $V-K$, globular cluster giants have somewhat *redder* $J-K$ colors than field giants (Cohen, Frogel, and Persson 1978; Frogel, Persson, and Cohen 1981, 1983). In contrast, Fig. 4 shows that nearly all of the BW giants from Table I have, at a given $V-K$, $J-K$ colors that are about 0.05 mag *bluer* than the mean field line. Three of the four stars with measured abundances which lie above the mean line in Fig. 4 do, in fact, belong to the low-Z group; their [Fe/H] values are -0.76, -0.72, and -1.03. The fourth, a high-Z star, has an [Fe/H] of 0.24 (Whitford and Rich 1983).

Since the $(J-K)/(V-K)$ reddening vector is nearly parallel to the mean sequence in Fig. 4, moderate changes in the color excess values will not affect the appearance of the fig-

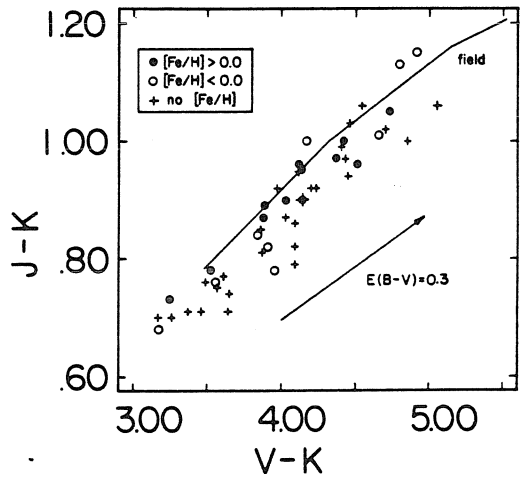

FIG. 4. The mean line for field giants is from Frogel *et al.* (1978).

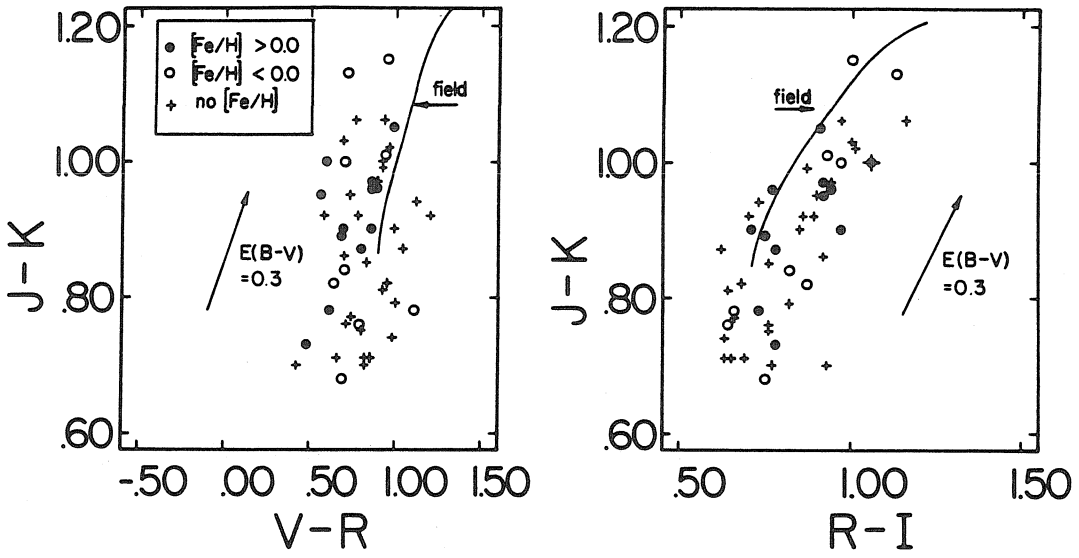

FIG. 5. *RI* values are on the Cousins photometric system with the mean lines for field giants derived from the relations given by Bessell (1979) and Frogel *et al.* (1978).

ure. Suppose that there is a residual systematic error in the V magnitudes such that the $V-K$ colors in Fig. 1 are too blue. Any correction would act to further increase the displacement of the BW giants with respect to the field line in Fig. 4.

b) (J−K), (V−R), and (R−I)

Whitford and Blanco (1979) pointed out that the giants in BW have an "R-band dip" with respect to the energy distributions of old disk giants. They attributed this dip to strong blanketing effects in super-metal-rich stars. The energy curves in Fig. 1 of Frogel and Whitford (1982) display the depth of the dip as observed in the coolest BW stars.

Figure 5(a) shows that the R-band dip may be present even in the K and early-M giants from BW in Table I. At constant $J-K$, the BW stars are displaced blueward, in $V-R$, of the mean field line. If the stars were forced redward in $J-K$ to match the field line in Fig. 4, the displacement in Fig. 5(a) would further increase. The displacement, though, depends hardly at all on a star's metallicity. The three low-Z stars noted in connection with Fig. 4 are not particularly less displaced here.

As would be expected if the source of the R-band dip has a relatively smaller effect on the I band, the $R-I$ colors of the BW stars are redder than those for field giants at the same $J-K$ as may be seen in Fig. 5(b). About one-half of the shift can be attributed to the $J-K$ displacement in Fig. 4. The rest must be due to differential blanketing effects in the R pass band.

In the $(J-K)$, $(V-I)$ plane (not shown), the BW giants from Table I lie close to the mean line for field giants.

c) (J−H), (H−K)

Figure 6 shows a tendency for the high-Z stars to lie redward, in $H-K$, of the low-Z giants. The low-Z star at $(J-H, H-K)$ of 0.62, 0.20 is II-146. Its [Fe/H] of -0.05 is the highest of any in the low-Z group. This tendency is similar to the separation observed between globular cluster giants of *all* metallicities and field giants shown in the figure (Frogel, Persson, and Cohen 1983).

d) The CO Indices

All of the high-Z giants and two of the low-Z ones in BW have CO indices greater than the mean for field giants at the

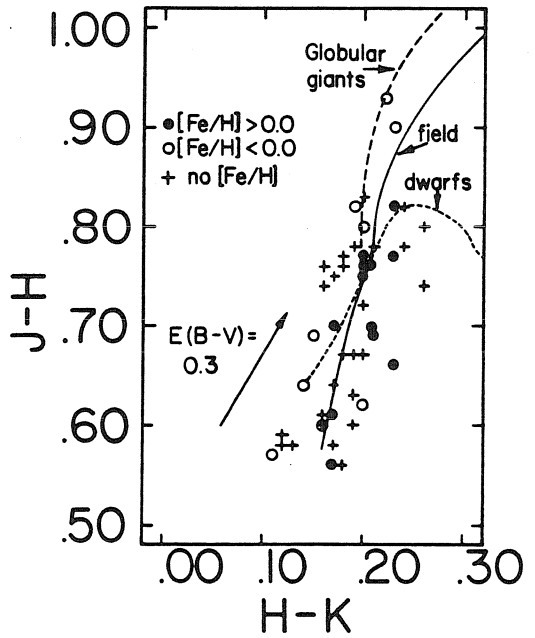

FIG. 6. Mean lines for giants and dwarfs are from Frogel *et al.* (1978); that for globular cluster giants is from Frogel, Persson, and Cohen (1983).

same $V-K$ (Fig. 7). NGC 5927, a globular cluster with a metallicity only slightly less than solar, has giants of similar color to the BW ones in Fig. 7. The NGC 5927 stars, too, have CO indices greater than the mean field line (Frogel, Persson, and Cohen 1983).

V. DISCUSSION

The K giants in Baade's Window are generally considered to be good representatives of the old stellar population found in the central regions of early-type galaxies and the bulges of spiral galaxies. Whitford and Rich (1983) have shown that the mean metallicity of these giants is several tenths of a dex greater than solar. In infrared color-magnitude diagrams, the giant branches of clusters ranging in metallicity from the most metal-poor globulars, such as M92, through metal-rich old disk clusters, such as M67, follow an orderly progression of increasing redness with increasing [Fe/H] (Frogel, Cohen, and Persson 1983). Therefore, it is quite surprising that the high-Z stars from BW in Figs. 1 and 2 are not particularly red. In fact, even the visual CM diagrams of Arp (1965) and van den Bergh (1971) placed the majority of the giants blueward of the giant branches of the metal-rich old disk clusters. The inconsistency of Arp's and van den Bergh's CM diagrams with a solar or greater than solar metal abundance has apparently not been remarked upon in the literature.

It is unlikely that there are systematic errors in the photometry which can affect both the $J-K$ and $V-K$ colors of the BW stars sufficiently so as to account for their relatively blue colors. We can not, of course, rule out a peculiar wavelength dependence for the interstellar absorption law, but consider it unlikely since nearly all of the extinction occurs in the galactic plane close to the Sun (Arp 1965; van den Bergh 1971). Two possible explanations are that these stars are much younger than usually thought or that there are large blanketing effects caused by their high metallicity. These possibilities will be fully considered in a later paper. The implications of these alternatives are, however, worth brief mention here. (We note that the adoption of 7 kpc rather than 9 kpc as the distance to the Galactic center will move the points in Figs. 1 and 2 *down* by 0.6 mag.)

Many of the M giants in BW have bolometric luminosities which are one to two magnitudes brighter than that which marks the termination point of a star's first ascent of the giant branch (Frogel 1981; Frogel and Whitford 1982). Frogel and Whitford concluded that while it is possible that some of these luminous giants are massive and young, the relatively long main-sequence lifetimes of SMR stars provide them with sufficient mass to rise to a high level on the asymptotic giant branch. Wood and Bessell (1983), on the other hand, argue that many of the red variables in the nuclear bulge are only a few Gyr old.

If the $J-K$ and $V-K$ colors of the BW stars are not significantly affected by blanketing, and the giant branch models of Sweigart and Gross (1978) are correct in a relative sense, then metal-rich stars would have to be of at least two solar masses with ages of about 2 Gyr to account for their relative positions in Figs. 1 and 2. According to the main-sequence calculations of Mengel *et al.* (1979), stars with a metallicity of five times solar would have the luminosity and color of an early-F star at the turnoff stage. In the BW, such stars would show a concentration at $V=18.2$, too faint to show on existing color-magnitude diagrams. However, since the metal-rich fraction of the BW giants is so large (Whitford and Rich 1983), such a population of young objects would have had a noticeable effect on the integrated light of BW as measured by Whitford (1978). A similar component of relatively bright, blue turnoff stars in the analogous population of elliptical galaxies would be nearer the case of continuous star birth in Larson and Tinsley's (1974) modeling of aging effects for which the calculated integrated color is $(B-V)=0.5$. Their single-burst case with fainter, not-so-blue turnoff stars matches the observed colors of ellipticals: $(B-V)=0.95$.

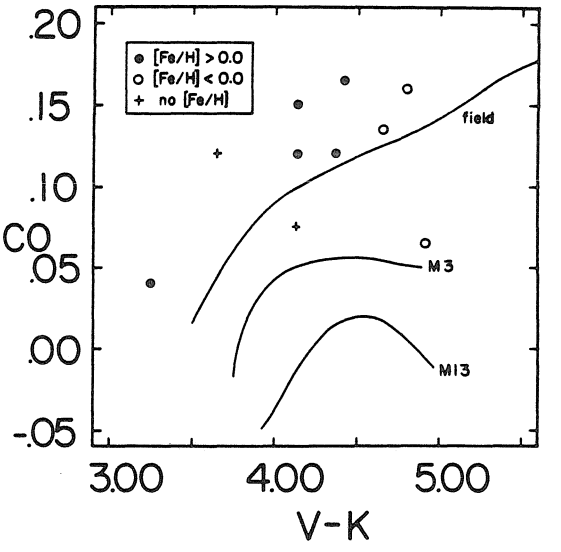

FIG. 7. The mean lines are from Cohen, Frogel, and Persson (1978).

What about blanketing effects? The displacement of the BW stars with respect to the mean for field giants in Fig. 4 is in the sense that the BW stars have too blue $J-K$ for given $V-K$ and/or too red $V-K$'s. The latter possibility is opposite to what is needed to help the more fundamental problem of Fig. 1. Hence, it is not unreasonable to conclude that blanketing effects on $J-K$ act to make the BW stars blue with respect to field giants. The large CO indices in the BW stars (Fig. 7) can account for only 0.02 mag of extra blanketing in the K passband.

Frogel, Persson, and Cohen (1983) demonstrate that the effect of H_2O absorption is greater in the K-filter bandpass than in the J filter (its effect on the H filter is several times greater than that on the other two filters). In Fig. 6, the high-Z group of stars are displaced with respect to the low-Z ones in the sense expected if H_2O absorption were important. However, for the sample of BW stars with measurements of the 1.9-μm H_2O index, there is no evidence of H_2O in excess of that for field giants of the same color (Frogel, Whitford, and Blanco 1984).

McGregor and Hyland (1981) have discussed the effects of the infrared CN bands on JHK colors of supergiants. From their work, it would appear that metal-rich stars with enhanced CN bands should be displaced to bluer $J-H$ and redder $H-K$ colors relative to weak-CN stars. Whether this effect is operative in stars of the luminosity of the BW K giants can be examined with high-resolution infrared spectra.

So, we conclude that while there is evidence for blanketing differences between solar neighborhood giants and the K

giants in BW, we can not, at present, quantify these differences in a manner which will allow us to understand the apparently anomalous location of the BW stars in color-magnitude diagrams.

The participation of A. E. Whitford and R. M. Rich in this work was supported in part by a grant from the National Science Foundation.

REFERENCES

Arp, H. (1965). Astrophys. J. **141**, 43.
Baade, W. (1963). In *Evolution of Stars and Galaxies*, edited by C. P. Gaposchkin (Harvard University, Cambridge, Mass.), p. 279.
Bessell, M. S. (1979). Publ. Astron. Soc. Pac. **91**, 589.
Blanco, B. M., Blanco, V. M., and McCarthy, M. F. (1978). Nature **271**, 638.
Blanco, V. M., and Blanco, B. M. (1984). Publ. Astron. Soc. Pac. **96**, 603.
Blanco, V. M., McCarthy, M. F., Blanco, B. M. (1984). Astron. J. **89**, 636.
Cohen, J. G., Frogel, J. A., and Persson, S. E. (1978). Astrophys. J. **222**, 165.
Dean, J. F., Warren, P. R., and Cousins, A. W. J. (1978). Mon. Not. R. Astron. Soc. **183**, 569.
Elias, J. H., Frogel, J. A., Mathews, K., and Neugebauer, G. (1982). Astron. J. **87**, 1029.
Elias, J. H., Frogel, J. A., and Humphreys, R. M. (1985). Astrophys. J. Suppl. (in press).
Frogel, J. A. (1981). In *Physical Processes in Red Giants*, edited by I. Iben, Jr., and A. Renzini (Reidel, Dordrecht), p. 55.
Frogel, J. A., Cohen, J. G., and Persson, S. E. (1983). Astrophys. J. **272**, 167.
Frogel, J. A., Persson, S. E., Aaronson, M., and Mathews, K. (1978). Astrophys. J. **220**, 75.
Frogel, J. A., Persson, S. E., and Cohen, J. G. (1981). Astrophys. J. **246**, 842.
Frogel, J. A., Persson, S. E., and Cohen, J. G. (1983). Astrophys. J. Suppl. **53**, 713.
Frogel, J. A., and Whitford, A. E. (1982). Astrophys. J. Lett. **259**, L7.
Frogel, J. A., Whitford, A. E., and Blanco, V. M. (1984). In preparation.
Glass, I. S., and Feast, M. W. (1982). Mon. Not. R. Astron. Soc. **198**, 199.
Larson, R. B., and Tinsley, B. M. (1974). Astrophys. J. **192**, 293.
Lee, T. A. (1970). Astrophys. J. **162**, 217.
McGregor, P. J., and Hyland, A. R. (1981). Astrophys. J. **250**, 116.
Mengel, J. G., Sweigart, A. V., Demarque, P., and Gross, P. G. (1979). Astrophys. J. Suppl. **40**, 733.
Morgan, W. (1959). Astron. J. **64**, 432.
Nassau, J. J., and Blanco, V. M. (1958). Astrophys. J. **128**, 46.
Persson, S. E., Frogel, J. A., Cohen, J. G., Aaronson, M., and Mathews, K. (1980). Astrophys. J. **230**, 452.
Sweigart, A. V., and Gross, P. G. (1978). Astrophys. J. Suppl. **36**, 405.
van den Bergh, S. (1971). Astron. J. **76**, 1082.
Whitford, A. E. (1978). Astrophys. J. **226**, 777.
Whitford, A. E., and Blanco, V. M. (1979). Bull. Am. Astron. Soc. **11**, 675.
Whitford, A. E., and Rich, R. M. (1983). Astrophys. J. **274**, 723.
Wood, P. R., and Bessell, M. S. (1983). Astrophys. J. **265**, 748.
Zinn, R. (1980). Astrophys. J. Suppl. **42**, 19.

APPENDIX 2

NEW RESULTS ON THE GALACTIC BULGE POPULATION: RELEVENCE TO THE POPULATION II VARIABLES

R. M. Rich

Reprinted from the *Memorie Della Societa Astronomica Italiana* (1985, **56** 23–35).

NEW RESULTS ON THE GALACTIC BULGE POPULATION: RELEVANCE TO THE POPULATION II VARIABLES

R. Michael Rich

Palomar Observatory, California Institute of Technology

The variable stars of population II have served as the luminous signposts of stellar populations. They are veritable storehouses of information, from which distances can be obtained, metal abundances estimated, and ages inferred. Stars old and metal poor enough to populate the instability strip as horizontal branch stars become RR Lyraes; metal rich stars become luminous enough to be Miras and LPV's. Of the stellar populations we can study in detail, the galactic bulge is unique in that it has an integrated spectrum resembling other late galaxy populations (Whitford, 1978) yet also contains both RR Lyrae stars and Mira variables. It also has none of the obvious hallmarks of very young populations, such as are found in the Magellanic Clouds.

The following table illustrates features that set the galactic bulge off from other resolved populations. The nearest comparable population resides in the bulge of M31, one hundred times as distant. Hence, if we are to understand the variable star content in old, metal rich populations, the galactic bulge is an excellent place to begin. A complete review of the characteristics of the bulge population can be found in Whitford's 1984 review article; this paper deals with more recent developments, and also contains a personal perspective on the significance of various developments.

Systems With Known Population II Variables

System	Age (Gyr)	[Fe/H]
Disk	0 – 15	−0.6 – 0.0
Halo	>10	< −1.0
Globular Clusters	>10	−2.0 – −0.8
Bulge	>10 (?)	−2.0 – +1.0
Dwarf Spheroidals	>7	−2.0 – −1.0
SMC, LMC Fields	0 – 15	−2.0 – −0.5
SMC, LMC Globular Clusters	> 10*	−2.0 – −0.8

*Graham and Nemec, 1984

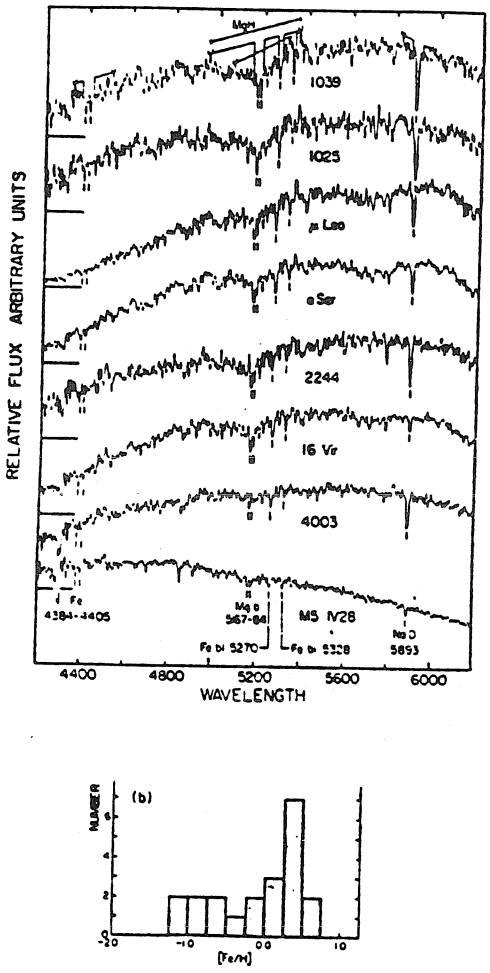

Fig. 1.—Spectra of four Baade's window K giants (four-digit numbers) and four standard stars. Ther vertical ticks mark the five features whose strength was measured; continuum placement and integration limits for these features are shown for the uppermost spectrum. The two bulge giants with the highest metallicity are at the top. *below*: Histogram of metal abundances *for bulge stars* derived relative to giants in the solar neighborhood which have been analysed at high dispersion (Whitford and Rich, 1983).

Baade (1951) used the RR Lyrae stars in his famous demonstration that there is in fact a galactic bulge. He also found LPV's in the NGC 6522 window (Baade, 1963) but the RR Lyraes proved immediately significant because of their value in confirming a spatially concentrated bulge, as well as in measuring R_0. For many years, galactic bulge populations were characterized as old and metal poor, largely based on the presence of the RR Lyrae stars. Morgan's 1956 spectroscopy revealed the bulge of M31 to be strong-lined; Spinrad and Taylor (1971) confirmed the result with digital spectroscopy, but attributed the strong lines to a dwarf-enhanced, as well as metal rich population. Even modern work, such as Gunn, Stryker and Tinsley, 1981, does not consider the possibility of an abundance range in the stars comprising strong-lined galaxy populations. The metal poor stars may contribute significant numbers of blue horizontal branch and UV bright stars, and thus could explain the hot UV flux seen in old galaxy populations, ***without requiring the presence of any young stars.*** Baade's population II variables illustrated that the bulge has a range in abundance and possibly in age, but the result has yet to be accepted, more than thirty years later. No galactic globular cluster has a population of variable stars which resembles that in Baade's window; why was this not pointed out soon after Baade's work was completed? With the Hubble Space Telescope, variable stars and the upper giant branch will be accessible in other more distant galaxies. I expect that the "metal rich" bulge of M31 will also show a considerable spread in the stellar abundances.

This report contains preliminary findings on the abundances and radial velocities of K giants in the nuclear bulge. I will also discuss work in progress with Donald Terndrup and A.E. Whitford to define the color-magnitude diagram of the bulge.

The best evidence for the abundance range in the galactic bulge, aside from the population II variables, are the spectra of 21 K giants in Baade's Window obtained by Whitford and Rich, 1983. The panel of spectra, and the derived abundance distribution, is reproduced in Figure 1. Note that the range in abundance, from -1 to nearly 1 dex, is greater than has been measured in any other resolved population.

About 30% of the K giants studied in a larger, 77 star sample are also metal poor ([Fe/H] $<$ -0.5 dex). We would expect these stars to be the progenitors of the RR Lyrae stars. However, while in normal globular clusters, the RR Lyrae population is only 4-10% of the K giants, in the bulge, this number is less than 5% (Whitford and Rich, 1983). The sample of bulge stars is too small to draw a firm conclusion at this time, although the halo also appears to lack a blue horizontal branch (Bahcall and Soneira, 1984). Radial velocities will undoubtedly prove the best means by which to link populations of variables with their progenitors.

The fraction of metal poor stars in Baade's Window is high, not only in number but also in their impact upon the appearance of the integrated light. Mould, Kristian, and Da Costa (1983,1984) have also found significant abundance spreads in the haloes of local group galaxies. It would be very interesting to assess the abundance distribution as a function of galactic latitude, because it would provide a detailed description of the enrichment history of the bulge. Toward this end, I developed a method to rapidly survey the bulge's metallicity, which will be done at latitudes of $-3°$, $-4°$,and $-8°$. The method employs filters centered on the MgH feature and two sideband continuum points. While the MgH feature is gravity sensitive, nearly all of the stars detected are giants, and the

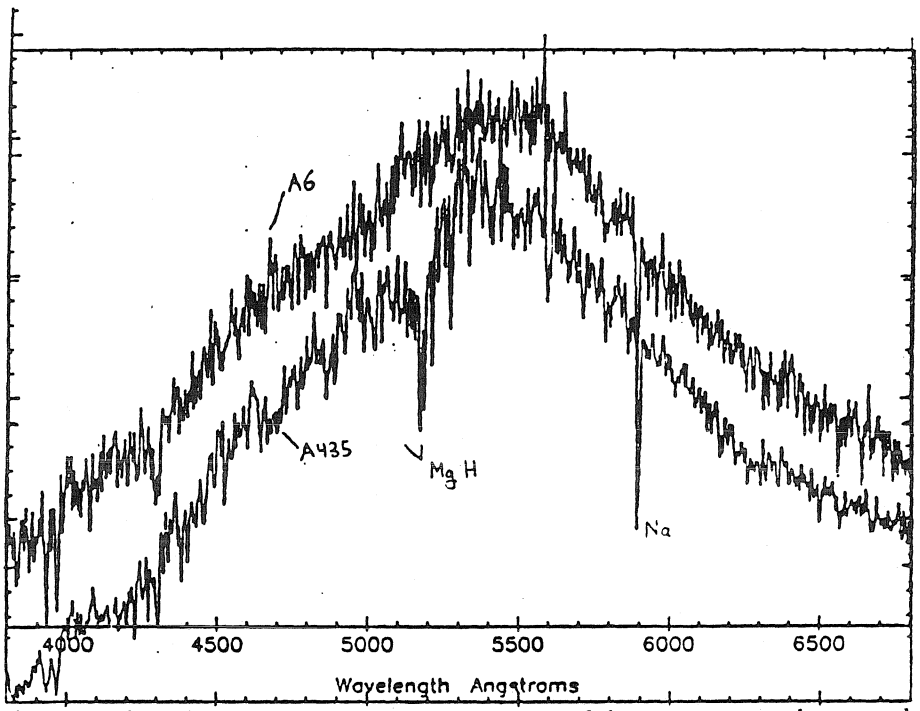

Fig. 2.—Two K giants in Baade's window, selected for spectroscopy because their narrow band indices indicated high and low metallicity, respectively. The narrow band photometry was done with the Cerro Tololo 4m prime focus CCD in a direct imaging mode.

large reddening helps to eliminate nearby stars from the sample, as well. These data will tell us if the abundance gradient results from a decline in the number of metal rich stars, or from a decrease in the mean metal abundance. At this time, the narrow band method has successfully identified stars of high and low abundance for spectroscopic study, which are shown in figure 2.

Are the metal rich K giants progenitors of the M giant population, and do the metal rich and metal poor stars belong to different kinematic populations? These questions can be answered by measuring radial velocities. Using the 2.5m du Pont telescope and the Shectman intensified reticon spectrograph, Rich and Whitford have measured about 50 stars. In the following table, the 1984 data are more significant because of the smaller errors. Some shift in the zero point also seems to be present in the 1982 data. More data will be obtained in 1985.

Velocity Dispersions of Giants in Baade's Window

Sample	σ km/sec	V km/sec	N	Error km/sec
Total, 1982	120 ± 12	-59 ± 17	50	40
Strong Line K	105 ± 14	-75 ± 20	29	
Weak Line K	137 ± 21	-38 ± 30	21	
Total, 1984	120 ± 15	-26 ± 21	33	20
Strong Line K	87 ± 17	-50 ± 23	14	
Weak Line K	143 ± 24	2 ± 33	18	
M Giants*	113 ± 11	-10 ± 16	49	11

*Mould, 1983

The dispersions are shown in figure 3. It appears that the metal rich K giants do have a smaller velocity dispersion. They also appear to have a bulk negative velocity, a curious result which does not appear in any other sample of objects studied. The M giants in Mould's sample have a dispersion intermediate between the strong and weak lined K giants. Feast et al. (1980) found an almost identical dispersion for the Miras in the Sgr I and Baade windows. Perhaps the progenitors of the M giants have a wider range of metal content. Recall that 47 Tuc, with an abundance of -1 dex, contains both M giants and Miras. If the M giants were young stars, they would have formed out of gas which would have interacted with the disk in what one would guess would be a dissipative collapse. In drawing general conclusions, one must be troubled that so few stars have reliable velocities. However, if the metal poor K giants were progenitors of the RR Lyrae stars, one would expect the RR Lyraes to have a velocity dispersion greater than 120 km/sec. Nonetheless, Rodgers (1977) measured 35 RR Lyrae stars in various bulge windows, and found a dispersion of 70 km/sec, very much less than that for any other bulge population.

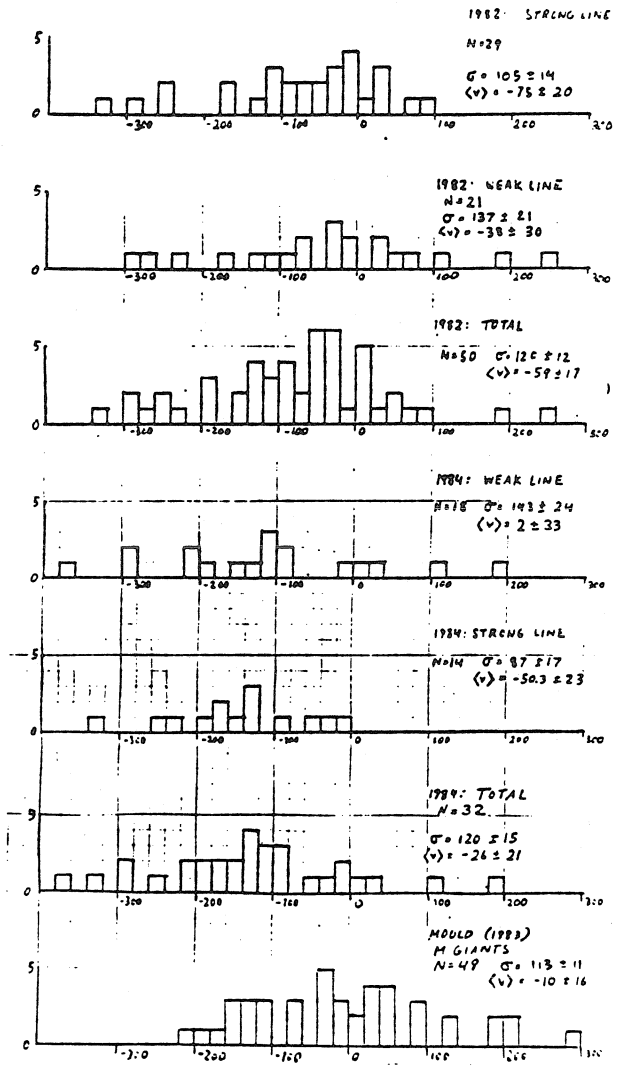

Fig. 3.—Velocity dispersions of K giants in Baade's Window. The 1984 data are more reliable, with errors of 20 km/s and less zero-point uncertainty.

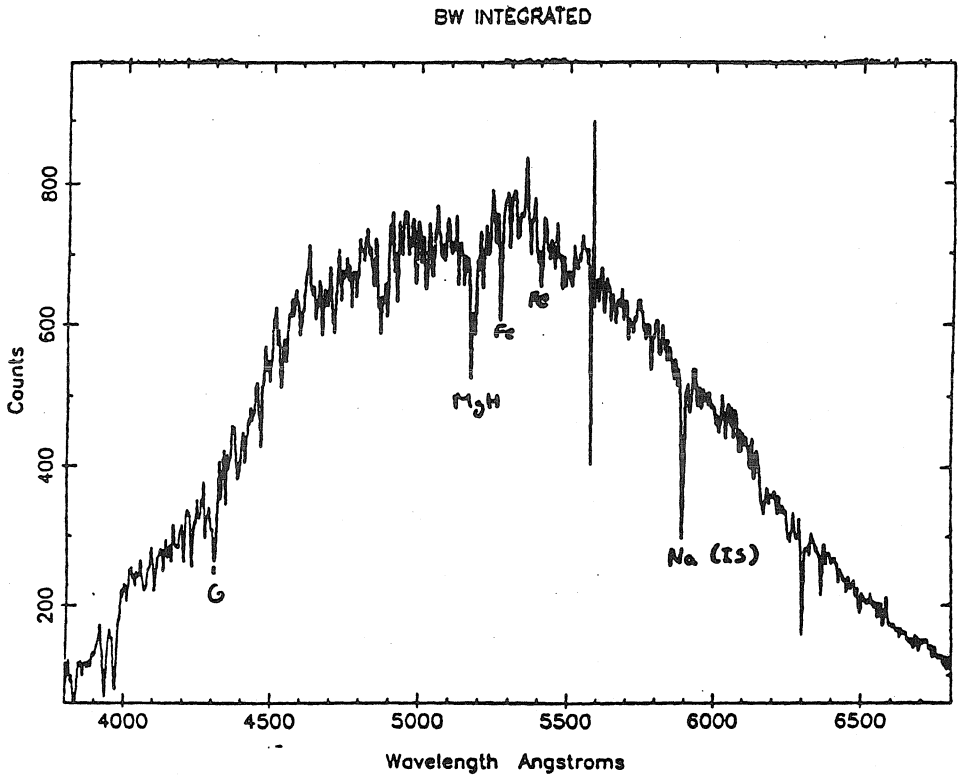

Fig. 4.—Integrated spectrum resulting from scanning over a patch of Baade's Window, and subtracting sky taken before and afterwards. The prominent "emission line" is poorly subtracted night sky emission.

II. Progenitors of Luminous Red Variables: Search for a Young Population

If one places the most luminous Baade's Window stars in the physical H-R diagram, a straightforward interpretation would suggest that the stars are on the upper AGB, and could be younger than 2 Gyr (Frogel and Whitford, 1982). Moreover, Wood and Bessell (1983) found large pulsation masses ($> 2M_{\odot}$) for the long period Miras. (For a more complete description, see Whitford's 1984 review article.) Figure 4 shows the integrated spectrum of a patch of Baade's Window; one sees no evidence for a signficant young star component, which should appear as Balmer lines. If there are young, metal-rich stars in the bulge, where did the material come from, and how was it enriched? Dissipative theories for galaxy formation generally predict short collapse times for the more dense, central portions of galaxies.

It should be possible to answer these questions by directly observing the bulge's color-magnitude diagram (Terndrup, Rich, and Whitford 1983). The bulge color-magnitude diagrams were measured from 4m Tololo prime focus CCD data using a point-spread function fitting program written by Terndrup at Lick Observatory. In the $-8°$ field, we confirm van den Bergh's reported turnoff, but the CCD photometry extends down to V=22. If one uses a distance of 7 kpc and E(B−V)=0.23, the Vanden Berg (1984) isochrones overlay the bulk of the apparent turnoff population. Best fitting are the solar metallicity, Y=0.25, 10 Gyr isochrones, from which one concludes that few, if any, stars are young. It will be most revealing to model the observed color-magnitude diagram with a range of abundances and ages, and taking into account the spatial thickness of the bulge. If there are metal poor stars in the bulge, they are older than 8−10 Gyr, because the bulge has no known luminous, red carbon stars like those associated with intermediate age populations in the Magellanic Clouds. As mentioned earlier, Wood and Bessell suggest that substantial numbers of AGB stars younger than 1 Gyr are present in the galactic bulge. Can we test this hypothesis using the CCD photometry, by looking for turnoff stars? In Baade's Window, Frogel and Whitford (1983) found that M giants more luminous than the helium flash comprised about 15% of their sample. If their sample was representative, then there are 360 such stars per square degree (Blanco et al. 1984). Iben and Renzini (1983) suggest that the time spent more luminous than the helium flash, $t_{\rm AGB}$, is about 10^6yrs, so the number of main sequence progenitors is:

$$N_{\rm MS} = \left(\frac{t_{\rm MS}}{t_{\rm AGB}}\right) N_{\rm RG}$$

For 2 Gyr old stars, the above formula requires 200 main sequence stars per square arc minute, or about 3000 of them per frame, in Baade's window. Although the crowding is severe, nothing like that many stars are there. Wood and Bessell suggested that stars younger than 1 Gyr are also present, but the observed number of main sequence stars is three orders of magnitude short! The number of late M giants falls precipitously with increasing galactic latitude, falling by a factor of 100 from $-4°$ to $-8°$ (Blanco, 1984). We would expect to see at least 10 stars near the 2 Gyr isochrone, but we can't draw any strong conclusions, except that there aren't many young stars at that latitude. Van den Bergh and Herbst (1974) surveyed a total of 72 square arcmin, so we would expect a minimum of

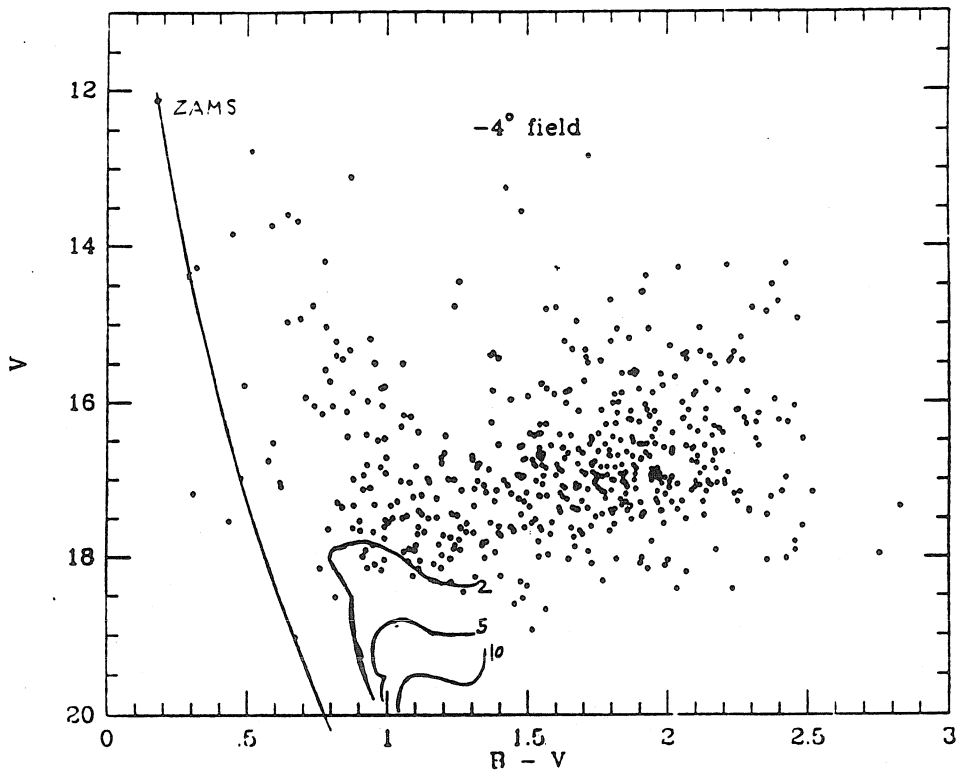

Fig. 5.—Color-magnitude diagram in Baade's Window, obtained with the Cerro Tololo 4m prime focus CCD *see text.* Isochrones are from Vanden Berg, 1984.

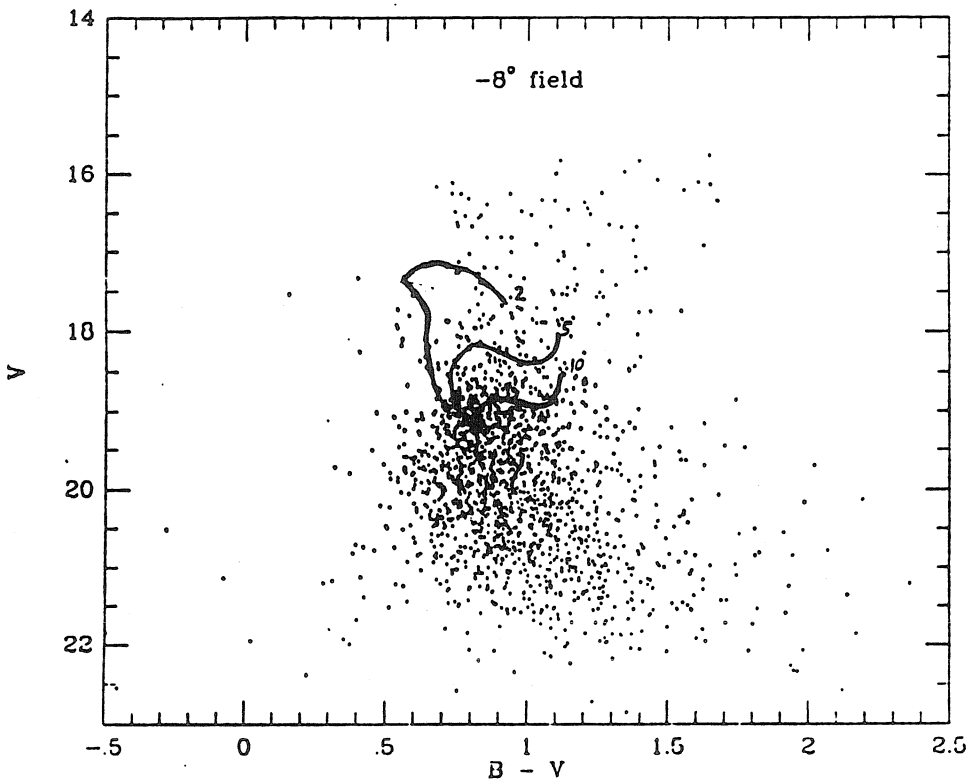

Fig. 6.—As above, for the $l = 0°, b = -8°$ field of the Galactic bulge.

70 stars in the proper location on their color-magnitude diagrams; instead, only a handful are there, and they don't define anything that appears to be a main sequence. These rough calculations are very generous, in that they don't require the young stars to have a sensible luminosity function, which would make them even more numerous.

The observations in Baade's Window were made in 1" seeing, and illustrate that we have little hope of ruling out anything but the youngest populations from the ground. Yet Blanco's counts of M giants indicate that the excess of luminous AGB stars is most severe in the inner windows, where we have the greatest difficulty in determining ages. Even so, the blue stars in Baade's Window are clearly too *red* to be main sequence stars. Because their numbers also fall short by three orders of magnitude, we are left seeking other explanations for the luminosities of the late M giants and long period Miras. The young main sequence stars are not present. Any limits set on the intermediate age population will come from Space Telescope.

III. Programs for the Future

The galactic bulge is a complex population, regardless of how closely its integrated light resembles an elliptical galaxy. The population II variables tell us that the population is considerably more complicated than single metal content populations used in galaxy population models. There probably is an age spread. More study of the bulge at different latitudes, with spectroscopy of large numbers of stars, would be very useful. It would also be interesting, though perhaps next to impossible, to find RR Lyrae stars in Sag I, the innermost of Baade's Windows, at $-2.7°$ galactic latitude. If we knew the velocity dispersion of the RR Lyrae stars in Baade's Window, we would at least have a homogeneous population, certain to be old, to use as a benchmark in comparing other populations. The luminous Miras would be unlikely to be young, formed in a dissipative infall of gas, if their velocity dispersion were identical to the RR Lyrae stars.

The luminosity function of the upper giant branch is as accessible in M31 as it is in the Galaxy. Further, the bulge of M31 can be well resolved close to the nucleus, even from the ground. Using the Space Telescope, we will certainly be able to detect Miras in M31's bulge, and RR Lyrae stars in its halo. Once again, the variable stars of population II will provide invaluable information on the properties of late-type stellar populations.

References

Baade, W. 1951, *Pub.Obs.Univ.Mich.*, **10**, 7.

Baade, W. 1963, in *Evolution of Stars and Galaxies* ed. C.P. Gaposchkin (Cambridge: Harvard University Press), p. 282.

Bahcall, J.N., and Soneira, R.M. 1984, *Ap.J.Suppl.Ser.*, **55**, 67.

Blanco, V.M. 1984 *preprint.*

Blanco, V.M., McCarthy, S.J., and Blanco, B.M. 1984, *A.J.*, **89**, 636.

Feast, M.W., Robertson, B.S.C., and Black, C. 1980, *M.N.R.A.S.*, **190**, 227.

Frogel, J.A., and Whitford, A.E. 1982, *Ap.J.Lett.*, **259**, L7.

Gunn, J.E., Stryker, L.L., and Tinsley, B.M. 1981, *Ap.J.*, **249**, 48.

Graham, J.A., and Nemec, J.M. 1984 in *Structure and Evolution of the Magellanic Clouds* eds. S. van den Bergh and K. S. de Boer (Dordrecht: Reidel) p.37.

Iben, I., and Renzini, A. 1983, *Ann.Rev.Astr.Ap.*, **21**, 271.

Morgan, W.W. 1956, *Pub.A.S.P.*, **68**, 509.

Mould, J.R. 1983, *Ap.J.*, **266**, 255.

Mould, J.R., Kristian,J., and Da Costa, G.S. 1983, *Ap.J.*, **270**, 471.

Mould, J.R., Kristian,J., and Da Costa, G.S. 1984, *Ap.J.*, **278**, 575.

Rodgers, A.W. 1977, *Ap.J.*, **226**, 255.

Spinrad, H., and Taylor, B.J. 1971, *Ap.J.Suppl.*, **22**, 445.

Terndrup, D.M., Rich, R.M., and Whitford, A.E. 1984, *Pub.A.S.P.*, **96**, 796.

Vanden Berg, D. 1984, *preprint.*

Van den Bergh, S., and Herbst, E. 1974, *A.J.*, **79**, 603.

Whitford, A.E. 1978, *Ap.J.*, **226**, 277.

Whitford, A.E. 1984, *preprint.*

Whitford, A.E., and Rich, R.M. 1983, *Ap.J.*, **274**, 723.

Wood, P.R., and Bessell, M.S. 983, *Ap.J.*, **265**, 748.

DISCUSSION

FEAST- It is interesting to try to see where the OH/IR sources fit into your picture. The OH/IR sources are generally regarded as relatively massive, very long period variables.

RICH- If there are many young stars in the bulge, they should show up as main sequence stars as well as giants. The requisite number of main sequence stars are not there. The OH/IR sources may be related to sources in the nuclear bulge discovered by the IRAS satellyte. Both classes of evolved giants will be better understood when the turn-off age is established.

BLANCO- I have two remarks. One, I am not too surprised about your finding about half as many RR Lyraes as one would expect from the number of K giants in the bulge. As we remarked earlier today, in our reanalysis of RR Lyraes in Baade's Window we found about 3 times as many RR Lyraes for unit volume as were found by Oort and Plaut. This factor of 3 for excess is not too different from the factor of 2 for scarcity you found. The second remark is about Mould's radial velocities. As Mould remarked, his measures were biased towards the brighter giants. In view of a possible disk-like distribution of late giants within the bulge, Mould's radial velocities may have favored the giants closest to us from the galactic center and therefore may not be truly representative of the kinematics near the galactic center but of stellar motions closer to the sun.

ZINN- Can you say something more on how the metallicities of the stars were determined? In particular, how the sensitivity of MgH and Mgb to surface gravity was handled.

RICH- For full details I refer you to the paper where the abundances are determined (Withford and Rich, 1983 Ap.J.274,723). Briefly, Fe5270, 5328 were used as well as Mg, and IR colors (J-K) were measured to get temeperatures. The same quantities were measured for local K giants and Baade's Window stars. It was found that for the local K giants there was a tight dependence of linestrength on metal abundance and (J-K) color. This relationship was applied to the bulge K giants, with reddening corrections.